Supporting Information

Catalytic Activation of N_2O at a Low-Valent Bismuth Redox Platform

Yue Pang, Markus Leutzsch, Nils Nöthling and Josep Cornella*

Max-Planck-Institut für Kohlenforschung, D-45470 Mülheim an der Ruhr, Germany

cornella@kofo.mpg.de

Table of Contents

1. General Information

Unless otherwise stated, all manipulations were performed under argon using standard Schlenk line techniques or in a MBraun argon-filled glove box.

Instruments: Flash chromatography: Merck silica gel 60 (40-63 μm). ESI-MS: ESQ 3000 (Bruker). Accurate mass determinations: Bruker APEX III FT-MS (7 T magnet) or MAT 95 (Finnigan). NMR spectra were recorded using a Bruker AVIII HD 300 MHz, Bruker Advance III HD 400 MHz or Bruker AVIII 500 MHz spectrometer. ^{1}H and ^{13}C chemical shifts are reported relative to the solvent residual peak as an internal standard. For ^{1}H NMR: $CDCl_3$, δ 7.26; THF-*d*$_8$, δ 3.58; toluene-*d*$_8$, δ 2.08; CD_3OD, δ 3.31. For ^{13}C NMR: $CDCl_3$, δ 77.16; THF-*d*$_8$, δ 67.57; toluene-*d*$_8$, δ 20.43; CD_3OD, δ 49.00. ^{11}B NMR chemical shifts were referenced to pinacolborane (28.0 ppm, THF-*d*$_8$). NMR yields were determined by using mesitilyene as internal standard. For each spectrum 16 FIDs were averaged and the relaxation delay between experiments was set to 30 s. GC-TCD measurements were performed on Agilent Technologies GC 7890B with a 30 m HP-Plot 5 Å Molsieve column. Melting points were measured with an EZ-Melt Automated Melting Point Apparatus from Standford Research Systems.

Chemicals: N_2O was provided by Air Liquide containing less than 5 ppm N_2, 1 ppm H_2O and 1 ppm air and O_2. THF-*d*$_8$ and toluene-*d*$_8$ were purchased from Eurisotop, degassed by repeated freeze-pump-thaw cycles, distilled from the proper drying agents, and stored over 4 Å molecular sieves. 4 Å molecular sieves were activated at 200 °C under high vacuum (1×10^{-4} bar) for 3 days. Anhydrous *n*-pentane, THF, Et_2O and toluene were distilled from appropriate drying agents and were transferred under argon. Anhydrous *n*-hexane and benzene were purchased from Millipore Sigma-Aldrich. Anhydrous $BiCl_3$ (99.9%, trace metal basis) was purchased from Alfa Aesar. Cobaltocene (min. 98%) was purchased from Strem Chemicals and stored in the freezer of the glove box prior to use. Bismuthinidene **1** was prepared by the reported method.[1] Unless otherwise noted, all reagents were obtained from commercial suppliers and used without further purification.

2. Synthesis and Characterization Data of Ligands

2.1. Synthesis of Ligand **S1**

2,6-Diphenylaniline

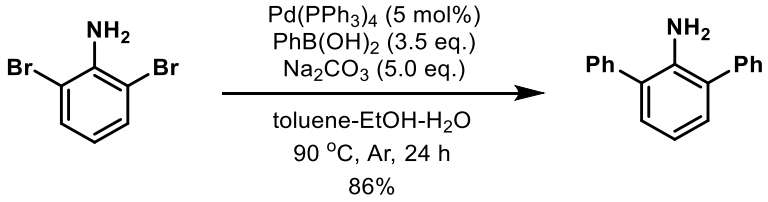

2,6-Diphenylaniline was prepared by the literature method with modifications.[2]

Procedure: a 500 mL three-necked flask equipped with a reflux condenser was charged with 2,6-dibromoaniline (10.0 g, 39.9 mmol), phenylboronic acid (17.0 g, 139.5 mmol, 3.5 equiv.), Na_2CO_3 (21.1 g, 199.3 mmol, 5.0 equiv.). The setup was evacuated and refilled with argon. A liquid mixture of toluene (100 mL), H_2O (40 mL) and EtOH (20 mL) was degassed by freeze-pump-thaw cycles and transferred to the flask under argon. After that, $Pd(PPh_3)_4$ (2.3 g, 2.0 mmol, 5 mol%) was added to the suspension under argon. After stirred at 90 °C for 24 h, the reaction mixture was cooled to room temperature, filtered through Celite pad, and the filtrate was partitioned with EtOAc and H_2O. The organic layer was separated and evaporated under reduced pressure. The residue was purified by column chromatography on silica gel (hexane/DCM, 5:1 to 4:1 to 3:1, *v*/*v*) to afford 8.4 g 2,6-diphenylaniline as a white crystalline solid in 86% yield.

^{1}H NMR (400 MHz, $CDCl_3$): δ 7.57 – 7.52 (m, 4H), 7.51 – 7.46 (m, 4H), 7.42 – 7.35 (m, 2H), 7.16 (d, *J* = 7.6 Hz, 2H), 6.92 (t, *J* = 7.5 Hz, 1H), 3.85 (br. s, 2H, NH_2).

^{13}C NMR (101 MHz, $CDCl_3$): δ 140.9, 139.9, 129.9, 129.4, 129.0, 128.1, 127.4, 118.3.

The spectral data matched with those reported in the literature.[2]

Ligand **S1**

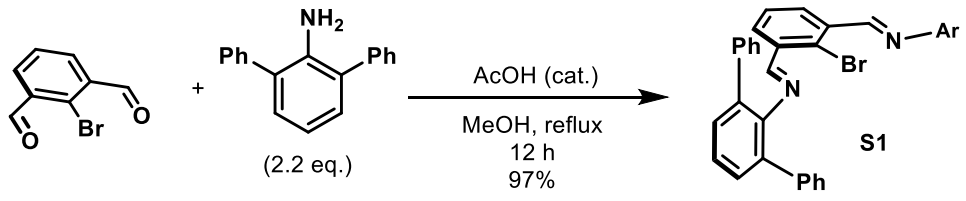

Procedure: to a 100 mL round-bottom flask equipped with a reflux condenser, 2-bromoisophthalaldehyde (1.00 g, 4.7 mmol), 2,6-diphenylaniline (2.53 g, 10.3 mmol), MeOH (25 mL) and AcOH (4 drops) were added in sequence. Then the mixture was heated to reflux with rapid stirring for 12 h, during which the pale yellow product crushed out. The solid was

filtered, washed with MeOH three times and dried at 110 °C under high vacuum. **S1** was obtained as a pale yellow powder (3.02 g, 96%).

^{1}H NMR (400 MHz, $CDCl_3$): δ 8.24 (s, 2H), 7.68 (d, *J* = 7.7 Hz, 2H), 7.40 – 7.33 (m, 12H), 7.33 – 7.26 (m, 10H), 7.25 – 7.19 (m, 4H), 7.16 (t, *J* = 7.7 Hz, 1H).

^{13}C NMR (101 MHz, $CDCl_3$): δ 164.2, 148.1, 140.0, 135.3, 133.9, 131.3, 130.3, 130.2, 128.2, 127.7, 127.5, 126.8, 125.1.

M.p.: 187.9 – 189.3 °C.

HRMS (ESI): calc'd for $C_{44}H_{31}N_2BrNa^+$ $[M+Na]^+$ 689.15629; found 689.15720.

2.2. Synthesis of Ligand **S2**

The synthetic route to ligand **S2**

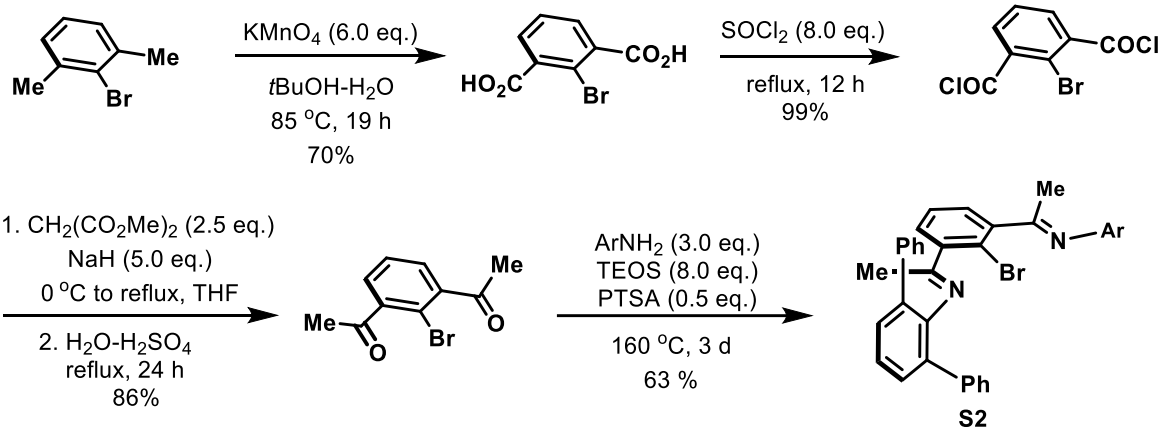

2-Bromoisophthalic acid

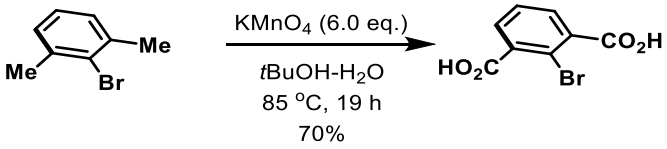

2-bromoisophthalic acid was prepared by the literature method with modifications.[3]

Procedure: to a 1 L round-bottom flask equipped with a condenser 2-bromo-1,3-dimethylbenzene (18.0 g, 97.3 mmol), H_2O (280 mL) and *t*BuOH (140 mL) were added. $KMnO_4$ (92.2 g, 583.6 mmol, 6.0 equiv.) was added portionwise and the solution was heated to reflux for 19 h. After this time, the reaction was quenched by adding 20 mL EtOH and filtered through Celite pad while still hot. The filtrate was evaporated to dryness and 140 mL

20% HCl was added. Filtration, washing with water and drying under high vacuum afforded 16.7 g (70%) title compound as a white solid.

^{1}H NMR (400 MHz, CD_3OD): δ 7.73 (d, *J* = 7.6 Hz, 2H), 7.49 (dd, *J* = 8.1, 7.4 Hz, 1H).

^{13}C NMR (101 MHz, CD_3OD): δ 169.9, 137.9, 132.5, 128.5, 118.4.

The spectral data matched with those reported in the literature.[3]

2,6-Diacetylbromobenzene

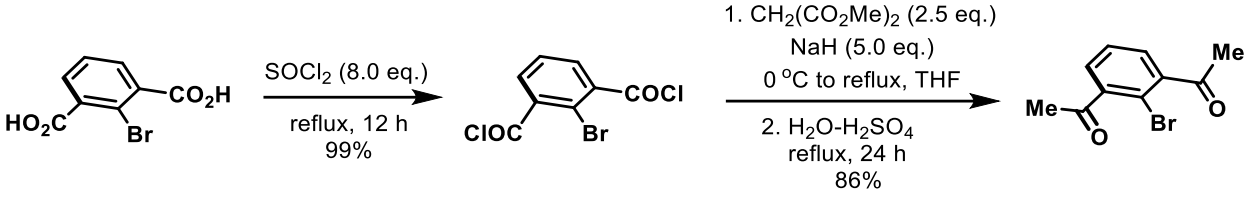

2,6-Diacetylbromobenzene was prepared by the literature method with modifications.[4]

Preparation of 2,6-bis(chlorocarbonyl)bromobenzene: 2-bromoisophtalic acid (12.7 g, 51.8 mmol) was suspended in 30 mL of thionyl chloride in a Schlenk flask equipped with a Teflon screw cap. The reaction mixture was heated to reflux for 12 h, during which the starting material completely dissolved. The reaction mixture was concentrated *in vacuo* and the residue was kept under high vacuum overnight. The 2,6-bis(chlorocarbonyl)bromobenzene was obtained as an off-white solid (14.5 g, 99%) and used for the next step without further purification.

Preparation of 2,6-diacetylbromobenzene: NaH (6.0 g, 248.3 mmol, 5.0 equiv.) and 50 mL dry THF were added to a 500 mL argon-filled three-necked flask equipped with a stirring bar, a dropping funnel and a reflux condenser. The mixture was cooled by an ice bath, and subsequently 100 mL THF solution of dimethyl malonate (16.4 g, 124.1 mmol, 2.5 equiv.) was added dropwise via the dropping funnel. After the addition, the mixture was heated to reflux and then a 60 mL THF solution of 2,6-diacetylbromobenzene (14.0 g, 49.7 mmol) was added dropwise. After 12 h of reflux, the reaction was quenched by slow addition of 100 mL 10% H_2SO_4. The reaction mixture was concentrated *in vacuo* and extracted with Et_2O. After removal of the solvent, the crude was refluxed for 24 h in a mixture of H_2O (22 mL), conc. H_2SO_4 (8.6 mL) and AcOH (40 mL). After this time, the reaction mixture was diluted with water and extracted with EtOAc twice. The combined organic layers were washed with brine, dried over K_2CO_3 and $NaSO_4$ and concentrated *in vacuo*. The residue was purified by column chromatography on silica gel (hexane/EtOAc, 4:1 to 2:1, *v*/*v*) to afford 10.3 g 2,6-diacetylbromobenzene as a pale yellow oil in 86% yield.

^{1}H NMR (400 MHz, $CDCl_3$): δ 7.46 – 7.37 (m, 3H), 2.62 (s, 6H).

^{13}C NMR (101 MHz, $CDCl_3$): δ 201.8, 143.9, 129.4, 128.0, 114.0, 30.8.

The spectral data matched with those reported in the literature.[4]

Ligand **S2**

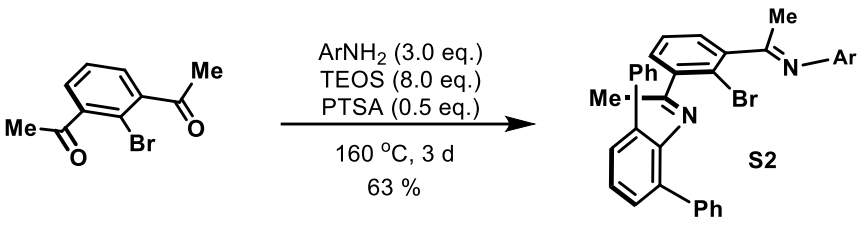

Ligand **S2** was prepared by the literature method with modifications.[5]

Procedure: a 50 mL pressure Schlenk fitted with a J-Young valve was charged with 2,6-diphenylaniline (4.00 g, 16.3 mmol, 3.0 equiv.) and *p*-toluenesulfonic acid monohydrate (PTSA, 0.52 g, 2.7 mmol, 0.5 equiv.). The Schlenk was evacuated and refilled with argon. 2,6-Diacetylbromobenzene (1.31 g, 5.4 mmol) and tetraethyl orthosilicate (TEOS, 9.7 mL, 8.0 equiv.) were added under argon. The reaction mixture was stirred at 160 °C for 3 days.

The reaction was quenched by addition of 20 mL NaOH (aq., 10%) and EtOH (15 mL) and SiO_2 crushed out. The mixture was stirred for additional 2 h and filtered through a pad of Celite. The pad was washed with a mixture of DCM and EtOAc, and the filtrate was concentrated *in vacuo*. The residue was dissolved in DCM and washed with H_2O. The organic layer was dried over anhydrous Na_2SO_4 and concentrated *in vacuo*. The residue was purified by column chromatography on silica gel (hexane/DCM, 4:1 to hexane/EtOAc, 15:1 to 10:1, *v*/*v*) to afford 2.38 g **S2** as a white crystalline solid in 63% yield.

^{1}H NMR (400 MHz, $CDCl_3$): δ 7.44 – 7.38 (m, 8H), 7.38 – 7.33 (m, 6H), 7.33 – 7.28 (m, 10H), 7.28 – 7.21 (m, 2H), 6.89 (t, *J* = 7.6 Hz, 1H), 6.24 (d, *J* = 7.6 Hz, 2H), 1.59 (s, 6H).

^{13}C NMR (101 MHz, $CDCl_3$): δ 169.7, 146.1, 143.8, 140.4, 132.7, 129.8, 129.7, 128.5, 128.3, 127.2, 126.9, 124.2, 116.3, 23.3.

M.p.: 213.4 – 214.8 °C.

HRMS (ESI): calc'd for $C_{46}H_{35}N_2BrNa^+$ $[M+Na]^+$ 717.18759; found 717.18860.

3. Synthesis and Characterization Data of Organobismuth Complexes

General note:

1. Carbons attached to Bi were observed by ^{13}C NMR. At room temperature these signals were generally broadened due to quadrupole relaxation effects of ^{209}Bi (100%, spin 9/2, quadrupole moment -0.4 x $10^{-28}m^{-2}$). At lower temperatures those ^{13}C signals were usually sharper.

2. The reducing agents (K-Selectride, and KC_8) for the preparation of the reported bismuthinidenes failed to give clean reduction of *N*,*C*,*N*-chelated-$BiCl_2$ **2** and **3**, complicating the purification.[1, 6] However, the reduction with Cp_2Co at room temperature gave NMR-pure **4** and **5**, which could be worked up by filtration and removal of solvents. The reduction reaction could be scaled up to gram-scale without noticeable decrease of yields. Bismuthinidenes **1** could be prepared in the same procedure.

3.1. Synthesis of *N*,*C*,*N*-Chelated-$BiCl_2$ (**2**)

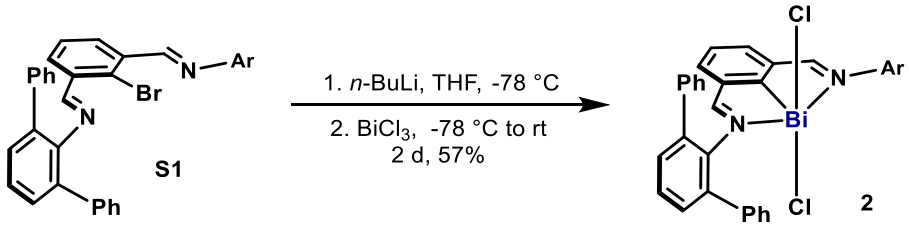

N,*C*,*N*-chelated-$BiCl_2$ (**2**) was prepared by the literature method with modifications.[7]

Procedure: To a dry ice/acetone-cooled solution of **S1** (2.34 g, 3.50 mmol) in dry THF (40 mL), *n*-BuLi (1.4 mL, 2.6 M in hexane, 3.68 mmol, 1.05 equiv.) was added dropwise under argon. The resulting dark red solution was stirred at this temperature for 4 h and then transferred via a cannula under argon to a precooled suspension of $BiCl_3$ (1.21 g, 3.85 mmol, 1.10 equiv.) in THF (20 mL) at -78 °C. The resulting dark brown mixture was stirred at room temperature for 2 days.

The work-up was carried out without the protection of argon. The reaction mixture was evaporated to dryness, re-dissolved in DCM and filtered through a Celite bed. The filtrate was concentrated *in vacuo* to ca. 20 mL and hexane was used for precipitation of the product. Filtration afforded *N*,*C*,*N*-chelated-$BiCl_2$ (**2**) as a bright yellow powder (1.99 g, 66%).

^{1}H NMR (400 MHz, $CDCl_3$): δ 9.19 (s, 2H), 7.54 – 7.45 (m, 10H), 7.42 (dd, *J* = 8.2, 6.7 Hz, 1H), 7.39 – 7.30 (m, 18H).

^{13}C NMR (101 MHz, $CDCl_3$): δ 226.2 (Bi-C), 177.2 (C=N), 146.7, 143.0, 138.9, 137.3, 136.7, 131.6, 130.3, 129.4, 128.5, 127.8, 127.2.

M.p.: 275 °C (dec.).

HRMS (ESI): calc'd for $C_{44}H_{31}N_2BiCl^+$ $[M\text{-}Cl]^+$ 831.19741; found 831.19741.

Single crystals suitable for X-ray crystallography were obtained by slow evaporation of a CH_2Cl_2 solution of **2** at room temperature.

3.2. Synthesis of *N*,*C*,*N*-Chelated-$BiCl_2$ (**3**)

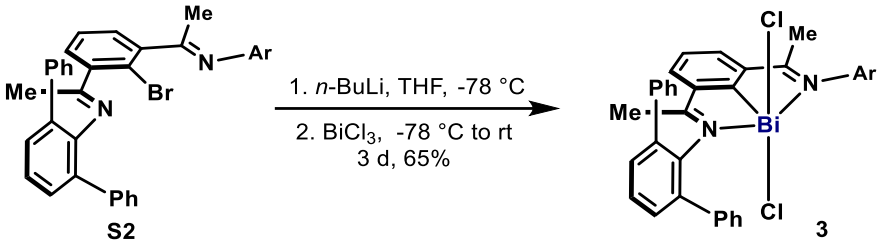

Procedure: to a dry ice/acetone-cooled solution of **S2** (1.50 g, 2.16 mmol) in dry THF (35 mL), *n*-BuLi (0.87 mL, 2.6 M in hexane, 2.26 mmol 1.05 equiv.) was added dropwise under argon. The resulting orange-red solution was stirred at this temperature for 5.5 h and then transferred via a cannula to a dry ice/acetone-cooled suspension of $BiCl_3$ (0.75 g, 2.37 mmol, 1.1 equiv.) in THF (15 mL). The resulting orange mixture was stirred at room temperature for 3 days.

The work-up was carried out without the protection of argon. The reaction mixture was evaporated to dryness, re-dissolved in CH_2Cl_2 and filtered through Celite bed. The filtrate was concentrated *in vacuo* to ca. 15 mL and hexane was used for precipitation of the product. Filtration and washing of the solid repeatedly with Et_2O afforded *N*,*C*,*N*-chelated-$BiCl_2$ (**3**) as a bright yellow powder (1.26 g, 65%).

Note: the procedure reported by Dostál[6] for the preparation of similar structures failed for this reaction because the excess amount of *n*-BuLi resulted in a severe *n*-butyl addition reaction to the imine site, which was confirmed by ESI-HRMS. Therefore, *n*-BuLi solution was titrated prior to use and the amount of *n*-BuLi used for lithiation was carefully controlled. Besides, hydrodebromonation byproduct crushed out from the mother liquor and was isolated in 14% yield.

^{1}H NMR (400 MHz, $CDCl_3$): δ 7.84 (d, *J* = 7.7 Hz, 2H), 7.51 – 7.41 (m, 9H), 7.37 (s, 6H), 7.32 – 7.23 (m, 12H), 1.91 (s, 6H).

^{13}C NMR (101 MHz, $CDCl_3$): δ 220.0 (Bi-C), 182.0 (C=N), 148.3, 140.9, 139.0, 136.5, 135.8, 131.1, 130.0, 129.2, 128.5, 127.8, 127.1, 22.5.

M.p.: 278 °C (dec.).

HRMS (ESI): calc'd for $C_{46}H_{35}N_2BiCl^+$ $[M\text{-}Cl]^+$ 859.22822; found 859.22882.

Single crystals suitable for X-ray crystallography were obtained by slow diffusion of *n*-pentane into a concentrated $CHCl_3$ solution of **3** at 0 °C overnight.

3.3. Synthesis of Bismuthinidene (**4**)

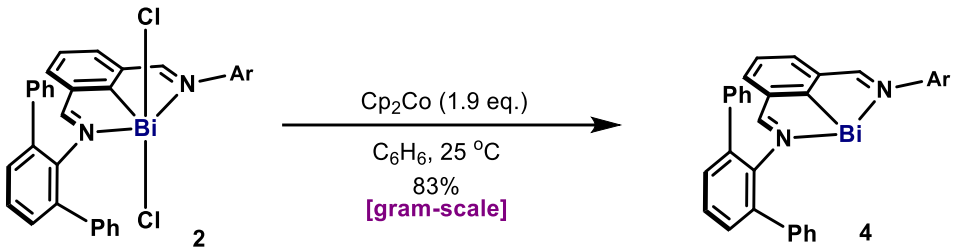

Procedure: in a glove box, **2** (1.50 g, 1.73 mmol) and benzene (anhydrous and degassed, 50 mL) were added to a 100 mL Schlenk flask. At room temperature, cobaltocene (0.62 g, 3.28 mmol, 1.9 equiv.) was added portionwise to this suspension under rapid stirring. The resulting dark purple mixture was stirred for an additional 2 h and the Schlenk flask was taken out of the glove box. Cobaltocenium chloride was filtered off under argon. The filtrate was frozen and benzene was removed by sublimation *in vacuo* to afford bismuthinidene (**4**) as a dark purple powder (1.14 g, 83%).

Characterization of **4**:

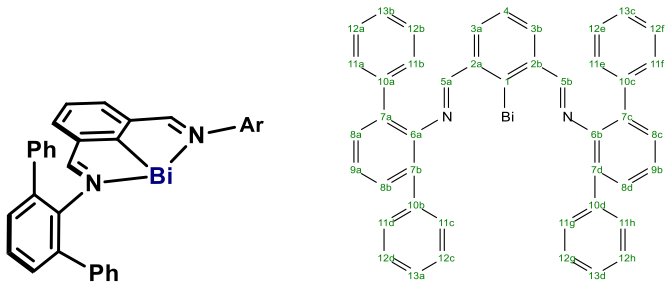

^{1}H NMR (500 MHz, THF-*d*$_8$): δ 9.18 (s, 2H, H-5), 7.65 (d, *J* = 7.4 Hz, 2H, H-3), 7.40 (d, *J* = 7.6 Hz, 4H, H-8), 7.27 (dd, *J* = 8.1, 7.2 Hz, 2H, H-9), 7.22 – 7.18 (m, 8H, H-11), 7.10 – 7.06 (m, 12H, H-12, H-13), 6.68 (t, *J* = 7.4 Hz, 1H, H-4).

^{13}C NMR (126 MHz, THF-*d*$_8$): δ 219.1 (C-1), 172.5 (C-5), 147.9 (C-6), 145.1 (C-2), 141.0 (C-10), 137.5 (C-7), 136.5 (C-3), 130.9 (C-11), 130.7 (C-8), 128.7 (C-12), 127.4 (C-13), 126.5 (C-9), 122.9 (C-4).

The protons and carbons are assigned according to HSQC and HMBC.

M.p.: 260.8 – 262.3 °C (dark oil).

HRMS (EI): calc'd for $C_{44}H_{31}N_2Bi^+$ $[M]^+$ 796.22915; found 796.22951.

Details of EI-MS measurement of Bi(I) (4 and 5)

For EI-MS analysis, the Bi(I) complexes were filled into a small crucible within the Schlenk tube under argon. The sample was then directly transferred into a direct insertion probe and then into the ion source, which was under vacuum. In the course of the experiment the probe

was heated up to a maximum of 400°C. At some temperatures the sample components sublimated in the vacuum and were directly ionized and measured.

For aldimine-based Bi(I) (**4**), a clear run was shown. However, there were partially decomposition compounds observed for ketimine-based Bi(I) (**5**). In both cases, the original molecular ions were found as the major peaks.

In an argon-filled Schlenk tube, single crystals suitable for X-ray crystallography were obtained by layer diffusion of *n*-pentane into a concentrated toluene solution of **4** at –35 °C overnight.

3.4. Synthesis of Bismuthinidene (**5**)

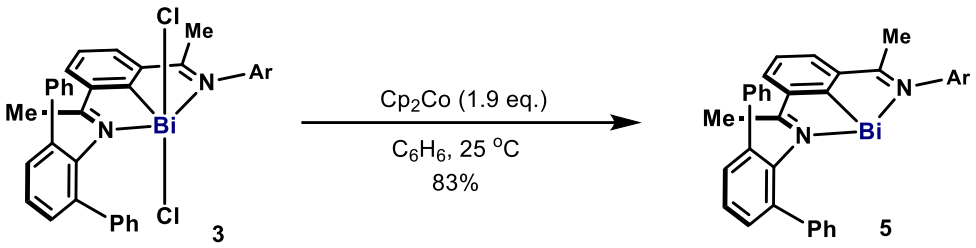

Procedure: in a glove box, **3** (421 mg, 0.47 mmol) and benzene (anhydrous and degassed, 20 mL) were added to a 100 mL Schlenk flask. At room temperature, cobaltocene (169 mg, 0.89 mmol, 1.9 equiv.) was added portionwise to this suspension under rapid stirring. The resulting dark red-purple mixture was stirred for 2 h and then the Schlenk flask was taken out of the glove box. Cobaltocenium chloride was filtered off under argon. The filtrate was frozen and benzene was removed by sublimation *in vacuo* to afford bismuthinidene (**5**) as a dark red-purple powder (322 mg, 83%).

Characterization of **5**:

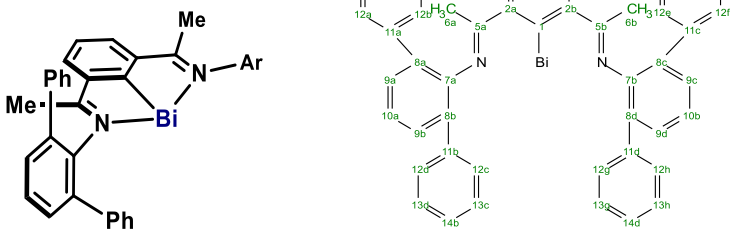

^{1}H NMR (400 MHz, THF-*d*$_8$): δ 7.87 (d, *J* = 7.6 Hz, 2H, H-3), 7.39 (d, *J* = 7.6 Hz, 4H, H-9), 7.27 (dd, *J* = 8.2, 7.0 Hz, 2H, H-10), 7.19 – 7.12 (m, 8H, H-12), 7.10 – 7.02 (m, 12H, H-13, H-14), 6.72 (t, *J* = 7.6 Hz, 1H, H-4), 2.71 (s, 6H, H-6).

^{13}C NMR (101 MHz, THF-*d*$_8$): δ 211.1 (C-1), 173.1 (C-5), 145.5 (C-2), 145.3 (C-7), 141.1 (C-11), 137.2 (C-8), 133.9 (C-3), 131.2 (C-12), 130.6 (C-9), 128.6 (C-13), 127.5 (C-14), 126.2 (C-10), 122.4 (C-4), 20.4 (C-6).

The protons and carbons are assigned according to HSQC and HMBC.

M.p.: 257.3 – 259.5 ^{o}C (dark oil).

HRMS (EI): calc'd for $C_{46}H_{35}N_2Bi^+$ $[M]^+$ 824.26044; found 824.26062.

In a glove box, single crystals suitable for X-ray crystallography were obtained by layer diffusion of *n*-pentane into a concentrated THF solution of **5** in a NMR tube for 4 days.

4. N_2O Oxidation of Bismuthinidenes

4.1. N_2O Oxidation of Bismuthinidene (**1**)

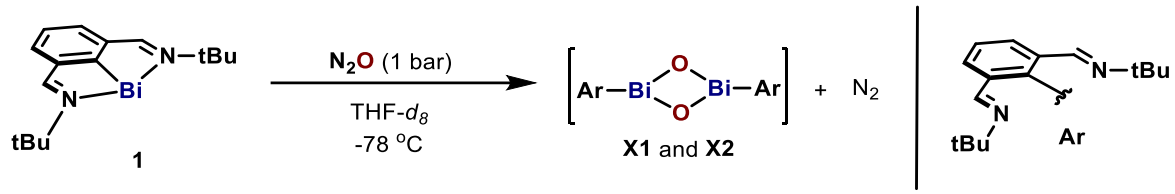

Procedure: in a glove box, bismuthinidene (**1**) (1.1 mg, 2.4 μmmol) and THF-d_8 (0.8 mL) were added to an oven-dried 10 mL pressure Schlenk tube fitted with a J-Young valve. The concentration of **1** is 3.0 μmol/mL. The Schlenk tube was taken out of the glove box and connected to a Schlenk line and a N_2O bottle via a three-way tubing system. The system was degassed by freeze-pump-thaw, backfilled with N_2O (1 bar) at –78 °C and stirred for about 45 min, during which the color of the solution changed gradually from green into pale yellow. The solution was immediately transferred into a J-Young NMR tube in the glove box. The J-Young NMR tube was cooled in dry ice prior to NMR study.

Summary of NMR, ESI-MS and GC-TCD studies of N_2O oxidation of bismuthinidene (**1**)**:**

- **Structures: X1** and **X2** contain intact ligand scaffolds and C–Bi bonds; **X1** has a symmetric structure while **X2** has an asymmetric structure; **X1** is in equilibrium with **X2** (**X1**/**X2** = 5:1); $[(LBiO)_2+H]^+$ was found in ESI-HRMS;
- **Stability: X1** and **X2** decomposed gradually at room temperature; the possible decomposition pathway is disproportionation to Bi_2O_3 and $(L_2Bi)_2O$;
- **N_2O activation:** N_2 formation was detected by GC-TCD (see GC Analysis of N_2 formation).

Based on above mentioned and the studies on dimeric bismuth oxide **6** (*vide infra*), **X1** and **X2** are postulated to be a *syn*- or an *anti*-dimeric bismuth oxide with dynamic imine coordination behavior. The low concentration of this stoichiometric reaction simulates the catalytic reaction condition, suggesting that dimeric bismuth oxide species might be involved in the catalytic reactions.

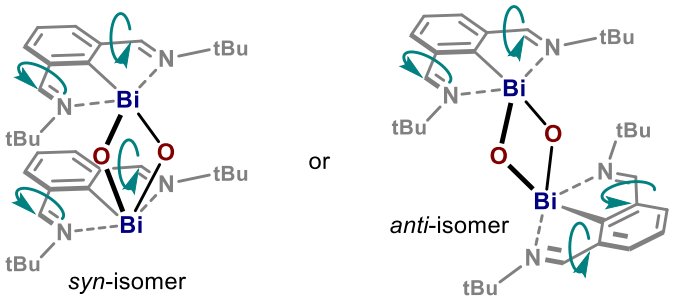

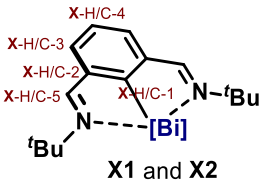

The peaks are named as ***X-H/C- position*** based on this numbering system.

$^1H/^{13}C$ chemical shifts and ROESY correlations:

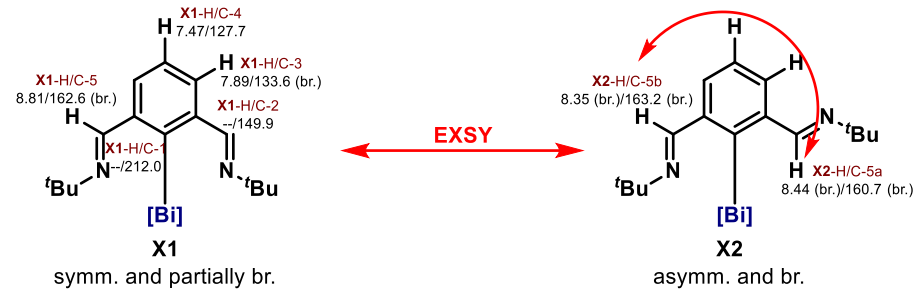

^{1}H NMR (THF-d_8, 600 MHz, –40 °C)

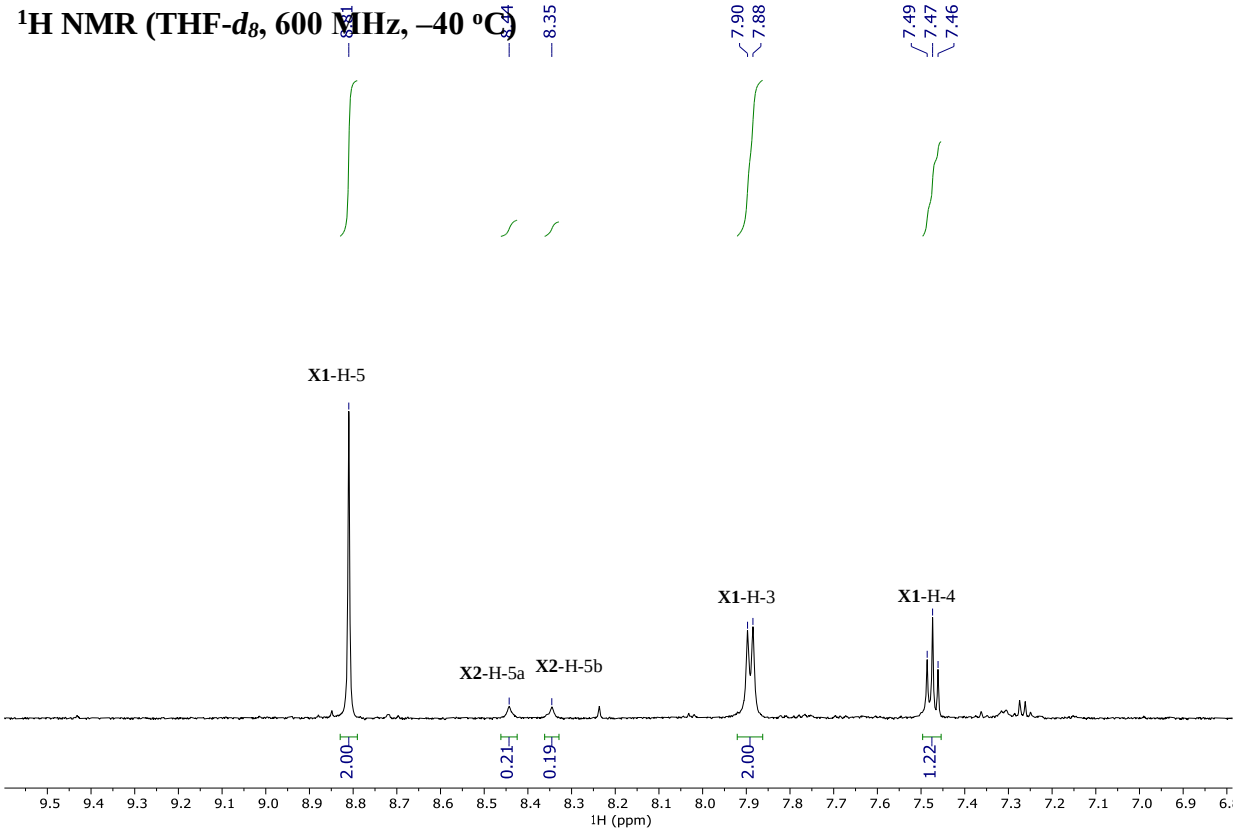

X1 has a symmetric structure while **X2** has an asymmetric structure.

^{13}C NMR (THF-d_8, 151 MHz, –40 °C)

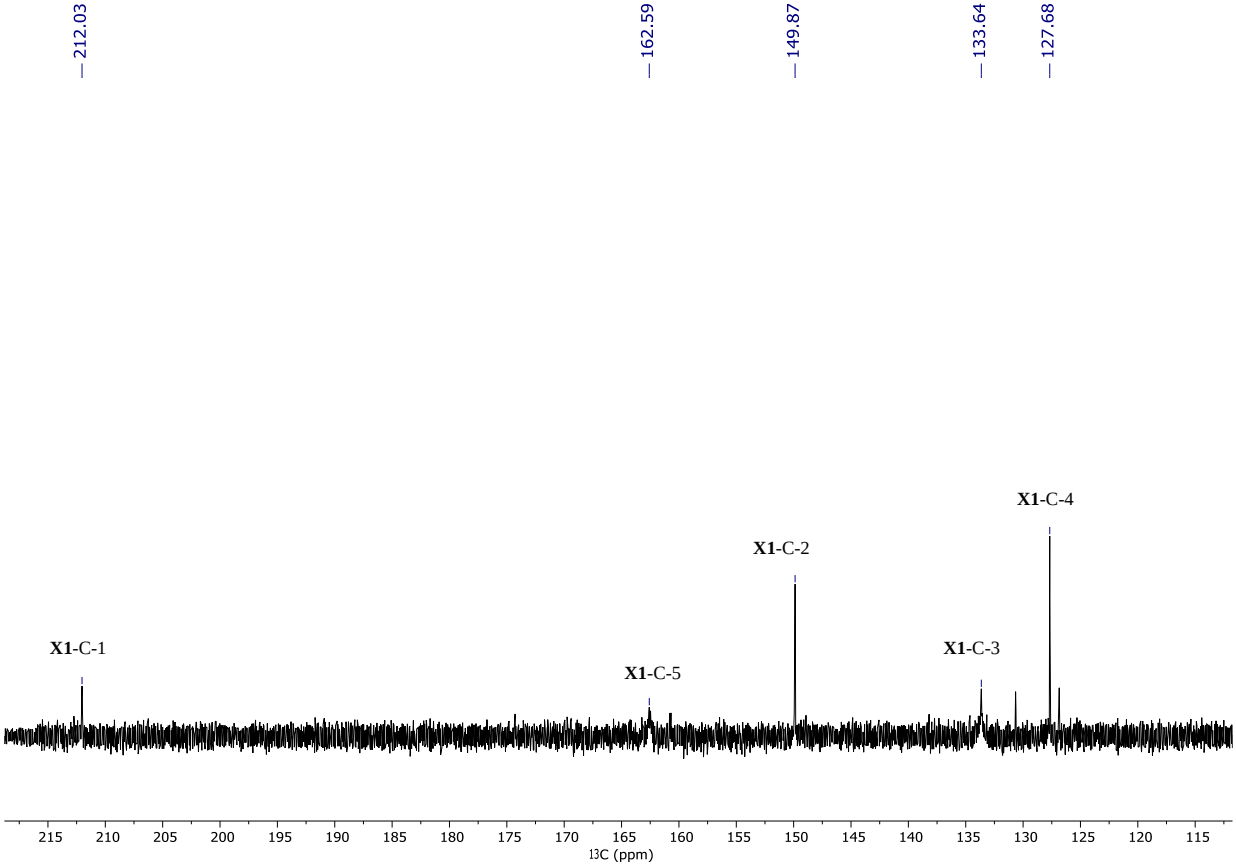

X1-C-3 and **X1**-C-5 are broadened because of the exchange of **X1** and **X2**. The carbons of **X2** are below are hidden within the noise.

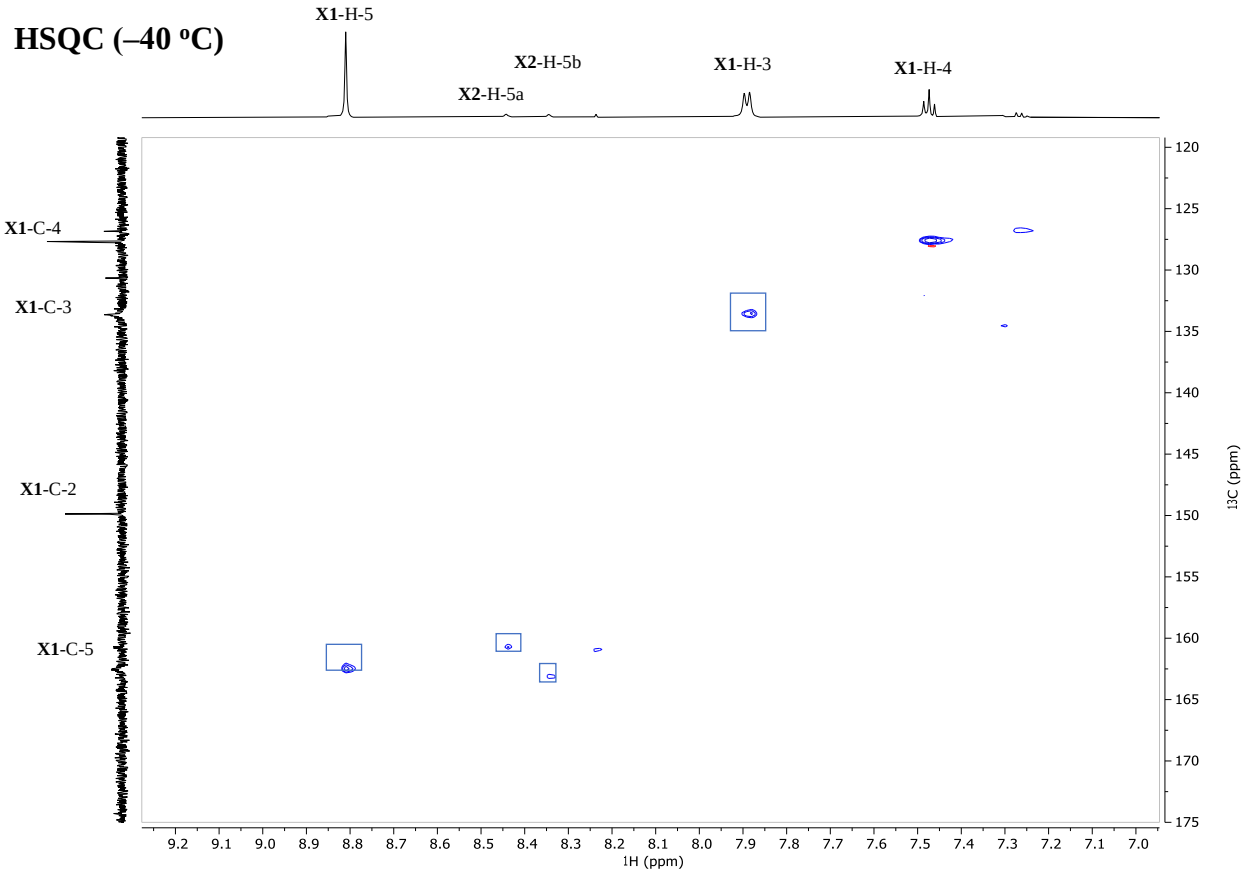

HSQC shows that **X1**-H-3 and **X1**-H-5 correlate to the broadened **X1**-C-3 and **X1**-C-5. The correlations between **X2**-H-5a/b and **X2**-C-5a/b (δ 160.7 and 163.2 ppm) can also be observed.

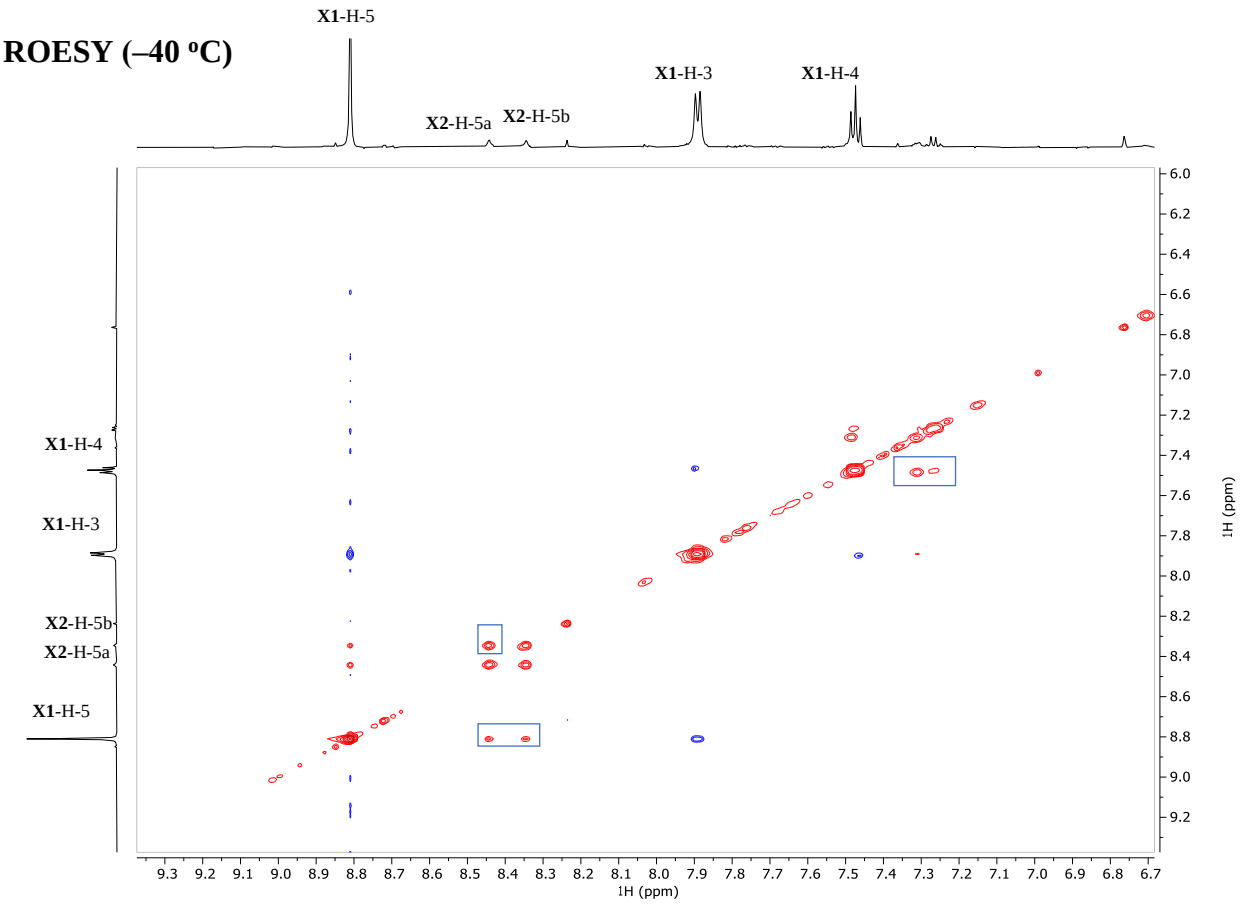

ROE signals are shown in blue (close to each other in space) while EXSY signals in red (chemical interconversions). An EXSY cross-peak identifies a signal that is converted into another signal by a process such as dissociation, coordination and rotation).

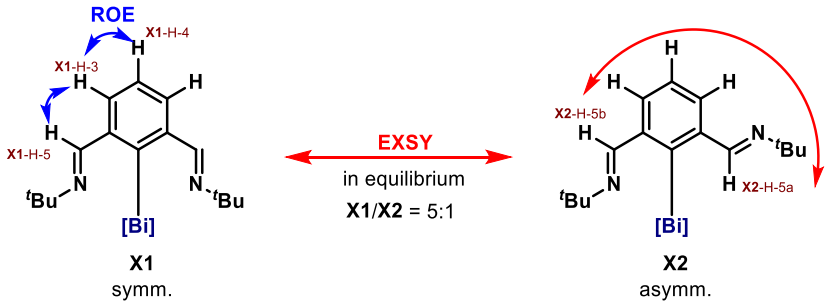

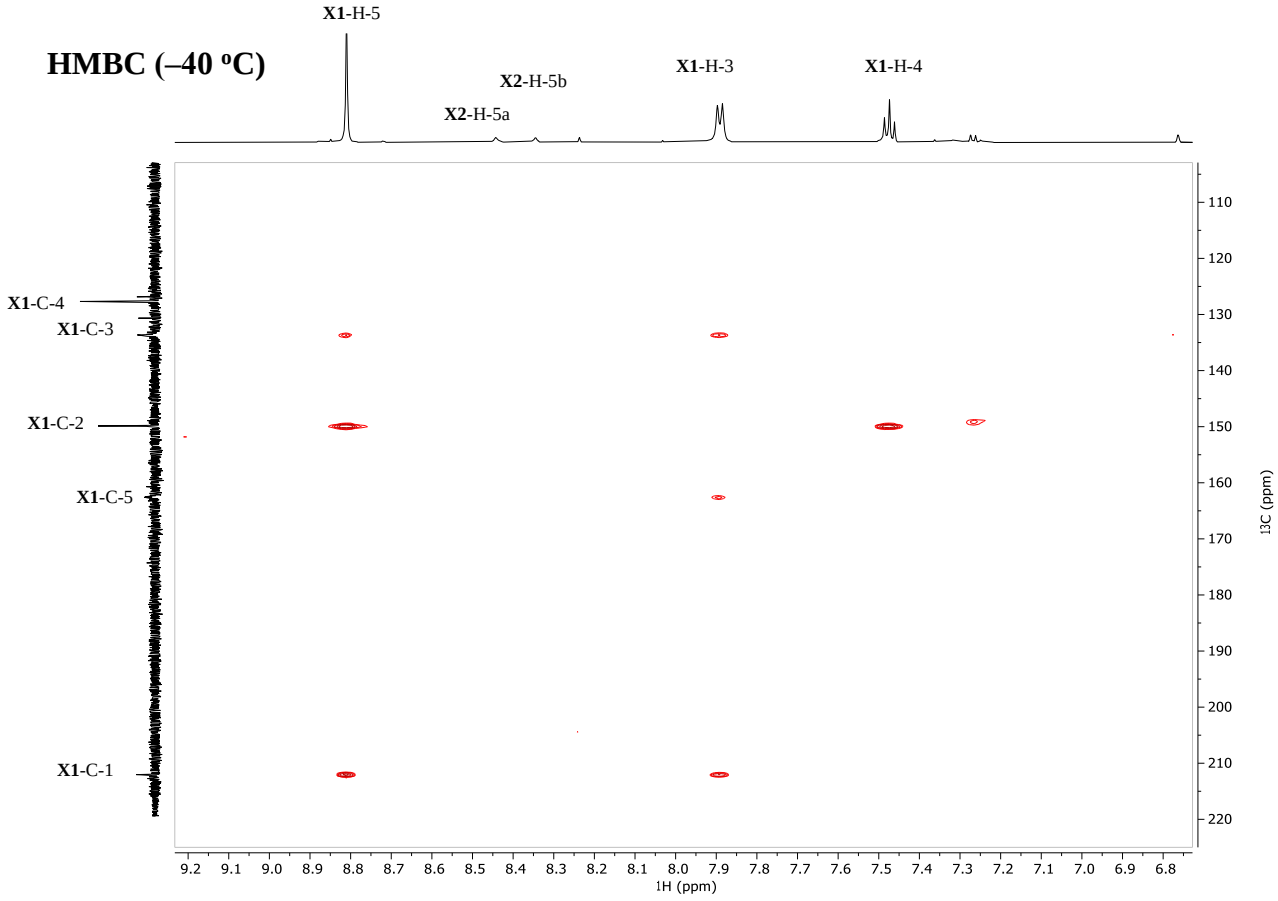
HMBC (–40 ºC)
X1-H-5
X2-H-5b
X2-H-5a
X1-H-3
X1-H-4
X1-C-4
X1-C-3
X1-C-2
X1-C-5
X1-C-1
110
120
130
140
150
160
170
180
190
200
210
220
13C (ppm)
9.2
9.1
9.0
8.9
8.8
8.7
8.6
8.5
8.4
8.3
8.2
8.1
8.0
7.9
7.8
7.7
7.6
7.5
7.4
7.3
7.2
7.1
7.0
6.9
6.8
1H (ppm)

^{1}H-NMR spectra at different temperatures (–40 °C to 25 °C)

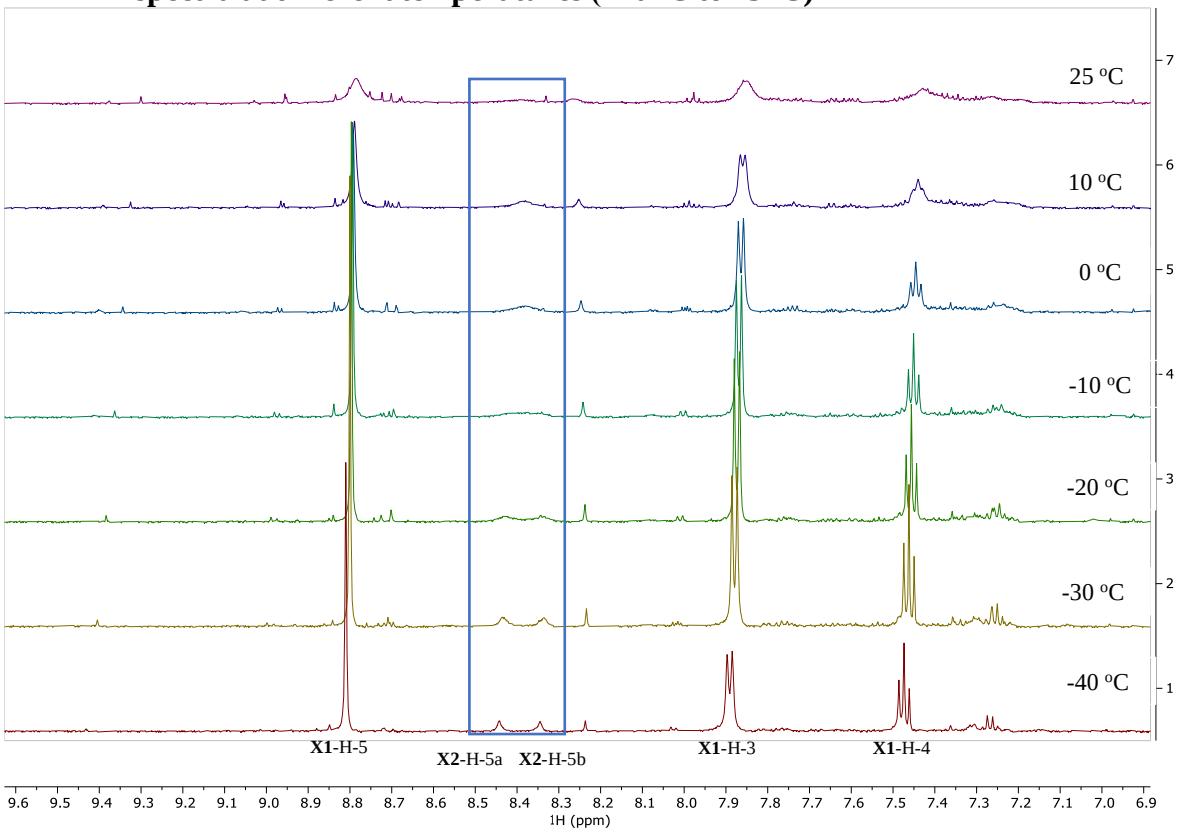

Variable temperature NMR data (–40 °C to 25 °C) shows that the signals of **X1** and **X2** are broadening with increasing temperatures. **X2**-H-5a and **X2**-H-5b are coalescent from approximately -10 °C.

The sample was stored at room temperature overnight and measured again. ^{1}H NMR (–40 °C) shows that **X1** and **X2** have fully decomposed.

MS studies:

After the reaction, ESI-MS experiments were performed immediately under argon and at low temperature. Characteristic ions found in ESI-MS are 469 $[ArBi=O+H]^+$ and 937 $[(ArBiO)_2+H]^+$. **HRMS (ESI)**: calc'd for $C_{32}H_{47}Bi_2N_4O_2^+$ $[(LBiO)_2+H]^+$ 937.33012; found 937.33070.

The result of ESI-MS supports that oxobismuth species might exist as dimeric forms in the solution.

ESI-MS was also performed for a long-stored reaction sample. The result shows that oxobismuth species were almost not detected, instead, the major peak was suggested to be $[L_2Bi]^+$. **HRMS (ESI)**: calc'd for $C_{32}H_{46}BiN_4^+$ $[L_2Bi]^+$ 695.35208; found 695.35243. And black precipitate was found on the bottom of the reaction tube. Based on these findings, it is suggested that one decomposition pathway could be ascribed to disproportionation.

Details of ESI-MS measurement of oxo-bismuth species:

All oxo-bismuth samples were stored in argon-filled Schlenk tubes and the procedures and results of the ESI-(HR)MS analysis were as follows:

For ESI-MS analysis, THF solutions of the mixture of oxo-bismuth compounds obtained from N_2O oxidation of Bi(I) (**1**) and Bi_2O_2 (**6**) and Bi-OH (**7**, in solid form), were diluted with anhydrous and degassed MeCN and quickly injected into ESI-source. After injection, the sample was surrounded by a N_2 flow supporting the formation of the spray, but exposure to air could not be completely discarded at this point. No chemical (e.g. protic solvents or acetic acid) was used to promote ionization. The decomposition of these compounds was not fast due to the reluctance of these oxo-bismuth species to react with O_2 or moisture (slow reaction) from the air. On the other hand, the very high sensitivity of the ESI-MS spectrometers in our institute ensures that a little part of intact target molecules in the solution is enough to give the high mass accuracy of the determined mass.

For Bi_2O_2 (**6**), the $[Bi_2O_2+H]^+$ peak was found but the major peak corresponds to $[Bi=O+H]^+$. This disaggregation process was also reported in previous literature (G. Strîmb, A. Pöllnitz, C. I. Raţ, C. Silvestru, *Dalton Trans.*, **2015**, *44*, 9927.). For Bi-OH (**7**), $[M+H]^+$ and $[M+CH_3]^+$ are the dominant peaks.

4.2. N_2O Oxidation of Bismuthinidene (**4**): the Formation of Dimeric Bismuth Oxide (**6**)

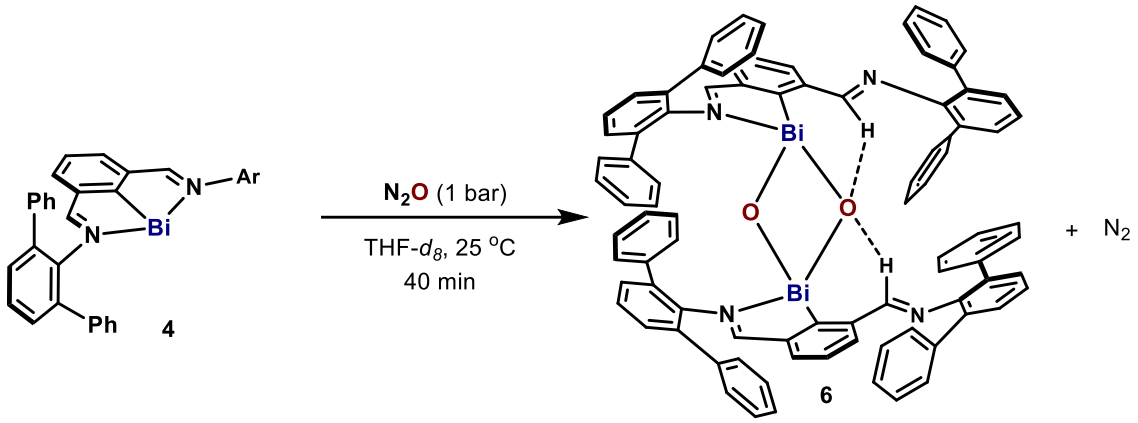

In a glove box, **4** (20.0 mg, 0.0251 mmol) and THF-d_8 (0.8 mL) were added to an oven-dried 10 mL pressure Schlenk tube fitted with a J-Young valve. The Schlenk tube was taken out of the glove box and connected to a Schlenk line and a N_2O bottle via a three-way tubing system. The system was degassed by freeze-pump-thaw, backfilled with N_2O (about 1 bar) and stirred at 25 °C for 40 min, during which slow formation of N_2 was observed and the color of the solution changed gradually from dark purple into pale yellow. The solution was transferred into a J-Young NMR tube in the glove box for the NMR study.

Characterization of **6**:

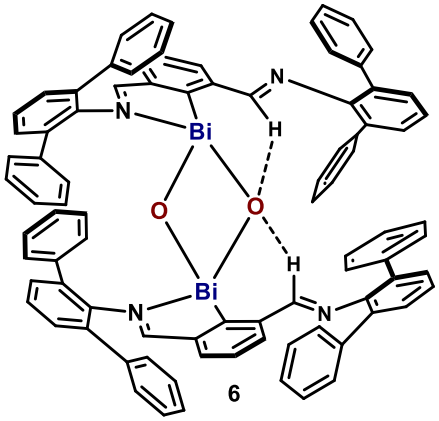

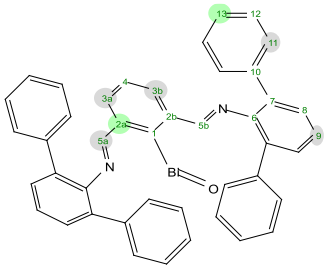

^{1}H NMR (400 MHz, THF-d_8, -50 °C): δ 10.04 (s, 2H, H-5b), 8.35 (dd, *J* = 7.1, 2.2 Hz, 2H), 8.25 – 8.15 (br. m, 2H), 8.11 (s, 2H, H-5a), 7.69 (d, *J* = 7.6 Hz, 4H), 7.58 – 7.35 (m, 20H), 7.32 – 7.25 (br. m, 4H), 7.17 (d, *J* = 7.6 Hz, 4H), 7.13 – 7.07 (br. m, 2H), 6.90 (t, *J* = 7.5 Hz, 4H), 6.83 (t, *J* = 7.8 Hz, 4H), 6.77 (t, *J* = 7.6 Hz, 2H), 6.64 (d, *J* = 7.6 Hz, 2H), 6.59 (t, *J* = 7.5 Hz, 2H), 6.48 (d, *J* = 7.9 Hz, 4H), 6.36 – 6.18 (br. m, 2H).

^{13}C NMR (101 MHz, THF-d_8, -50 °C): δ 211.8 (C-1), 176.1 (C-5a), 166.9 (C-5b), 150.2, 147.8, 147.1, 145.2, 142.0, 141.3, 141.0, 139.3, 137.7, 135.5, 135.3, 135.1, 134.1, 133.7, 132.6, 132.4

(br.), 131.5, 131.5 , 131.1 (br.), 130.8 (br.), 130.4 (br.), 130.2, 129.9 (br.), 129.7, 129.2 (br.), 128.6 (br.), 128.5 (br.), 128.3 (br.), 127.7 (br.), 127.6 (br.), 126.8 (br.), 126.4 (br.), 126.0 (br.).

^{1}H NMR (400 MHz, THF-*d*$_8$, 60 ^{o}C): δ 8.99 (s, 4H, H-5), 7.74 (d, *J* = 7.6 Hz, 4H, H-3), 7.32 – 7.20 (m, 18H, H-4, H-11), 7.11 – 6.98 (m, 36H, H-8, H-9, H-12, H-13).

^{13}C NMR (101 MHz, THF-*d*$_8$, 60 ^{o}C): δ 213.9 (C-1), 171.1 (C-5), 148.4 (C-2), 147.3 (C-6), 141.3 (C-10), 135.6 (C-3), 134.9 (C-7), 131.4 (C-11), 131.2 (C-8), 128.6 (C-12), 128.2 (C-4), 127.4 (C-13), 125.9 (C-9).

The protons and carbons are assigned according to HSQC and HMBC.

HRMS (ESI): calc'd for $C_{88}H_{63}Bi_2N_4O_2^+$ $[M+H]^+$ 1625.45532; found 1625.45673.

In an argon-filled Schlenk flask, single crystals suitable for X-ray crystallography were obtained by slow diffusion of *n*-pentane into a concentrated toluene solution of **6** at –78 ^{o}C (dry ice) for a 1 week.

Stability:

1. **6** is a moisture-sensitive compound. The imine moiety hydrolyzed gradually when trace amount of H_2O existed in the system. 2,6-Diphenylaniline was detected by ^{1}H NMR.

2. **6** partially decomposed when the solvent was removed. The sublimation of a C_6D_6 solution of **6** gave an off-white solid, which could not be fully re-dissolved in C_6D_6. ^{1}H NMR showed that decomposition occurred to certain degree in the solution phase.

^{1}H-NMR at different temperatures:

a. Decrease of the temperatures (25 ºC to –90 ºC)

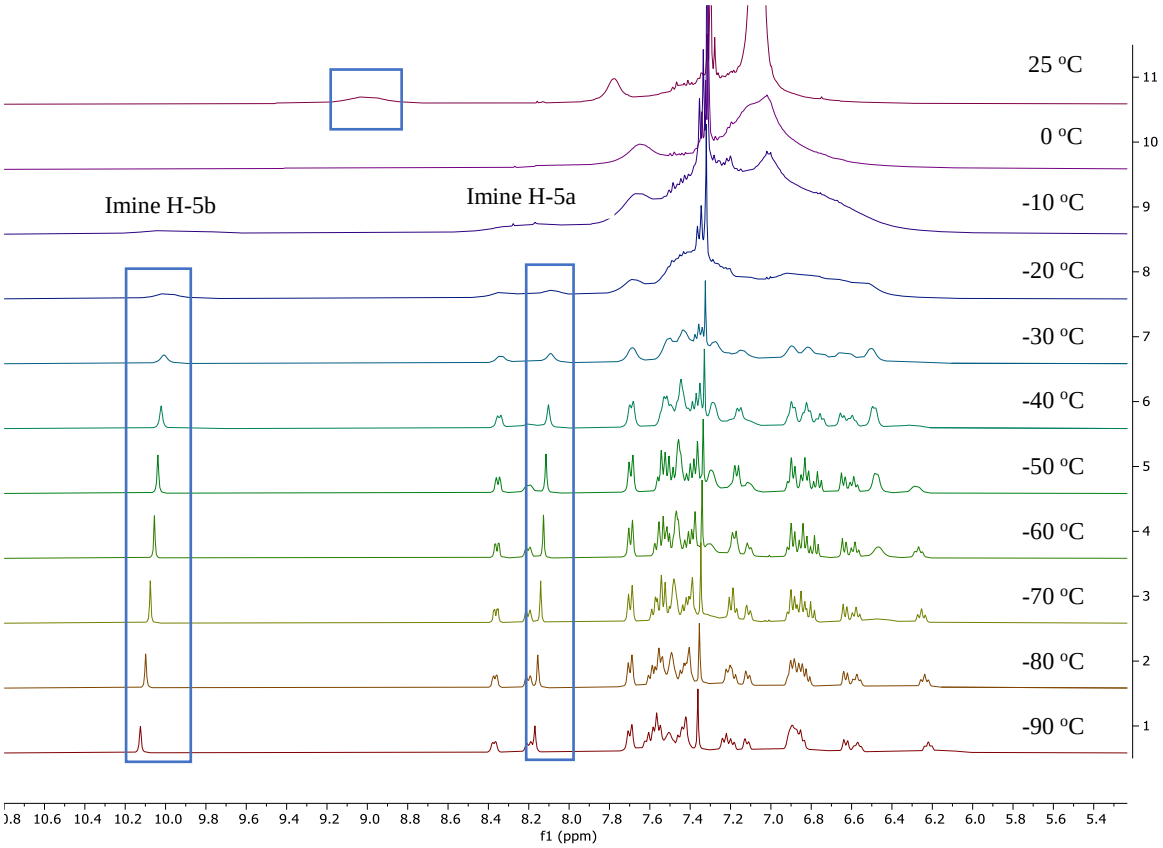

At 25 °C, all ^{1}H signals are very broad and two imine protons (H-5a and H-5b) are averaged (δ 9.01 ppm). ^{1}H signals are even more broadened at 0 ºC and gradually sharpen as temperature decreases.

The ^{1}H NMR at low temperature reveals an asymmetric structure where the two imine protons (H-5a and H-5b) have dramatically different chemical shifts (δ 8.11 and 10.04 ppm). In comparison to X-ray structure, very high chemical shift of H-5b can be explained by forming a hydrogen bond with one of the two oxo groups. Another imine group is weakly coordinated, and as a result H-5a has a normal chemical shift. The dynamic behavior can be explained by the switch of two imines and bond rotations of *m*-terphenyl groups.

Since most signals are sharp at –50 ºC, the ^{13}C NMR and 2D NMR are recorded at this temperature.

b. Increase of the temperatures (from 25 °C to 60 °C)

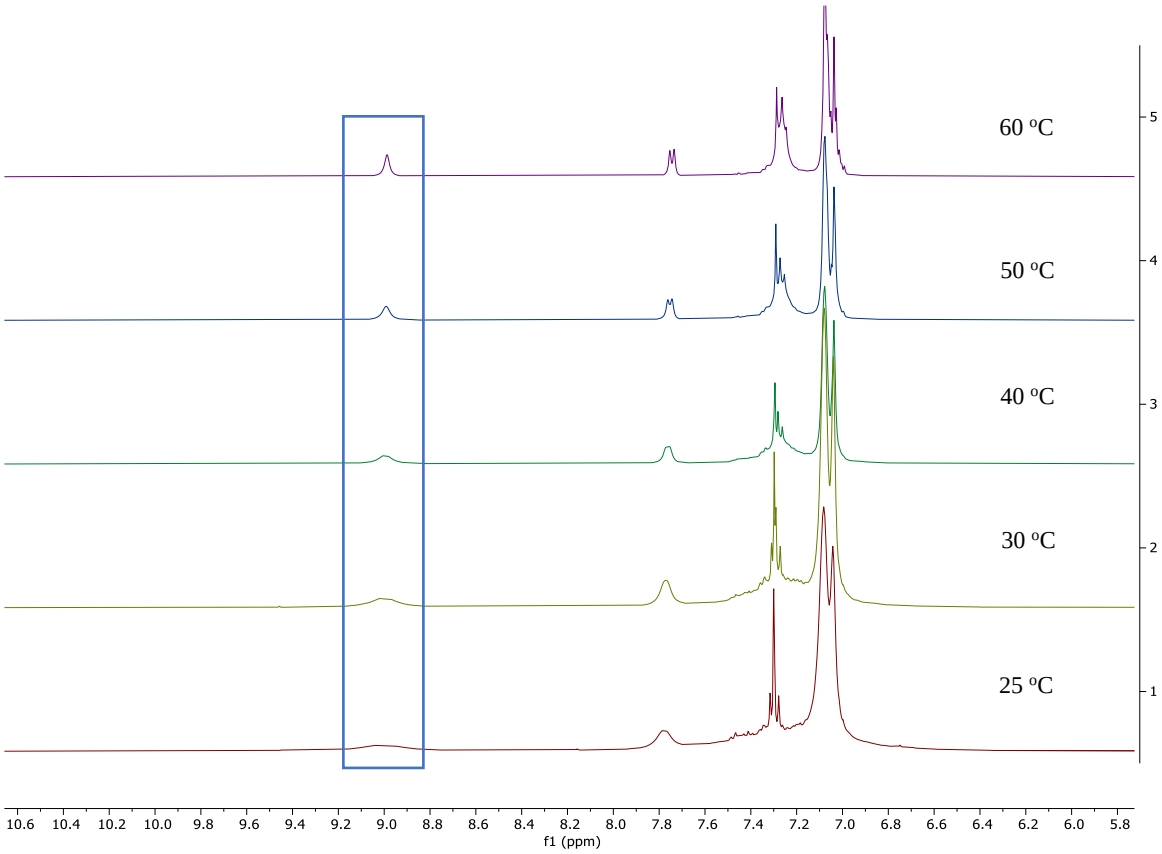

The proton signals also sharpen when the sample were gradually heated. Rapid switch of two imines and bond rotations of *m*-terphenyl groups leads to a simplified ^{1}H NMR at high temperature. The ^{13}C NMR and 2D NMR were also recorded at 60 °C.

HSQC (–50 ºC)

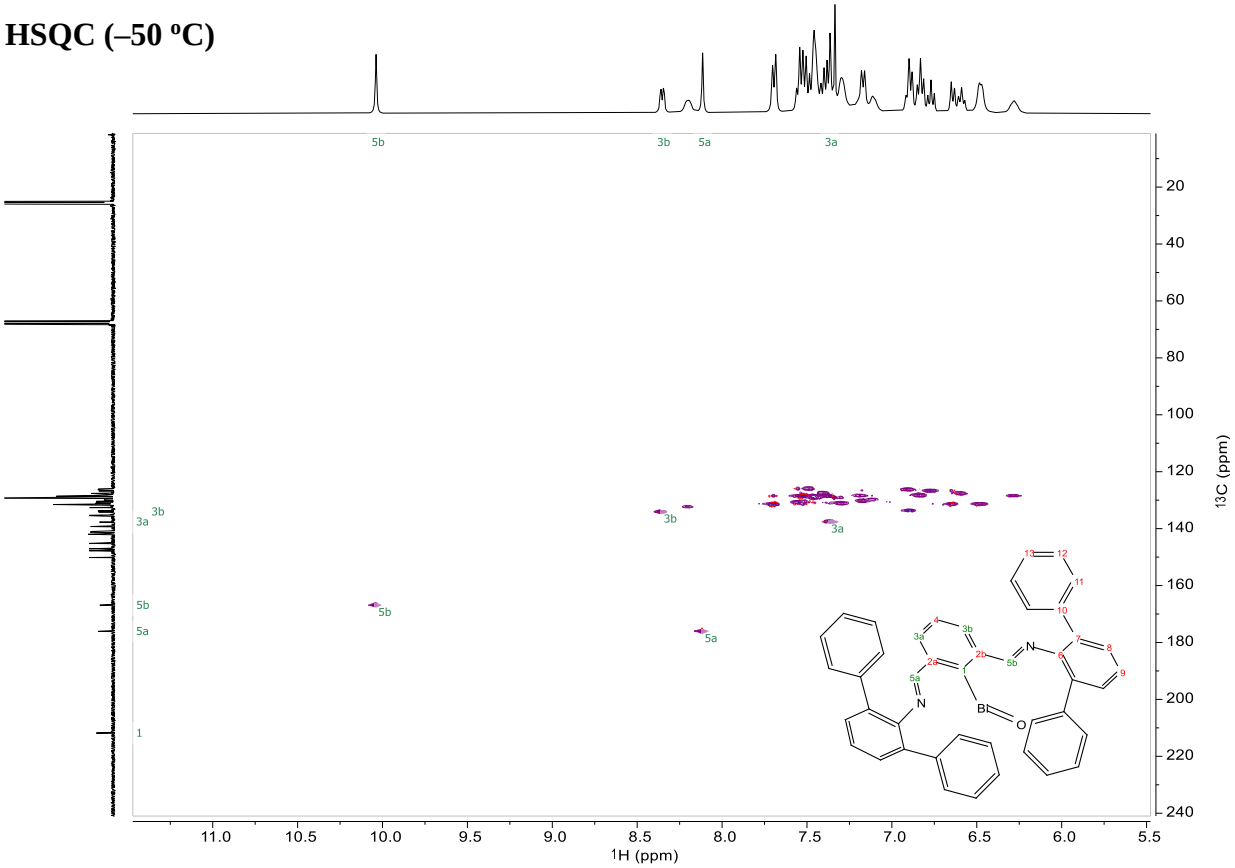

HSQC (–50 ºC) reveals that H-5a and H-5b (δ 8.11 and 10.04 ppm) are attached to C-5a and C-5b (δ 176.1, 166.9). The imine C-5b is distinctly de-shielded because of the hydrogen bonding.

HMBC (–50 ºC)

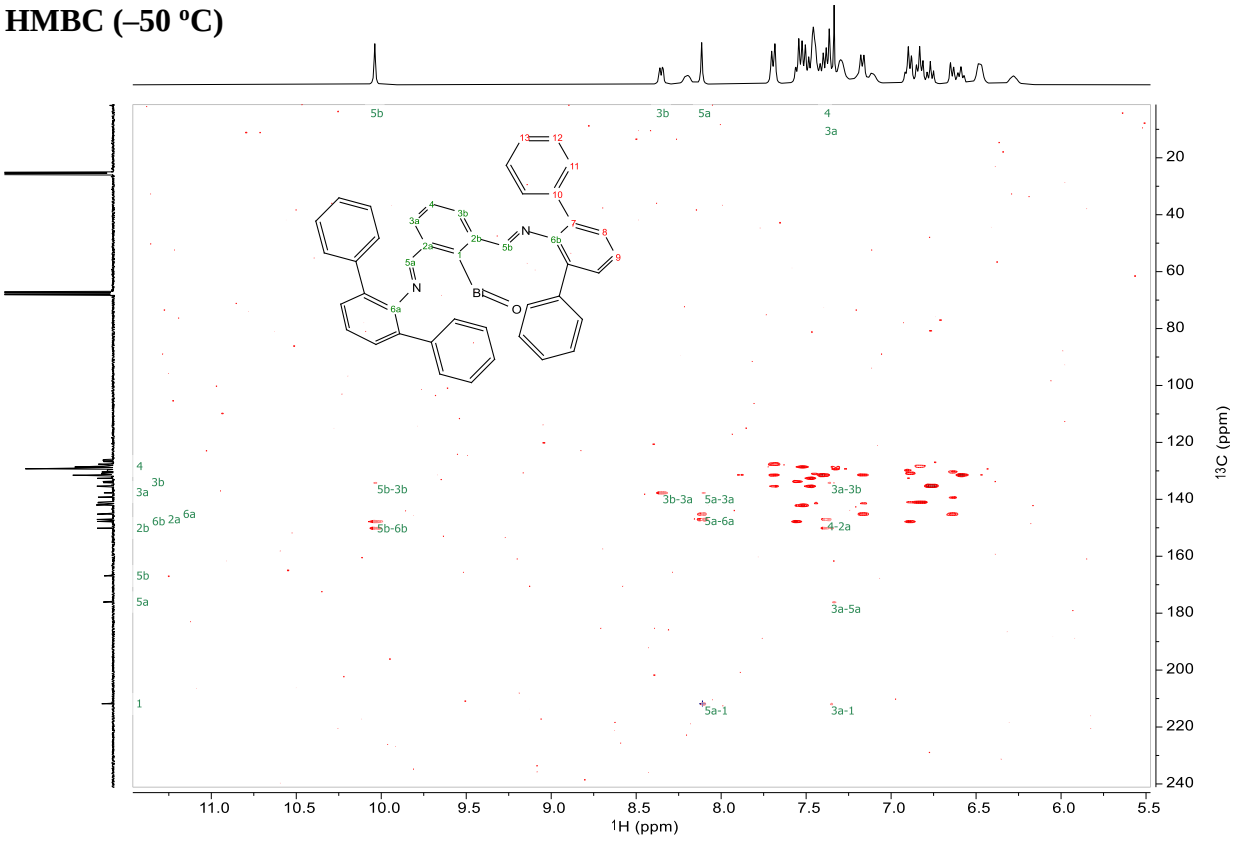

In the 2D-HMBC spectrum at –50 ºC a cross peak between H-5a and C-1 (C-Bi, δ 211.8 ppm) is observed, while the correlation between H-5b and C-1 cannot be observed. In the X-ray structure, C-5b imine points away from the oxo group.

ROESY (–50 ºC)

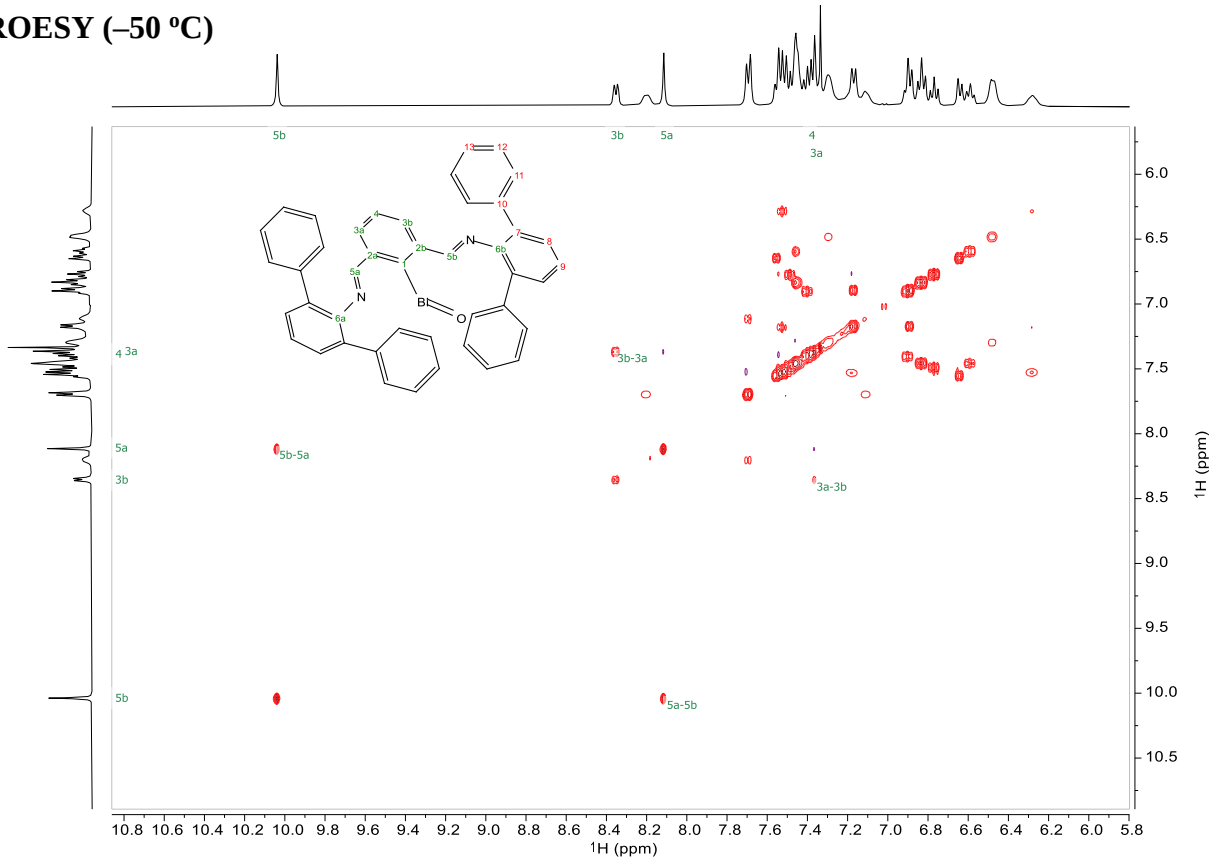

Overall, the ROESY NMR data (–50 ºC) reveals a dynamic structure of **4**. Particularly, an chemical exchange cross peak (EXSY peak) is observed between the two imine protons as well between the meta-H of the central Ar-Bi ring, indicating that they are in exchange even at –50 ºC.

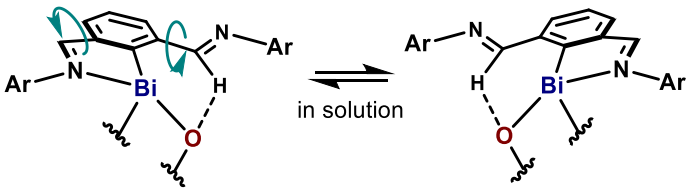

DOSY (Diffusion-Ordered NMR Spectroscopy) Experiments:

Diffusion coefficients were obtained from a double stimulated echo sequence with bipolar gradient pulses, convection compensation, longitudinal eddy current delay (LED) and three spoiler gradients (Bruker sequence: dstebpgp3s). The gradient pulse strength G was incremented from 5% to 98% of the maximum G_{max} with a linear gradient ramp in 64 steps. For measurements temperatures above 233 K, the diffusion time (Δ) used was 75 ms and the length of a gradient pulse gradient pulse (δ/2) of the encoding gradient was 1.3 ms. For lower temperatures <= 233K a diffusion time Δ = 200 ms was used. The maximum gradient strength G_{max} of the NMR probe (PA BBO 400S1 BBF-H-D-05 Z PLUS) was 53.5 G·cm^{-1}. Diffusion coefficients were obtained by averaging three diffusion coefficients obtained from fitting the signal decay of three different resonance integrals to the Stejskal-Tanner equation (1) in the Bruker TOPSPIN T1T2 relaxation module.

$$I(G) = I_0 e^{-D(\gamma G\delta)^2(\Delta-\delta/3)} \quad (1)$$

Diffusion values were predicted with an EXCEL spreadsheet using the Stokes−Einstein Gierer-Wirtz Estimation (SEGWE) method.[8]

In order to test the SEGWE method, the diffusion coefficients of bismuthinidene **4** were determined at different temperatures and compared to the predicted diffusion coefficients in toluene-d_8 (see Table S1). Overall, the predictions were underestimating the experimental diffusion values, but all the results were within 10% of the experimental value.

When a ~50:50 mixture of **4** and mono-organobismuth oxide **6** was analyzed, which was prepared by partial conversion of **4** with N_2O, the measured diffusion coefficient of **4** at 223 K still fits the predicted values for a monomeric species quite well. In contrast to this, the experimental value values for **6** at 223 K [(1.02 ± 0.02) × 10^{-10} m^2/s] were not matching the prediction for a monomeric species **6** (1.39 × 10^{-10} m^2/s) but the dimeric species (1.02 ×10^{-10} m^2/s). This is in very good agreement with the obtained X-ray structure and supports that organobismuth oxide **6** is a dimer in solution.

When the mixture of **4** and **6** were fully converted to **6,** the measured diffusion coefficients for **6** still agree with the results from the mixture.

Table S1: Overview over all the diffusion experiments

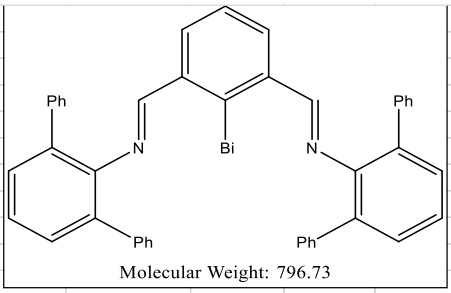

Molecular Weight: 796.73

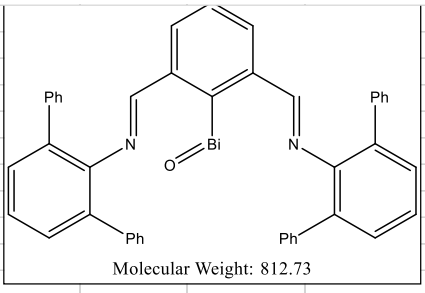

Molecular Weight: 812.73

		Dimer					Dimer				
	MW:	1593.46	g mol-1			MW:	1625.46	g mol-1			
		Monomer					Monomer				
	MW:	796.73	g mol-1			MW:	812.73	g mol-1			
		Temp	**D_{pred} (m^2/s)**		**D_{exp}**					$\frac{D_{exp}-D_{pred}}{D_{pred}}$
					D1	**D2**	**D3**	average	Stdev	
4		298K	6.46E-10	± 1.9E-10	6.92E-10	7.14E-10	6.81E-10	6.96E-10	0.17E-10	7.69%
		273 K	4.22E-10	± 1.2E-10	4.62E-10	4.58E-10	4.50E-10	4.57E-10	0.06E-10	8.14%
		233 K	1.80E-10	± 5.2E-11	1.91E-10	1.93E-10	1.89E-10	1.91E-10	0.02E-10	5.77%
		223 K	1.40E-10	± 4.1E-11	1.40E-10	1.41E-10	1.47E-10	1.43E-10	0.04E-10	2.19%
Mixture of 4 and 6	SM - Monomer	223	1.40E-10	± 4.1E-11	1.40E-10	1.35E-10		1.38E-10	0.04E-10	-1.50%
	SM - Dimer		1.03E-10	± 3.0E-11	1.4E-10	1.35E-10		1.38E-10	0.04E-10	34.10%
	Produkt - Monomer		1.39E-10	± 4.0E-11	1.01E-10	1.02E-10	1.04E-10	1.02E-10	0.02E-10	-26.23%
	Produkt - Dimer		1.02E-10	± 3.0E-11	1.01E-10	1.02E-10	1.043E-10	1.02E-10	0.02E-10	0.39%
	SM - Monomer	233	1.80E-10	± 5.2E-11	1.92E-10	1.83E-10		1.872E-10	0.06E-10	3.69%
	SM - Dimer		1.33E-10	± 3.8E-11	1.92E-10	1.83E-10		1.8715E-10	0.06E-10	41.17%
	Produkt - Monomer		1.79E-10	± 5.2E-11	1.35E-10	1.44E-10	1.44E-10	1.410E-10	0.05E-10	-21.17%
	Produkt - Dimer		1.31E-10	± 3.8E-11	1.35E-10	1.44E-10	1.438E-10	1.41E-10	0.05E-10	7.28%
6 (fully converted from the mixture of 4 and 6)	Produkt - Monomer	233	1.79E-10	± 5.2E-11	1.40E-10	1.44E-10	1.43E-10	1.41E-10	0.02E-10	-21.17%
	Produkt - Dimer		1.31E-10	± 3.8E-11	1.4E-10	1.44E-10	1.426E-10	1.41E-10	0.02E-10	7.28%

NMR Monitoring:

NMR monitoring was performed for a toluene-d_8 solution of **4** in a N_2O-filled J-Young NMR tube, however, the reaction proceeded very slowly in the NMR tube while standing still. The reaction was accelerated by gently shaking the NMR tube. After each shake, a ^1H NMR spectrum was recorded. According to NMR monitoring, no intermediate (proposed monomeric oxobismuth species) was detected, which indicated the dimerization after N_2O oxidation is a fast process.

4.3. N_2O Oxidation of Bismuthinidene (**5**): the Formation of Bismuth Hydroxide (**7**)

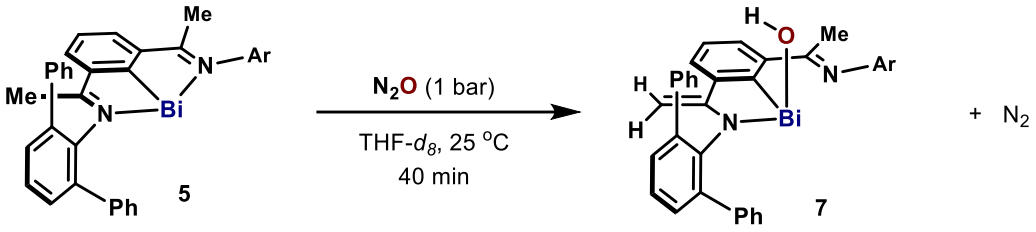

NMR study: in a glove box, bismuthinidene (**5**) (20.0 mg, 0.0238 mmol) and THF-d_8 (0.8 mL) were added to an oven-dried 10 mL pressure Schlenk tube fitted with a J-Young valve. The Schlenk tube was taken out of the glove box and connected to a Schlenk line and a N_2O bottle via a three-way tubing system. The system was degassed by freeze-pump-thaw, backfilled with N_2O (1 bar) and stirred at 25 °C for 40 min, during which slow formation of N_2 was observed and the color of the solution changed gradually from dark purple-red into orange-red. The solution was transferred into a J-Young NMR tube in the glove box for the NMR study.

Preparative reaction: in a glove box, bismuthinidene (**5**) (150 mg, 0.182 mmol) and dry THF (7 mL) were added to an oven-dried 100 mL pressure Schlenk flask fitted with a J-Young valve. The Schlenk flask was taken out of the glove box and connected to a Schlenk line and a N_2O bottle via a three-way tubing system. The system was degassed by freeze-pump-thaw, backfilled with N_2O (1 bar). The reaction mixture was stirred at 25 °C for 45 min until a clear orange-red solution formed. After the removal of THF *in vacuo*, the crude product was washed with dry *n*-pentane on a fritted glass filter under argon and dried under high vacuum, giving bismuth hydroxide (**7**) as an orange-yellow powder (142 mg, 93%).

Characterization of **7**:

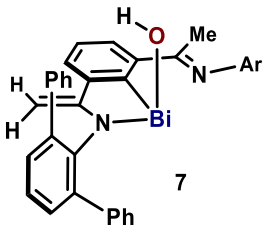

7

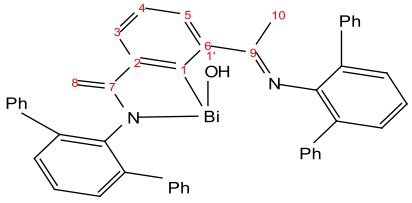

^{1}H NMR (400 MHz, THF-*d*$_8$): δ 7.82 (dd, *J* = 8.2, 0.8 Hz, 1H, H-3), 7.71 – 7.63 (m, 5H), 7.42 – 7.03 (m, 23H), 4.14 (s, 1H, H-8trans), 3.27 (s, 1H, H-8cis), 1.86 (s, 3H, H-10), 0.92 (s, 1H, H-1).

^{13}C NMR (101 MHz, THF-*d*$_8$): δ 195.0 (C-1), 173.9 (C-9), 164.0 (C-7), 153.1 (C-2), 147.2, 144.5 (C-6), 144.3, 143.2, 142.8, 142.5, 141.2, 141.0, 140.8, 135.7, 135.4, 131.8 (C-3), 131.6, 131.3, 131.1, 130.9, 130.5, 130.3, 130.1, 129.6, 129.2, 129.0, 128.8, 128.7 (C-4), 128.7, 128.4, 127.7, 127.5, 127.1, 126.2, 124.7, 84.8 (C-8), 19.3 (C-10).

HRMS (ESI): calc'd for $C_{46}H_{36}BiN_2O^+$ $[M+H]^+$ 841.26260; found 841.26360.

M.p.: 229 ^{o}C (dec.).

Stability: the titled compound is stable in the solid state in the glove box for at least two months, however, it reacts slowly with H_2O to give white amorphous precipitate. Therefore, the solvents used for single crystal growth were anhydrous.

In the glove box, single crystals suitable for X-ray crystallography were obtained by layer diffusion of *n*-hexane into a concentrated THF solution of **7** in a NMR tube for a week.

^{1}H-^{1}H COSY

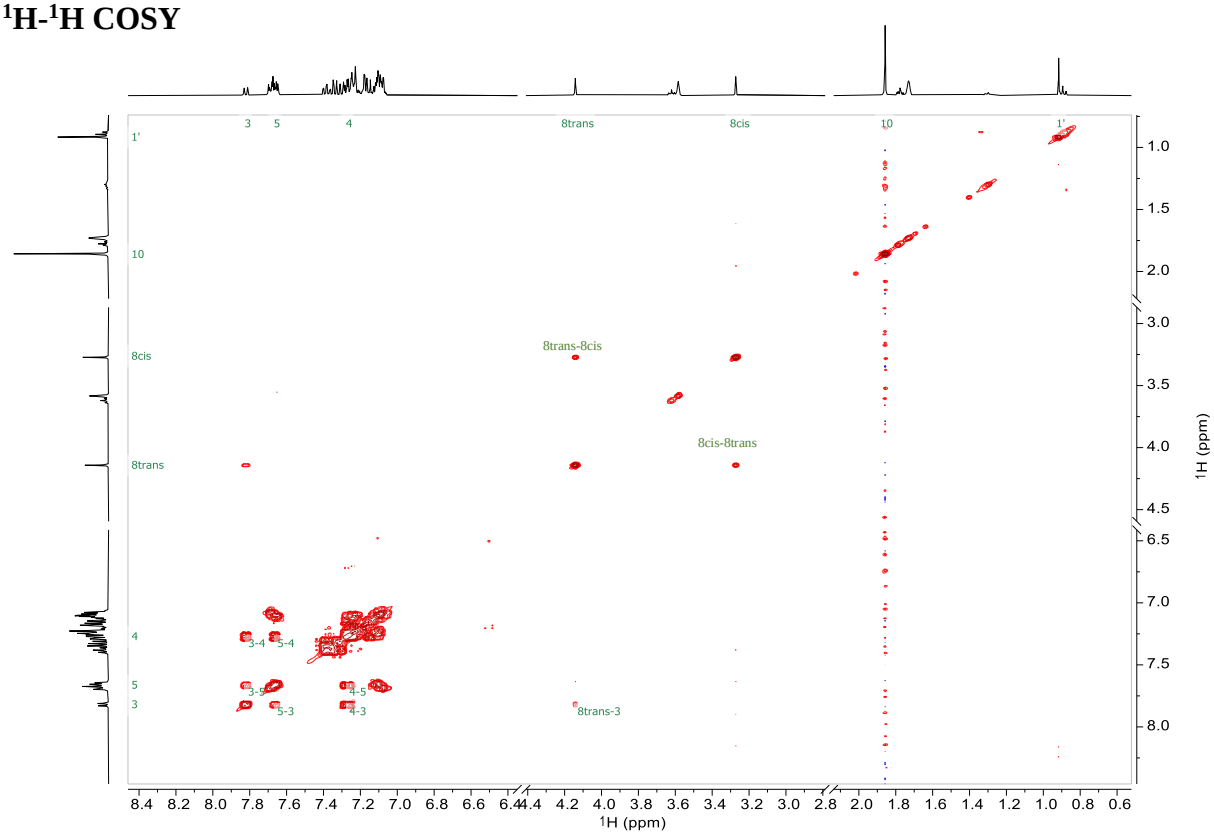

The coupling between H-8cis/trans is observed in ^{1}H-^{1}H COSY, although this germinal coupling is too weak to be observed in ^{1}H NMR.

Edited-HSQC

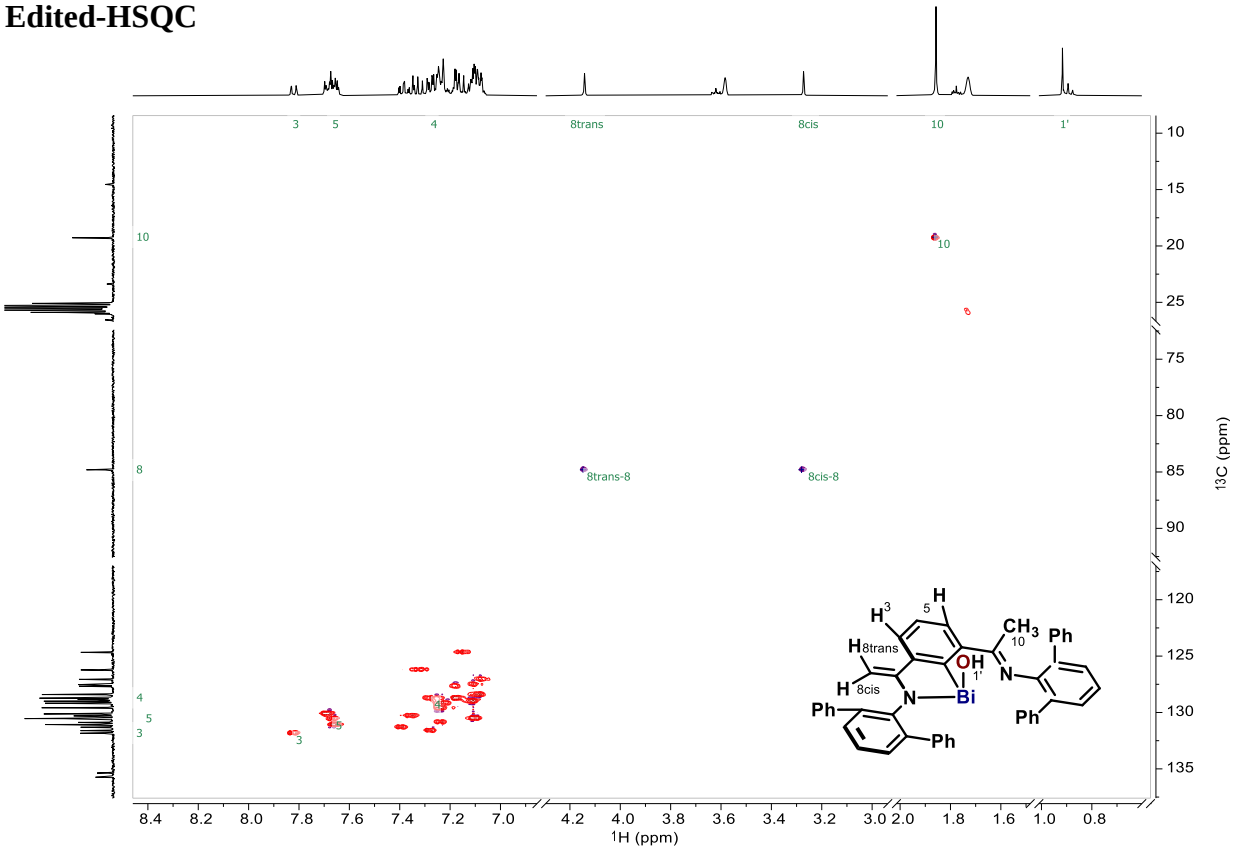

The DEPT135-edited-HSQC shows that H-8$_{cis}$ and H8$_{trans}$ are attached to the same carbon C-8 as indicated by the opposite phase of the signals compared to all other carbons in the molecule while H-10s belong to CH_3. H-1' (OH) has no correlation with any carbon.

HMBC

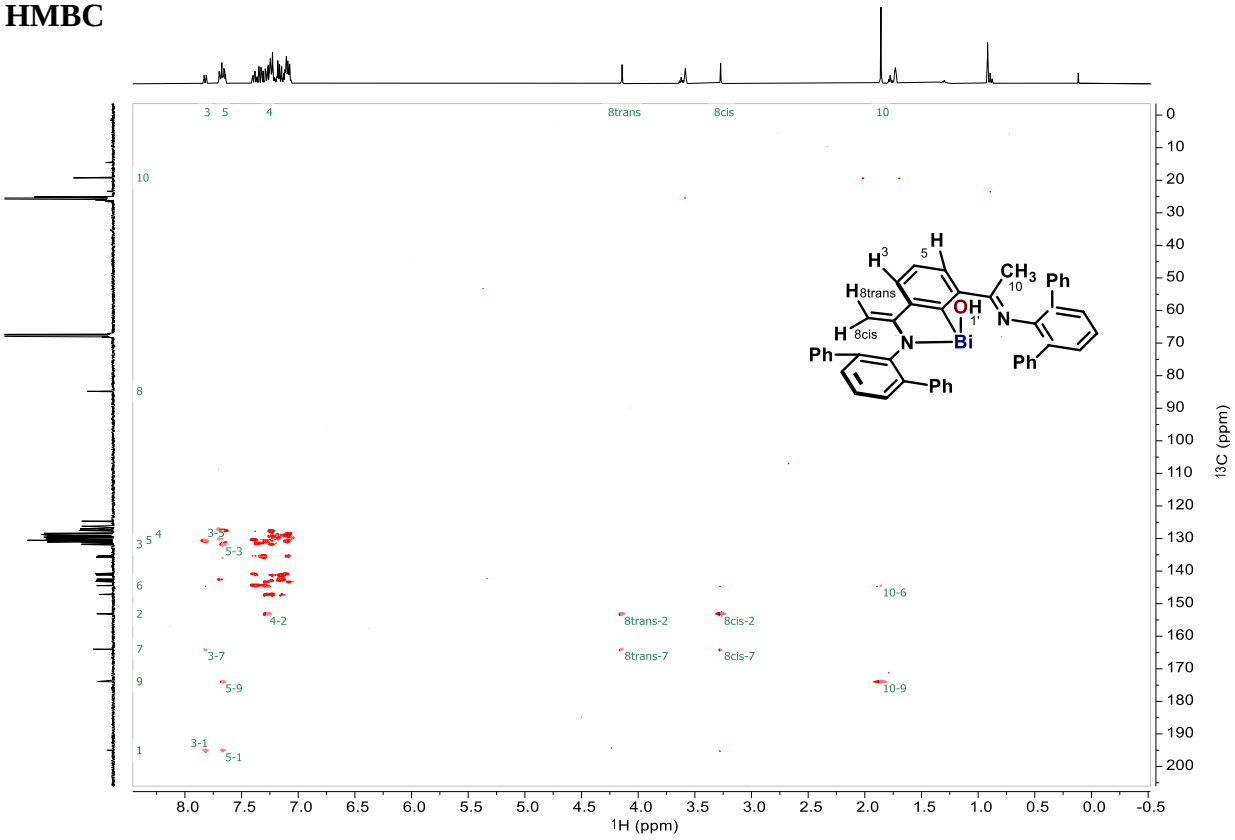

HMBC further confirms the nature of CH_2 (attaching to enamine) and CH_3 (attaching to imine).

ROESY

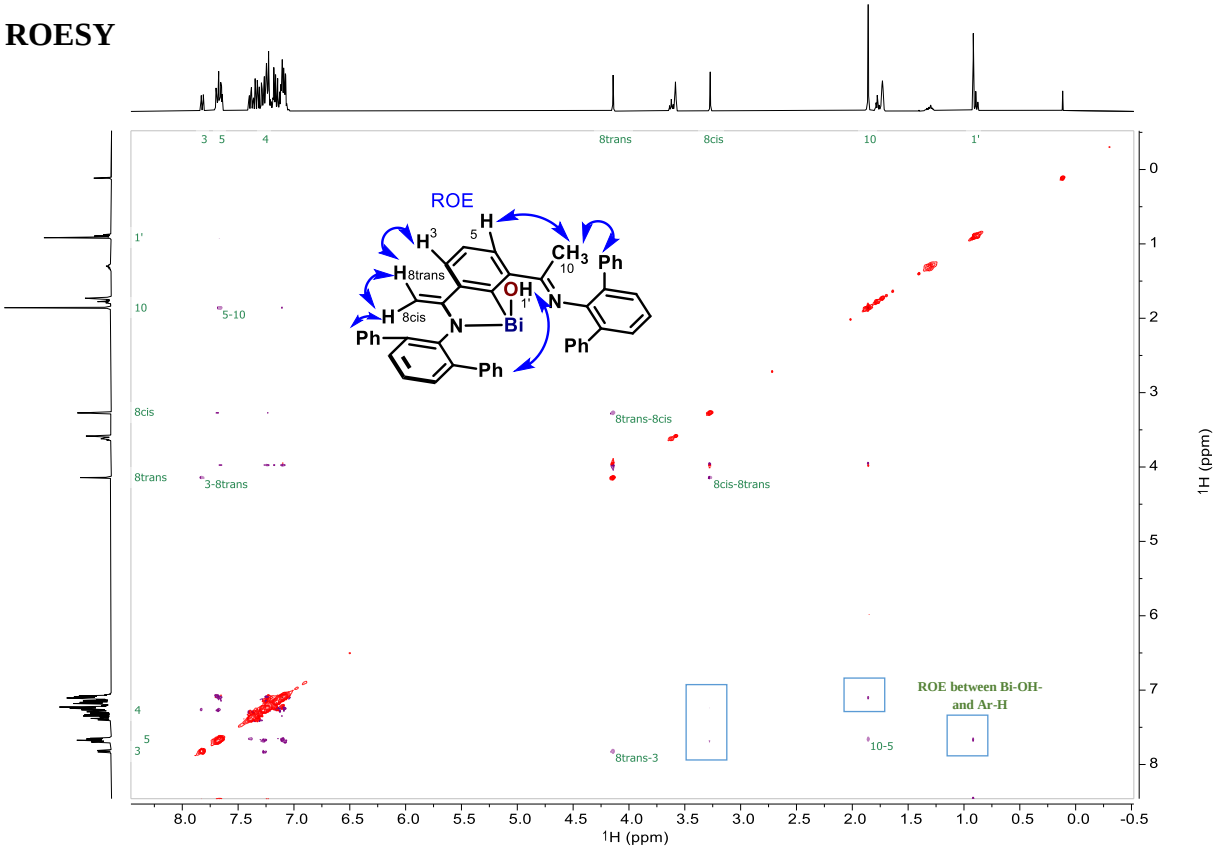

Multiple ROE cross peaks and the absence of EXSY peaks reveal that **7** has a rather non-dynamic structure. All ROE correlations are consistent with the structural information in the X-ray.

NMR Monitoring:

NMR monitoring was performed for a THF-d_8 solution of **5** in a N_2O-filled J-Young NMR tube, however, the reaction proceeded very slowly in the NMR tube while standing still. The reaction was accelerated by gently shaking the NMR tube. After each shake, a ^1H NMR spectrum was recorded. According to NMR monitoring, no intermediate (proposed monomeric oxobismuth species) was detected, which indicated the tautomerization after N_2O oxidation is a fast process.

5. HBpin Reduction of 6 and 7

5.1. HBpin Reduction of Dimeric Bismuth Oxide (**6**)

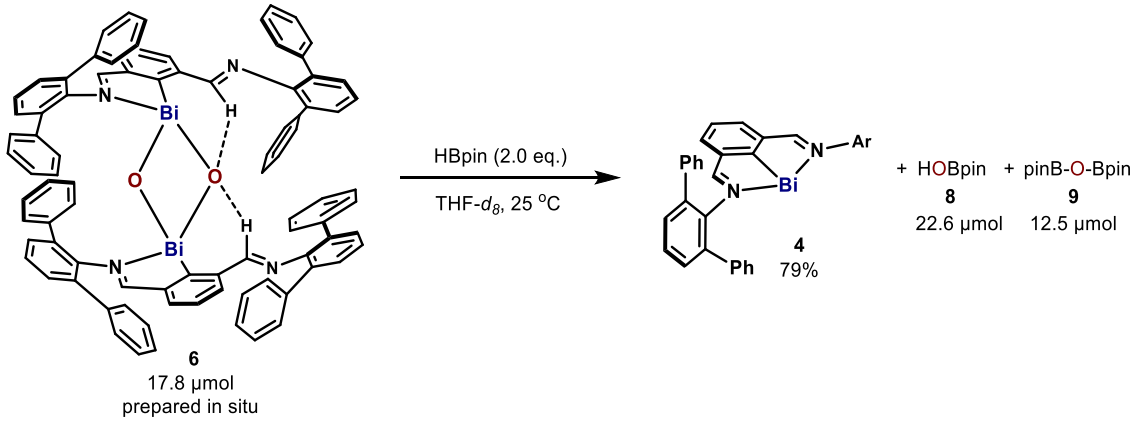

Due to its instability in solid state, a 1 mL THF-d_8 solution of **6** (17.8 μmol, 0.5 equiv.) was prepared *in situ* by N_2O oxidation of **4** (28.4 mg, 35.7 μmol, 1.0 equiv.). After oxidation, the excess of N_2O was removed *in vacuo*.

In the glove box, a 250 μL THF-d_8 solution of HBpin (10.4 μL, 2.0 equiv., 71.4 μmol) was added *slowly and dropwise* to **6** solution *under rapid stirring*. The pale yellow solution turned into dark purple immediately. After stirring for 5 min, mesitylene (5.0 μL, 1.0 equiv., 35.7 μmol) was added as internal standard and the solution was transferred into a J-Young NMR tube for NMR study.

^{1}H NMR (THF-d_8, 500 MHz)

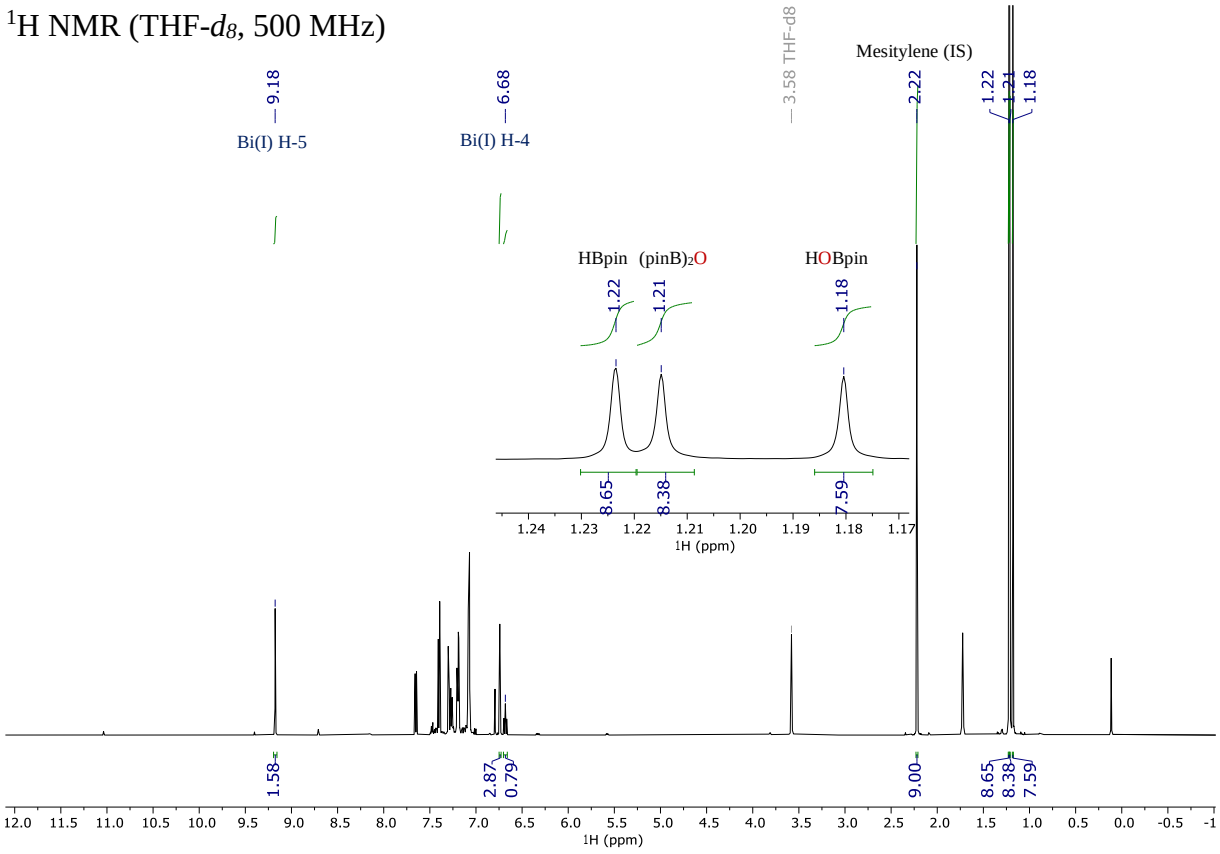

^{11}B NMR (THF-d_8, 160 MHz)

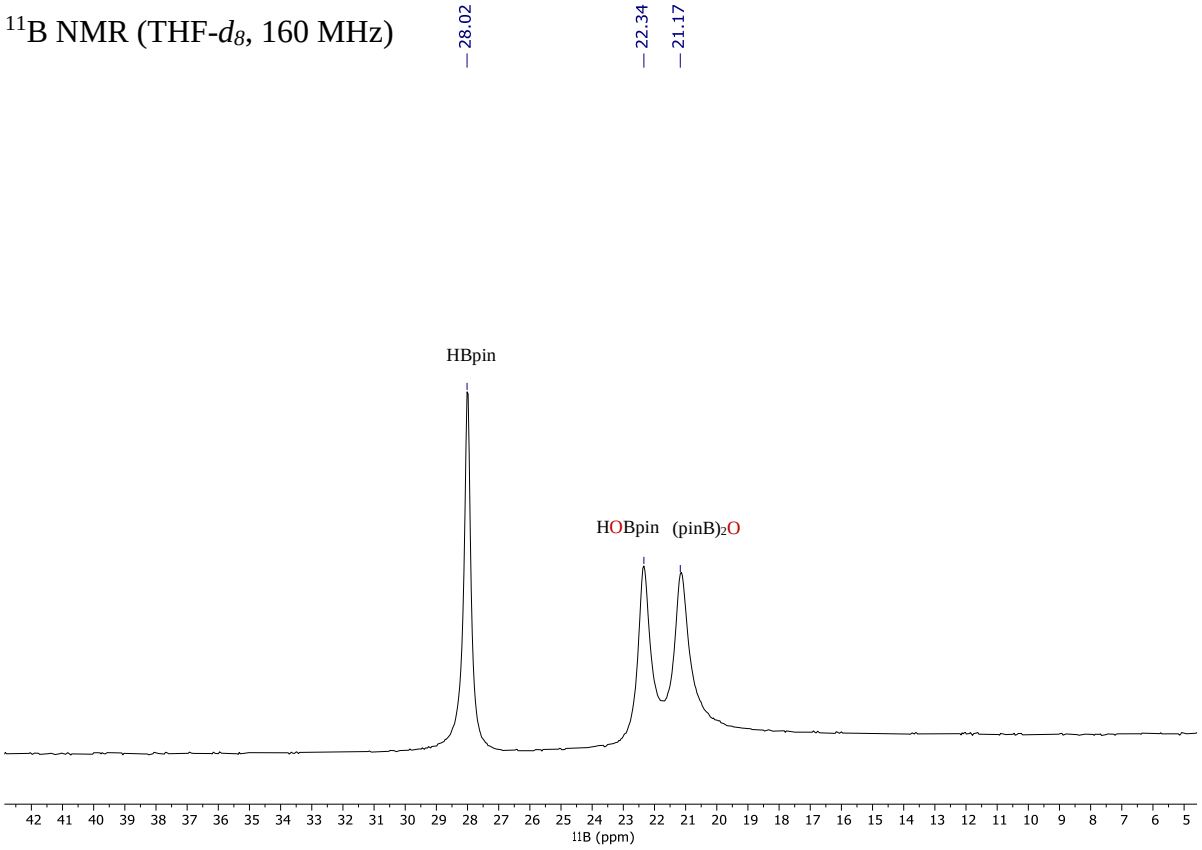

*Pure bismuthinidene (**4**)*

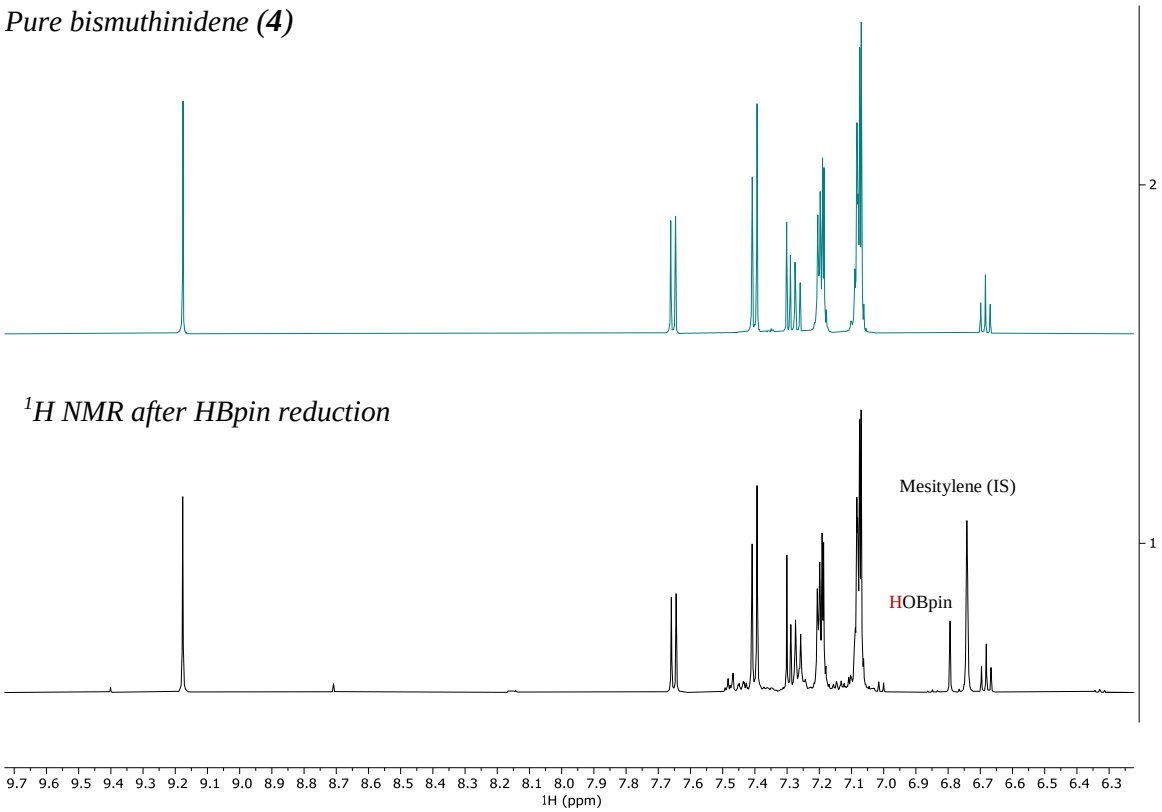

^{1}H NMR after HBpin reduction

Bismuthinidene (**4**) formed in 79% yield during HBpin reduction, accompanied with the formation of HOBpin (**8**, 22.6 μmol) and $(pinB)_2O$ (**9**, 12.5 μmol). The results confirmed that

the stoichiometry of the oxygen transfer reaction between bismuth oxide (**6**) and HBpin was 1:2. The rest of bismuth oxide (**6**) was converted into black precipitate. The fast and unselective reduction at high concentration might lead to relatively low yield of bismuthinidene (**4**) in stoichiometric reduction.

After 4 days, NMR data of the sample was recorded again and 0.73 equiv. bismuthinidene (**4**) remained, indicating that bismuthinidene (**4**) was stable at the reaction condition (HBpin and products).

5.2. HBpin Reduction of Bismuth Hydroxide (**7**)

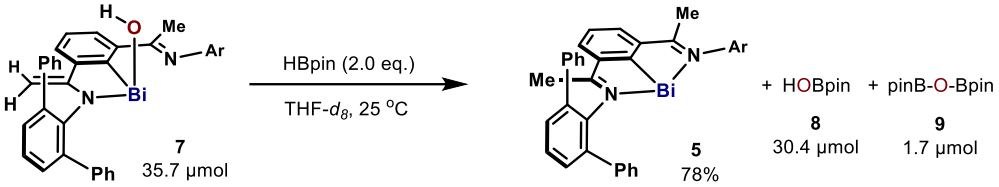

In the glove box, a 250 μL THF-d_8 solution of HBpin (10.4 μL, 2.0 equiv., 71.4 μmol) was added *slowly and dropwise* to a 1 mL THF-d_8 solution bismuth hydroxide (**7**) (30.0 mg, 35.7 μmol) *under rapid stirring*. The orange-red solution turned into dark red-purple immediately. After stirring for 5 min, mesitylene (5.0 μL, 1.0 equiv., 35.7 μmol) was added as internal standard and the solution was transferred into a J-Young NMR tube for NMR study.

^{1}H NMR (THF-d_8, 500 MHz)

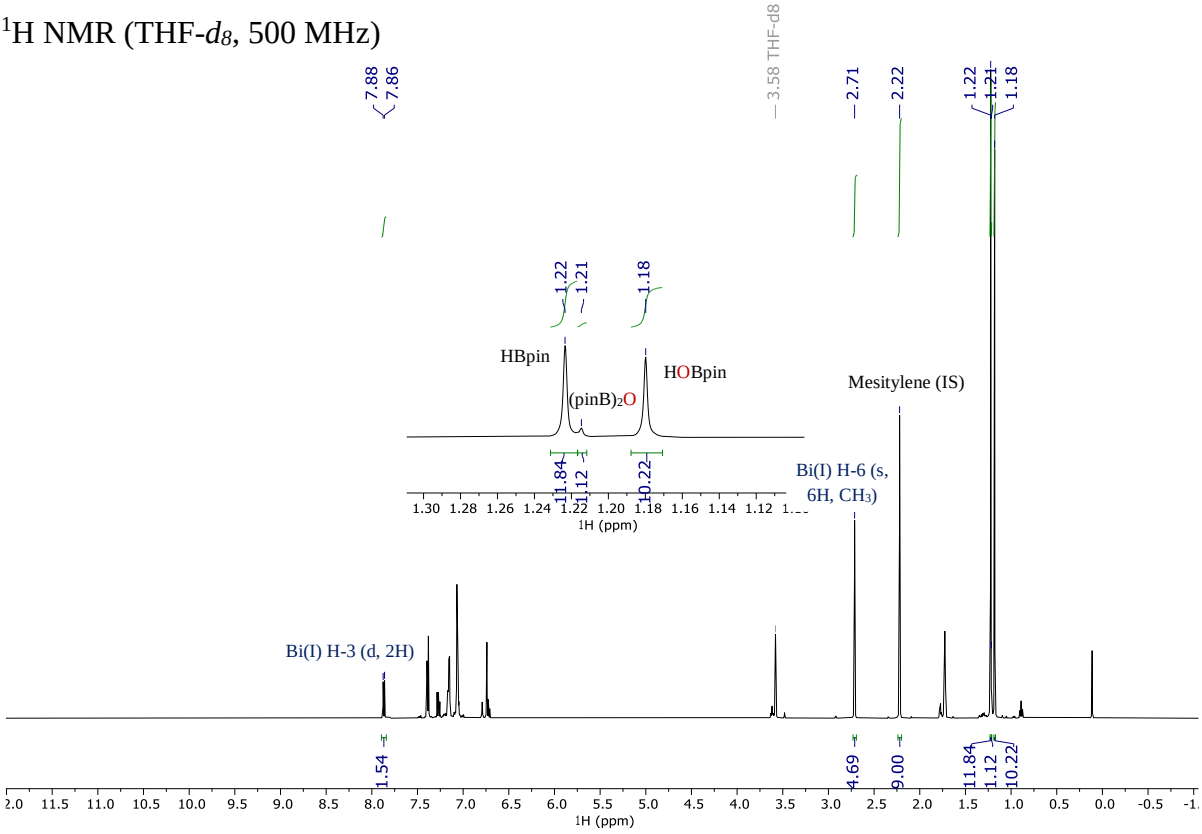

^{11}B NMR (THF-d_8, 160 MHz)

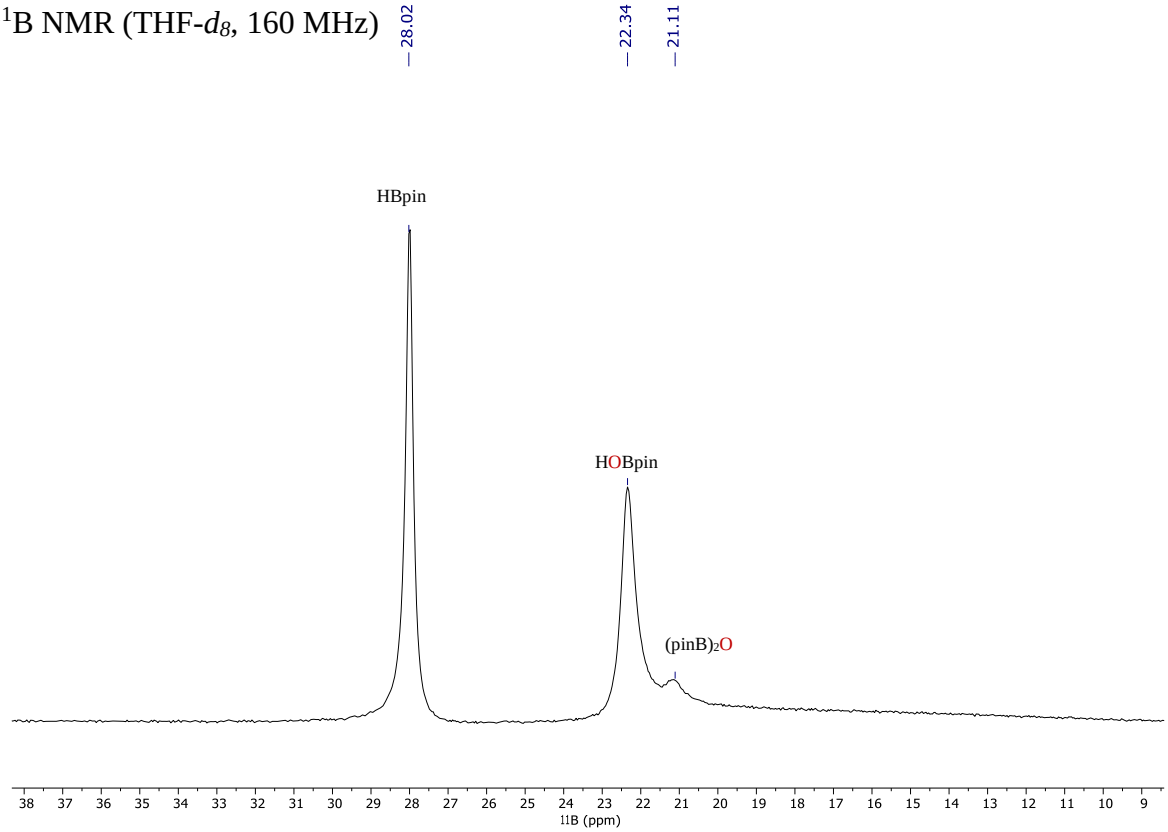

*Pure bismuthinidene (**5**)*

^{1}H NMR after HBpin reduction

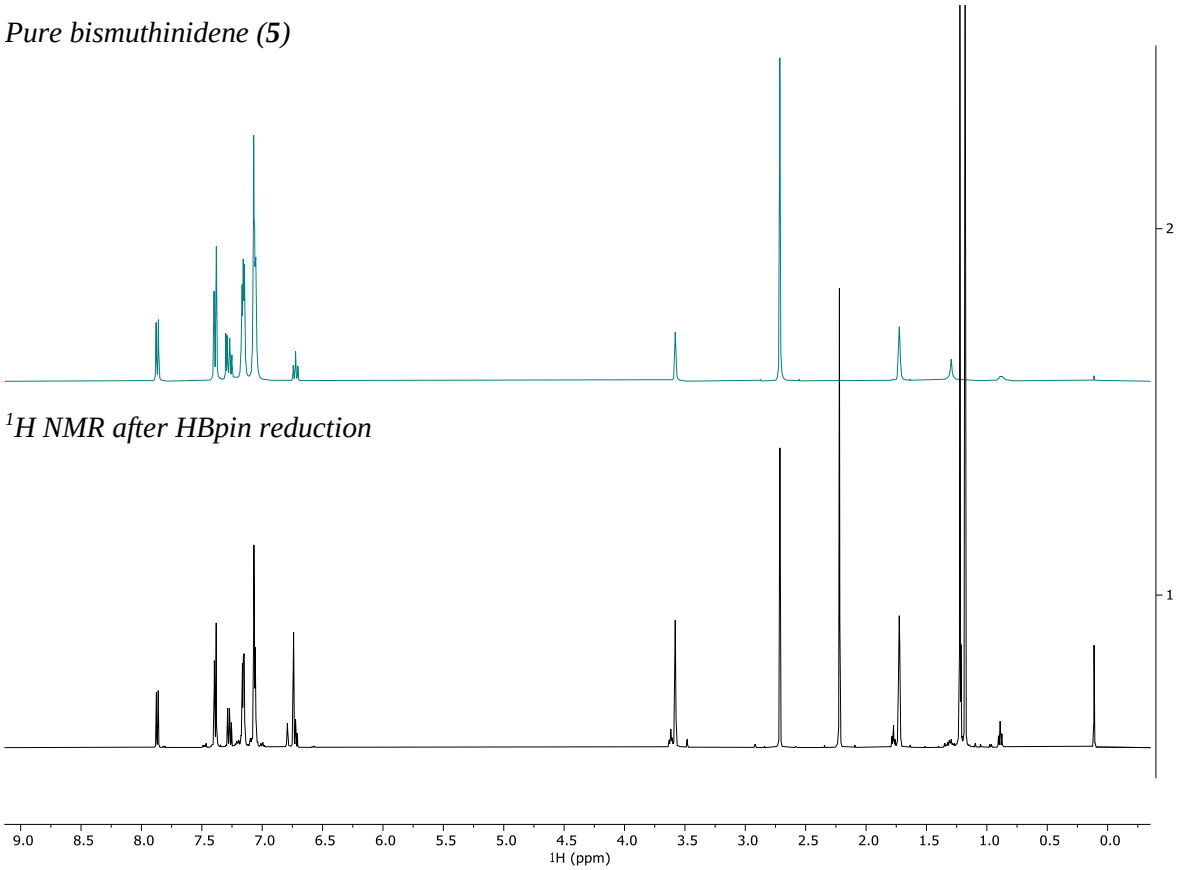

Bismuthinidene (**5**) formed in 78% yield during HBpin reduction, accompanied with the formation of HOBpin (**8**, 30.4 µmol) and (pinB)$_2$O (**9**, 1.7 µmol). The results confirmed that

the stoichiometry of the oxygen transfer reaction between bismuth oxide (**7**) and HBpin was 1:1. The rest of bismuth oxide (**7**) was converted into black precipitate. *Since the free ligand is not detected in ^{1}H NMR, this black precipitate is more likely dimerized or oligomerized Bi(I) instead of metallic Bi.* The fast and unselective reduction at high concentration might lead to relatively low yield of bismuthinidene (**5**) in stoichiometric reduction. This assumption was supported by the fact that direct addition of undiluted HBpin afforded lower yield of bismuthinidene (**5**) (65%) and more black precipitate.

After 4 days, a NMR data of the sample was recorded again and no change of the amount of bismuthinidene (**5**) in solution was observed, indicating that bismuthinidene (**5**) was stable at the reaction condition (HBpin and products).

6. Catalytic N_2O Deoxygenation

6.1. Characterization of Products **8** and **9**

HOBpin (**8**)[9] and $(pinB)_2O$ (**9**)[10] have been characterized in the previous literature, however, the data in THF-d_8 has not been reported. Herein, the NMR characterization of HOBpin (**8**) and $(pinB)_2O$ (**9**) were reported and in THF-d_8.

4,4,5,5-tetramethyl-1,3,2-dioxaborolan-2-ol (**8**)

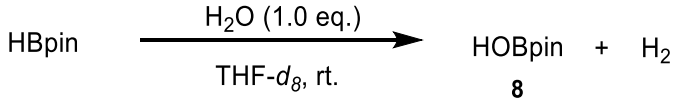

Procedure: in a glove box, HBpin (0.4 mmol, 58.0 µL) and THF-d_8 (0.6 mL) were added to a 10 mL vial. H_2O (degassed, 7.2 µL, 1.0 equiv.) was added to the solution outside the glove box. The solution was stirred at room temperature for 1 h, during which continuous formation of H_2 was observed. After reaction, the solution was diluted and transferred into a J-Young NMR tube in the glove box for NMR characterization.

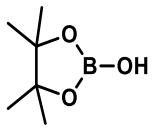

8

^{1}H NMR (500 MHz, THF-d_8): δ 6.80 (s, 1H, OH), 1.18 (s, 12H, CH_3).

^{13}C NMR (126 MHz, THF-d_8): δ 82.4 (C_q), 25.2 (CH_3).

^{11}B NMR (160 MHz, THF-d_8): δ 22.3.

2,2'-oxybis(4,4,5,5-tetramethyl-1,3,2-dioxaborolane) (**9**)

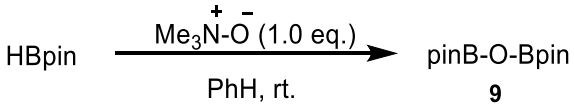

$(pinB)_2O$ was prepared by the literature method with modifications.[10]

Procedure: to an oven-dried 50 mL Schlenk flask, trimethylamine *N*-oxide (130 mg, 1.73 mmol, 1.0 equiv.) and anhydrous benzene (10 mL) were added under argon. To this suspension, HBpin (251 µL, 1.73 mmol) was slowly added. The reaction mixture was stirred 4 h. Then, the solution was frozen and benzene and trimethylamine were removed *in vacuo* and the resulting white solid was dried under high vacuum for 10 h. $(pinB)_2O$ was isolated as a white solid in 95% yield (440 mg).

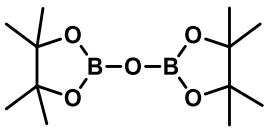

9

^{1}H NMR (500 MHz, THF-*d*$_8$): δ 1.21 (s, 12H).

^{13}C NMR (126 MHz, THF-*d*$_8$): δ 83.5 (C_q), 25.0 (CH_3).

^{11}B NMR (160 MHz, THF-*d*$_8$): δ 21.1.

6.2. General Procedure for Catalytic N_2O Deoxygenation

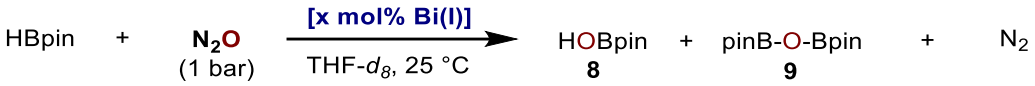

In a glove box, mesitylene (20.9 µL, 0.15 mmol, 1.0 equiv.), THF-d_8 and HBpin (21.8 µL, 0.15 mmol) were added successively to a 10 mL pressure Schlenk tube fitted with a J-Young valve. And then corresponding Bi(I) catalyst (THF-d_8 stock solution) was added. The total amount of THF-d_8 was 0.8 mL. The Schlenk tube was taken out of the glove box and connected to a Schlenk line and a N_2O bottle via a three-way tubing system. The system was degassed by freeze-pump-thaw, backfilled with N_2O (1 bar) and rapidly stirred (750 rpm), during which formation of N_2 was observed. The ending point of the reaction was judged by the disappearance of characteristic color of Bi(I) catalyst or the formation of black precipitate. The solution was transferred into a J-Young NMR tube in the glove box for the NMR study.

6.3. Table S2: Catalytic N_2O Deoxygenation with HBpin

Because the product HOBpin (**8**) reacted with HBpin to give $(pinB)_2O$ (**9**), the TONs are always lower than theoretical TON [1/cat. (%)] even though full conversions were achieved in most cases.

$$TON = [HOBpin\ (\%) + (pinB)_2O\ (\%)] \times [1/cat.\ (\%)]$$

$$TOF = TON/time\ (min)$$

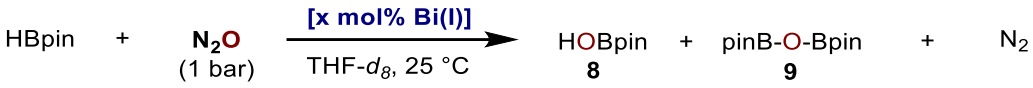

Table S2: Catalytic N_2O deoxygenation with HBpin[a]

Entry	**Bi(I)** (mol%)	Time	Conv. (%)[b]	**8** (%)	**9** (%)	TON	TOF
1	---	15 h	0	---	---	---	---
2	**4** (1.0)	15 h	79	27	27	54	---
3	**5** (1.0)	15 h	100	79	10	89	---
4	**1** (2.5)	< 1 min[c]	100	58	18	30	> 30 min^{-1}
5	**1** (1.0)	~ 3 min[c]	100	60	20	80	~ 27 min^{-1}
6	**1** (0.5)	~ 5 min[c]	100	62	20	162	~ 32 min^{-1}
7	**1** (0.1)	~ 15 min[c]	100	57	21	780	~ 52 min^{-1}
8	**1** (0.05)	~ 30 min[c]	100	53	23	1520	~ 51 min^{-1}
9	**1** (0.01)	11 h	97	36	31	6700	---

[a]Yields and TONs calculated by ^1H NMR using mesitylene as internal standard. [b]Based on HBpin. [c]Determined by disappearance of the characteristic color of Bi(I).

6.4. NMR Spectra of Catalytic N_2O Deoxygenation

- Blank Reaction

^{1}H NMR (THF-d_8, 500 MHz)

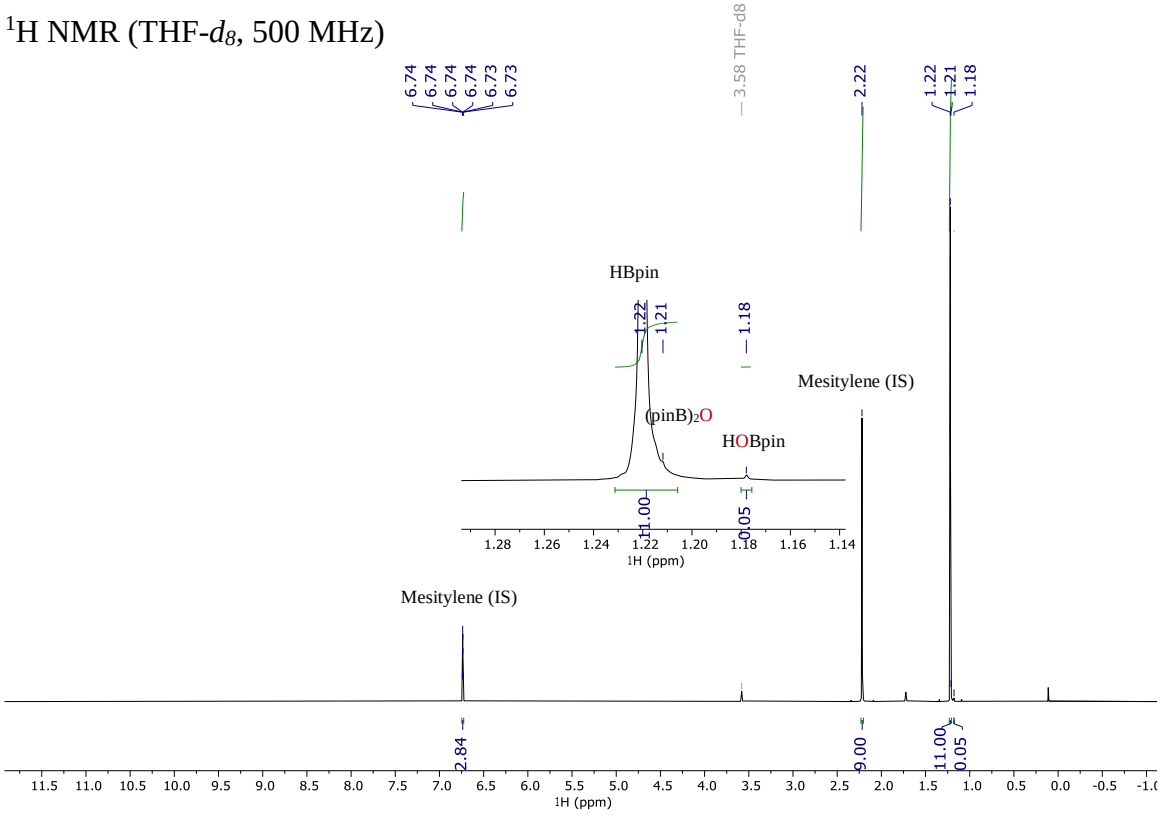

^{11}B NMR (THF-d_8, 160 MHz)

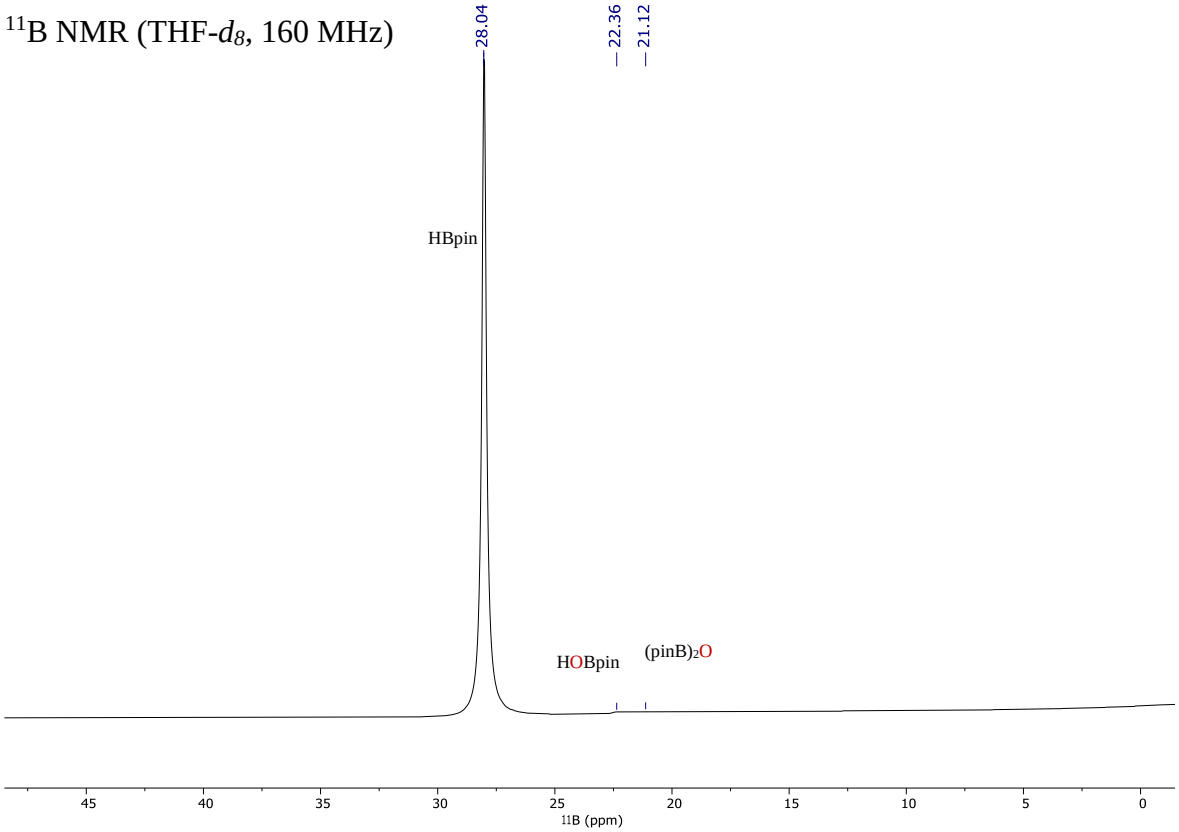

- Catalytic N_2O Deoxygenation by Bismuthinidene (**4**)

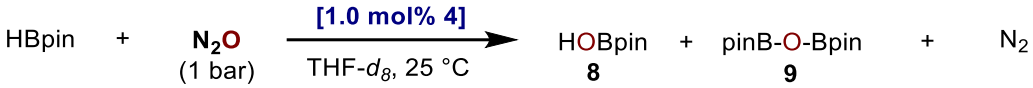

The stock solution was prepared by dissolving 4.8 mg bismuthinidene (**4**) in 1.0 mL THF-d_8 and 250 µL of this solution was used for each reaction. The conversion, yields and TONs were calculated by ^{1}H NMR integration relative to the mesitylene as internal standard, from an average of three independent reactions.

Slow N_2 formation was observed during the reaction. The solution remained dark purple until black precipitate formed after about 4 h.

^{1}H NMR (THF-d_8, 500 MHz)

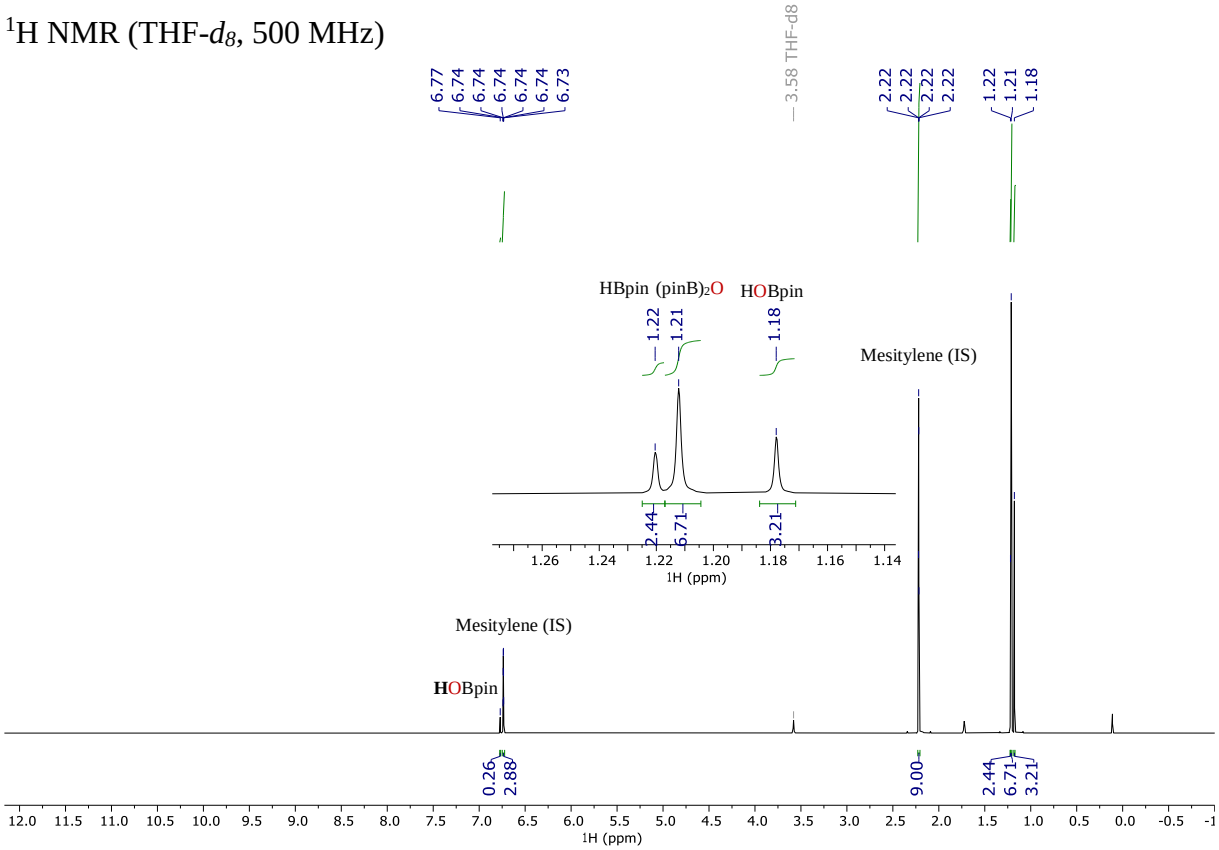

^{11}B NMR (THF-d_8, 160 MHz)

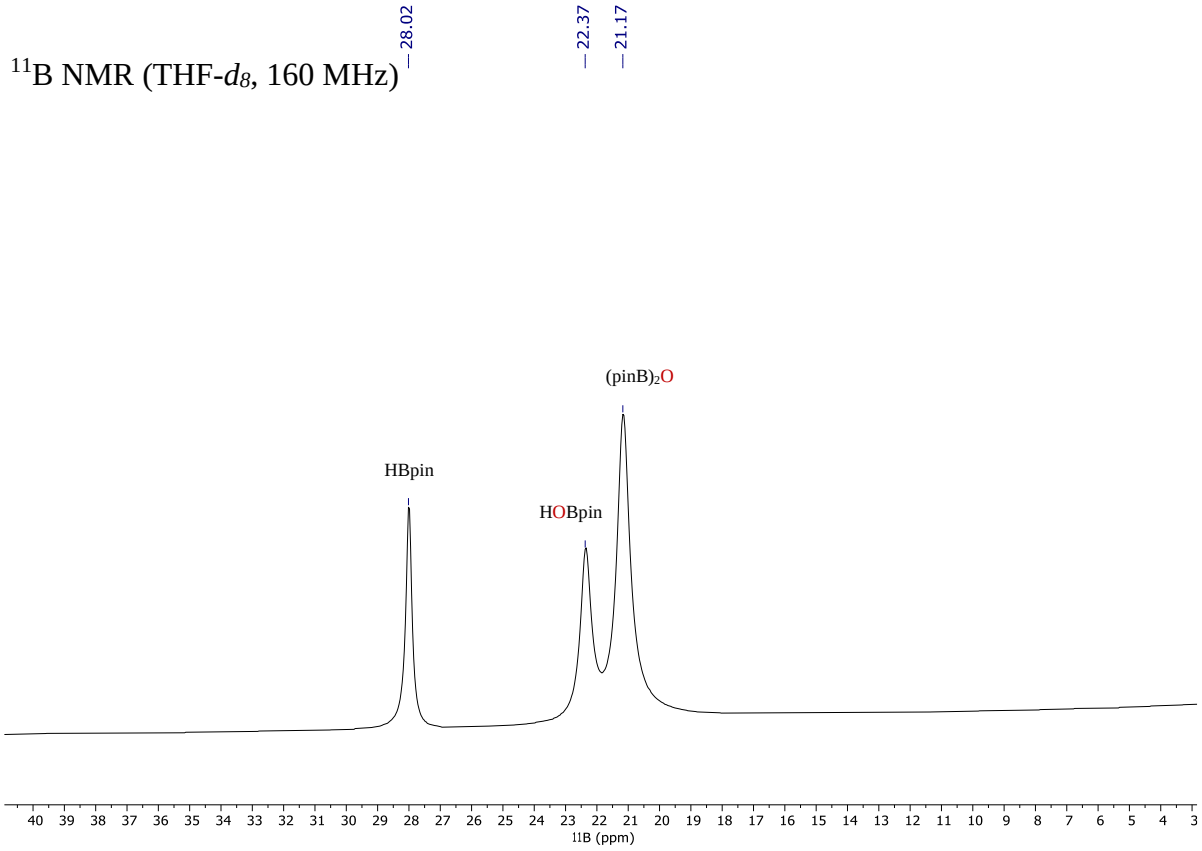

- Catalytic N_2O Deoxygenation by Bismuthinidene (**5**)

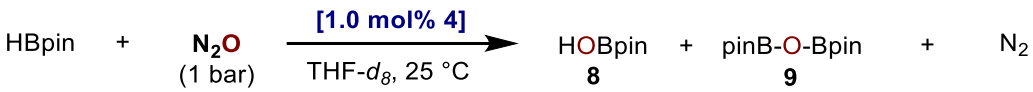

The stock solution was prepared by dissolving 5.0 mg bismuthinidene (**5**) in 1.0 mL THF-d_8 and 250 µL of this solution was used for each reaction. The conversion, yields and TON were calculated by ^{1}H NMR integration relative to the mesitylene as internal standard, from an average of three independent reactions.

Slow N_2 formation was observed during the reaction. The solution remained dark red-purple until black precipitate formed after about 4 h.

^{1}H NMR (THF-d_8, 500 MHz)

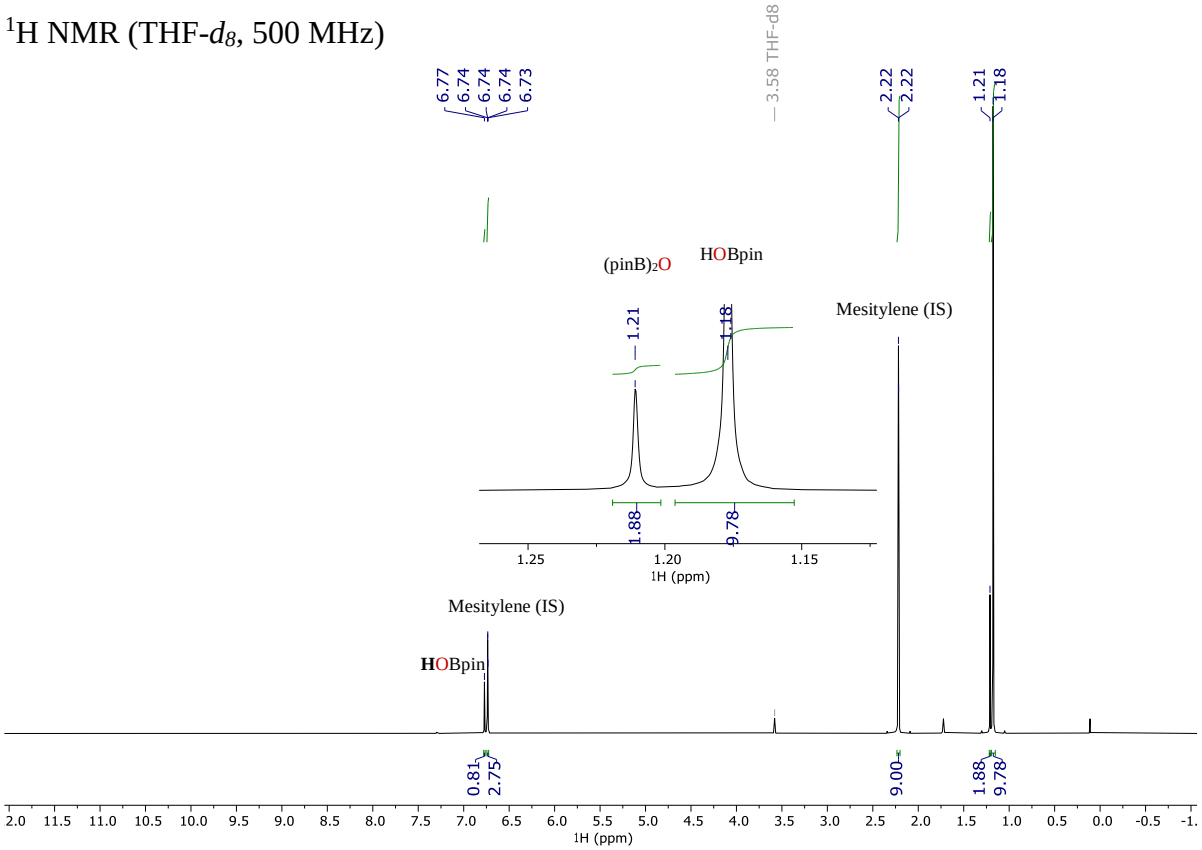

^{11}B NMR (THF-d_8, 160 MHz)

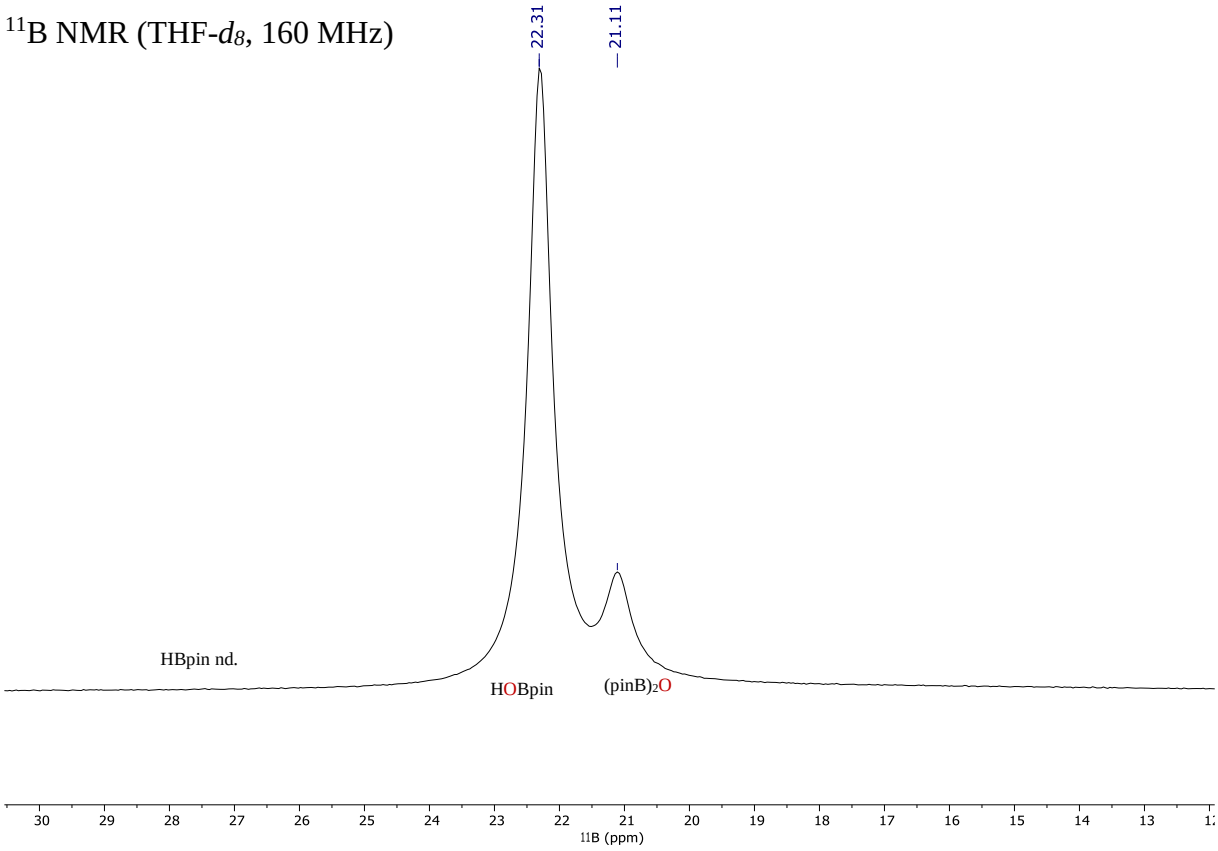

- Catalytic N_2O Deoxygenation by Bismuthinidene (**1**)

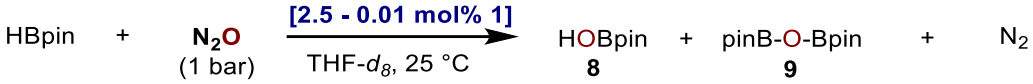

The stock solution was prepared by dissolving 2.7 mg bismuthinidene (**1**) in 1.0 mL THF-d_8. 250 µL, 125 µL, 25.0 µL and 12.5 µL of this solution was used for 1.0 mol%, 0.5 mol%, 0.1 mol% and 0.05 mol% catalytic reactions.

For 0.01 mol% reaction, the stock solution was prepared by dissolving 2.7 mg bismuthinidene (**1**) in 2.0 mL THF-d_8 and 10.0 µL of this solution was used. The scale for 0.01 mol% reaction was 0.30 mmol. 25 mL pressure Schlenk flasks were used.

The conversions, yields and TONs were calculated by ^{1}H NMR integration relative to the mesitylene as internal standard. The conversion, yields and TON of 0.01 mol% catalytic reactions were obtained from an average of three independent reactions.

1.0 mol% reaction:

Violent release of N_2 was observed and the color of the solution remained green until completion of the reaction. The reaction time was estimated to be about 3 min.

The CH_3 of HOBpin (**8**) was very broad possibly due to the interaction between the deactivated catalyst and HOBpin (**8**). This effect was not observed when the catalyst loading was below 0.5 mol%. The amount of HOBpin (**8**) was calculated based on the integration of the OH. The amount of $(pinB)_2O$ (**9**) was calculated by subtracting the calculated amount of HOBpin (**8**) from the total amount of HOBpin (**8**) and $(pinB)_2O$ (**9**).

^{1}H NMR (THF-d_8, 500 MHz)

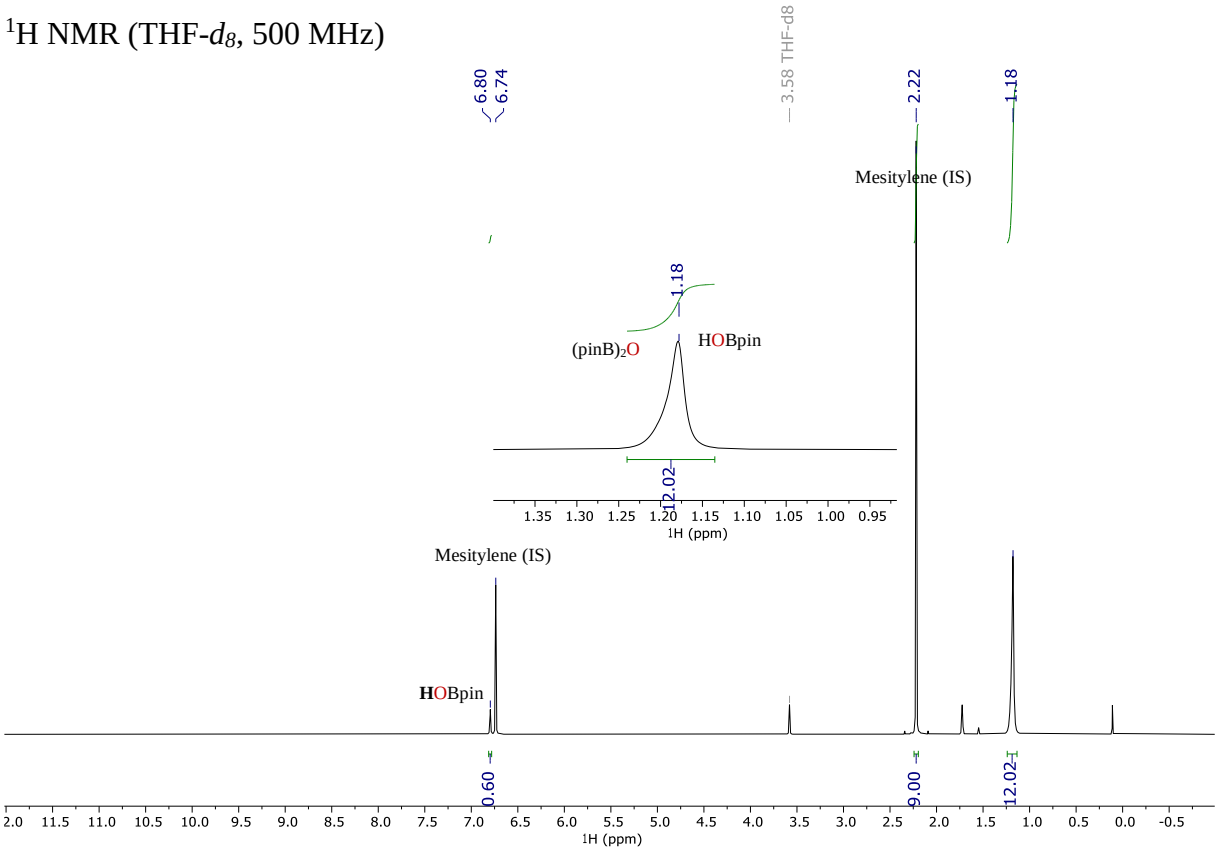

^{11}B NMR (THF-d_8, 160 MHz)

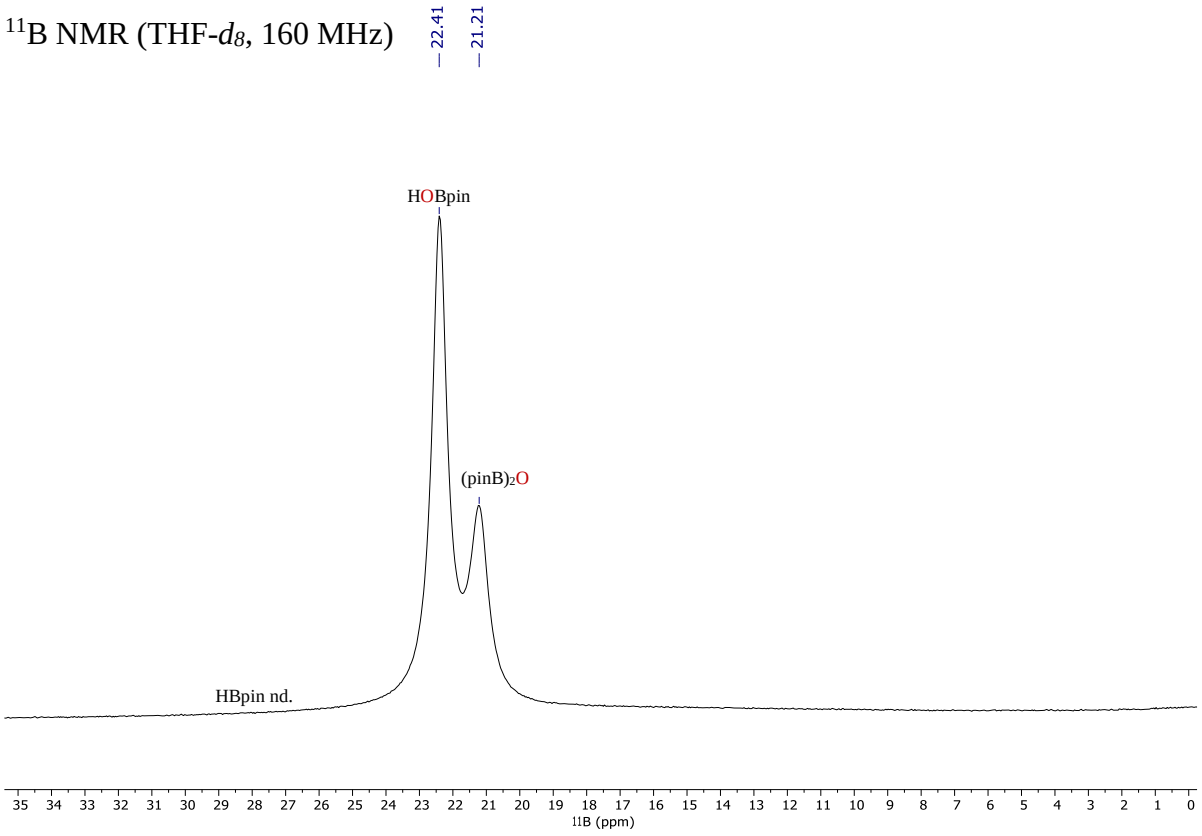

0.01 mol% reaction:

Gentle release of N_2 was observed and the color of the Bi(I) catalyst was barely observed. The reaction mixture was stirred for 11 h.

^{1}H NMR (THF-d_8, 500 MHz)

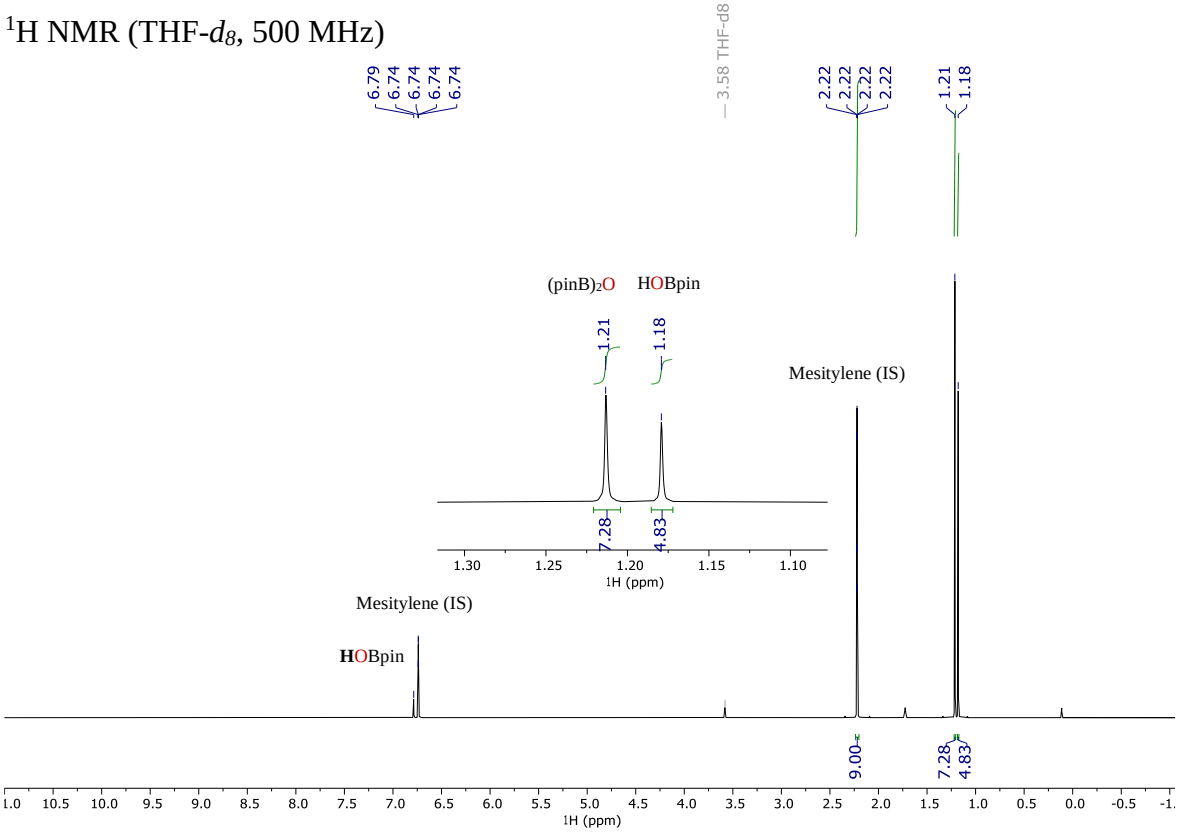

^{11}B NMR (THF-d_8, 160 MHz)

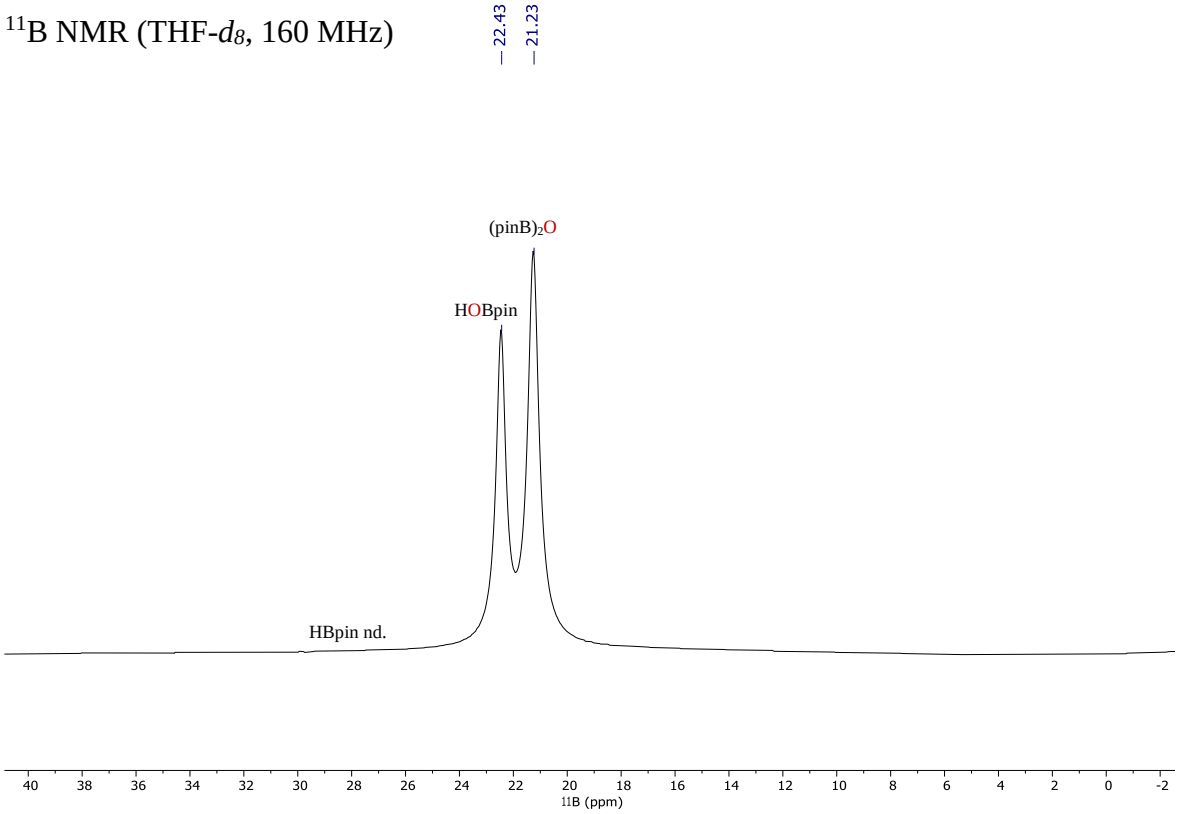

7. The Mechanistic Proposal

A simplidied catalytic cycle was proposed as follows:

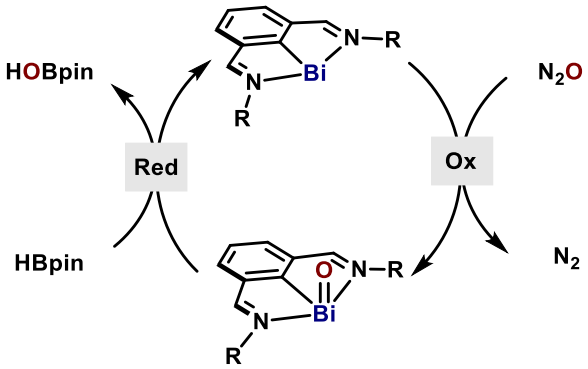

Detailed mechanistic suggestions:

1. N_2O activation on Bi center

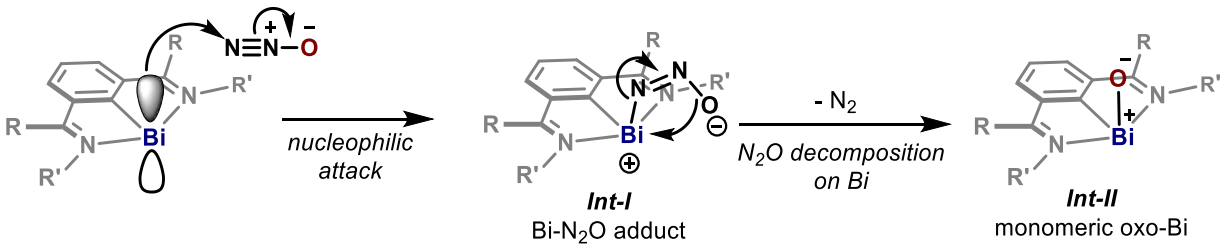

The initial step of N_2O activation on Bi center is proposed to occur in analogy to NHCs.[11] Namely, bismuthinidenes (**1**, **4** and **5**) utilize electrons in the HOMO orbital (mainly consist of the p_z orbital of the bismuth center)[1a, 6] to attack the terminal N of N_2O. As a result, Bi-N_2O adduct (***Int-I***) forms. Subsequently, the release of N_2 gives transient monomeric bismuth oxides (***Int-II***). Due to the high polarity of the Bi–O bond and the large difference in orbital size between Bi and O atoms, the transient ***Int-II*** are proposed to exist in ylide form.[12]

2. The stabilization of transient monomeric oxo-Bi (***Int-II***)

Because of the high instability of ***Int-II***, they tend to be stabilized rapidly via dimerization or deprotonation/tautomerization process. The hydrogen-bonding between O and imine H suggested in **6** let us propose that the imine arms of ***Int-II*** readily rotate. After bond rotation, dimerization gives dimeric bismuth oxide **6** while deprotonation of CH_3 gives monomeric bismuth oxide **7**. **6** is a *trans*-isomer (with respect to the relative orientation of the Bi–Ar to a Bi_2O_2 ring)[13,14] and has a dynamic structure where two imines are in dissociation/coordination equilibrium.

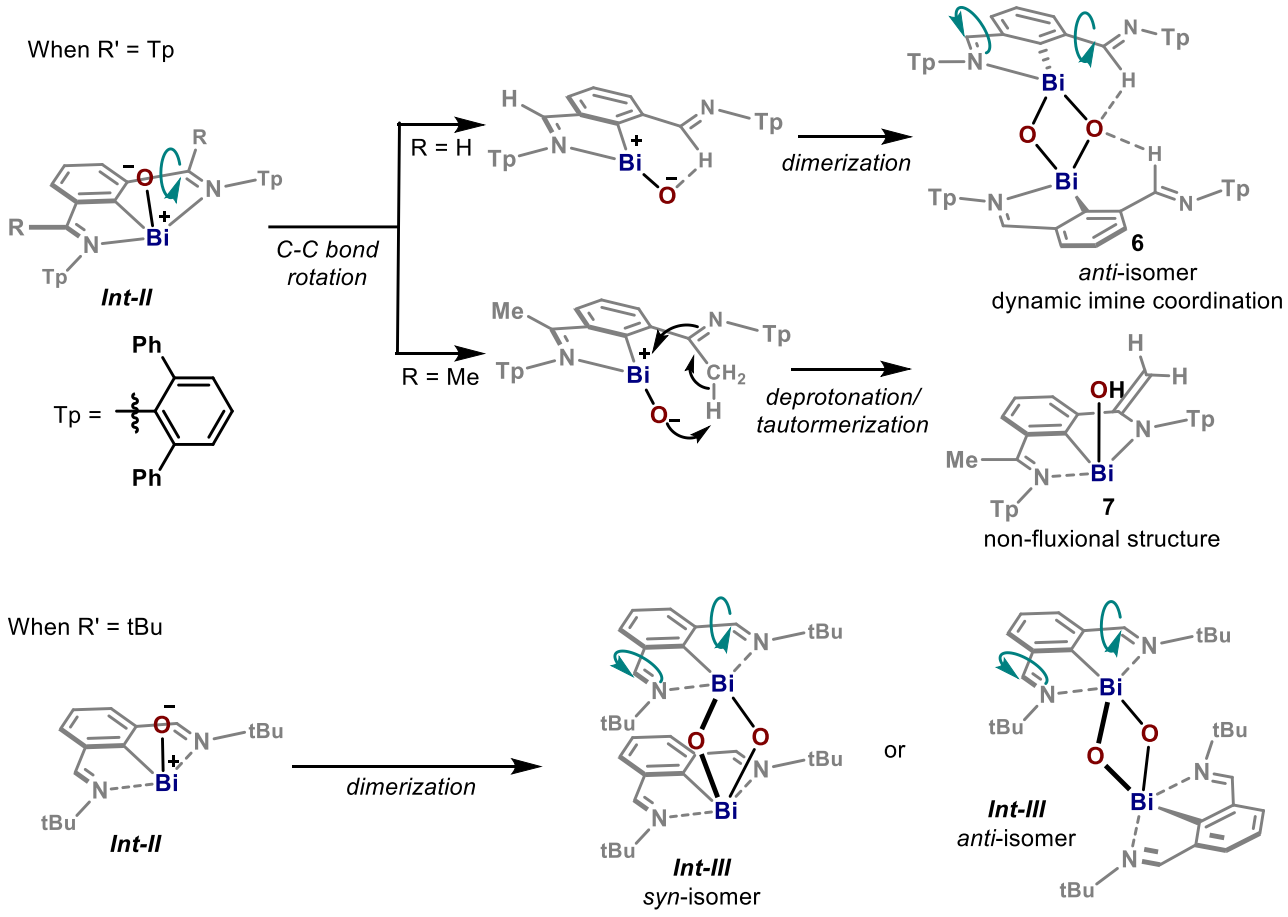

Based on the X-ray structure of **7** and NMR studies of the N_2O oxidation of **1**, we propose that ***Int-II*** with tBu substituents would dimerize to form ***Int-III*** as an *anti*- or a *syn*-isomer.[13,14,15] Both isomers have dynamic behaviors.

3. Formation of Bi-oxo-HBpin adduct (***Int-V***)

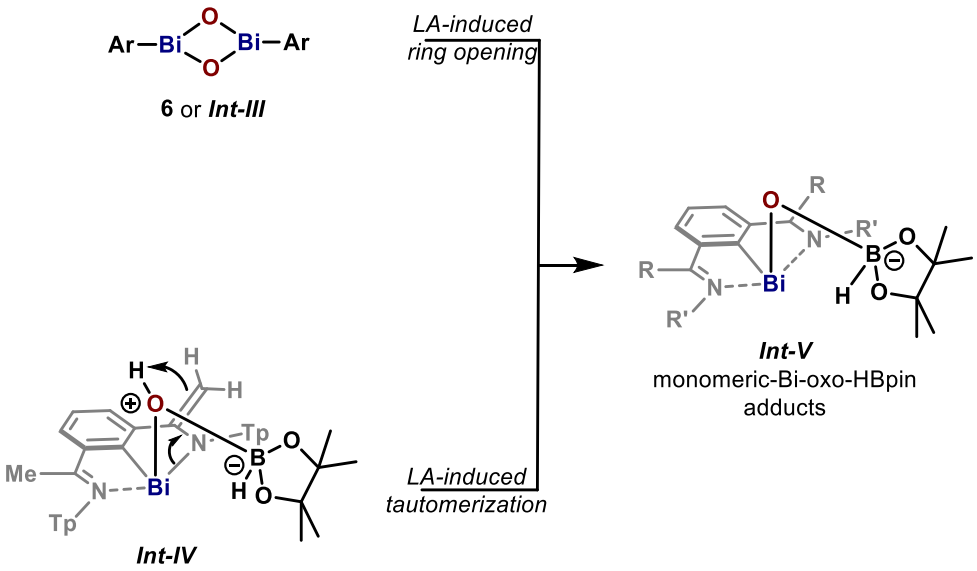

The coordination of the oxo group of **6** or ***Int-III*** to the Lewis-acidic B center of HBpin would probably lead to the ring-opening (this process has been reported for a $(LSbO)_2$ with $B(C_6F_5)_3$[16]). As for **7**, on the contrary, the acidity of the proton on OH enhances after HBpin coordination and this proton transfers to the enamine arm (this process has been reported for a $B(C_6F_5)_3$-stabilized *β*-diketiminate-derived boracarbonyl compound[17]). Both processes give monomeric-Bi-oxo-HBpin adduct ***Int-V***.

4. Hydride transfer and reductive elimination

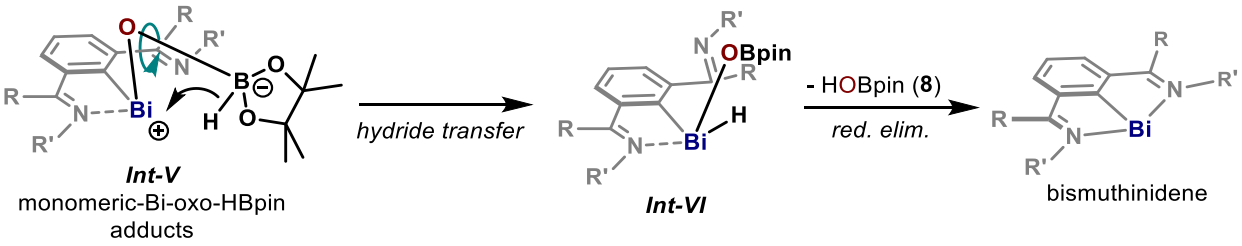

The hydridic H atom on tetrahedron B center migrates to cationic Bi center to form bismuth hydride ***Int-VI***. Bismuth hydrides have been reported to be unstable,[1, 6, 18] and therefore it is proposed that ***Int-VI*** readily undergoes reductive elimination to yield HOBpin (**8**) and regenerates bismuthinidene catalysts.

8. X-ray Crystallographic Studies

8.1. Single Crystal Structure Analysis of **2, 1·DCM**

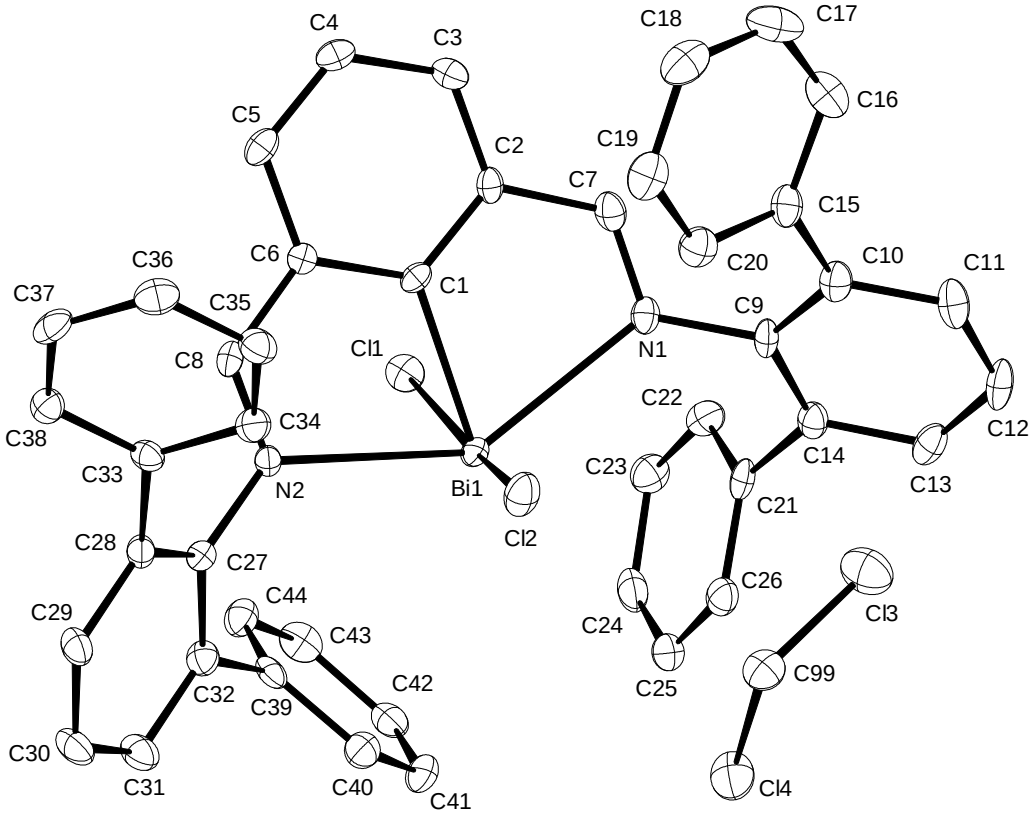

Figure S1. The molecular structure of complex **2, 1·DCM**. H atoms have been removed for clarity.

X-ray Crystal Structure Analysis of complex 2 1·DCM: C_{45} H_{33} Bi Cl_4 N_2, M_r = 952.51 g mol^{-1}, yellow prism, crystal size 0.11 x 0.09 x 0.08 mm^3, monoclinic, P $2_1/n$ [14], a = 12.6023(6) Å, b = 14.1992(16) Å, c = 21.007(2) Å, β = 92.842(6)°, V = 3754.4(6) $Å^3$, T = 100(2) K, Z = 4, D_{calc} = 1.685 g·cm^3, λ = 0.71073 Å, μ(*Mo-K*α) = 5.017 mm^{-1}, analytical absorption correction (T_{min} = 0.63212, T_{max} = 0.76390), Bruker AXS Enraf-Nonius KappaCCD diffractometer with a FR591 rotating Mo-anode X-ray source, 2.852 < θ < 27.498°, 54781 measured reflections, 8629 independent reflections, 7293 reflections with $I > 2\sigma(I)$, R_{int} = 0.0487. The structure was solved by *SHELXT* and refined by full-matrix least-squares (*SHELXL*) against F^2 to R_1 = 0.0309 [$I > 2\sigma(I)$], wR_2 = 0.0580, 469 parameters.

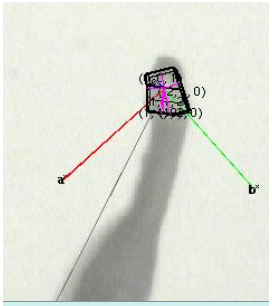

	h	k	l	distance (mm)
1.	-2	1	0	0.03
2.	1	-1	0	0.03
3.	-1	-2	0	0.03
4.	1	2	0	0.05
5.	0	0	1	0.06
6.	0	0	-1	0.05
7.	1	1	2	0.04
8.	1	1	-2	0.05
9.	1	1	0	0.045

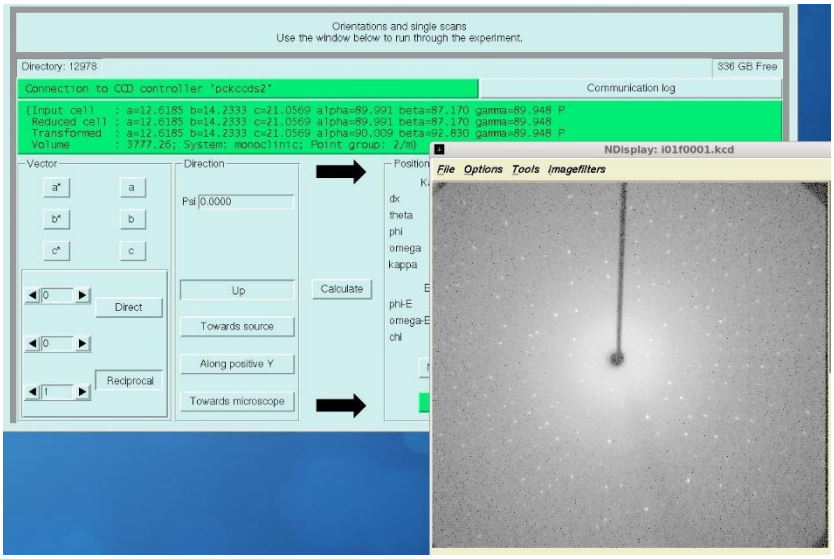

INTENSITY STATISTICS FOR DATASET

Resolution	#Data	#Theory	%Complete	Redundancy	Mean I	Mean I/s	Rmerge	Rsigma
Inf - 2.55	260	273	95.2	8.95	129.32	76.48	0.0300	0.0096
2.55 - 1.70	606	606	100.0	7.67	94.64	55.52	0.0278	0.0125
1.70 - 1.34	881	881	100.0	7.33	58.59	40.43	0.0325	0.0173
1.34 - 1.17	856	856	100.0	6.99	48.58	32.70	0.0374	0.0216
1.17 - 1.06	865	865	100.0	6.72	38.61	26.65	0.0450	0.0272
1.06 - 0.98	928	928	100.0	6.35	31.55	21.64	0.0560	0.0344
0.98 - 0.92	896	896	100.0	5.99	27.26	18.12	0.0657	0.0419
0.92 - 0.88	740	740	100.0	5.69	21.48	14.42	0.0827	0.0534
0.88 - 0.84	871	871	100.0	5.50	21.93	14.04	0.0857	0.0563
0.84 - 0.81	816	816	100.0	5.21	18.52	11.45	0.1030	0.0694
0.81 - 0.78	912	912	100.0	5.00	17.11	10.35	0.1113	0.0787
0.78 - 0.75	1038	1039	99.9	4.76	14.92	8.85	0.1307	0.0945
0.75 - 0.73	815	815	100.0	4.53	12.94	7.45	0.1482	0.1138
0.73 - 0.71	908	909	99.9	4.34	12.32	6.80	0.1711	0.1271
0.71 - 0.69	1013	1013	100.0	4.17	10.74	5.74	0.1972	0.1530
0.69 - 0.68	542	542	100.0	4.06	9.77	5.19	0.2059	0.1750
0.68 - 0.66	1195	1196	99.9	3.89	8.76	4.45	0.2389	0.2082
0.66 - 0.65	655	655	100.0	3.80	8.92	4.26	0.2387	0.2182
0.65 - 0.64	696	698	99.7	3.62	8.07	3.69	0.2668	0.2644
0.64 - 0.62	1668	1687	98.9	3.47	6.78	2.82	0.3225	0.3559
0.72 - 0.62	6224	6246	99.6	3.83	8.82	4.33	0.2389	0.2238
Inf - 0.62	17161	17198	99.8	5.17	24.68	15.36	0.0679	0.0605

The high residual electron density (highest peak: 4.22 at 0.75 Å from Bi1 and deepest hole: -2.08 at 0.62 Å from Bi1) could possibly be caused by anharmonic displacement of the Bi atom.

Complete .cif-data of the compound are avaliable under the CCDC number **CCDC-2031447**.

Table S3. Crystal data and structure refinement.

Identification code	12978	
Empirical formula	$C_{45}H_{33}BiCl_4N_2$	
Color	yellow	
Formula weight	952.51 g·mol^{-1}	
Temperature	100(2) K	
Wavelength	0.71073 Å	
Crystal system	monoclinic	
Space group	$P2_1/n$, (No. 14)	
Unit cell dimensions	a = 12.6023(6) Å	α= 90°.
	b = 14.1992(16) Å	β= 92.842(6)°.
	c = 21.007(2) Å	γ = 90°.
Volume	3754.4(6) Å^3	
Z	4	
Density (calculated)	1.685 Mg · m^{-3}	
Absorption coefficient	5.017 mm^{-1}	
F(000)	1872 e	
Crystal size	0.11 x 0.09 x 0.08 mm^3	
θ range for data collection	2.852 to 27.498°.	
Index ranges	-16 ≤ h ≤ 15, -18≤ k ≤ 18, -27 ≤ l ≤ 27	
Reflections collected	54781	
Independent reflections	8629 [R_{int} = 0.0487]	
Reflections with I>2σ(I)	7293	
Completeness to θ = 25.242°	99.9 %	
Absorption correction	Gaussian	
Max. and min. transmission	0.76 and 0.63	
Refinement method	Full-matrix least-squares on F^2	
Data / restraints / parameters	8629 / 0 / 469	
Goodness-of-fit on F^2	1.074	
Final R indices [I>2σ(I)]	R_1 = 0.0309	wR^2 = 0.0580
R indices (all data)	R_1 = 0.0435	wR^2 = 0.0633
Largest diff. peak and hole	4.2 and -2.1 e · Å^{-3}	

Table S4. Bond lengths [Å] and angles [°].

Cl(1)-Bi(1)	2.6635(10)	Cl(2)-Bi(1)	2.6624(10)
Cl(4)-C(99)	1.775(4)	Cl(3)-C(99)	1.762(4)
N(2)-C(8)	1.279(5)	N(2)-C(27)	1.429(5)
N(2)-Bi(1)	2.601(3)	N(1)-C(7)	1.281(5)
N(1)-C(9)	1.435(5)	N(1)-Bi(1)	2.549(3)
C(6)-C(8)	1.461(5)	C(6)-C(1)	1.388(5)
C(6)-C(5)	1.392(5)	C(39)-C(40)	1.395(5)
C(39)-C(32)	1.492(5)	C(39)-C(44)	1.384(6)
C(8)-H(8)	0.9500	C(2)-C(1)	1.390(5)
C(2)-C(3)	1.393(5)	C(2)-C(7)	1.463(5)
C(27)-C(32)	1.402(5)	C(27)-C(28)	1.416(5)
C(40)-H(40)	0.9500	C(40)-C(41)	1.387(6)
C(21)-C(26)	1.389(6)	C(21)-C(22)	1.389(5)
C(21)-C(14)	1.495(5)	C(1)-Bi(1)	2.209(4)
C(3)-C(4)	1.391(5)	C(23)-C(22)	1.388(6)
C(23)-C(24)	1.373(6)	C(26)-C(25)	1.387(6)
C(41)-C(42)	1.381(6)	C(32)-C(31)	1.391(5)
C(43)-C(44)	1.396(6)	C(43)-C(42)	1.377(6)
C(28)-C(33)	1.495(5)	C(28)-C(29)	1.391(5)
C(5)-C(4)	1.385(6)	C(33)-C(38)	1.394(5)
C(33)-C(34)	1.396(5)	C(38)-C(37)	1.392(5)
C(14)-C(9)	1.399(5)	C(14)-C(13)	1.391(5)
C(9)-C(10)	1.413(5)	C(35)-C(34)	1.389(5)
C(35)-C(36)	1.396(6)	C(25)-C(24)	1.385(6)
C(13)-C(12)	1.386(6)	C(29)-C(30)	1.388(6)
C(10)-C(15)	1.495(6)	C(10)-C(11)	1.396(5)
C(20)-C(15)	1.406(6)	C(20)-C(19)	1.392(6)
C(12)-C(11)	1.379(6)	C(15)-C(16)	1.394(6)
C(31)-C(30)	1.382(6)	C(37)-C(36)	1.376(6)
C(18)-C(17)	1.366(7)	C(18)-C(19)	1.394(6)
C(17)-C(16)	1.398(7)		

C(8)-N(2)-C(27)	119.7(3)	C(8)-N(2)-Bi(1)	109.1(2)
C(27)-N(2)-Bi(1)	131.0(2)	C(7)-N(1)-C(9)	119.0(3)

C(7)-N(1)-Bi(1)	110.0(2)	C(9)-N(1)-Bi(1)	130.5(2)
C(1)-C(6)-C(8)	117.7(3)	C(1)-C(6)-C(5)	120.2(3)
C(5)-C(6)-C(8)	122.0(3)	C(40)-C(39)-C(32)	118.8(4)
C(44)-C(39)-C(40)	119.0(4)	C(44)-C(39)-C(32)	121.9(4)
N(2)-C(8)-C(6)	121.7(3)	C(1)-C(2)-C(3)	119.8(3)
C(1)-C(2)-C(7)	117.3(3)	C(3)-C(2)-C(7)	122.8(3)
C(32)-C(27)-N(2)	118.7(3)	C(32)-C(27)-C(28)	119.7(3)
C(28)-C(27)-N(2)	121.4(3)	C(41)-C(40)-C(39)	120.8(4)
C(26)-C(21)-C(22)	119.2(4)	C(26)-C(21)-C(14)	121.1(4)
C(22)-C(21)-C(14)	119.4(4)	C(6)-C(1)-C(2)	120.0(3)
C(6)-C(1)-Bi(1)	120.3(3)	C(2)-C(1)-Bi(1)	119.4(3)
C(4)-C(3)-C(2)	120.0(4)	C(24)-C(23)-C(22)	119.8(4)
C(25)-C(26)-C(21)	120.1(4)	C(42)-C(41)-C(40)	119.6(4)
C(27)-C(32)-C(39)	122.9(3)	C(31)-C(32)-C(39)	117.3(3)
C(31)-C(32)-C(27)	119.8(4)	C(42)-C(43)-C(44)	120.4(4)
C(27)-C(28)-C(33)	125.2(3)	C(29)-C(28)-C(27)	118.5(3)
C(29)-C(28)-C(33)	116.1(3)	N(1)-C(7)-C(2)	121.1(3)
C(4)-C(5)-C(6)	119.8(3)	C(23)-C(22)-C(21)	120.5(4)
C(38)-C(33)-C(28)	120.1(3)	C(38)-C(33)-C(34)	119.4(4)
C(34)-C(33)-C(28)	120.2(3)	C(39)-C(44)-C(43)	120.0(4)
C(43)-C(42)-C(41)	120.2(4)	C(37)-C(38)-C(33)	120.1(4)
C(9)-C(14)-C(21)	122.2(3)	C(13)-C(14)-C(21)	118.5(3)
C(13)-C(14)-C(9)	119.2(4)	C(14)-C(9)-N(1)	119.3(3)
C(14)-C(9)-C(10)	120.8(3)	C(10)-C(9)-N(1)	119.8(3)
C(34)-C(35)-C(36)	120.2(4)	C(24)-C(25)-C(26)	120.0(4)
C(12)-C(13)-C(14)	120.3(4)	C(30)-C(29)-C(28)	121.7(4)
C(5)-C(4)-C(3)	120.2(4)	C(35)-C(34)-C(33)	120.1(4)
C(9)-C(10)-C(15)	122.3(3)	C(11)-C(10)-C(9)	117.9(4)
C(11)-C(10)-C(15)	119.7(4)	Cl(3)-C(99)-Cl(4)	111.3(2)
C(19)-C(20)-C(15)	120.7(4)	C(11)-C(12)-C(13)	120.4(4)
C(20)-C(15)-C(10)	120.1(4)	C(16)-C(15)-C(10)	121.7(4)
C(16)-C(15)-C(20)	118.2(4)	C(12)-C(11)-C(10)	121.2(4)
C(30)-C(31)-C(32)	120.9(4)	C(36)-C(37)-C(38)	120.6(4)
C(23)-C(24)-C(25)	120.3(4)	C(17)-C(18)-C(19)	119.8(4)
C(18)-C(17)-C(16)	120.9(4)	C(15)-C(16)-C(17)	120.3(4)
C(31)-C(30)-C(29)	119.2(4)	C(20)-C(19)-C(18)	119.9(4)
C(37)-C(36)-C(35)	119.7(4)	Cl(2)-Bi(1)-Cl(1)	168.36(3)
N(2)-Bi(1)-Cl(1)	93.54(7)	N(2)-Bi(1)-Cl(2)	79.95(7)

N(1)-Bi(1)-Cl(1)	90.78(7)	N(1)-Bi(1)-Cl(2)	87.91(7)
N(1)-Bi(1)-N(2)	138.69(10)	C(1)-Bi(1)-Cl(1)	78.20(9)
C(1)-Bi(1)-Cl(2)	90.47(9)	C(1)-Bi(1)-N(2)	70.12(12)
C(1)-Bi(1)-N(1)	70.67(12)		

8.2. Single Crystal Structure Analysis of **3, 1· TCM**

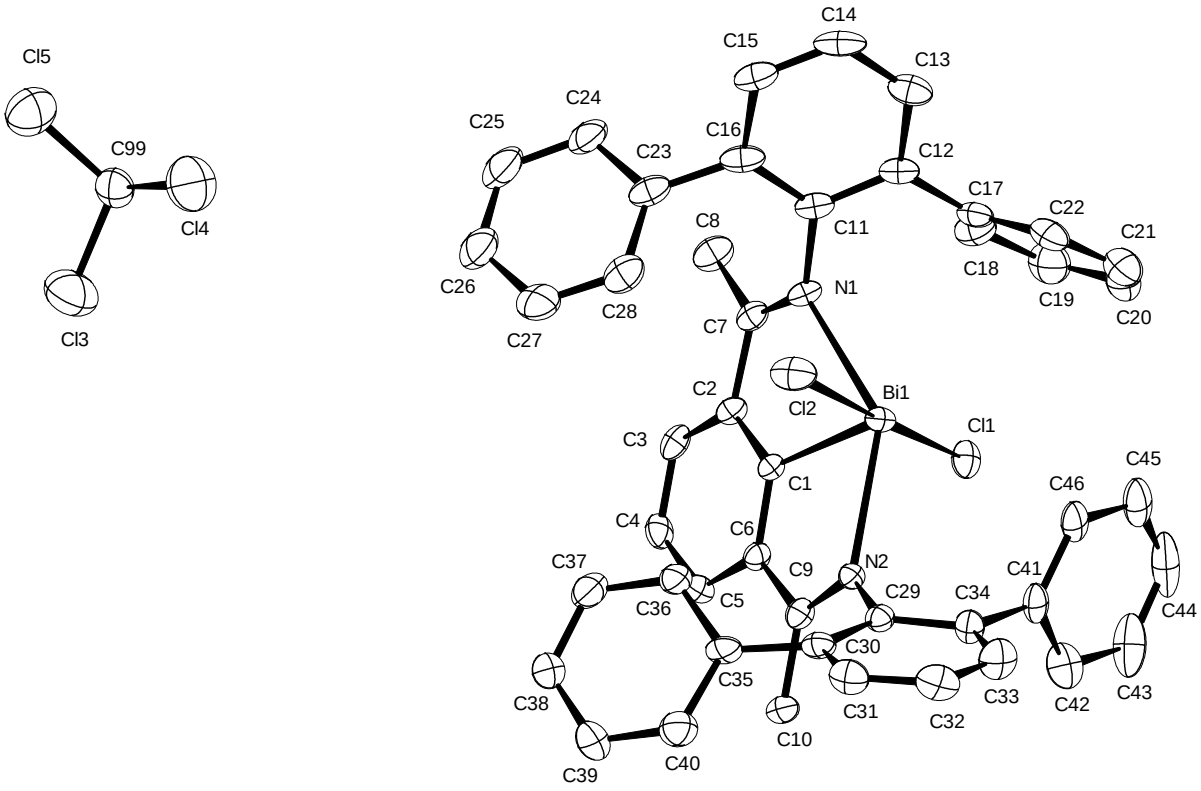

Figure S2. The molecular structure of complex **3 1· TCM**. H atoms have been removed for clarity.

X-ray Crystal Structure Analysis of complex 3 1·TCM: $C_{47}H_{36}BiCl_5N_2$, M_r = 4198.1(7) g mol^{-1}, light yellow plate, crystal size 0.11 x 0.09 x 0.04 mm^3, orthorhombic, *P*na2$_1$ [33], a = 17.5685(13) Å, b = 10.9004(5) Å, c = 21.922(3) Å, V = 4198.1(7) Å^3, T = 100(2) K, Z = 4, D_{calc} = 1.606 g·cm^3, λ = 0.71073 Å, μ(*Mo-K*α) = 4.554 mm^{-1}, analytical absorption correction (T_{min} = 0.62820, T_{max} = 0.84300), Bruker AXS Enraf-Nonius KappaCCD diffractometer with a FR591 rotating Mo-anode X-ray source, 2.879 < θ < 33.134°, 94400 measured reflections, 15965 independent reflections, 10813 reflections with $I > 2\sigma(I)$, R_{int} = 0.0855. The structure was solved by *SHELXS* and refined by full-matrix least-squares (*SHELXL*) against F^2 to R_1 = 0.0405 [$I > 2\sigma(I)$], wR_2 = 0.0630, 499 parameters.

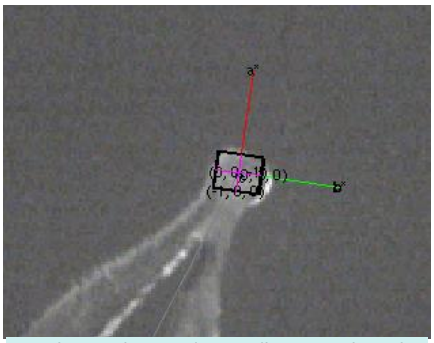

	h	k	l	distance (mm)
1.	0	0	-1	0.02
2.	0	0	1	0.02
3.	0	1	0	0.055
4.	0	-1	0	0.055
5.	-1	0	0	0.045
6.	1	0	0	0.045

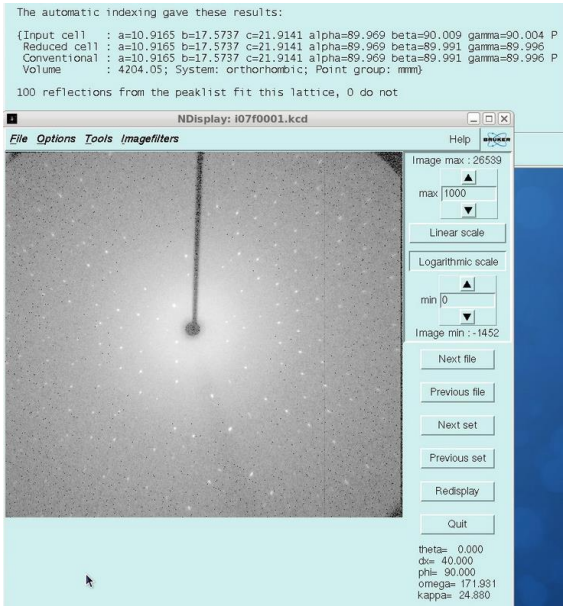

INTENSITY STATISTICS FOR DATASET

Resolution	#Data	#Theory	%Complete	Redundancy	Mean I	Mean I/s	Rmerge	Rsigma
Inf - 2.80	132	143	92.3	19.69	78.01	76.06	0.0352	0.0090
2.80 - 1.84	309	309	100.0	16.11	55.56	57.07	0.0364	0.0114
1.84 - 1.45	437	437	100.0	14.96	35.90	42.37	0.0424	0.0146
1.45 - 1.25	454	454	100.0	14.66	26.30	35.67	0.0510	0.0179
1.25 - 1.13	444	444	100.0	13.81	22.54	30.83	0.0550	0.0214
1.13 - 1.05	419	419	100.0	13.28	18.12	25.58	0.0674	0.0262
1.05 - 0.98	471	471	100.0	12.83	15.16	22.11	0.0795	0.0317
0.98 - 0.93	445	445	100.0	12.47	12.60	18.39	0.0933	0.0381
0.93 - 0.89	420	420	100.0	11.85	10.64	15.71	0.1085	0.0467
0.89 - 0.85	497	497	100.0	11.43	9.97	14.53	0.1200	0.0517
0.85 - 0.82	447	447	100.0	10.89	8.53	12.08	0.1406	0.0638
0.82 - 0.79	499	499	100.0	10.52	7.00	10.01	0.1723	0.0781
0.79 - 0.77	386	386	100.0	10.09	7.38	10.06	0.1759	0.0809
0.77 - 0.75	437	437	100.0	9.70	5.85	8.04	0.2191	0.1042
0.75 - 0.73	453	453	100.0	9.36	5.23	7.00	0.2532	0.1230
0.73 - 0.71	546	546	100.0	9.01	4.86	6.19	0.2672	0.1427
0.71 - 0.70	267	267	100.0	8.75	4.24	5.29	0.3003	0.1732
0.70 - 0.68	623	623	100.0	8.56	3.93	4.58	0.3474	0.2050
0.68 - 0.67	344	344	100.0	8.23	3.54	3.76	0.3897	0.2524
0.67 - 0.66	367	367	100.0	7.95	3.20	3.18	0.4272	0.3067
0.66 - 0.65	360	364	98.9	7.74	3.20	2.88	0.4508	0.3506
0.75 - 0.65	2960	2964	99.9	8.57	4.10	4.84	0.3259	0.2008
Inf - 0.65	8757	8772	99.8	11.24	13.67	17.28	0.0831	0.0459

The crystal appears to be twinned by inversion (TWIN -1 0 0 0 -1 0 0 0 -1) with a refined (BASF) 54.4% occupancy of the inverse structure.

Complete .cif-data of the compound are avaliable under the CCDC number **CCDC-2031446**.

Table S5. Crystal data and structure refinement.

Identification code	13155	
Empirical formula	$C_{47}H_{36}BiCl_5N_2$	
Color	yellow	
Formula weight	1015.01 $g \cdot mol^{-1}$	
Temperature	100(2) K	
Wavelength	0.71073 Å	
Crystal system	ORTHORHOMBIC	
Space group	*P*na2_1, (No. 33)	
Unit cell dimensions	a = 17.5685(13) Å	α= 90°.
	b = 10.9004(5) Å	β= 90°.
	c = 21.922(3) Å	γ = 90°.
Volume	4198.1(7) $Å^3$	
Z	4	
Density (calculated)	1.606 $Mg \cdot m^{-3}$	
Absorption coefficient	4.554 mm^{-1}	
F(000)	2000 e	
Crystal size	0.11 x 0.09 x 0.04 mm^3	
θ range for data collection	2.879 to 33.134°.	
Index ranges	$-27 \le h \le 27$, $-16 \le k \le 16$, $-33 \le l \le 33$	
Reflections collected	94400	
Independent reflections	15965 [R_{int} = 0.0855]	
Reflections with I>2σ(I)	10813	
Completeness to θ = 25.242°	99.8 %	
Absorption correction	Gaussian	
Max. and min. transmission	0.84 and 0.63	
Refinement method	Full-matrix least-squares on F^2	
Data / restraints / parameters	15965 / 1 / 499	
Goodness-of-fit on F^2	1.028	
Final R indices [I>2σ(I)]	R_1 = 0.0405	wR^2 = 0.0630
R indices (all data)	R_1 = 0.0827	wR^2 = 0.0727
Absolute structure parameter	0.544(6)	
Largest diff. peak and hole	1.8 and -1.4 $e \cdot Å^{-3}$	

Table S6. Bond lengths [Å] and angles [°].

Bi(1)-Cl(1)	2.6209(17)	Bi(1)-Cl(2)	2.7438(16)
Bi(1)-N(1)	2.493(5)	Bi(1)-N(2)	2.499(5)
Bi(1)-C(1)	2.212(6)	N(1)-C(7)	1.293(8)
N(1)-C(11)	1.428(8)	N(2)-C(9)	1.296(8)
N(2)-C(29)	1.435(8)	C(1)-C(2)	1.382(8)
C(1)-C(6)	1.386(8)	C(2)-C(3)	1.391(8)
C(2)-C(7)	1.493(9)	C(3)-C(4)	1.387(9)
C(4)-C(5)	1.385(9)	C(5)-C(6)	1.409(8)
C(6)-C(9)	1.483(8)	C(7)-C(8)	1.486(8)
C(9)-C(10)	1.494(9)	C(11)-C(12)	1.402(9)
C(11)-C(16)	1.406(9)	C(12)-C(13)	1.402(9)
C(12)-C(17)	1.489(9)	C(13)-C(14)	1.373(10)
C(14)-C(15)	1.389(11)	C(15)-C(16)	1.401(9)
C(16)-C(23)	1.510(11)	C(17)-C(18)	1.379(10)
C(17)-C(22)	1.385(10)	C(18)-C(19)	1.403(12)
C(19)-C(20)	1.368(11)	C(20)-C(21)	1.378(13)
C(21)-C(22)	1.390(11)	C(23)-C(24)	1.383(9)
C(23)-C(28)	1.403(12)	C(24)-C(25)	1.398(11)
C(25)-C(26)	1.343(12)	C(26)-C(27)	1.385(11)
C(27)-C(28)	1.392(11)	C(29)-C(30)	1.407(9)
C(29)-C(34)	1.402(8)	C(30)-C(31)	1.386(9)
C(30)-C(35)	1.481(10)	C(31)-C(32)	1.384(9)
C(32)-C(33)	1.388(10)	C(33)-C(34)	1.389(9)
C(34)-C(41)	1.495(9)	C(35)-C(36)	1.422(10)
C(35)-C(40)	1.411(10)	C(36)-C(37)	1.381(10)
C(37)-C(38)	1.389(10)	C(38)-C(39)	1.391(10)
C(39)-C(40)	1.375(10)	C(41)-C(42)	1.401(10)
C(41)-C(46)	1.389(10)	C(42)-C(43)	1.386(10)
C(43)-C(44)	1.357(13)	C(44)-C(45)	1.359(12)
C(45)-C(46)	1.396(10)	Cl(3)-C(99)	1.751(8)
Cl(4)-C(99)	1.743(7)	Cl(5)-C(99)	1.757(8)
Cl(1)-Bi(1)-Cl(2)	178.29(6)	N(1)-Bi(1)-Cl(1)	93.30(13)
N(1)-Bi(1)-Cl(2)	86.18(12)	N(1)-Bi(1)-N(2)	138.97(17)

N(2)-Bi(1)-Cl(1)	92.05(12)	N(2)-Bi(1)-Cl(2)	89.41(12)
C(1)-Bi(1)-Cl(1)	80.16(16)	C(1)-Bi(1)-Cl(2)	101.19(16)
C(1)-Bi(1)-N(1)	70.37(19)	C(1)-Bi(1)-N(2)	70.57(19)
C(7)-N(1)-Bi(1)	113.4(4)	C(7)-N(1)-C(11)	123.7(5)
C(11)-N(1)-Bi(1)	122.8(4)	C(9)-N(2)-Bi(1)	113.3(4)
C(9)-N(2)-C(29)	122.8(5)	C(29)-N(2)-Bi(1)	123.4(4)
C(2)-C(1)-Bi(1)	119.2(5)	C(2)-C(1)-C(6)	121.0(6)
C(6)-C(1)-Bi(1)	118.5(4)	C(1)-C(2)-C(3)	120.1(6)
C(1)-C(2)-C(7)	117.8(5)	C(3)-C(2)-C(7)	122.1(5)
C(4)-C(3)-C(2)	119.2(6)	C(5)-C(4)-C(3)	121.2(6)
C(4)-C(5)-C(6)	119.4(6)	C(1)-C(6)-C(5)	119.0(5)
C(1)-C(6)-C(9)	118.6(5)	C(5)-C(6)-C(9)	122.3(6)
N(1)-C(7)-C(2)	116.8(5)	N(1)-C(7)-C(8)	123.9(6)
C(8)-C(7)-C(2)	119.3(5)	N(2)-C(9)-C(6)	116.7(6)
N(2)-C(9)-C(10)	123.9(5)	C(6)-C(9)-C(10)	119.4(5)
C(12)-C(11)-N(1)	118.3(6)	C(12)-C(11)-C(16)	120.9(6)
C(16)-C(11)-N(1)	120.5(6)	C(11)-C(12)-C(17)	121.9(6)
C(13)-C(12)-C(11)	118.3(6)	C(13)-C(12)-C(17)	119.7(6)
C(12)-C(13)-H(13)	119.4	C(14)-C(13)-C(12)	121.1(7)
C(13)-C(14)-C(15)	120.5(6)	C(14)-C(15)-C(16)	120.2(6)
C(11)-C(16)-C(23)	123.4(6)	C(15)-C(16)-C(11)	118.8(7)
C(15)-C(16)-C(23)	117.8(6)	C(18)-C(17)-C(12)	119.9(6)
C(18)-C(17)-C(22)	118.7(7)	C(22)-C(17)-C(12)	121.1(7)
C(17)-C(18)-C(19)	121.0(8)	C(20)-C(19)-C(18)	120.0(9)
C(19)-C(20)-C(21)	119.1(9)	C(20)-C(21)-C(22)	121.4(8)
C(17)-C(22)-C(21)	119.8(8)	C(24)-C(23)-C(16)	118.8(8)
C(24)-C(23)-C(28)	118.7(8)	C(28)-C(23)-C(16)	122.5(6)
C(23)-C(24)-C(25)	119.3(7)	C(26)-C(25)-C(24)	122.1(7)
C(25)-C(26)-C(27)	119.7(8)	C(26)-C(27)-C(28)	119.7(8)
C(27)-C(28)-C(23)	120.4(7)	C(30)-C(29)-N(2)	120.4(5)
C(34)-C(29)-N(2)	118.9(6)	C(34)-C(29)-C(30)	120.6(6)
C(29)-C(30)-C(35)	122.8(6)	C(31)-C(30)-C(29)	118.4(6)
C(31)-C(30)-C(35)	118.5(6)	C(32)-C(31)-C(30)	121.3(7)
C(31)-C(32)-C(33)	119.9(6)	C(32)-C(33)-C(34)	120.4(7)
C(29)-C(34)-C(41)	121.5(5)	C(33)-C(34)-C(29)	119.2(6)
C(33)-C(34)-C(41)	119.3(6)	C(36)-C(35)-C(30)	123.2(7)
C(40)-C(35)-C(30)	120.5(7)	C(40)-C(35)-C(36)	116.2(8)
C(37)-C(36)-C(35)	120.4(8)	C(36)-C(37)-C(38)	121.0(7)

C(37)-C(38)-C(39)	120.3(7)	C(40)-C(39)-C(38)	118.4(7)
C(39)-C(40)-C(35)	123.6(7)	C(42)-C(41)-C(34)	120.5(7)
C(46)-C(41)-C(34)	122.0(6)	C(46)-C(41)-C(42)	117.4(7)
C(43)-C(42)-C(41)	120.4(8)	C(44)-C(43)-C(42)	121.3(9)
C(43)-C(44)-C(45)	119.4(8)	C(44)-C(45)-C(46)	120.8(9)
C(41)-C(46)-C(45)	120.6(8)	Cl(3)-C(99)-Cl(5)	110.2(4)
Cl(4)-C(99)-Cl(3)	110.7(4)	Cl(4)-C(99)-Cl(5)	110.5(5)

8.3. Single Crystal Structure Analysis of **4, 1·*n*-Pentane**

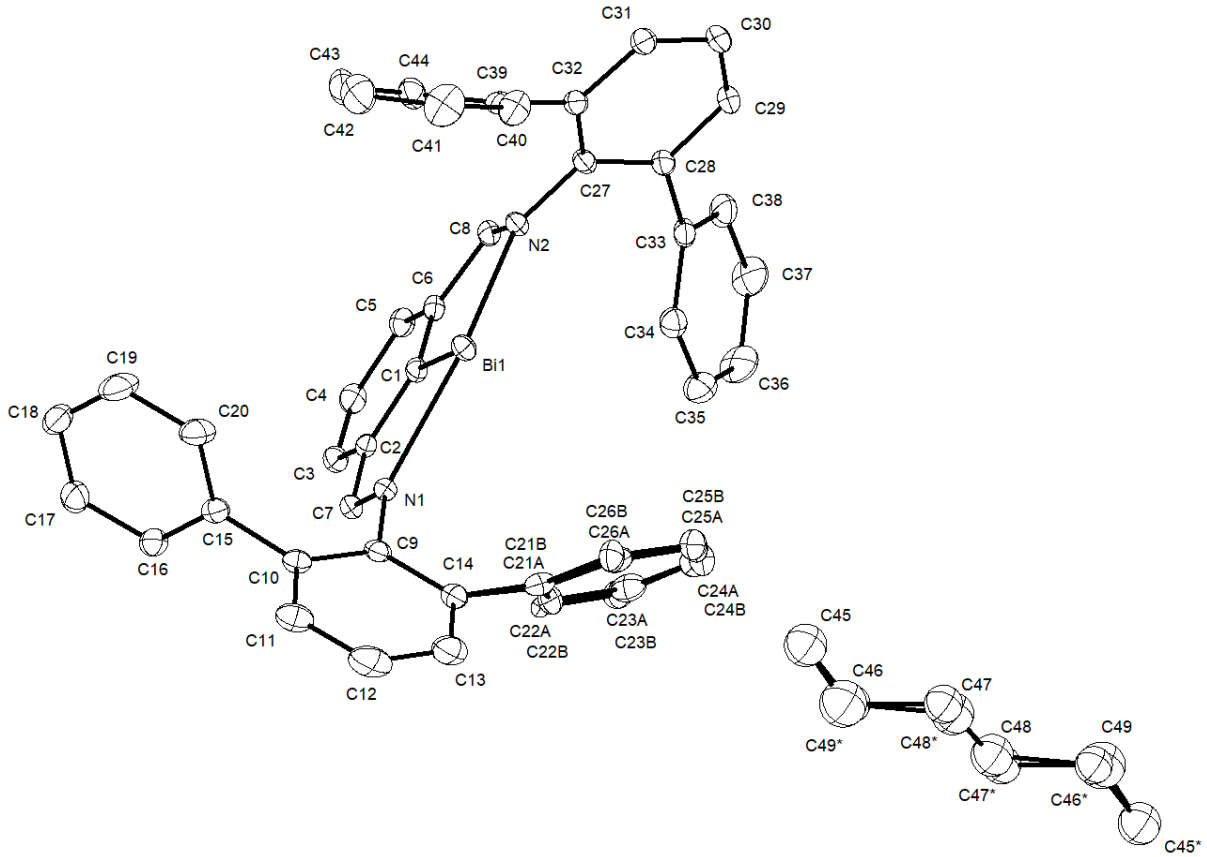

Figure S3. The molecular structure of complex **4 1·*n*-pentane**. H atoms have been removed for clarity.

X-ray Crystal Structure Analysis of complex 4 1·*n*-Pentane: $C_{46.50}H_{37}BiN_2$, M_r = 832.76 g mol^{-1}, red plate, crystal size 0.067 x 0.037 x 0.012 mm^3, triclinic, space group $P\bar{1}$ [2], a = 11.4047(5) Å, b = 12.3940(5) Å, c = 14.2472(6) Å, α = 71.805(2)°, β = 69.902(2) °, γ = 75.783(2)°, V = 1774.93(13) Å^3, T = 100(2) K, Z = 2, D_{calc} = 1.558 g·cm^3, λ = 0.71073 Å, μ(*Mo-K*$_\alpha$) = 5.003 mm^{-1}, analytical absorption correction (T_{min} = 0.77530, T_{max} = 0.95494), Bruker-AXS Kappa Mach3 with APEX-II detector and IμS micro focuse source, 1.751 < θ < 34.091°, 68161 measured reflections, 14308 independent reflections, 12427 reflections with $I > 2\sigma(I)$, R_{int} = 0.0361. The structure was solved by *SHELXT* and refined by full-matrix least-squares (*SHELXL*) against F^2 to R_1 = 0.0272 [$I > 2\sigma(I)$], wR_2 = 0.0498, 500 parameters.

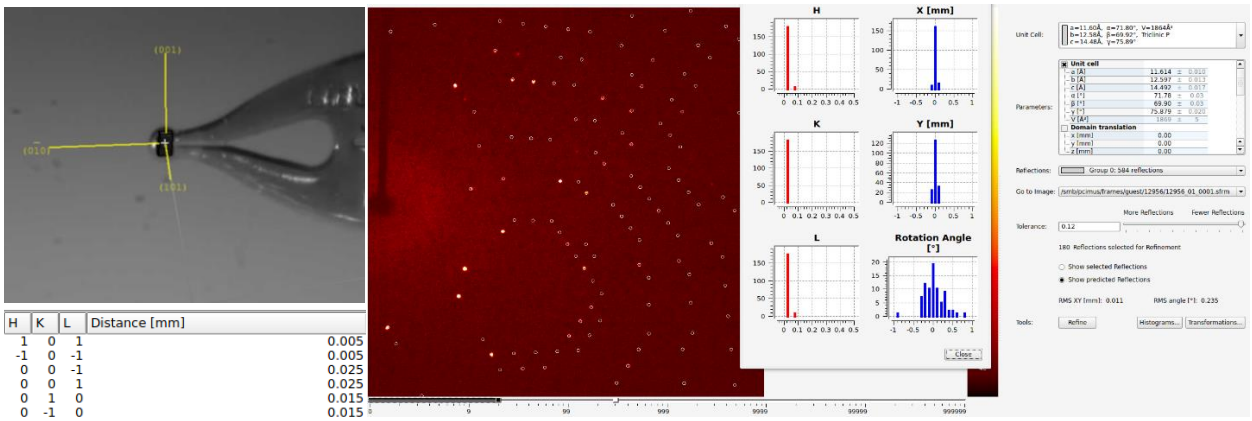

H	K	L	Distance [mm]
1	0	1	0.005
-1	0	-1	0.005
0	0	-1	0.025
0	0	1	0.025
0	1	0	0.015
0	-1	0	0.015

INTENSITY STATISTICS FOR DATASET

Resolution	#Data	#Theory	%Complete	Redundancy	Mean I	Mean I/s	Rmerge	Rsigma
Inf - 2.59	215	215	100.0	9.48	137.25	112.43	0.0169	0.0074
2.59 - 1.73	507	507	100.0	9.50	91.06	95.73	0.0182	0.0086
1.73 - 1.37	724	724	100.0	9.48	61.74	79.15	0.0221	0.0103
1.37 - 1.20	713	713	100.0	9.16	48.75	66.26	0.0271	0.0125
1.20 - 1.09	721	721	100.0	8.50	40.01	54.41	0.0327	0.0152
1.09 - 1.01	730	730	100.0	6.26	34.42	40.35	0.0374	0.0213
1.01 - 0.95	719	719	100.0	5.20	29.24	32.36	0.0427	0.0270
0.95 - 0.90	772	772	100.0	4.48	24.34	25.58	0.0520	0.0342
0.90 - 0.86	747	747	100.0	4.05	22.33	22.19	0.0517	0.0396
0.86 - 0.83	654	654	100.0	3.90	18.71	18.51	0.0595	0.0471
0.83 - 0.80	770	770	100.0	3.68	17.98	17.01	0.0653	0.0524
0.80 - 0.77	862	862	100.0	3.59	15.53	14.51	0.0730	0.0615
0.77 - 0.75	674	674	100.0	3.42	14.84	13.46	0.0789	0.0683
0.75 - 0.73	749	749	100.0	3.32	12.86	11.37	0.0903	0.0792
0.73 - 0.71	834	835	99.9	3.20	11.40	10.04	0.1024	0.0918
0.71 - 0.70	445	446	99.8	3.16	11.19	9.67	0.1125	0.0958
0.70 - 0.68	966	973	99.3	2.99	9.40	8.13	0.1234	0.1150
0.68 - 0.67	546	549	99.5	2.93	8.50	7.33	0.1442	0.1304
0.67 - 0.66	562	567	99.1	2.90	7.62	6.60	0.1545	0.1441
0.66 - 0.64	1215	1256	96.7	2.55	7.19	5.78	0.1723	0.1706
0.64 - 0.63	184	403	45.7	0.69	6.39	3.54	0.2004	0.2646
0.73 - 0.63	4752	5029	94.5	2.73	8.92	7.56	0.1315	0.1278
Inf - 0.63	14309	14586	98.1	4.67	25.66	27.73	0.0358	0.0363

One low-angle reflection [0 0 1] was shadowed by the beamstop and removed from the data set before the final refinement cycles. One phenyl ring shows disorder over two positions with 50:50 occupancy. The structure contains an *n*-pentane molecule disordered about a crystallographic special position (inversion centre) with 50:50 occupancy.

Complete .cif-data of the compound are avaliable under the CCDC number **CCDC-2031445**.

Table S7. Crystal data and structure refinement.

Identification code	12956	
Empirical formula	$C_{46.50}H_{37}BiN_2$	
Color	red	
Formula weight	832.76 $g \cdot mol^{-1}$	
Temperature	100(2) K	
Wavelength	0.71073 Å	
Crystal system	Triclinic	
Space group	$P\bar{1}$, (No. 2)	
Unit cell dimensions	a = 11.4047(5) Å	α= 71.805(2)°.
	b = 12.3940(5) Å	β= 69.902(2)°.
	c = 14.2472(6) Å	γ = 75.783(2)°.
Volume	1774.93(13) $Å^3$	
Z	2	
Density (calculated)	1.558 $Mg \cdot m^{-3}$	
Absorption coefficient	5.003 mm^{-1}	
F(000)	826 e	
Crystal size	0.067 x 0.037 x 0.012 mm^3	
θ range for data collection	1.751 to 34.091°.	
Index ranges	$-17 \le h \le 17$, $-19 \le k \le 19$, $-22 \le l \le 22$	
Reflections collected	68161	
Independent reflections	14308 [R_{int} = 0.0361]	
Reflections with I>2σ(I)	12427	
Completeness to θ = 25.242°	100.0 %	
Absorption correction	Gaussian	
Max. and min. transmission	0.95494 and 0.77530	
Refinement method	Full-matrix least-squares on F^2	
Data / restraints / parameters	14308 / 0 / 500	
Goodness-of-fit on F^2	1.050	
Final R indices [I>2σ(I)]	R_1 = 0.0272	wR^2 = 0.0498
R indices (all data)	R_1 = 0.0374	wR^2 = 0.0521
Extinction coefficient	n/a	
Largest diff. peak and hole	1.244 and -1.359 $e \cdot Å^{-3}$	

Table S8. Bond lengths [Å] and angles [°].

Bi(1)-N(1)	2.4601(15)	Bi(1)-N(2)	2.5066(15)
Bi(1)-C(1)	2.1487(19)	N(1)-C(7)	1.301(3)
N(1)-C(9)	1.420(2)	N(2)-C(8)	1.300(2)
N(2)-C(27)	1.425(2)	C(1)-C(2)	1.412(2)
C(1)-C(6)	1.410(3)	C(2)-C(3)	1.403(3)
C(2)-C(7)	1.437(3)	C(3)-H(3)	0.9500
C(3)-C(4)	1.388(3)	C(4)-H(4)	0.9500
C(4)-C(5)	1.398(3)	C(5)-H(5)	0.9500
C(5)-C(6)	1.397(3)	C(6)-C(8)	1.443(2)
C(7)-H(7)	0.9500	C(8)-H(8)	0.9500
C(9)-C(10)	1.406(3)	C(9)-C(14)	1.409(3)
C(10)-C(11)	1.397(3)	C(10)-C(15)	1.496(3)
C(11)-H(11)	0.9500	C(11)-C(12)	1.386(3)
C(12)-H(12)	0.9500	C(12)-C(13)	1.379(4)
C(13)-H(13)	0.9500	C(13)-C(14)	1.387(3)
C(14)-C(21A)	1.611(8)	C(14)-C(21B)	1.395(10)
C(15)-C(20)	1.387(3)	C(15)-C(16)	1.391(3)
C(20)-H(20)	0.9500	C(20)-C(19)	1.392(4)
C(19)-H(19)	0.9500	C(19)-C(18)	1.376(4)
C(18)-H(18)	0.9500	C(18)-C(17)	1.382(3)
C(17)-H(17)	0.9500	C(17)-C(16)	1.391(3)
C(16)-H(16)	0.9500	C(27)-C(28)	1.416(3)
C(27)-C(32)	1.405(3)	C(28)-C(29)	1.400(3)
C(28)-C(33)	1.493(3)	C(29)-H(29)	0.9500
C(29)-C(30)	1.379(3)	C(30)-H(30)	0.9500
C(30)-C(31)	1.381(3)	C(31)-H(31)	0.9500
C(31)-C(32)	1.400(3)	C(33)-C(34)	1.401(3)
C(33)-C(38)	1.394(3)	C(34)-H(34)	0.9500
C(34)-C(35)	1.384(3)	C(35)-H(35)	0.9500
C(35)-C(36)	1.383(3)	C(36)-H(36)	0.9500
C(36)-C(37)	1.377(4)	C(37)-H(37)	0.9500
C(37)-C(38)	1.396(3)	C(38)-H(38)	0.9500
C(39)-C(40)	1.403(3)	C(39)-C(44)	1.391(3)
C(39)-C(32)	1.490(3)	C(40)-H(40)	0.9500
C(40)-C(41)	1.390(3)	C(41)-H(41)	0.9500
C(41)-C(42)	1.385(4)	C(42)-H(42)	0.9500

C(42)-C(43)	1.391(4)	C(43)-H(43)	0.9500
C(43)-C(44)	1.385(3)	C(44)-H(44)	0.9500
C(21A)-C(22A)	1.372(9)	C(21A)-C(26A)	1.397(11)
C(22A)-H(22A)	0.9500	C(22A)-C(23A)	1.427(11)
C(23A)-H(23A)	0.9500	C(23A)-C(24A)	1.369(9)
C(24A)-H(24A)	0.9500	C(24A)-C(25A)	1.366(10)
C(25A)-H(25A)	0.9500	C(25A)-C(26A)	1.413(10)
C(26A)-H(26A)	0.9500	C(21B)-C(22B)	1.397(10)
C(21B)-C(26B)	1.374(11)	C(22B)-H(22B)	0.9500
C(22B)-C(23B)	1.367(13)	C(23B)-H(23B)	0.9500
C(23B)-C(24B)	1.390(9)	C(24B)-H(24B)	0.9500
C(24B)-C(25B)	1.376(8)	C(25B)-H(25B)	0.9500
C(25B)-C(26B)	1.394(9)	C(26B)-H(26B)	0.9500
C(48)-H(48A)	0.9900	C(48)-H(48B)	0.9900
C(48)-C(49)	1.514(10)	C(48)-C(47)	1.424(9)
C(46)-H(46A)	0.9900	C(46)-H(46B)	0.9900
C(46)-C(45)	1.470(8)	C(46)-C(47)	1.543(9)
C(45)-H(45A)	0.9800	C(45)-H(45B)	0.9800
C(45)-H(45C)	0.9800	C(49)-H(49A)	0.9800
C(49)-H(49B)	0.9800	C(49)-H(49C)	0.9800
C(47)-H(47A)	0.9900	C(47)-H(47B)	0.9900

N(1)-Bi(1)-N(2)	142.49(5)	C(1)-Bi(1)-N(1)	71.44(6)
C(1)-Bi(1)-N(2)	71.22(6)	C(7)-N(1)-Bi(1)	112.81(12)
C(7)-N(1)-C(9)	120.80(15)	C(9)-N(1)-Bi(1)	126.36(12)
C(8)-N(2)-Bi(1)	111.50(11)	C(8)-N(2)-C(27)	118.65(16)
C(27)-N(2)-Bi(1)	128.22(12)	C(2)-C(1)-Bi(1)	120.12(14)
C(6)-C(1)-Bi(1)	120.69(13)	C(6)-C(1)-C(2)	119.18(17)
C(1)-C(2)-C(7)	117.06(17)	C(3)-C(2)-C(1)	119.77(17)
C(3)-C(2)-C(7)	123.14(17)	C(2)-C(3)-H(3)	119.8
C(4)-C(3)-C(2)	120.41(17)	C(4)-C(3)-H(3)	119.8
C(3)-C(4)-H(4)	119.8	C(3)-C(4)-C(5)	120.31(18)
C(5)-C(4)-H(4)	119.8	C(4)-C(5)-H(5)	120.0
C(6)-C(5)-C(4)	119.99(18)	C(6)-C(5)-H(5)	120.0
C(1)-C(6)-C(8)	117.24(17)	C(5)-C(6)-C(1)	120.33(17)
C(5)-C(6)-C(8)	122.35(17)	N(1)-C(7)-C(2)	118.49(16)
N(1)-C(7)-H(7)	120.8	C(2)-C(7)-H(7)	120.8
N(2)-C(8)-C(6)	119.25(17)	N(2)-C(8)-H(8)	120.4

C(6)-C(8)-H(8)	120.4	C(10)-C(9)-N(1)	120.57(17)
C(10)-C(9)-C(14)	120.43(19)	C(14)-C(9)-N(1)	118.82(17)
C(9)-C(10)-C(15)	122.13(17)	C(11)-C(10)-C(9)	118.43(19)
C(11)-C(10)-C(15)	119.34(18)	C(10)-C(11)-H(11)	119.5
C(12)-C(11)-C(10)	121.1(2)	C(12)-C(11)-H(11)	119.5
C(11)-C(12)-H(12)	120.0	C(13)-C(12)-C(11)	120.1(2)
C(13)-C(12)-H(12)	120.0	C(12)-C(13)-H(13)	119.6
C(12)-C(13)-C(14)	120.8(2)	C(14)-C(13)-H(13)	119.6
C(9)-C(14)-C(21A)	116.2(3)	C(13)-C(14)-C(9)	119.2(2)
C(13)-C(14)-C(21A)	124.3(4)	C(13)-C(14)-C(21B)	115.1(4)
C(21B)-C(14)-C(9)	125.3(4)	C(20)-C(15)-C(10)	119.21(19)
C(20)-C(15)-C(16)	118.2(2)	C(16)-C(15)-C(10)	122.42(17)
C(15)-C(20)-H(20)	119.5	C(15)-C(20)-C(19)	121.0(2)
C(19)-C(20)-H(20)	119.5	C(20)-C(19)-H(19)	119.9
C(18)-C(19)-C(20)	120.1(2)	C(18)-C(19)-H(19)	119.9
C(19)-C(18)-H(18)	120.2	C(19)-C(18)-C(17)	119.7(2)
C(17)-C(18)-H(18)	120.2	C(18)-C(17)-H(17)	119.9
C(18)-C(17)-C(16)	120.2(2)	C(16)-C(17)-H(17)	119.9
C(15)-C(16)-H(16)	119.6	C(17)-C(16)-C(15)	120.8(2)
C(17)-C(16)-H(16)	119.6	C(28)-C(27)-N(2)	119.85(17)
C(32)-C(27)-N(2)	119.68(16)	C(32)-C(27)-C(28)	120.34(16)
C(27)-C(28)-C(33)	123.67(16)	C(29)-C(28)-C(27)	118.25(18)
C(29)-C(28)-C(33)	117.81(17)	C(28)-C(29)-H(29)	119.3
C(30)-C(29)-C(28)	121.45(19)	C(30)-C(29)-H(29)	119.3
C(29)-C(30)-H(30)	120.1	C(29)-C(30)-C(31)	119.83(18)
C(31)-C(30)-H(30)	120.1	C(30)-C(31)-H(31)	119.5
C(30)-C(31)-C(32)	121.05(19)	C(32)-C(31)-H(31)	119.5
C(34)-C(33)-C(28)	121.17(18)	C(38)-C(33)-C(28)	120.41(18)
C(38)-C(33)-C(34)	118.20(19)	C(33)-C(34)-H(34)	119.6
C(35)-C(34)-C(33)	120.8(2)	C(35)-C(34)-H(34)	119.6
C(34)-C(35)-H(35)	119.8	C(36)-C(35)-C(34)	120.3(2)
C(36)-C(35)-H(35)	119.8	C(35)-C(36)-H(36)	120.1
C(37)-C(36)-C(35)	119.8(2)	C(37)-C(36)-H(36)	120.1
C(36)-C(37)-H(37)	119.9	C(36)-C(37)-C(38)	120.3(2)
C(38)-C(37)-H(37)	119.9	C(33)-C(38)-C(37)	120.6(2)
C(33)-C(38)-H(38)	119.7	C(37)-C(38)-H(38)	119.7
C(40)-C(39)-C(32)	118.93(18)	C(44)-C(39)-C(40)	118.06(19)
C(44)-C(39)-C(32)	122.92(19)	C(39)-C(40)-H(40)	119.6

C(41)-C(40)-C(39)	120.8(2)	C(41)-C(40)-H(40)	119.6
C(40)-C(41)-H(41)	119.9	C(42)-C(41)-C(40)	120.2(2)
C(42)-C(41)-H(41)	119.9	C(41)-C(42)-H(42)	120.3
C(41)-C(42)-C(43)	119.4(2)	C(43)-C(42)-H(42)	120.3
C(42)-C(43)-H(43)	119.9	C(44)-C(43)-C(42)	120.2(2)
C(44)-C(43)-H(43)	119.9	C(39)-C(44)-H(44)	119.4
C(43)-C(44)-C(39)	121.2(2)	C(43)-C(44)-H(44)	119.4
C(27)-C(32)-C(39)	123.34(16)	C(31)-C(32)-C(27)	118.87(18)
C(31)-C(32)-C(39)	117.78(17)	C(22A)-C(21A)-C(14)	124.5(7)
C(22A)-C(21A)-C(26A)	119.0(7)	C(26A)-C(21A)-C(14)	116.4(5)
C(21A)-C(22A)-H(22A)	119.7	C(21A)-C(22A)-C(23A)	120.7(6)
C(23A)-C(22A)-H(22A)	119.7	C(22A)-C(23A)-H(23A)	120.4
C(24A)-C(23A)-C(22A)	119.2(6)	C(24A)-C(23A)-H(23A)	120.4
C(23A)-C(24A)-H(24A)	119.5	C(25A)-C(24A)-C(23A)	121.0(6)
C(25A)-C(24A)-H(24A)	119.5	C(24A)-C(25A)-H(25A)	120.0
C(24A)-C(25A)-C(26A)	120.0(6)	C(26A)-C(25A)-H(25A)	120.0
C(21A)-C(26A)-C(25A)	120.0(6)	C(21A)-C(26A)-H(26A)	120.0
C(25A)-C(26A)-H(26A)	120.0	C(14)-C(21B)-C(22B)	116.4(7)
C(26B)-C(21B)-C(14)	126.1(5)	C(26B)-C(21B)-C(22B)	117.4(9)
C(21B)-C(22B)-H(22B)	118.6	C(23B)-C(22B)-C(21B)	122.8(7)
C(23B)-C(22B)-H(22B)	118.6	C(22B)-C(23B)-H(23B)	120.4
C(22B)-C(23B)-C(24B)	119.2(6)	C(24B)-C(23B)-H(23B)	120.4
C(23B)-C(24B)-H(24B)	120.5	C(25B)-C(24B)-C(23B)	118.9(7)
C(25B)-C(24B)-H(24B)	120.5	C(24B)-C(25B)-H(25B)	119.4
C(24B)-C(25B)-C(26B)	121.2(7)	C(26B)-C(25B)-H(25B)	119.4
C(21B)-C(26B)-C(25B)	120.4(6)	C(21B)-C(26B)-H(26B)	119.8
C(25B)-C(26B)-H(26B)	119.8	H(48A)-C(48)-H(48B)	107.0
C(49)-C(48)-H(48A)	107.6	C(49)-C(48)-H(48B)	107.6
C(47)-C(48)-H(48A)	107.6	C(47)-C(48)-H(48B)	107.6
C(47)-C(48)-C(49)	118.9(5)	H(46A)-C(46)-H(46B)	107.2
C(45)-C(46)-H(46A)	107.9	C(45)-C(46)-H(46B)	107.9
C(45)-C(46)-C(47)	117.5(5)	C(47)-C(46)-H(46A)	107.9
C(47)-C(46)-H(46B)	107.9	C(46)-C(45)-H(45A)	109.5
C(46)-C(45)-H(45B)	109.5	C(46)-C(45)-H(45C)	109.5
H(45A)-C(45)-H(45B)	109.5	H(45A)-C(45)-H(45C)	109.5
H(45B)-C(45)-H(45C)	109.5	C(48)-C(49)-H(49A)	109.5
C(48)-C(49)-H(49B)	109.5	C(48)-C(49)-H(49C)	109.5
H(49A)-C(49)-H(49B)	109.5	H(49A)-C(49)-H(49C)	109.5

H(49B)-C(49)-H(49C)	109.5	C(48)-C(47)-C(46)	120.3(5)
C(48)-C(47)-H(47A)	107.3	C(48)-C(47)-H(47B)	107.3
C(46)-C(47)-H(47A)	107.3	C(46)-C(47)-H(47B)	107.3
H(47A)-C(47)-H(47B)	106.9		

8.4. Single Crystal Structure Analysis of **5**

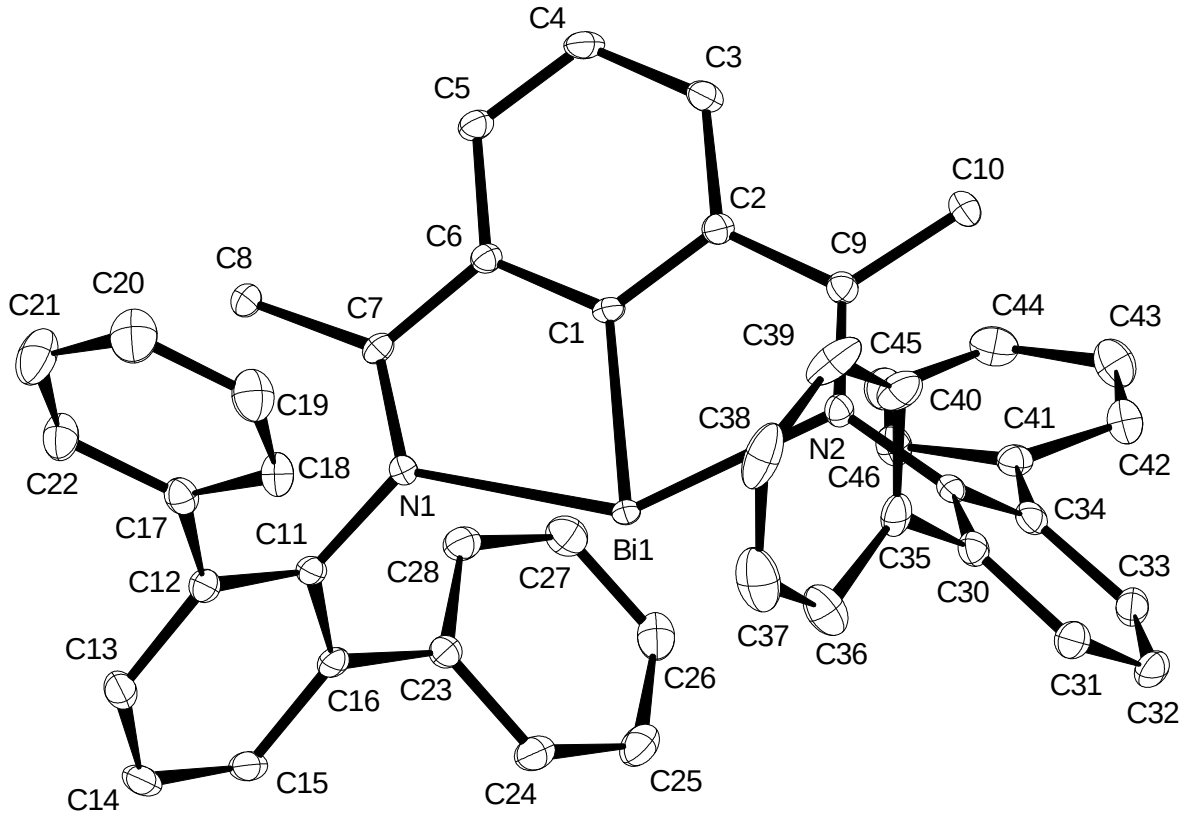

Figure S4. The molecular structure of complex **5**. H atoms have been removed for clarity.

X-ray Crystal Structure Analysis of complex 5 $C_{46}H_{35}BiN_2$, M_r = 824.74 g mol^{-1}, dark brown prism, crystal size 0.23 x 0.17 x 0.10 mm^3, triclinic, $P\bar{1}$ [2], a = 11.5135(13) Å, b = 11.9576(6) Å, c = 13.7914(16) Å, α= 88.445(7)°, β= 73.593(11)°, γ = 78.419(7)°, V = 1783.4(3) Å^3, T = 100(2) K, Z = 2, D_{calc} = 1.536 g·cm^3, λ = 0.71073 Å, μ(*Mo-K*$_\alpha$) = 4.978 mm^{-1}, analytical absorption correction (T_{min} = 0.35936, T_{max} = 0.64959), Bruker AXS Enraf-Nonius KappaCCD diffractometer with a FR591 rotating Mo-anode X-ray source, 2.749 < θ < 27.500°, 37792 measured reflections, 8180 independent reflections, 7986 reflections with $I > 2\sigma(I)$, R_{int} = 0.0374. The structure was solved by *SHELXS* and refined by full-matrix least-squares (*SHELXL*) against F^2 to R_1 = 0.0177 [$I > 2\sigma(I)$], wR_2 = 0.0445, 444 parameters.

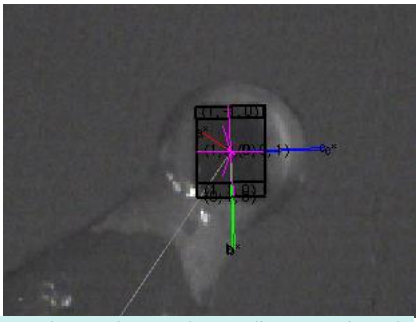

	h	k	l	distance (mm)
1.	0	0	-1	0.085
2.	0	0	1	0.085
3.	0	-1	0	0.115
4.	0	1	0	0.115
5.	-1	0	0	0.05
6.	1	0	0	0.05
7.	1	-1	0	0.085
8.	1	1	0	0.1

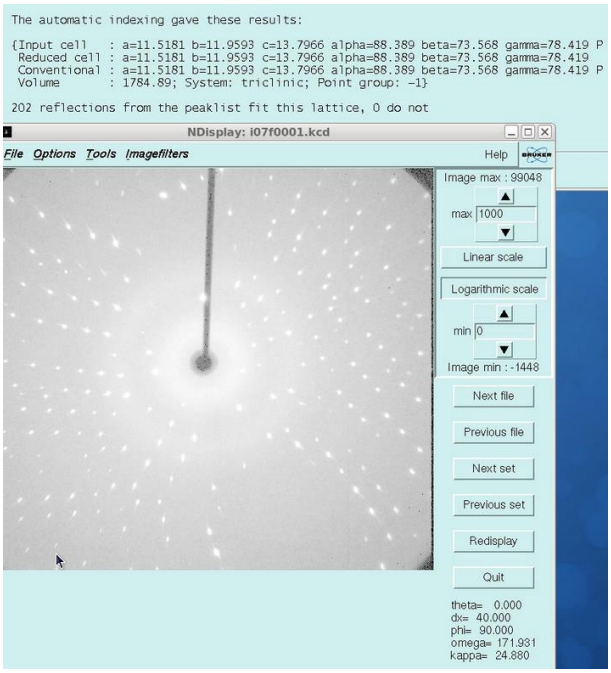

INTENSITY STATISTICS FOR DATASET

Resolution	#Data	#Theory	%Complete	Redundancy	Mean I	Mean I/s	Rmerge	Rsigma
Inf - 2.22	333	343	97.1	4.47	202.93	43.10	0.0429	0.0238
2.22 - 1.49	783	783	100.0	5.09	149.07	44.48	0.0373	0.0208
1.49 - 1.19	1096	1096	100.0	5.15	100.69	41.53	0.0354	0.0212
1.19 - 1.03	1203	1203	100.0	4.97	78.22	38.55	0.0352	0.0224
1.03 - 0.94	1082	1082	100.0	4.69	63.43	35.28	0.0371	0.0240
0.94 - 0.87	1172	1172	100.0	4.45	50.21	31.60	0.0373	0.0261
0.87 - 0.82	1087	1087	100.0	4.25	43.70	30.11	0.0379	0.0281
0.82 - 0.78	1104	1104	100.0	4.05	36.74	27.20	0.0392	0.0308
0.78 - 0.75	969	969	100.0	3.87	34.78	25.55	0.0405	0.0326
0.75 - 0.72	1169	1169	100.0	3.67	30.47	22.95	0.0410	0.0356
0.72 - 0.69	1379	1379	100.0	3.54	26.00	20.92	0.0449	0.0393
0.69 - 0.67	1036	1036	100.0	3.40	23.63	19.54	0.0481	0.0429
0.67 - 0.65	1172	1172	100.0	3.22	21.03	17.77	0.0492	0.0472
0.65 - 0.63	1346	1346	100.0	3.08	18.45	16.24	0.0548	0.0525
0.63 - 0.62	728	729	99.9	2.95	17.40	14.83	0.0601	0.0575
0.62 - 0.60	1619	1623	99.8	2.84	16.12	13.77	0.0638	0.0617
0.60 - 0.59	919	922	99.7	2.72	13.83	12.36	0.0702	0.0698
0.59 - 0.58	912	914	99.8	2.59	12.58	11.23	0.0735	0.0777
0.58 - 0.57	1014	1016	99.8	2.60	12.11	10.97	0.0842	0.0805
0.57 - 0.56	1146	1149	99.7	2.41	11.16	9.83	0.0837	0.0921
0.56 - 0.55	810	837	96.8	2.29	9.73	8.70	0.0981	0.1073
0.65 - 0.55	8494	8536	99.5	2.71	14.21	12.48	0.0684	0.0698
Inf - 0.55	22079	22131	99.8	3.61	39.83	22.94	0.0411	0.0326

Several low angle reflections were shadowed by beam stop and were removed from the data before the final refinement cycles.

Complete .cif-data of the compound are avaliable under the CCDC number **CCDC-2031448**.

Table S9. Crystal data and structure refinement.

Identification code	13192	
Empirical formula	$C_{46}H_{35}BiN_2$	
Color	dark brown	
Formula weight	824.74 g · mol^{-1}	
Temperature	100(2) K	
Wavelength	0.71073 Å	
Crystal system	TRICLINIC	
Space group	$P\bar{1}$, (No. 2)	
Unit cell dimensions	a = 11.5135(13) Å	α= 88.445(7)°.
	b = 11.9576(6) Å	β= 73.593(11)°.
	c = 13.7914(16) Å	γ = 78.419(7)°.
Volume	1783.4(3) Å^3	
Z	2	
Density (calculated)	1.536 Mg · m^{-3}	
Absorption coefficient	4.978 mm^{-1}	
F(000)	816 e	
Crystal size	0.23 x 0.17 x 0.10 mm^3	
θ range for data collection	2.749 to 27.500°.	
Index ranges	-14 ≤ h ≤ 14, -15≤ k ≤ 15, -17 ≤ l ≤ 17	
Reflections collected	37792	
Independent reflections	8180 [R_{int} = 0.0374]	
Reflections with I>2σ(I)	7986	
Completeness to θ = 25.242°	99.7 %	
Absorption correction	Gaussian	
Max. and min. transmission	0.65 and 0.36	
Refinement method	Full-matrix least-squares on F^2	
Data / restraints / parameters	8180 / 0 / 444	
Goodness-of-fit on F^2	1.094	
Final R indices [I>2σ(I)]	R_1 = 0.0177	wR^2 = 0.0445
R indices (all data)	R_1 = 0.0183	wR^2 = 0.0449
Largest diff. peak and hole	1.3 and -1.5 e · Å^{-3}	

Table S10. Bond lengths [Å] and angles [°].

Bi(1)-N(1)	2.4621(15)	Bi(1)-N(2)	2.4552(16)
Bi(1)-C(1)	2.1503(18)	N(1)-C(7)	1.301(2)
N(1)-C(11)	1.422(2)	N(2)-C(9)	1.305(2)
N(2)-C(29)	1.423(2)	C(1)-C(2)	1.412(3)
C(1)-C(6)	1.418(2)	C(2)-C(3)	1.403(3)
C(2)-C(9)	1.461(3)	C(3)-C(4)	1.393(3)
C(4)-C(5)	1.394(3)	C(5)-C(6)	1.400(3)
C(6)-C(7)	1.461(3)	C(7)-C(8)	1.515(2)
C(9)-C(10)	1.506(3)	C(11)-C(12)	1.413(3)
C(11)-C(16)	1.412(3)	C(12)-C(13)	1.399(3)
C(12)-C(17)	1.491(3)	C(13)-C(14)	1.388(3)
C(14)-C(15)	1.386(3)	C(15)-C(16)	1.394(3)
C(16)-C(23)	1.494(3)	C(17)-C(18)	1.396(3)
C(17)-C(22)	1.397(3)	C(18)-C(19)	1.388(3)
C(19)-C(20)	1.386(3)	C(20)-C(21)	1.399(3)
C(21)-C(22)	1.390(3)	C(23)-C(24)	1.400(3)
C(23)-C(28)	1.396(3)	C(24)-C(25)	1.388(3)
C(25)-C(26)	1.392(3)	C(26)-C(27)	1.392(3)
C(27)-C(28)	1.390(3)	C(29)-C(30)	1.412(3)
C(29)-C(34)	1.412(3)	C(30)-C(31)	1.395(3)
C(30)-C(35)	1.496(3)	C(31)-C(32)	1.386(3)
C(32)-C(33)	1.385(3)	C(33)-C(34)	1.402(3)
C(34)-C(41)	1.491(3)	C(35)-C(36)	1.397(3)
C(35)-C(40)	1.392(3)	C(36)-C(37)	1.395(3)
C(37)-C(38)	1.380(4)	C(38)-C(39)	1.387(4)
C(39)-C(40)	1.395(3)	C(41)-C(42)	1.400(3)
C(41)-C(46)	1.400(3)	C(42)-C(43)	1.392(3)
C(43)-C(44)	1.387(3)	C(44)-C(45)	1.386(3)
C(45)-C(46)	1.390(3)		

N(2)-Bi(1)-N(1)	142.37(5)	C(1)-Bi(1)-N(1)	71.47(6)
C(1)-Bi(1)-N(2)	71.19(6)	C(7)-N(1)-Bi(1)	114.06(12)
C(7)-N(1)-C(11)	123.61(16)	C(11)-N(1)-Bi(1)	122.33(11)
C(9)-N(2)-Bi(1)	114.65(12)	C(9)-N(2)-C(29)	124.03(16)

C(29)-N(2)-Bi(1)	119.68(12)	C(2)-C(1)-Bi(1)	120.28(13)
C(2)-C(1)-C(6)	119.96(16)	C(6)-C(1)-Bi(1)	119.76(13)
C(1)-C(2)-C(9)	117.69(16)	C(3)-C(2)-C(1)	119.65(17)
C(3)-C(2)-C(9)	122.66(17)	C(4)-C(3)-C(2)	120.28(18)
C(3)-C(4)-C(5)	120.18(17)	C(4)-C(5)-C(6)	120.97(17)
C(1)-C(6)-C(7)	117.73(16)	C(5)-C(6)-C(1)	118.92(17)
C(5)-C(6)-C(7)	123.30(17)	N(1)-C(7)-C(6)	116.61(16)
N(1)-C(7)-C(8)	122.86(17)	C(6)-C(7)-C(8)	120.46(16)
N(2)-C(9)-C(2)	116.03(17)	N(2)-C(9)-C(10)	123.47(17)
C(2)-C(9)-C(10)	120.50(17)	C(12)-C(11)-N(1)	121.76(17)
C(16)-C(11)-N(1)	118.21(17)	C(16)-C(11)-C(12)	119.87(17)
C(11)-C(12)-C(17)	122.03(17)	C(13)-C(12)-C(11)	118.96(18)
C(13)-C(12)-C(17)	118.99(17)	C(14)-C(13)-C(12)	121.26(18)
C(15)-C(14)-C(13)	119.34(18)	C(14)-C(15)-C(16)	121.47(19)
C(11)-C(16)-C(23)	121.92(17)	C(15)-C(16)-C(11)	119.06(18)
C(15)-C(16)-C(23)	119.01(17)	C(18)-C(17)-C(12)	120.73(18)
C(18)-C(17)-C(22)	119.24(19)	C(22)-C(17)-C(12)	119.98(18)
C(19)-C(18)-C(17)	120.39(19)	C(20)-C(19)-C(18)	120.2(2)
C(19)-C(20)-C(21)	119.9(2)	C(22)-C(21)-C(20)	119.9(2)
C(21)-C(22)-C(17)	120.4(2)	C(24)-C(23)-C(16)	119.82(18)
C(28)-C(23)-C(16)	121.49(17)	C(28)-C(23)-C(24)	118.66(18)
C(25)-C(24)-C(23)	120.68(19)	C(24)-C(25)-C(26)	120.24(19)
C(27)-C(26)-C(25)	119.5(2)	C(28)-C(27)-C(26)	120.24(19)
C(27)-C(28)-C(23)	120.66(18)	C(30)-C(29)-N(2)	118.49(17)
C(30)-C(29)-C(34)	120.06(17)	C(34)-C(29)-N(2)	121.10(16)
C(29)-C(30)-C(35)	121.91(17)	C(31)-C(30)-C(29)	119.60(18)
C(31)-C(30)-C(35)	118.46(17)	C(32)-C(31)-C(30)	120.76(18)
C(33)-C(32)-C(31)	119.45(18)	C(32)-C(33)-C(34)	121.94(18)
C(29)-C(34)-C(41)	123.90(17)	C(33)-C(34)-C(29)	118.12(17)
C(33)-C(34)-C(41)	117.98(17)	C(36)-C(35)-C(30)	120.48(19)
C(40)-C(35)-C(30)	120.79(18)	C(40)-C(35)-C(36)	118.6(2)
C(37)-C(36)-C(35)	120.4(2)	C(38)-C(37)-C(36)	120.4(2)
C(37)-C(38)-C(39)	119.9(2)	C(38)-C(39)-C(40)	119.9(2)
C(35)-C(40)-C(39)	120.8(2)	C(42)-C(41)-C(34)	118.75(17)
C(46)-C(41)-C(34)	123.07(18)	C(46)-C(41)-C(42)	118.17(18)
C(43)-C(42)-C(41)	121.12(19)	C(44)-C(43)-C(42)	119.96(19)
C(45)-C(44)-C(43)	119.42(19)	C(44)-C(45)-C(46)	120.91(19)
C(45)-C(46)-C(41)	120.34(19)		

8.5. Single Crystal Structure Analysis of **6, 3·toluene**

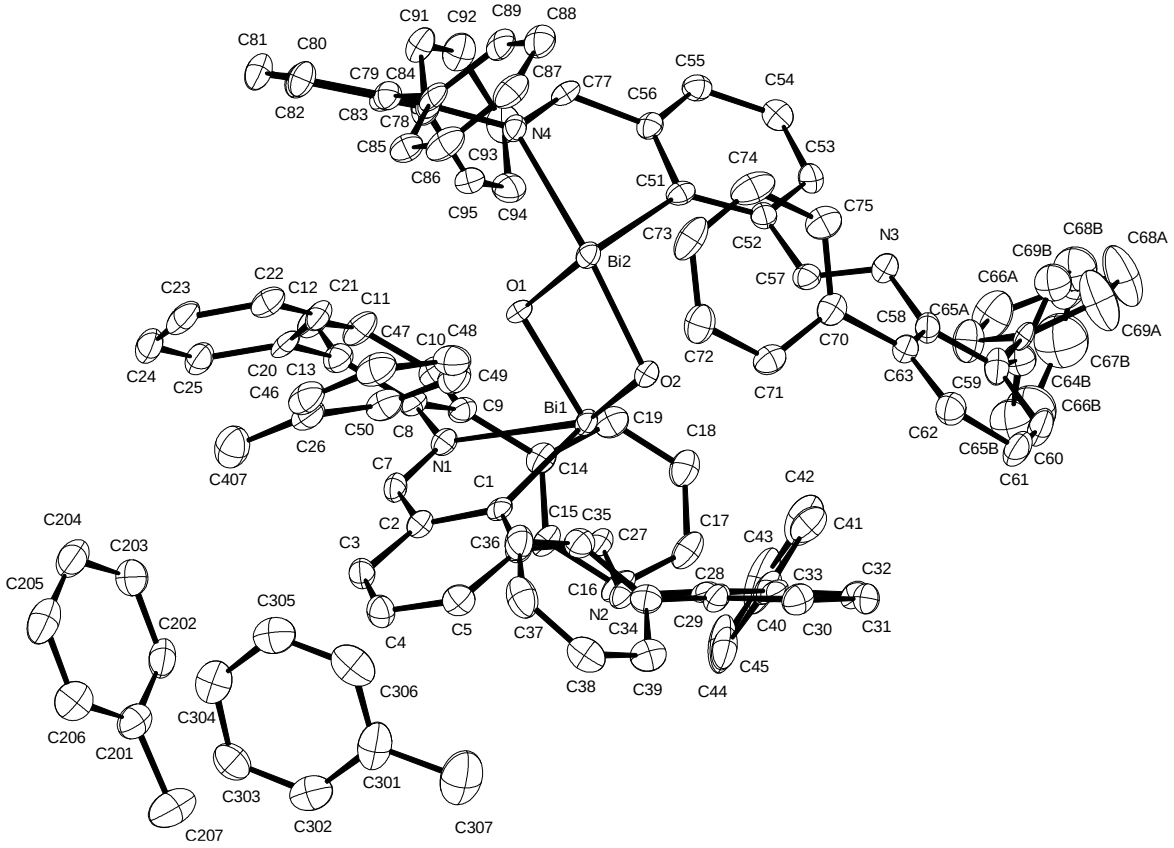

Figure S5. The molecular structure of complex **6 3·toluene**. H atoms have been removed for clarity.

X-ray Crystal Structure Analysis of complex 6 3·Toluene: $C_{109}H_{86}Bi_2N_4O_2$, M_r = 1901.77 g mol^{-1}, yellow plate, crystal size 0.10 x 0.08 x 0.04 mm^3, triclinic, $P\bar{1}$ [2], a = 15.364(2) Å, b = 16.4700(12) Å, c = 19.869(2) Å, α = 86.379(7)°, β = 67.786(8)°, γ = 84.375(8)°, V = 4630.2(9) Å^3, T = 100(2) K, Z = 2, D_{calc} = 1.364 g·cm^3, λ = 0.71073 Å, μ(*Mo-K*α) = 3.846 mm^{-1}, analytical absorption correction (T_{min} = 0.69230, T_{max} = 0.86804), Bruker AXS Enraf-Nonius KappaCCD diffractometer with a FR591 rotating Mo-anode X-ray source, 2.664 < θ < 27.499°, 94882 measured reflections, 21180 independent reflections, 16659 reflections with $I > 2\sigma(I)$, R_{int} = 0.0689. The structure was solved by *SHELXS* and refined by full-matrix least-squares (*SHELXL*) against F^2 to R_1 = 0.0437 [$I > 2\sigma(I)$], wR_2 = 0.1012, 1081 parameters.

	h	k	l	distance (mm)
1.	0	-1	0	0.04
2.	0	1	0	0.04
3.	-1	0	0	0.045
4.	1	0	0	0.05
5.	-1	1	0	0.04
6.	0	0	-1	0.02
7.	0	0	1	0.02

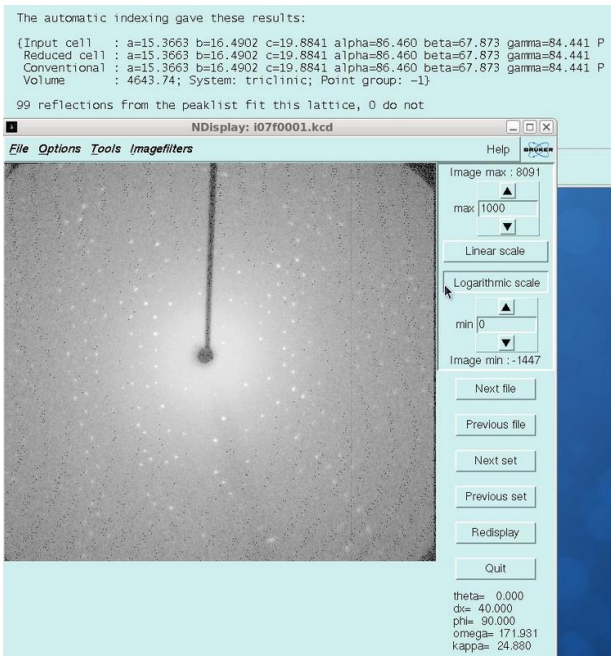

INTENSITY STATISTICS FOR DATASET

Resolution	#Data	#Theory	%Complete	Redundancy	Mean I	Mean I/s	Rmerge	Rsigma
Inf - 2.60	531	551	96.4	8.40	100.68	39.88	0.0560	0.0207
2.60 - 1.75	1256	1262	99.5	6.03	64.41	27.99	0.0535	0.0278
1.75 - 1.39	1774	1788	99.2	5.35	46.44	23.31	0.0562	0.0324
1.39 - 1.22	1751	1761	99.4	5.02	32.30	19.45	0.0563	0.0373
1.22 - 1.10	1903	1906	99.8	4.82	26.00	16.76	0.0609	0.0430
1.10 - 1.03	1596	1599	99.8	4.64	22.77	15.19	0.0656	0.0484
1.03 - 0.96	2076	2084	99.6	4.36	19.55	13.20	0.0755	0.0583
0.96 - 0.92	1491	1495	99.7	4.10	17.18	11.54	0.0850	0.0654
0.92 - 0.88	1802	1803	99.9	3.99	13.89	9.76	0.0957	0.0777
0.88 - 0.84	2127	2127	100.0	3.83	12.26	8.54	0.1067	0.0904
0.84 - 0.81	1865	1867	99.9	3.65	10.85	7.53	0.1242	0.1056
0.81 - 0.79	1436	1436	100.0	3.50	9.59	6.67	0.1373	0.1210
0.79 - 0.77	1547	1551	99.7	3.33	9.80	6.51	0.1379	0.1264
0.77 - 0.75	1771	1771	100.0	3.24	8.19	5.41	0.1717	0.1549
0.75 - 0.73	1955	1956	99.9	3.11	7.66	4.93	0.1814	0.1719
0.73 - 0.71	2147	2147	100.0	2.96	6.68	4.27	0.2027	0.2023
0.71 - 0.70	1167	1168	99.9	2.92	6.09	3.84	0.2194	0.2254
0.70 - 0.68	2583	2584	100.0	2.79	5.43	3.39	0.2414	0.2594
0.68 - 0.67	1375	1377	99.9	2.67	4.63	2.81	0.2894	0.3188
0.67 - 0.66	1481	1483	99.9	2.65	4.52	2.68	0.3009	0.3373
0.66 - 0.65	1585	1673	94.7	2.40	4.21	2.38	0.3134	0.3861
0.75 - 0.65	12293	12388	99.2	2.80	5.71	3.55	0.2327	0.2505
Inf - 0.65	35219	35389	99.5	3.82	17.33	10.08	0.0802	0.0752

Several low-order reflections were shadowed by the beamstop and removed from the least-squares refinement. A resolution cut off (0.77 Å) was applied. The relatively poor crystal quality is reflected in the diffraction data, which do not allow an exact description of the disordered solute. To improve signal-to-noise ratio quality the SQUEEZE routine in PLATON was applied to dataset. This results in a residual electron density of 3.48 and -3.99 $eÅ^{-3}$ as well as a void volume of 506.21 Å³ (10.9% of unit cell volume) using 1.2 Å probe radius and a 0.7 Å grid size (CCDC Mercury) after final refinement. The residual electron density of 3.48 and

-3.99 $e \cdot A^{-3}$ close to the Bi atom may be a result of anharmonic displacement of the heavy atom. Complete .cif-data of the compound are available under the CCDC number **CCDC-2031449**.

Table S11. Crystal data and structure refinement.

Identification code	13008	
Empirical formula	$C_{109}H_{86}Bi_2N_4O_2$	
Color	yellow	
Formula weight	1901.77 $g \cdot mol^{-1}$	
Temperature	100(2) K	
Wavelength	0.71073 Å	
Crystal system	TRICLINIC	
Space group	$P\bar{1}$, (No. 2)	
Unit cell dimensions	a = 15.364(2) Å	α= 86.379(7)°.
	b = 16.4700(12) Å	β= 67.786(8)°.
	c = 19.869(2) Å	γ = 84.375(8)°.
Volume	4630.2(9) $Å^3$	
Z	2	
Density (calculated)	1.364 $Mg \cdot m^{-3}$	
Absorption coefficient	3.846 mm^{-1}	
F(000)	1900 e	
Crystal size	0.10 x 0.08 x 0.04 mm^3	
θ range for data collection	2.664 to 27.499°.	
Index ranges	$-19 \le h \le 19$, $-21 \le k \le 21$, $-25 \le l \le 25$	
Reflections collected	94882	
Independent reflections	21180 [R_{int} = 0.0689]	
Reflections with I>2σ(I)	16659	
Completeness to θ = 25.242°	99.6 %	
Absorption correction	Gaussian	
Max. and min. transmission	0.87and 0.69	
Refinement method	Full-matrix least-squares on F^2	
Data / restraints / parameters	21180 / 0 / 1081	
Goodness-of-fit on F^2	1.049	
Final R indices [I>2σ(I)]	R_1 = 0.0437	wR^2 = 0.1012
R indices (all data)	R_1 = 0.0609	wR^2 = 0.1104
Remarks	Solvent accessible void with two disordered toluene was suppressed	
Largest diff. peak and hole	2.8 and -2.6 $e \cdot Å^{-3}$	

Table S12. Bond lengths [Å] and angles [°].

Bi(1)-Bi(2)	3.2380(5)	Bi(1)-O(1)	2.103(3)
Bi(1)-O(2)	2.120(3)	Bi(1)-N(1)	2.672(4)
Bi(1)-C(1)	2.300(5)	Bi(2)-O(1)	2.104(3)
Bi(2)-O(2)	2.129(3)	Bi(2)-N(4)	2.648(4)
Bi(2)-C(51)	2.297(5)	N(1)-C(7)	1.276(6)
N(1)-C(8)	1.436(6)	N(2)-C(27)	1.270(6)
N(2)-C(28)	1.422(6)	N(3)-C(57)	1.276(6)
N(3)-C(58)	1.421(6)	N(4)-C(77)	1.269(6)
N(4)-C(78)	1.434(6)	C(1)-C(2)	1.415(7)
C(1)-C(6)	1.412(7)	C(2)-C(3)	1.383(7)
C(2)-C(7)	1.460(7)	C(3)-C(4)	1.395(7)
C(4)-C(5)	1.376(7)	C(5)-C(6)	1.412(7)
C(6)-C(27)	1.474(7)	C(8)-C(9)	1.407(7)
C(8)-C(13)	1.415(7)	C(9)-C(10)	1.408(7)
C(9)-C(14)	1.486(7)	C(10)-C(11)	1.386(7)
C(11)-C(12)	1.383(8)	C(12)-C(13)	1.393(7)
C(13)-C(20)	1.495(7)	C(14)-C(15)	1.396(7)
C(14)-C(19)	1.400(7)	C(15)-C(16)	1.384(7)
C(16)-C(17)	1.371(8)	C(17)-C(18)	1.384(8)
C(18)-C(19)	1.392(8)	C(20)-C(21)	1.390(7)
C(20)-C(25)	1.403(7)	C(21)-C(22)	1.385(7)
C(22)-C(23)	1.386(8)	C(23)-C(24)	1.377(9)
C(24)-C(25)	1.389(8)	C(28)-C(29)	1.401(7)
C(28)-C(33)	1.408(7)	C(29)-C(30)	1.404(7)
C(29)-C(34)	1.498(7)	C(30)-C(31)	1.384(8)
C(31)-C(32)	1.381(7)	C(32)-C(33)	1.399(7)
C(33)-C(40)	1.496(7)	C(34)-C(35)	1.403(7)
C(34)-C(39)	1.396(7)	C(35)-C(36)	1.393(8)
C(36)-C(37)	1.376(8)	C(37)-C(38)	1.383(9)
C(38)-C(39)	1.395(8)	C(40)-C(41)	1.391(8)
C(40)-C(45)	1.400(8)	C(41)-C(42)	1.387(9)
C(42)-C(43)	1.373(12)	C(43)-C(44)	1.374(12)
C(44)-C(45)	1.383(9)	C(51)-C(52)	1.396(7)
C(51)-C(56)	1.416(6)	C(52)-C(53)	1.409(7)
C(52)-C(57)	1.484(7)	C(53)-C(54)	1.384(7)

C(54)-C(55)	1.390(7)	C(55)-C(56)	1.384(7)
C(56)-C(77)	1.470(7)	C(58)-C(59)	1.414(7)
C(58)-C(63)	1.402(7)	C(59)-C(60)	1.396(8)
C(59)-C(64A)	1.527(16)	C(59)-C(64B)	1.48(3)
C(60)-C(61)	1.373(9)	C(61)-C(62)	1.395(8)
C(62)-C(63)	1.390(7)	C(63)-C(70)	1.501(7)
C(64A)-C(65A)	1.446(18)	C(64A)-C(69A)	1.363(18)
C(64B)-C(65B)	1.31(3)	C(64B)-C(69B)	1.40(3)
C(65A)-C(66A)	1.378(15)	C(65B)-C(66B)	1.41(3)
C(66A)-C(67A)	1.314(17)	C(66B)-C(67B)	1.30(3)
C(67A)-C(68A)	1.371(19)	C(67B)-C(68B)	1.48(4)
C(68A)-C(69A)	1.385(18)	C(68B)-C(69B)	1.41(3)
C(70)-C(71)	1.395(8)	C(70)-C(75)	1.400(8)
C(71)-C(72)	1.394(8)	C(72)-C(73)	1.376(9)
C(73)-C(74)	1.381(9)	C(74)-C(75)	1.395(8)
C(78)-C(79)	1.404(7)	C(78)-C(83)	1.405(7)
C(79)-C(80)	1.403(7)	C(79)-C(84)	1.504(7)
C(80)-C(81)	1.384(8)	C(81)-C(82)	1.382(8)
C(82)-C(83)	1.395(7)	C(83)-C(90)	1.502(7)
C(84)-C(85)	1.389(7)	C(84)-C(89)	1.387(7)
C(85)-C(86)	1.393(8)	C(86)-C(87)	1.370(9)
C(87)-C(88)	1.394(8)	C(88)-C(89)	1.386(8)
C(90)-C(91)	1.404(7)	C(90)-C(95)	1.390(7)
C(91)-C(92)	1.377(8)	C(92)-C(93)	1.390(8)
C(93)-C(94)	1.379(8)	C(94)-C(95)	1.400(8)
C(26)-C(46)	1.390(8)	C(26)-C(50)	1.415(8)
C(26)-C(407)	1.500(8)	C(46)-C(47)	1.378(9)
C(47)-C(48)	1.403(9)	C(48)-C(49)	1.372(8)
C(49)-C(50)	1.380(8)	C(201)-C(202)	1.390(9)
C(201)-C(206)	1.397(9)	C(201)-C(207)	1.517(8)
C(202)-C(203)	1.390(8)	C(203)-C(204)	1.381(9)
C(204)-C(205)	1.375(10)	C(205)-C(206)	1.371(9)
C(301)-C(302)	1.395(10)	C(301)-C(306)	1.405(10)
C(301)-C(307)	1.488(9)	C(302)-C(303)	1.374(9)
C(303)-C(304)	1.374(9)	C(304)-C(305)	1.357(9)
C(305)-C(306)	1.357(10)		

O(1)-Bi(1)-Bi(2)	39.67(9)	O(1)-Bi(1)-O(2)	79.70(13)
O(1)-Bi(1)-N(1)	73.95(12)	O(1)-Bi(1)-C(1)	97.84(15)
O(2)-Bi(1)-Bi(2)	40.45(9)	O(2)-Bi(1)-N(1)	147.42(13)
O(2)-Bi(1)-C(1)	94.87(15)	N(1)-Bi(1)-Bi(2)	112.75(9)
C(1)-Bi(1)-Bi(2)	102.83(11)	C(1)-Bi(1)-N(1)	70.55(14)
O(1)-Bi(2)-Bi(1)	39.65(9)	O(1)-Bi(2)-O(2)	79.48(13)
O(1)-Bi(2)-N(4)	76.11(12)	O(1)-Bi(2)-C(51)	93.95(15)
O(2)-Bi(2)-Bi(1)	40.26(9)	O(2)-Bi(2)-N(4)	150.24(13)
O(2)-Bi(2)-C(51)	94.38(15)	N(4)-Bi(2)-Bi(1)	112.33(9)
C(51)-Bi(2)-Bi(1)	90.90(12)	C(51)-Bi(2)-N(4)	70.79(15)
Bi(1)-O(1)-Bi(2)	100.68(13)	Bi(1)-O(2)-Bi(2)	99.29(13)
C(7)-N(1)-Bi(1)	108.7(3)	C(7)-N(1)-C(8)	119.4(4)
C(8)-N(1)-Bi(1)	131.4(3)	C(27)-N(2)-C(28)	119.6(4)
C(57)-N(3)-C(58)	119.1(4)	C(77)-N(4)-Bi(2)	109.5(3)
C(77)-N(4)-C(78)	120.2(4)	C(78)-N(4)-Bi(2)	129.7(3)
C(2)-C(1)-Bi(1)	116.7(3)	C(6)-C(1)-Bi(1)	126.2(3)
C(6)-C(1)-C(2)	117.1(4)	C(1)-C(2)-C(7)	121.4(4)
C(3)-C(2)-C(1)	121.6(4)	C(3)-C(2)-C(7)	117.0(4)
C(2)-C(3)-C(4)	120.6(5)	C(5)-C(4)-C(3)	119.3(5)
C(4)-C(5)-C(6)	120.9(5)	C(1)-C(6)-C(27)	122.1(4)
C(5)-C(6)-C(1)	120.5(4)	C(5)-C(6)-C(27)	117.4(4)
N(1)-C(7)-C(2)	122.6(4)	C(9)-C(8)-N(1)	118.0(4)
C(9)-C(8)-C(13)	120.5(4)	C(13)-C(8)-N(1)	121.5(4)
C(8)-C(9)-C(10)	119.2(4)	C(8)-C(9)-C(14)	122.4(4)
C(10)-C(9)-C(14)	118.4(5)	C(11)-C(10)-C(9)	120.3(5)
C(12)-C(11)-C(10)	119.8(5)	C(11)-C(12)-C(13)	122.0(5)
C(8)-C(13)-C(20)	123.8(4)	C(12)-C(13)-C(8)	118.1(5)
C(12)-C(13)-C(20)	118.0(5)	C(15)-C(14)-C(9)	122.3(5)
C(15)-C(14)-C(19)	118.4(5)	C(19)-C(14)-C(9)	119.1(5)
C(16)-C(15)-C(14)	120.8(5)	C(17)-C(16)-C(15)	120.5(5)
C(16)-C(17)-C(18)	119.8(5)	C(17)-C(18)-C(19)	120.5(5)
C(18)-C(19)-C(14)	120.0(5)	C(21)-C(20)-C(13)	121.9(5)
C(21)-C(20)-C(25)	119.0(5)	C(25)-C(20)-C(13)	119.2(5)
C(22)-C(21)-C(20)	120.6(5)	C(21)-C(22)-C(23)	120.0(5)
C(24)-C(23)-C(22)	120.1(5)	C(23)-C(24)-C(25)	120.4(5)
C(24)-C(25)-C(20)	119.9(5)	N(2)-C(27)-C(6)	120.1(5)
C(29)-C(28)-N(2)	118.9(5)	C(29)-C(28)-C(33)	119.9(4)
C(33)-C(28)-N(2)	121.0(4)	C(28)-C(29)-C(30)	119.5(5)

C(28)-C(29)-C(34)	123.1(4)	C(30)-C(29)-C(34)	117.4(5)
C(31)-C(30)-C(29)	120.6(5)	C(32)-C(31)-C(30)	119.7(5)
C(31)-C(32)-C(33)	121.3(5)	C(28)-C(33)-C(40)	123.4(4)
C(32)-C(33)-C(28)	118.9(5)	C(32)-C(33)-C(40)	117.6(5)
C(35)-C(34)-C(29)	122.2(5)	C(39)-C(34)-C(29)	119.4(5)
C(39)-C(34)-C(35)	118.4(5)	C(36)-C(35)-C(34)	119.9(5)
C(37)-C(36)-C(35)	121.3(5)	C(36)-C(37)-C(38)	119.4(5)
C(37)-C(38)-C(39)	120.3(5)	C(38)-C(39)-C(34)	120.8(5)
C(41)-C(40)-C(33)	118.8(5)	C(41)-C(40)-C(45)	119.0(5)
C(45)-C(40)-C(33)	122.1(5)	C(42)-C(41)-C(40)	120.4(6)
C(43)-C(42)-C(41)	119.9(7)	C(42)-C(43)-C(44)	120.3(6)
C(43)-C(44)-C(45)	120.7(7)	C(44)-C(45)-C(40)	119.6(7)
C(52)-C(51)-Bi(2)	126.9(3)	C(52)-C(51)-C(56)	116.7(4)
C(56)-C(51)-Bi(2)	116.4(3)	C(51)-C(52)-C(53)	120.9(5)
C(51)-C(52)-C(57)	122.0(4)	C(53)-C(52)-C(57)	117.1(4)
C(54)-C(53)-C(52)	120.8(5)	C(53)-C(54)-C(55)	119.2(5)
C(56)-C(55)-C(54)	120.1(5)	C(51)-C(56)-C(77)	121.0(4)
C(55)-C(56)-C(51)	122.1(5)	C(55)-C(56)-C(77)	116.9(4)
N(3)-C(57)-C(52)	118.6(4)	C(59)-C(58)-N(3)	115.8(5)
C(63)-C(58)-N(3)	124.3(5)	C(63)-C(58)-C(59)	119.9(5)
C(58)-C(59)-C(64A)	118.3(6)	C(58)-C(59)-C(64B)	125.3(11)
C(60)-C(59)-C(58)	118.8(5)	C(60)-C(59)-C(64A)	122.9(7)
C(60)-C(59)-C(64B)	115.0(11)	C(61)-C(60)-C(59)	121.3(5)
C(60)-C(61)-C(62)	119.9(5)	C(63)-C(62)-C(61)	120.5(5)
C(58)-C(63)-C(70)	121.3(4)	C(62)-C(63)-C(58)	119.6(5)
C(62)-C(63)-C(70)	119.0(5)	C(65A)-C(64A)-C(59)	121.1(10)
C(69A)-C(64A)-C(59)	123.2(12)	C(69A)-C(64A)-C(65A)	115.6(13)
C(65B)-C(64B)-C(59)	123(2)	C(65B)-C(64B)-C(69B)	122(2)
C(69B)-C(64B)-C(59)	114.6(18)	C(66A)-C(65A)-C(64A)	121.7(11)
C(64B)-C(65B)-C(66B)	122(2)	C(67A)-C(66A)-C(65A)	119.0(12)
C(67B)-C(66B)-C(65B)	119(2)	C(66A)-C(67A)-C(68A)	122.1(13)
C(66B)-C(67B)-C(68B)	123(3)	C(67A)-C(68A)-C(69A)	119.8(12)
C(69B)-C(68B)-C(67B)	115(2)	C(64A)-C(69A)-C(68A)	121.4(13)
C(64B)-C(69B)-C(68B)	119(2)	C(71)-C(70)-C(63)	119.8(5)
C(71)-C(70)-C(75)	118.7(5)	C(75)-C(70)-C(63)	121.4(5)
C(72)-C(71)-C(70)	120.4(5)	C(73)-C(72)-C(71)	120.6(6)
C(72)-C(73)-C(74)	119.5(6)	C(73)-C(74)-C(75)	120.8(6)
C(74)-C(75)-C(70)	119.9(6)	N(4)-C(77)-C(56)	122.1(4)

C(79)-C(78)-N(4)	118.1(4)	C(79)-C(78)-C(83)	120.5(5)
C(83)-C(78)-N(4)	121.1(4)	C(78)-C(79)-C(84)	122.4(4)
C(80)-C(79)-C(78)	118.8(5)	C(80)-C(79)-C(84)	118.7(5)
C(81)-C(80)-C(79)	120.6(5)	C(82)-C(81)-C(80)	120.3(5)
C(81)-C(82)-C(83)	120.7(5)	C(78)-C(83)-C(90)	122.2(4)
C(82)-C(83)-C(78)	119.0(5)	C(82)-C(83)-C(90)	118.8(5)
C(85)-C(84)-C(79)	120.4(5)	C(89)-C(84)-C(79)	120.3(5)
C(89)-C(84)-C(85)	119.3(5)	C(84)-C(85)-C(86)	119.9(5)
C(87)-C(86)-C(85)	120.7(5)	C(86)-C(87)-C(88)	119.6(5)
C(89)-C(88)-C(87)	119.9(5)	C(88)-C(89)-C(84)	120.5(5)
C(91)-C(90)-C(83)	119.6(5)	C(95)-C(90)-C(83)	121.6(5)
C(95)-C(90)-C(91)	118.8(5)	C(92)-C(91)-C(90)	121.2(5)
C(91)-C(92)-C(93)	119.6(5)	C(94)-C(93)-C(92)	120.3(5)
C(93)-C(94)-C(95)	120.3(5)	C(90)-C(95)-C(94)	120.0(5)
C(46)-C(26)-C(50)	117.8(5)	C(46)-C(26)-C(407)	121.1(5)
C(50)-C(26)-C(407)	121.0(5)	C(47)-C(46)-C(26)	121.0(6)
C(46)-C(47)-C(48)	120.7(6)	C(49)-C(48)-C(47)	118.6(6)
C(48)-C(49)-C(50)	121.4(5)	C(49)-C(50)-C(26)	120.4(5)
C(202)-C(201)-C(206)	117.7(6)	C(202)-C(201)-C(207)	120.0(6)
C(206)-C(201)-C(207)	122.3(6)	C(201)-C(202)-C(203)	120.5(6)
C(204)-C(203)-C(202)	121.0(6)	C(205)-C(204)-C(203)	118.4(6)
C(206)-C(205)-C(204)	121.4(6)	C(205)-C(206)-C(201)	121.1(6)
C(302)-C(301)-C(306)	116.4(6)	C(302)-C(301)-C(307)	122.2(7)
C(306)-C(301)-C(307)	121.4(7)	C(303)-C(302)-C(301)	121.0(6)
C(302)-C(303)-C(304)	120.7(6)	C(305)-C(304)-C(303)	119.1(6)
C(306)-C(305)-C(304)	121.2(6)	C(305)-C(306)-C(301)	121.5(6)

8.6. Single Crystal Structure Analysis of **7**

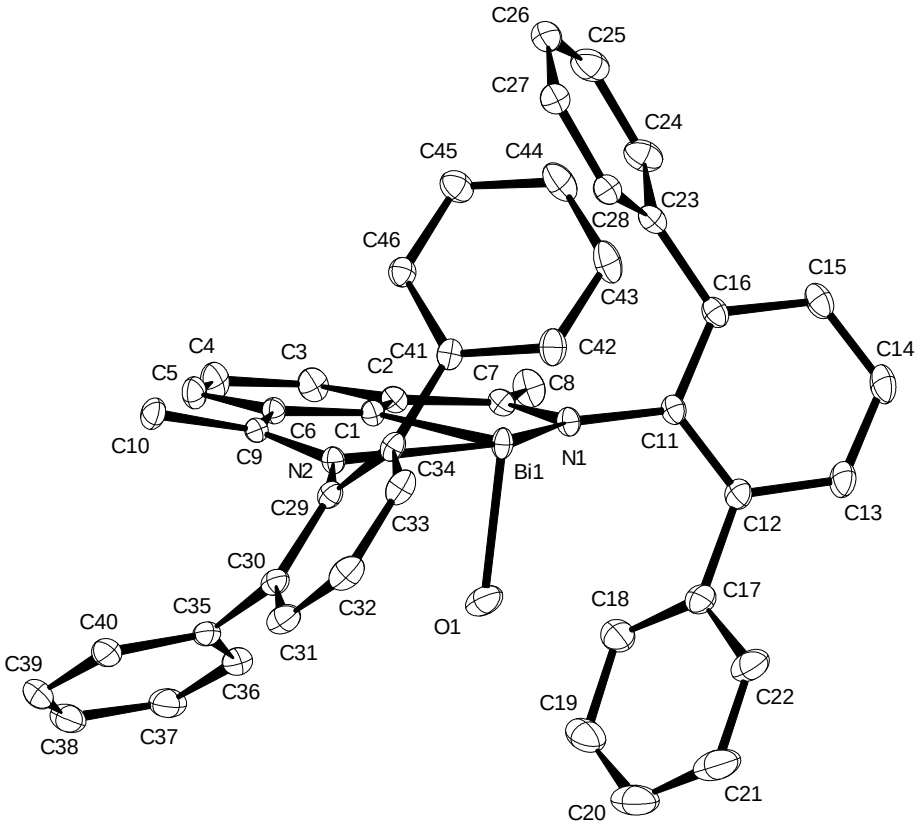

Figure S6. The molecular structure of complex **7**. H atoms have been removed for clarity.

X-ray Crystal Structure Analysis of complex 7: C_{46} H_{35} Bi N_2 O, M_r = 840.74 g mol^{-1}, orange prism, crystal size 0.134 x 0.047 x 0.021 mm^3, triclinic, $P\bar{1}$ [2], a = 11.9494(7) Å, b = 12.1997(7) Å, c = 14.6767(8) Å, α= 101.774(2)°, β= 94.585(2)°, γ = 113.825(2)°, V = 1884.29(19) Å^3, T = 100(2) K, Z = 2, D_{calc} = 1.482 g·cm^3, λ = 0.71073 Å, μ(*Mo-K*α) = 4.715 mm^{-1}, analytical absorption correction (T_{min} = 0.64576, T_{max} = 0.91743), Bruker-AXS Kappa Mach3 with APEX-II detector and IμS micro focuse source, 1.889 < θ < 36.318°, 147263 measured reflections, 18168 independent reflections, 17403 reflections with $I > 2\sigma(I)$, R_{int} = 0.0248. The structure was solved by *SHELXT* and refined by full-matrix least-squares (*SHELXL*) against F^2 to R_1 = 0.0180 [$I > 2\sigma(I)$], wR_2 = 0.0431, 475 parameters.

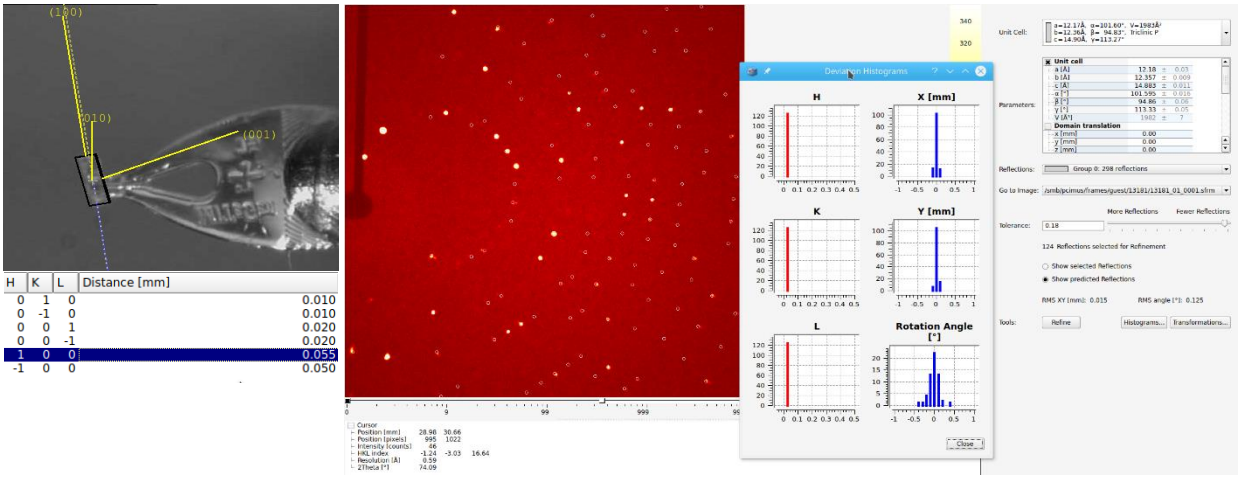

INTENSITY STATISTICS FOR DATASET

Resolution	#Data	#Theory	%Complete	Redundancy	Mean I	Mean I/s	Rmerge	Rsigma
Inf - 2.41	275	275	100.0	12.79	148.61	131.83	0.0201	0.0068
2.41 - 1.63	639	639	100.0	14.56	98.94	131.99	0.0188	0.0066
1.63 - 1.29	926	926	100.0	14.49	65.94	119.52	0.0191	0.0071
1.29 - 1.13	890	890	100.0	14.00	52.74	106.31	0.0204	0.0077
1.13 - 1.02	992	992	100.0	11.60	43.60	92.22	0.0226	0.0091
1.02 - 0.95	880	880	100.0	9.75	35.44	77.54	0.0237	0.0106
0.95 - 0.89	989	989	100.0	8.55	31.14	69.63	0.0254	0.0121
0.89 - 0.85	832	832	100.0	8.00	25.98	61.24	0.0270	0.0135
0.85 - 0.81	998	998	100.0	7.65	23.03	55.51	0.0286	0.0150
0.81 - 0.78	896	896	100.0	7.32	21.24	51.75	0.0302	0.0164
0.78 - 0.75	1034	1034	100.0	6.98	18.88	45.19	0.0327	0.0185
0.75 - 0.73	788	788	100.0	6.77	18.09	43.15	0.0348	0.0199
0.73 - 0.71	884	884	100.0	6.54	16.64	39.22	0.0372	0.0218
0.71 - 0.69	998	999	99.9	6.30	14.16	34.72	0.0418	0.0249
0.69 - 0.67	1103	1103	100.0	6.12	13.69	32.28	0.0433	0.0267
0.67 - 0.66	599	602	99.5	5.89	13.19	31.18	0.0461	0.0284
0.66 - 0.64	1331	1337	99.6	5.75	11.36	27.34	0.0511	0.0324
0.64 - 0.63	679	689	98.5	5.46	10.74	25.61	0.0544	0.0348
0.63 - 0.62	820	830	98.8	5.37	10.01	23.17	0.0548	0.0376
0.62 - 0.61	781	794	98.4	5.27	10.10	23.32	0.0600	0.0383
0.61 - 0.60	863	888	97.2	5.02	8.72	20.32	0.0673	0.0441
0.70 - 0.60	6708	6776	99.0	5.63	11.40	26.97	0.0510	0.0327
Inf - 0.60	18197	18265	99.6	8.08	28.17	56.06	0.0248	0.0140

Several low angle reflections were shadowed by the beam stop and removed from the data before the final refinement cycles. The H atom of the -OH group appeared as a residual electron density peak and refined satisfactorily in this position. There are no suitable acceptors around this H atom, though we note that there is a possible interaction of the (O-)H atom with the neighbouring phenyl group: O1---centroid(C17-C22) = 3.35 Å; O-H---centroid(C17-C22) = 159 °.

The structure contains a disordered *n*-hexane molecule which could not be described in satisfactory way. To improve signal-to-noise ratio quality the SQUEEZE routine in PLATON was applied to the dataset and led to solvent accessible void of 211.03 Å^3 (11.2% of unit cell volume) using a 1.2 Å probe radius and a grid size of 0.7 Å (CCDC Mercury).

Complete .cif-data of the compound are avaliable under the CCDC number **CCDC-2031450**.

Table S13. Crystal data and structure refinement.

Identification code	13181	
Empirical formula	C_{46} H_{35} Bi N_2 O	
Color	orange	
Formula weight	840.74 g·mol^{-1}	
Temperature	100(2) K	
Wavelength	0.71073 Å	
Crystal system	Triclinic	
Space group	*P* $\bar{1}$, (no. 2)	
Unit cell dimensions	a = 11.9494(7) Å	α= 101.774(2)°.
	b = 12.1997(7) Å	β= 94.585(2)°.
	c = 14.6767(8) Å	γ = 113.825(2)°.
Volume	1884.29(19) Å^3	
Z	2	
Density (calculated)	1.482 Mg·m^{-3}	
Absorption coefficient	4.715 mm^{-1}	
F(000)	832 e	
Crystal size	0.134 x 0.047 x 0.021 mm^3	
θ range for data collection	1.889 to 36.318°.	
Index ranges	-19 ≤ h ≤ 19, -20≤ k ≤ 20, -24 ≤ l ≤ 24	
Reflections collected	147263	
Independent reflections	18168 [R_{int} = 0.0248]	
Reflections with I>2σ(I)	17403	
Completeness to θ = 25.242°	99.6 %	
Absorption correction	Gaussian	
Max. and min. transmission	0.91743 and 0.64576	
Refinement method	Full-matrix least-squares on F^2	
Data / restraints / parameters	18168 / 0 / 475	
Goodness-of-fit on F^2	1.102	
Final R indices [I>2σ(I)]	R_1 = 0.0180	wR^2 = 0.0431
R indices (all data)	R_1 = 0.0193	wR^2 = 0.0435
Extinction coefficient	n/a	
Largest diff. peak and hole	3.472 and -1.491 e·Å^{-3}	

Table S14. Bond lengths [Å] and angles [°].

Bi(1)-O(1)	2.0984(10)	Bi(1)-N(1)	2.2319(9)
Bi(1)-N(2)	2.6117(9)	Bi(1)-C(1)	2.1869(11)
O(1)-H(1)	0.77(3)	N(1)-C(11)	1.4170(15)
N(1)-C(7)	1.3832(15)	N(2)-C(29)	1.4158(14)
N(2)-C(9)	1.2848(14)	C(1)-C(2)	1.3902(15)
C(1)-C(6)	1.3969(15)	C(29)-C(34)	1.4051(17)
C(29)-C(30)	1.4107(16)	C(11)-C(12)	1.4107(16)
C(11)-C(16)	1.4109(17)	C(8)-C(7)	1.3552(16)
C(8)-H(8A)	0.90(2)	C(8)-H(8B)	0.91(2)
C(35)-C(36)	1.3981(18)	C(35)-C(30)	1.4829(18)
C(35)-C(40)	1.4007(18)	C(2)-C(3)	1.4026(16)
C(2)-C(7)	1.4891(16)	C(23)-C(28)	1.3959(18)
C(23)-C(16)	1.4875(17)	C(23)-C(24)	1.3970(18)
C(46)-H(46)	0.9500	C(46)-C(45)	1.3872(18)
C(46)-C(41)	1.4006(16)	C(5)-H(5)	0.9500
C(5)-C(4)	1.3926(18)	C(5)-C(6)	1.3934(16)
C(15)-H(15)	0.9500	C(15)-C(16)	1.3981(17)
C(15)-C(14)	1.387(2)	C(4)-H(4)	0.9500
C(4)-C(3)	1.3878(18)	C(9)-C(6)	1.4826(16)
C(9)-C(10)	1.4969(16)	C(36)-H(36)	0.9500
C(36)-C(37)	1.394(2)	C(12)-C(13)	1.4016(17)
C(12)-C(17)	1.4862(18)	C(33)-H(33)	0.9500
C(33)-C(34)	1.3987(16)	C(33)-C(32)	1.387(2)
C(28)-H(28)	0.9500	C(28)-C(27)	1.3903(18)
C(10)-H(10A)	0.96(2)	C(10)-H(10B)	0.94(2)
C(10)-H(10C)	0.90(2)	C(34)-C(41)	1.4805(17)
C(13)-H(13)	0.9500	C(13)-C(14)	1.385(2)
C(30)-C(31)	1.3978(17)	C(45)-H(45)	0.9500
C(45)-C(44)	1.390(2)	C(3)-H(3)	0.9500
C(32)-H(32)	0.9500	C(32)-C(31)	1.387(2)
C(41)-C(42)	1.3969(17)	C(14)-H(14)	0.9500
C(40)-H(40)	0.9500	C(40)-C(39)	1.388(2)
C(42)-H(42)	0.9500	C(42)-C(43)	1.391(2)
C(25)-H(25)	0.9500	C(25)-C(24)	1.393(2)
C(25)-C(26)	1.380(2)	C(18)-H(18)	0.9500
C(18)-C(17)	1.398(2)	C(18)-C(19)	1.393(2)

C(17)-C(22)	1.398(2)	C(39)-H(39)	0.9500
C(39)-C(38)	1.383(3)	C(24)-H(24)	0.9500
C(22)-H(22)	0.9500	C(22)-C(21)	1.395(2)
C(37)-H(37)	0.9500	C(37)-C(38)	1.388(2)
C(38)-H(38)	0.9500	C(44)-H(44)	0.9500
C(44)-C(43)	1.384(2)	C(27)-H(27)	0.9500
C(27)-C(26)	1.386(2)	C(31)-H(31)	0.9500
C(43)-H(43)	0.9500	C(26)-H(26)	0.9500
C(19)-H(19)	0.9500	C(19)-C(20)	1.385(3)
C(20)-H(20)	0.9500	C(20)-C(21)	1.377(3)
C(21)-H(21)	0.9500		

O(1)-Bi(1)-N(1)	98.95(4)	O(1)-Bi(1)-N(2)	79.95(4)
O(1)-Bi(1)-C(1)	94.68(4)	N(1)-Bi(1)-N(2)	143.98(3)
C(1)-Bi(1)-N(1)	75.49(4)	C(1)-Bi(1)-N(2)	68.78(3)
Bi(1)-O(1)-H(1)	108(2)	C(11)-N(1)-Bi(1)	123.03(7)
C(7)-N(1)-Bi(1)	116.90(7)	C(7)-N(1)-C(11)	119.18(9)
C(29)-N(2)-Bi(1)	122.21(7)	C(9)-N(2)-Bi(1)	112.90(7)
C(9)-N(2)-C(29)	124.81(9)	C(2)-C(1)-Bi(1)	115.54(8)
C(2)-C(1)-C(6)	122.33(10)	C(6)-C(1)-Bi(1)	122.09(8)
C(34)-C(29)-N(2)	117.84(10)	C(34)-C(29)-C(30)	120.82(10)
C(30)-C(29)-N(2)	120.90(10)	C(12)-C(11)-N(1)	120.52(10)
C(12)-C(11)-C(16)	119.22(10)	C(16)-C(11)-N(1)	120.20(10)
C(7)-C(8)-H(8A)	120.1(14)	C(7)-C(8)-H(8B)	120.4(14)
H(8A)-C(8)-H(8B)	119.5(19)	C(36)-C(35)-C(30)	122.42(11)
C(36)-C(35)-C(40)	118.86(13)	C(40)-C(35)-C(30)	118.69(12)
C(1)-C(2)-C(3)	117.85(10)	C(1)-C(2)-C(7)	118.35(10)
C(3)-C(2)-C(7)	123.79(10)	C(28)-C(23)-C(16)	120.80(11)
C(28)-C(23)-C(24)	118.56(12)	C(24)-C(23)-C(16)	120.48(11)
C(45)-C(46)-H(46)	119.7	C(45)-C(46)-C(41)	120.61(11)
C(41)-C(46)-H(46)	119.7	C(4)-C(5)-H(5)	120.4
C(4)-C(5)-C(6)	119.18(11)	C(6)-C(5)-H(5)	120.4
C(16)-C(15)-H(15)	119.6	C(14)-C(15)-H(15)	119.6
C(14)-C(15)-C(16)	120.75(12)	C(5)-C(4)-H(4)	119.3
C(3)-C(4)-C(5)	121.30(11)	C(3)-C(4)-H(4)	119.3
N(2)-C(9)-C(6)	115.97(9)	N(2)-C(9)-C(10)	124.80(10)
C(6)-C(9)-C(10)	119.23(10)	C(35)-C(36)-H(36)	120.0
C(37)-C(36)-C(35)	119.98(12)	C(37)-C(36)-H(36)	120.0

C(11)-C(12)-C(17)	122.51(11)	C(13)-C(12)-C(11)	119.26(11)
C(13)-C(12)-C(17)	118.23(11)	C(1)-C(6)-C(9)	119.20(9)
C(5)-C(6)-C(1)	119.06(10)	C(5)-C(6)-C(9)	121.72(10)
C(34)-C(33)-H(33)	119.5	C(32)-C(33)-H(33)	119.5
C(32)-C(33)-C(34)	120.92(12)	C(23)-C(28)-H(28)	119.7
C(27)-C(28)-C(23)	120.61(12)	C(27)-C(28)-H(28)	119.7
C(9)-C(10)-H(10A)	109.5(13)	C(9)-C(10)-H(10B)	109.0(14)
C(9)-C(10)-H(10C)	112.7(15)	H(10A)-C(10)-H(10B)	107.3(19)
H(10A)-C(10)-H(10C)	110(2)	H(10B)-C(10)-H(10C)	108(2)
C(29)-C(34)-C(41)	121.05(10)	C(33)-C(34)-C(29)	118.82(11)
C(33)-C(34)-C(41)	120.13(11)	C(11)-C(16)-C(23)	122.18(10)
C(15)-C(16)-C(11)	119.90(11)	C(15)-C(16)-C(23)	117.88(11)
C(12)-C(13)-H(13)	119.4	C(14)-C(13)-C(12)	121.29(12)
C(14)-C(13)-H(13)	119.4	C(29)-C(30)-C(35)	122.26(10)
C(31)-C(30)-C(29)	118.36(12)	C(31)-C(30)-C(35)	119.36(11)
C(46)-C(45)-H(45)	119.9	C(46)-C(45)-C(44)	120.24(12)
C(44)-C(45)-H(45)	119.9	C(2)-C(3)-H(3)	119.9
C(4)-C(3)-C(2)	120.23(11)	C(4)-C(3)-H(3)	119.9
C(33)-C(32)-H(32)	120.1	C(31)-C(32)-C(33)	119.76(11)
C(31)-C(32)-H(32)	120.1	C(46)-C(41)-C(34)	121.24(10)
C(42)-C(41)-C(46)	118.33(11)	C(42)-C(41)-C(34)	120.43(11)
C(15)-C(14)-H(14)	120.2	C(13)-C(14)-C(15)	119.53(11)
C(13)-C(14)-H(14)	120.2	C(35)-C(40)-H(40)	119.8
C(39)-C(40)-C(35)	120.49(14)	C(39)-C(40)-H(40)	119.8
N(1)-C(7)-C(2)	113.67(9)	C(8)-C(7)-N(1)	124.50(11)
C(8)-C(7)-C(2)	121.83(11)	C(41)-C(42)-H(42)	119.5
C(43)-C(42)-C(41)	121.01(12)	C(43)-C(42)-H(42)	119.5
C(24)-C(25)-H(25)	119.9	C(26)-C(25)-H(25)	119.9
C(26)-C(25)-C(24)	120.20(13)	C(17)-C(18)-H(18)	119.8
C(19)-C(18)-H(18)	119.8	C(19)-C(18)-C(17)	120.41(15)
C(18)-C(17)-C(12)	121.93(12)	C(22)-C(17)-C(12)	119.77(13)
C(22)-C(17)-C(18)	118.28(13)	C(40)-C(39)-H(39)	119.8
C(38)-C(39)-C(40)	120.43(13)	C(38)-C(39)-H(39)	119.8
C(23)-C(24)-H(24)	119.7	C(25)-C(24)-C(23)	120.54(13)
C(25)-C(24)-H(24)	119.7	C(17)-C(22)-H(22)	119.7
C(21)-C(22)-C(17)	120.56(16)	C(21)-C(22)-H(22)	119.7
C(36)-C(37)-H(37)	119.7	C(38)-C(37)-C(36)	120.59(14)
C(38)-C(37)-H(37)	119.7	C(39)-C(38)-C(37)	119.58(14)

C(39)-C(38)-H(38)	120.2	C(37)-C(38)-H(38)	120.2
C(45)-C(44)-H(44)	120.1	C(43)-C(44)-C(45)	119.86(13)
C(43)-C(44)-H(44)	120.1	C(28)-C(27)-H(27)	119.9
C(26)-C(27)-C(28)	120.15(13)	C(26)-C(27)-H(27)	119.9
C(30)-C(31)-H(31)	119.4	C(32)-C(31)-C(30)	121.29(12)
C(32)-C(31)-H(31)	119.4	C(42)-C(43)-H(43)	120.0
C(44)-C(43)-C(42)	119.91(12)	C(44)-C(43)-H(43)	120.0
C(25)-C(26)-C(27)	119.93(13)	C(25)-C(26)-H(26)	120.0
C(27)-C(26)-H(26)	120.0	C(18)-C(19)-H(19)	119.6
C(20)-C(19)-C(18)	120.81(17)	C(20)-C(19)-H(19)	119.6
C(19)-C(20)-H(20)	120.4	C(21)-C(20)-C(19)	119.18(15)
C(21)-C(20)-H(20)	120.4	C(22)-C(21)-H(21)	119.6
C(20)-C(21)-C(22)	120.75(17)	C(20)-C(21)-H(21)	119.6

9. GC Analysis of N_2 Formation

Although N_2O provided by Air Liquide contains less than 1 ppm air and O_2, qualitative GC-TCD analysis of the headspace after the catalytic reactions was performed to provide additional proofs of the activation of N_2O.

The samples were measured on an Agilent Technologies GC 7890B.

The parameters:

Column: 30 m HP-Plot 5 Å Molsieve, inner diameter: 0,32 mm, film thickness: 10 µm

Temperature: injector: 220°C (split injection, Split 40:1), detector: 250°C (TCD)

Program: 30°C, 10 min isotherm 6°C/min 250°C, 12°C/min 320 °C, 5 min isotherm

Gas: 0.5 bar helium

The spectrum of 1:1 mixture of N_2O and N_2:

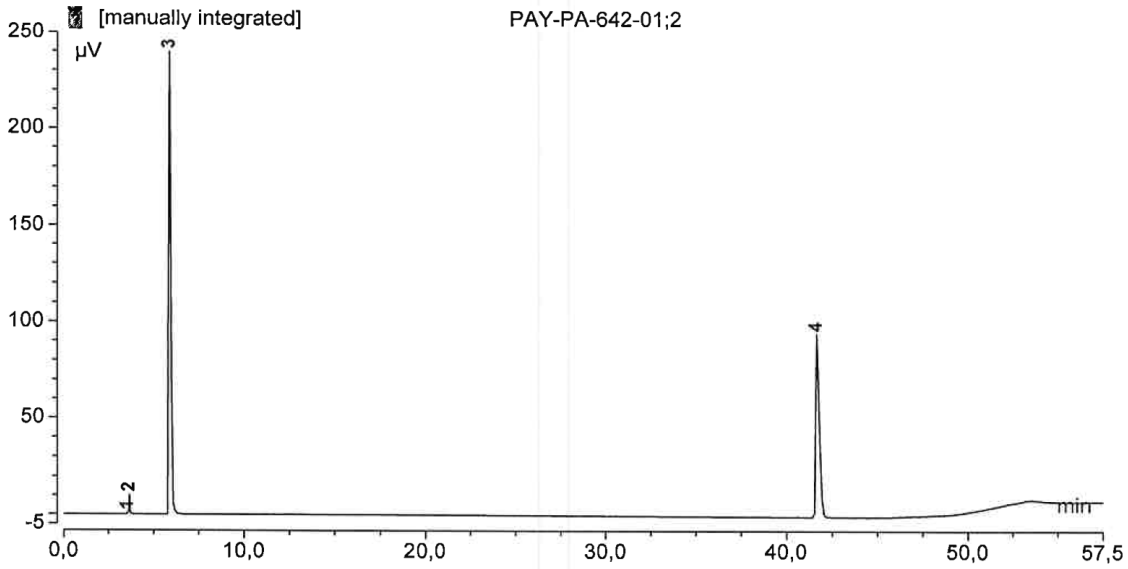

Sample:	**PAY-PA-642-01;2**	Instrument:	**GC_113**
Sequenz:	**7477 PAY-PA VD**	Measured:	**30.06.20 13:42**
Sequenz date:	**30.06.20**	Processing M.:	**PAY-PA**
		Report-File:	**PAY-PA**

Testmessung: N2 und N2O
Zuordnung mit Vergleichssubstanzen

No.	Ret.Time min	area-% %	Peak Name
1	3,58	0,04	Argon
2	3,66	1,04	O2
3	5,88	56,87	N2
4	41,67	42,05	N2O

Instrument parameters:

Column:	30,0 m	HP-Plot 5A Molsieve 0,32/10,0df G/764
Temperature:	220/ 30, 10 min iso 6/min 250 12/min 320, 5 min iso/ 250	
Gas:	0,50 bar	He
Sample size:	250,0 µL	

V. Diehl

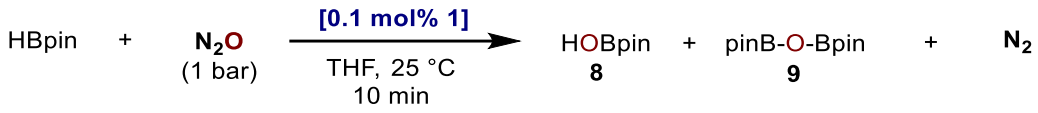

The stock solution of bismuthinidene (**1**) was prepared by dissolving 2.3 mg bismuthinidene (**1**) in 1.0 mL anhydrous and degassed THF in the glove box.

In the glove box, bismuthinidene (0.5 μmol, 100 μL stock solution, 0.1 mol%), 0.9 mL THF and HBpin (0.5 mmol, 72.5 μL) were added to a 15 mL oven-dried Schlenk tube. The Schlenk tube was sealed by a rubber septum and parafilm. And then it was taken out of the glove box and connected to a Schlenk line and a N_2O bottle via a three-way tubing system. The system was degassed by freeze-pump-thaw, backfilled with N_2O (1.0 bar) and rapidly stirred (750 rpm) for reaction. Violent release of N_2 was observed and the color of the solution remained green. As the consumption of N_2O in the headspace, the N_2 generation rate slowed down gradually. The ending point of the reaction was judged by the disappearance of green color of Bi(I) catalyst and the formation of black precipitate. The reaction time was about 10 min.

In the department of chromatography and electrophoresis, the headspace of the reaction was analyzed by GC-TCD.

The GC spectrum of catalytic N_2O activation by bismuthinidene (**1**):

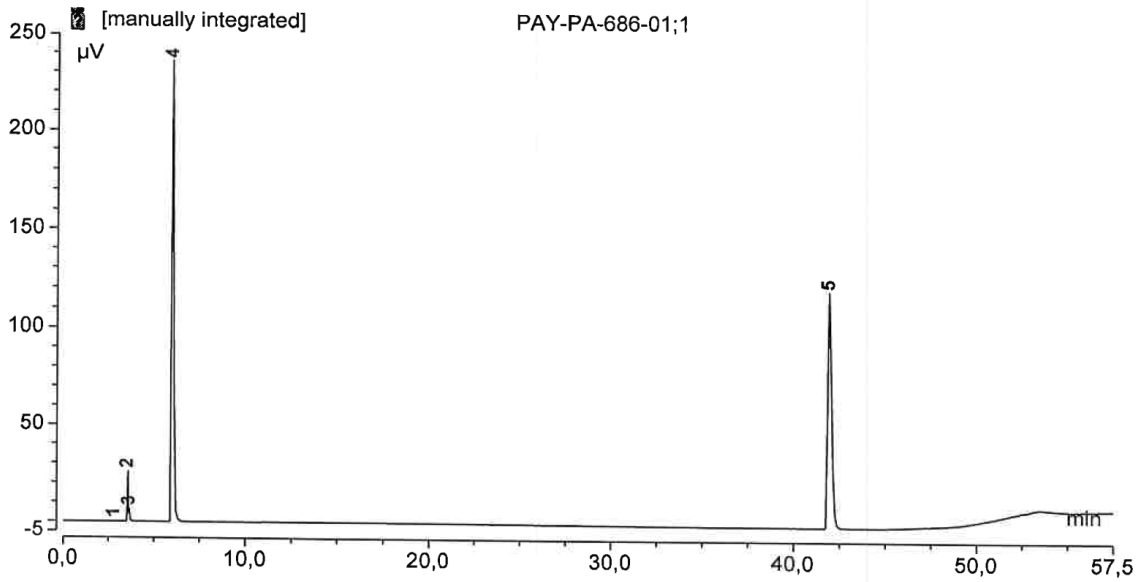

Sample:	**PAY-PA-686-01;1**	Instrument:	**GC_113**
Sequenz:	**7587 PAY-PA VD**	Measured:	**18.08.20 14:11**
Sequenz date:	**18.08.20**	Processing M.:	**PAY-PA**
		Report-File:	**PAY-PA-686-01**

Zuordnung mit Vergleichssubstanzen

No.	Ret.Time min	area-% %	Peak Name
1	2,84	0,02	
2	3,58	1,98	Argon
3	3,66	0,61	O2
4	5,95	50,27	N2
5	41,91	47,12	N2O

Instrument parameters:

Column:	30,0 m	HP-Plot 5A Molsieve 0,32/10,0df G/764
Temperature:	220/ 30, 10 min iso 6/min 250 12/min 320, 5 min iso/ 250	
Gas:	0,50 bar	He
Sample size:	250,0 µL	

V. Diehl

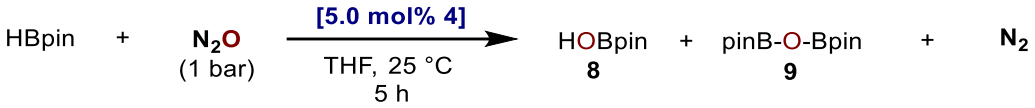

In the glove box, bismuthinidene (**4**) (19.9 mg, 25 μmol, 5.0 mol%), 1.0 mL anhydrous and degassed THF and HBpin (0.5 mmol, 72.5 μL) were added to a 12 mL oven-dried Schlenk tube. The Schlenk tube was sealed by a rubber septum and parafilm. And then it was taken out of the glove box and connected to a Schlenk line and a N_2O bottle via a three-way tubing system. The system was degassed by freeze-pump-thaw, backfilled with N_2O (1.0 bar) and rapidly stirred (750 rpm) for reaction. Slow release of N_2 was observed and the color of the solution remained dark purple. The ending point of the reaction was judged by the disappearance of purple color of Bi(I) catalyst and the formation of black precipitate. The reaction time was about 5 h.

In the department of chromatography and electrophoresis, the headspace of the reaction was analyzed by GC-TCD.

The GC spectrum of catalytic N_2O activation by bismuthinidene (**4**):

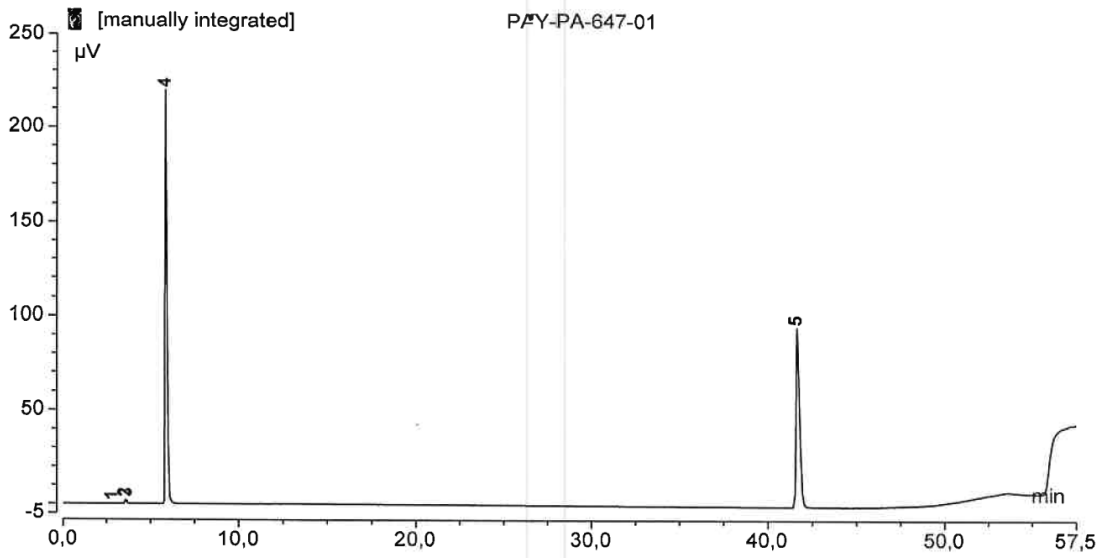

Sample:	**PAY-PA-647-01**	Instrument:	**GC_113**
Sequenz:	**7484 PAY-PA VD**	Measured:	**02.07.20 15:35**
Sequenz date:	**02.07.20**	Processing M.:	**PAY-PA**
		Report-File:	**PAY-PA-647-01**

Zuordnung mit Vergleichssubstanzen

No.	Ret.Time min	area-% %	Peak Name
1	2,84	0,01	
2	3,57	0,19	Argon
3	3,64	0,18	O2
4	5,84	55,82	N2
5	41,66	43,80	N2O

Instrument parameters:

Column:	30,0 m	HP-Plot 5A Molsieve 0,32/10,0df G/764
Temperature:	220/ 30, 10 min iso 6/min 250 12/min 320, 5 min iso/ 250	
Gas:	0 50 bar	He
Sample size:	350,0 µL	

V. Dizdl

10.References

(1) (a) Vránová, I.; Alonso, M.; Lo, R.; Sedlák, R.; Jambor, R.; Růžička, A.; Proft, F. D.; Hobza, P.; Dostál, L., From Dibismuthenes to Three- and Two-Coordinated Bismuthinidenes by Fine Ligand Tuning: Evidence for Aromatic BiC_3N Rings through a Combined Experimental and Theoretical Study. *Chem. Eur. J.* **2015,** *21*, 16917-16928; (b) Wang, F.; Planas, O.; Cornella, J., Bi(I)-Catalyzed Transfer-Hydrogenation with Ammonia-Borane. *J. Am. Chem. Soc.* **2019,** *141*, 4235-4240.

(2) Hashimoto, T.; Shimazaki, Y.; Omatsu, Y.; Maruoka, K., Indanol-Based Chiral Organoiodine Catalysts for Enantioselective Hydrative Dearomatization. *Angew. Chem., Int. Ed.* **2018,** *57*, 7200-7204.

(3) Courchay, F. C.; Sworen, J. C.; Ghiviriga, I.; Abboud, K. A.; Wagener, K. B., Understanding Structural Isomerization during Ruthenium-Catalyzed Olefin Metathesis: A Deuterium Labeling Study. *Organometallics* **2006,** *25*, 6074-6086.

(4) Déziel, R.; Malenfant, E.; Bélanger, G., Practical Synthesis of (*R*,*R*)- and (*S*,*S*)-Bis[2,6-bis(1-ethoxyethyl)phenyl] Diselenide. *J. Org. Chem.* **1996,** *61*, 1875-1876.

(5) Hyvl, J.; Yoshida, W. Y.; Rheingold, A. L.; Hughes, R. P.; Cain, M. F., A Masked Phosphinidene Trapped in a Fluxional NCN Pincer. *Chem. Eur. J.* **2016,** *22*, 17562-17565.

(6) Šimon, P.; de Proft, F.; Jambor, R.; Růžička, A.; Dostál, L., Monomeric Organoantimony(I) and Organobismuth(I) Compounds Stabilized by an NCN Chelating Ligand: Syntheses and Structures. *Angew. Chem., Int. Ed.* **2010,** *49*, 5468-5471.

(7) Vránová, I.; Jambor, R.; Růžička, A.; Jirásko, R.; Dostál, L., Reactivity of N,C,N-Chelated Antimony(III) and Bismuth(III) Chlorides with Lithium Reagents: Addition vs Substitution. *Organometallics* **2015,** *34*, 534-541.

(8) Evans, R.; Dal Poggetto, G.; Nilsson, M.; Morris, G. A., Improving the Interpretation of Small Molecule Diffusion Coefficients. *Anal. Chem.* **2018,** *90*, 3987-3994.

(9) Bagherzadeh, S.; Mankad, N. P., Catalyst Control of Selectivity in CO_2 Reduction Using a Tunable Heterobimetallic Effect. *J. Am. Chem. Soc.* **2015,** *137*, 10898-10901.

(10) Hawkeswood, S.; Stephan, D. W., Syntheses and Reactions of the Bis-boryloxide $O(Bpin)_2$ (pin = $O_2C_2Me_4$). *Dalton Trans.* **2005**, 2182-2187.

(11) (a) Tskhovrebov, A. G.; Solari, E.; Wodrich, M. D.; Scopelliti, R.; Severin, K., Covalent Capture of Nitrous Oxide by *N*-Heterocyclic Carbenes. *Angew. Chem., Int. Ed.* **2012,** *51*, 232-234; (b) Tskhovrebov, A. G.; Vuichoud, B.; Solari, E.; Scopelliti, R.; Severin, K., Adducts of Nitrous Oxide and *N*-Heterocyclic Carbenes: Syntheses, Structures, and Reactivity. *J. Am. Chem. Soc.* **2013,** *135*, 9486-9492.

(12) (a) Matano, Y.; Nomura, H., Dimeric Triarylbismuthane Oxide: A Novel Efficient Oxidant for the Conversion of Alcohols to Carbonyl Compounds. *J. Am. Chem. Soc.* **2001,** *123*, 6443-6444; (b) Matano, Y.; Nomura, H.; Hisanaga, T.; Nakano, H.; Shiro, M.; Imahori, H., Diverse Structures and Remarkable Oxidizing Ability of Triarylbismuthane Oxides. Comparative Study on the Structure and Reactivity of a Series of Triarylpnictogen Oxides. *Organometallics* **2004,** *23*, 5471-5480.

(13) (a) Sasamori, T.; Arai, Y.; Takeda, N.; Okazaki, R.; Furukawa, Y.; Kimura, M.; Nagase, S.; Tokitoh, N., Syntheses, Structures and Properties of Kinetically Stabilized Distibenes and Dibismuthenes, Novel Doubly Bonded Systems between Heavier Group 15 Elements. *Bull. Chem. Soc. Jpn.* **2002,** *75*, 661-675; (b) Tokitoh, N.; Arai, Y.; Okazaki, R.; Nagase, S., Synthesis and Characterization of a Stable Dibismuthene: Evidence for a Bi-Bi Double Bond. *Science* **1997,** *277*, 78-80.

(14) Strîmb, G.; Pöllnitz, A.; Raţ, C. I.; Silvestru, C., A General Route to Monoorganopnicogen(III) (M = Sb, Bi) Compounds with a Pincer (N,C,N) Group and Oxo Ligands. *Dalton Trans.* **2015,** *44*, 9927-9942.

(15) (a) Breunig, H. J.; Königsmann, L.; Lork, E.; Nema, M.; Philipp, N.; Silvestru, C.; Soran, A.; Varga, R. A.; Wagner, R., Hypervalent Organobismuth(III) Carbonate, Chalcogenides and Halides with the Pendant Arm Ligands 2-(Me_2NCH_2)C_6H_4 and 2,6-(Me_2NCH_2)$_2C_6H_3$. *Dalton Trans.* **2008**, 1831-1842; (b) Chovancová, M.; Jambor, R.; Růžička, A.; Jirásko, R.; Císařová, I.; Dostál, L., Synthesis, Structure, and Reactivity of Intramolecularly Coordinated Organoantimony and Organobismuth Sulfides. *Organometallics* **2009,** *28*, 1934-1941.

(16) Kather, R.; Svoboda, T.; Wehrhahn, M.; Rychagova, E.; Lork, E.; Dostál, L.; Ketkov, S.; Beckmann, J., Lewis-acid Induced Disaggregation of Dimeric Arylantimony Oxides. *Chem. Commun.* **2015,** *51*, 5932-5935.

(17) Wang, Y.; Hu, H.; Zhang, J.; Cui, C., Comparison of Anionic and Lewis Acid Stabilized *N*-Heterocyclic Oxoboranes: Their Facile Synthesis from a Borinic Acid. *Angew. Chem., Int. Ed.* **2011,** *50*, 2816-2819.

(18) (a) Hardman, N. J.; Twamley, B.; Power, P. P., (2,6-$Mes_2H_3C_6$)$_2$BiH, a Stable, Molecular Hydride of a Main Group Element of the Sixth Period, and Its Conversion to the Dibismuthene (2,6-$Mes_2H_3C_6$)BiBi(2,6-$Mes_2C_6H_3$). *Angew. Chem., Int. Ed.* **2000,** *39*, 2771-2773; (b) Balázs, G.; Breunig, H. J.; Lork, E., Synthesis and Characterization of R_2SbH, R_2BiH, and $R_2Bi{-}BiR_2$ [R = (Me_3Si)$_2$CH]. *Organometallics* **2002,** *21*, 2584-2586.

11. NMR Spectra

^{1}H NMR ($CDCl_3$, 400 MHz)

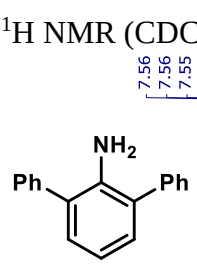

2,6-diphenylaniline

^{13}C NMR ($CDCl_3$, 101 MHz)

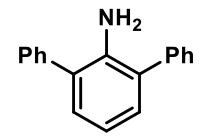

2,6-diphenylaniline

^{1}H NMR ($CDCl_3$, 400 MHz)

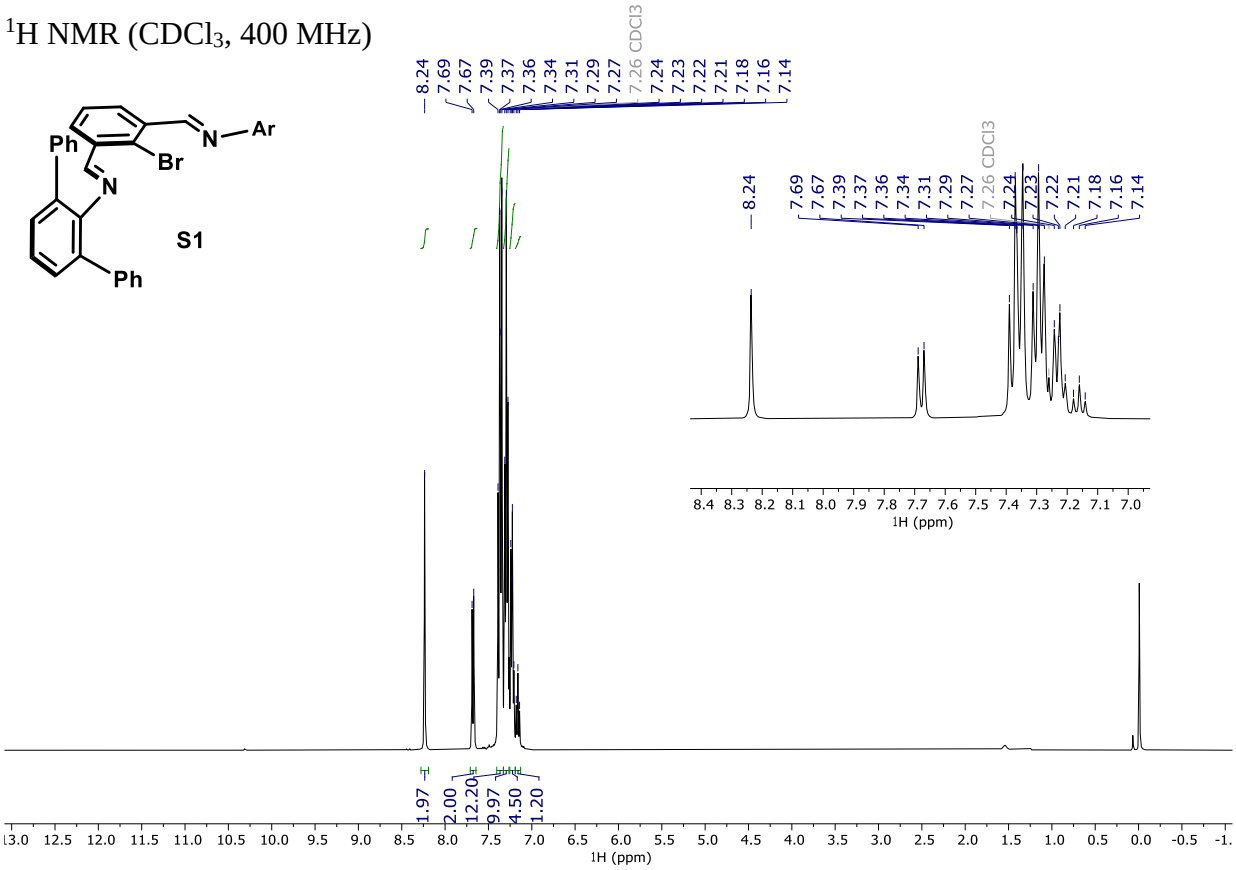

^{13}C NMR ($CDCl_3$, 101 MHz)

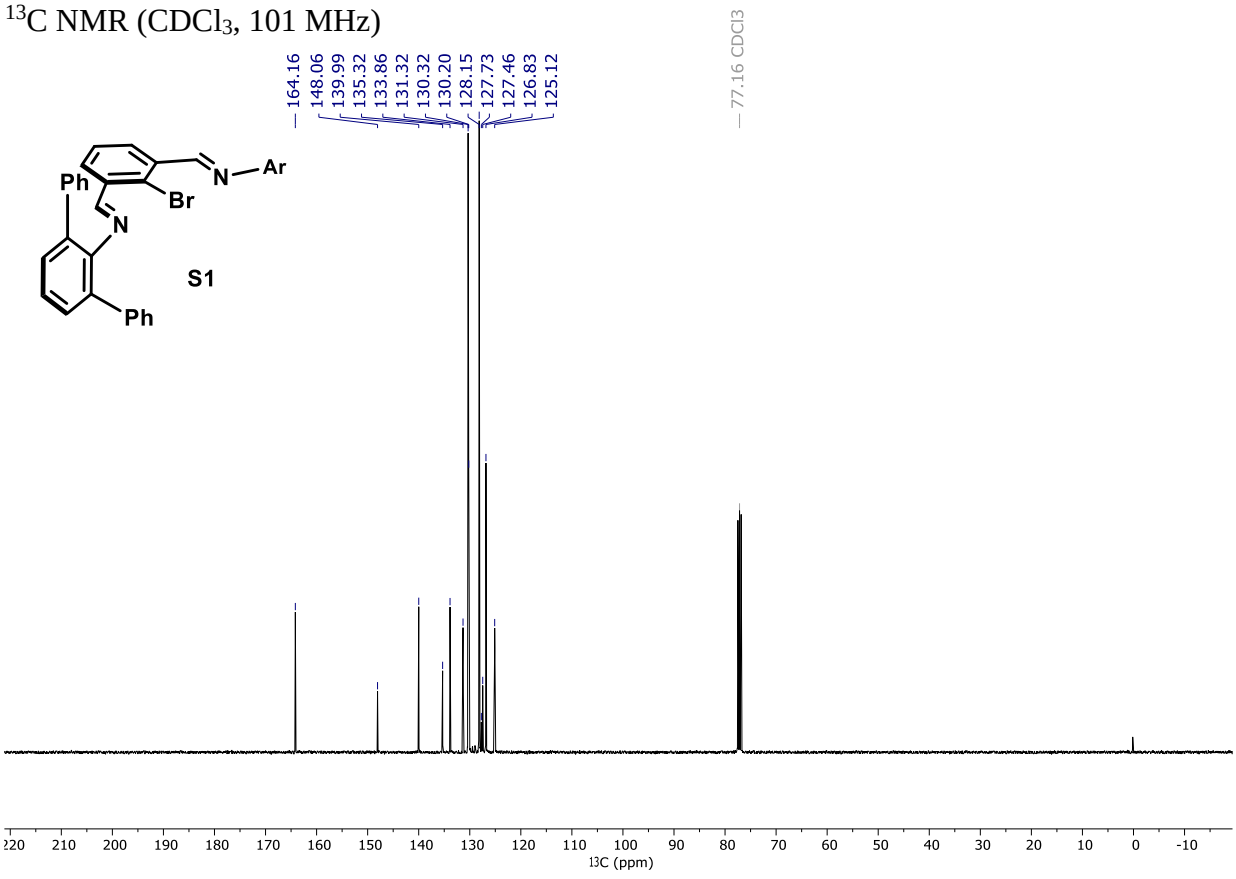

^{1}H NMR (CD_3OD, 400 MHz)

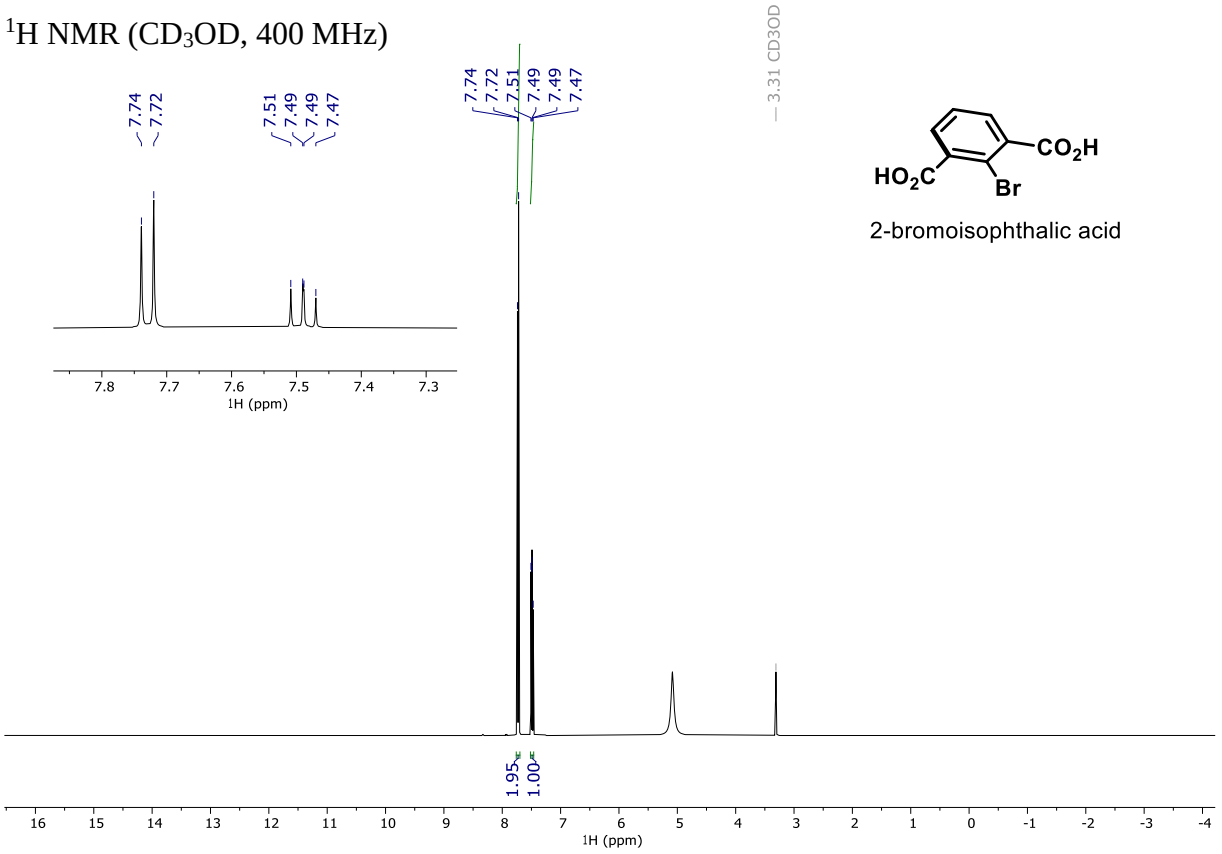

2-bromoisophthalic acid

^{13}C NMR (CD_3OD, 101 MHz)

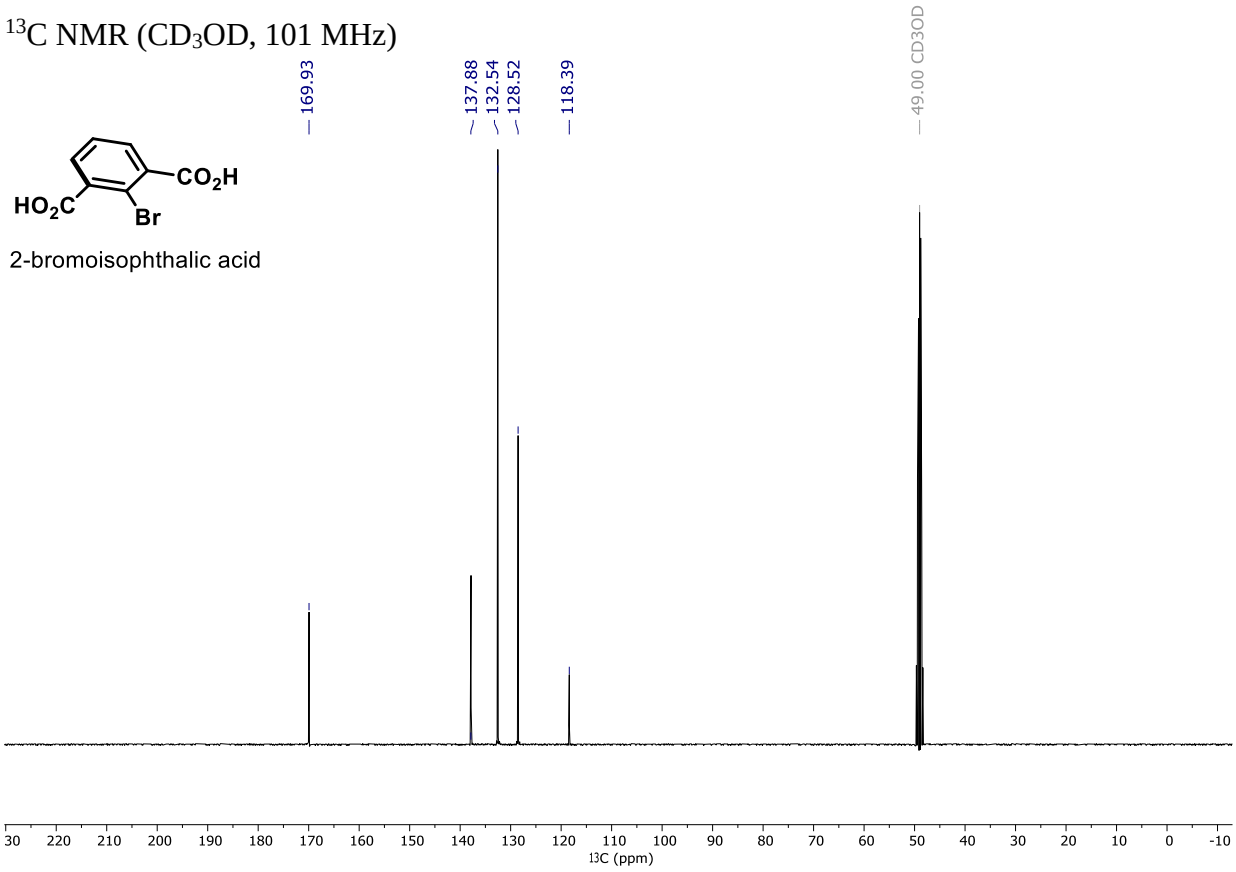

2-bromoisophthalic acid

^{1}H NMR ($CDCl_3$, 400 MHz)

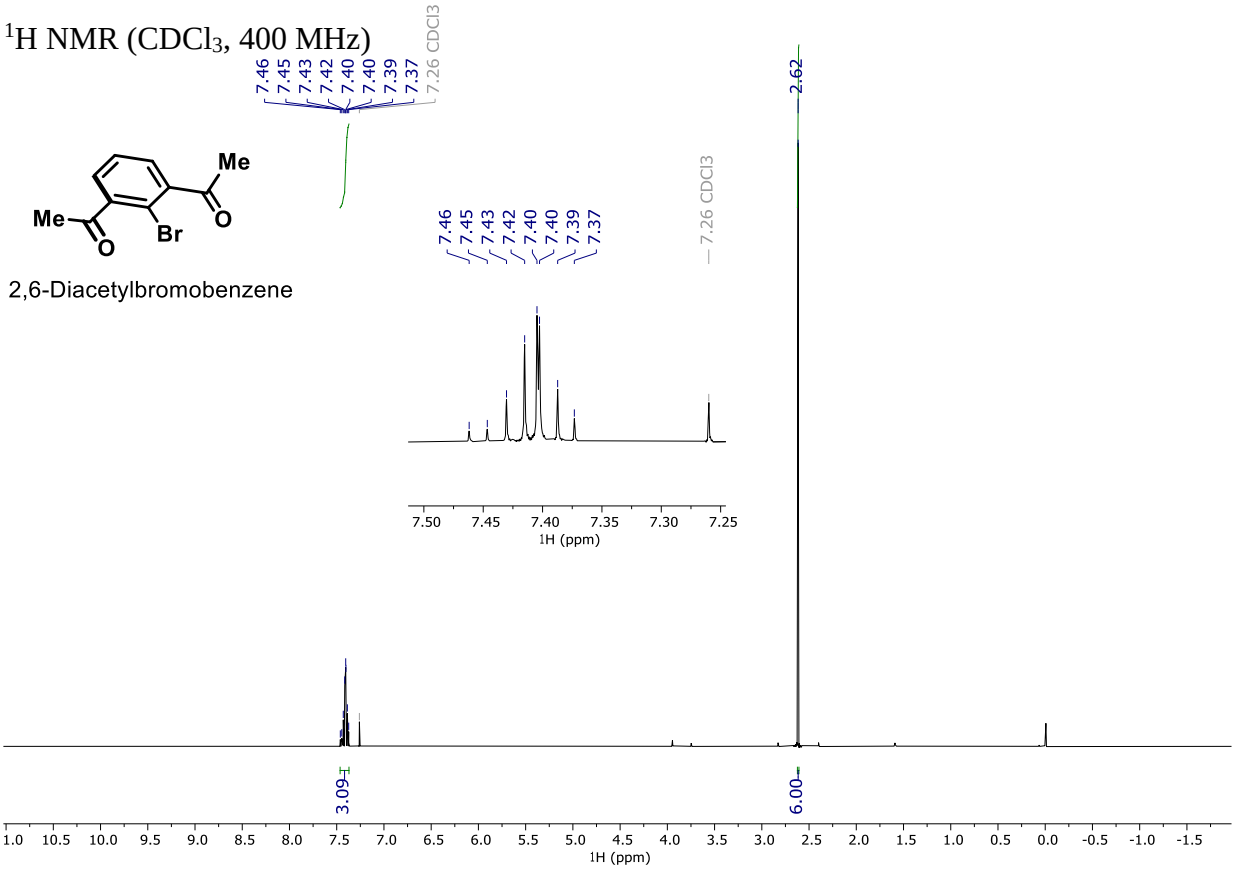

2,6-Diacetylbromobenzene

^{13}C NMR ($CDCl_3$, 101 MHz)

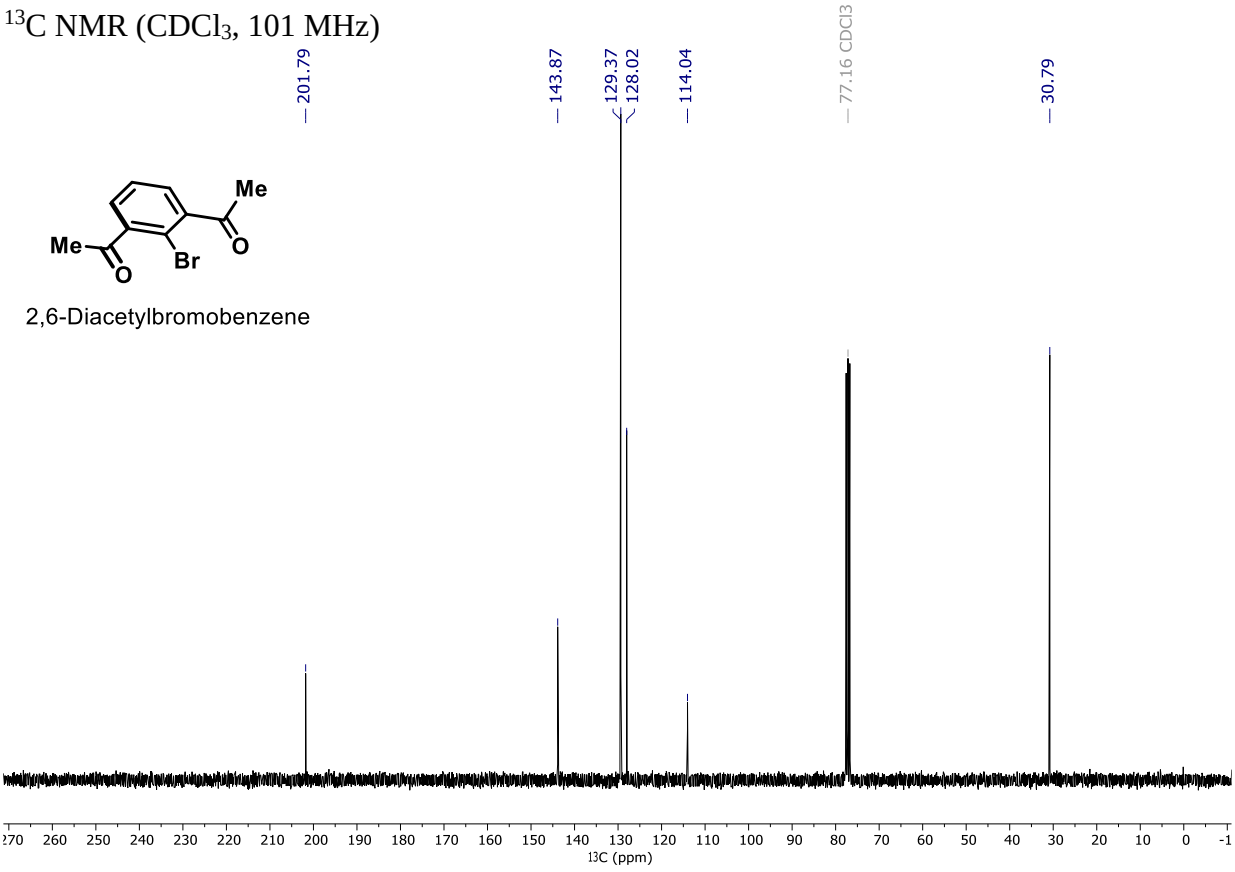

2,6-Diacetylbromobenzene

^{1}H NMR ($CDCl_3$, 400 MHz)

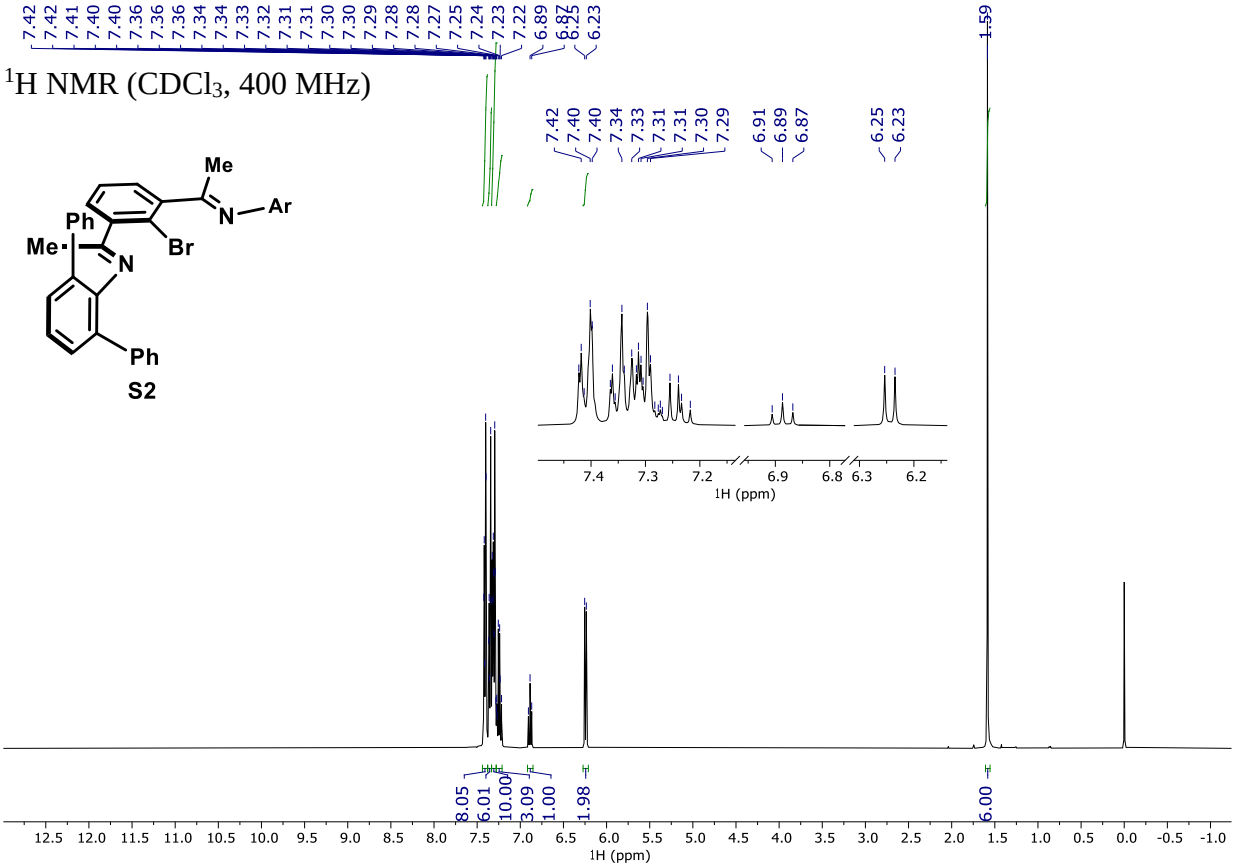

^{13}C NMR ($CDCl_3$, 101 MHz)

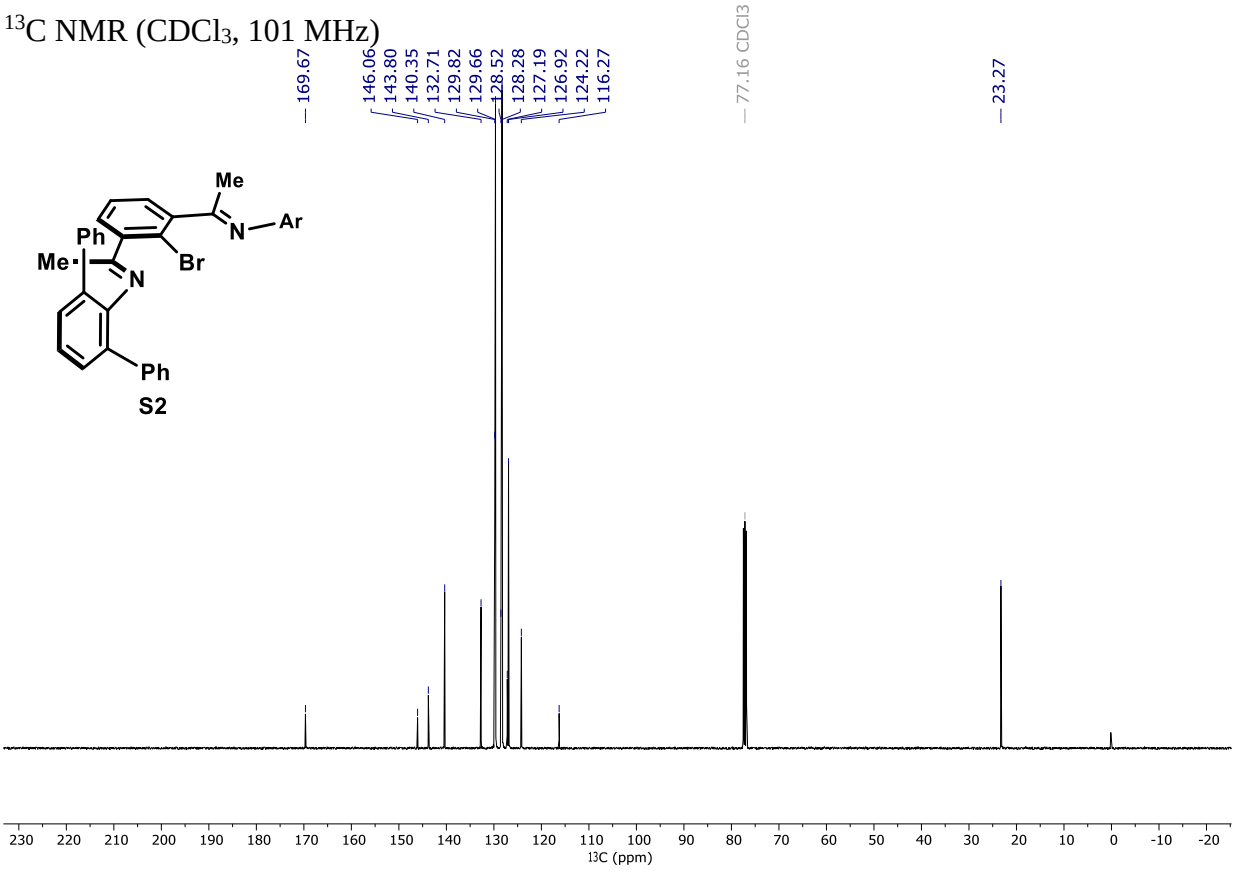

^{1}H NMR ($CDCl_3$, 400 MHz)

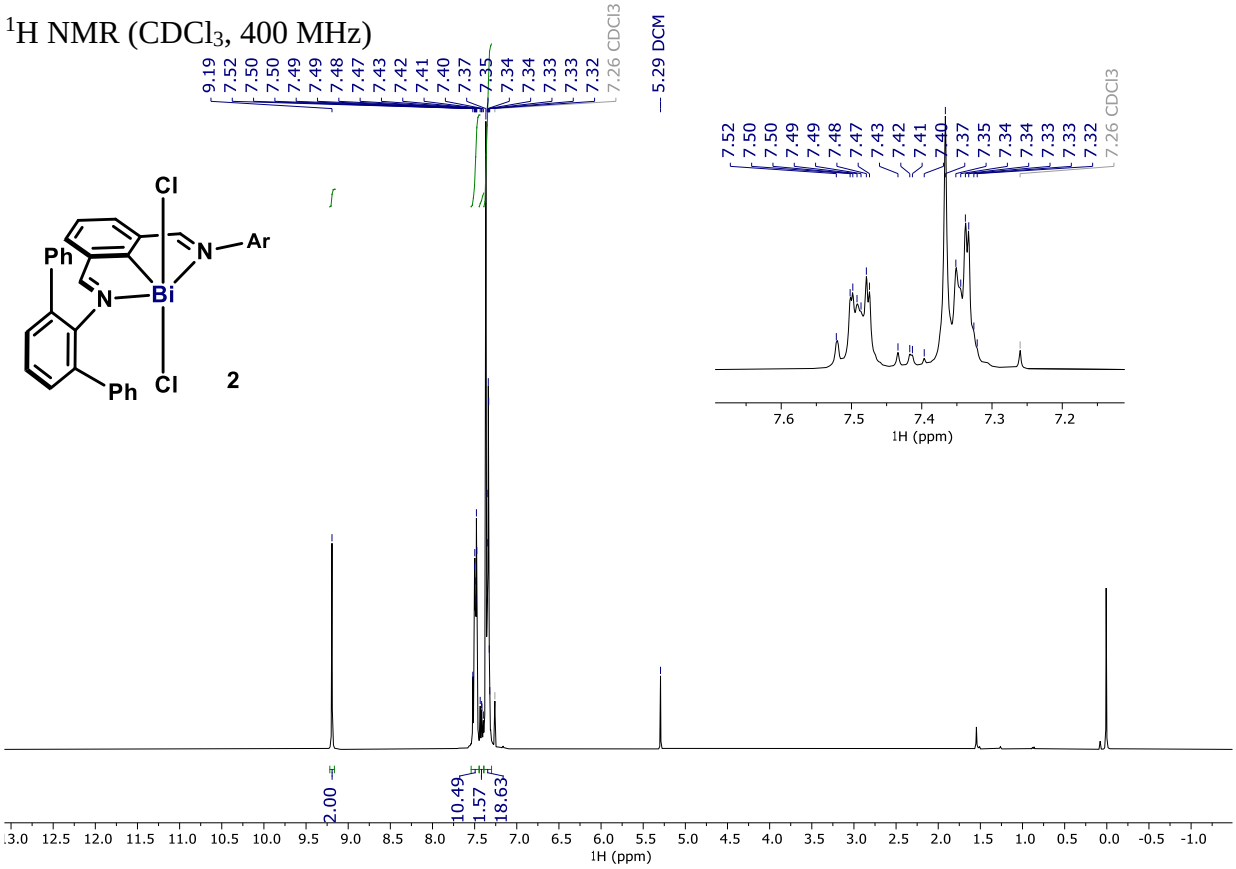

^{13}C NMR ($CDCl_3$, 101 MHz)

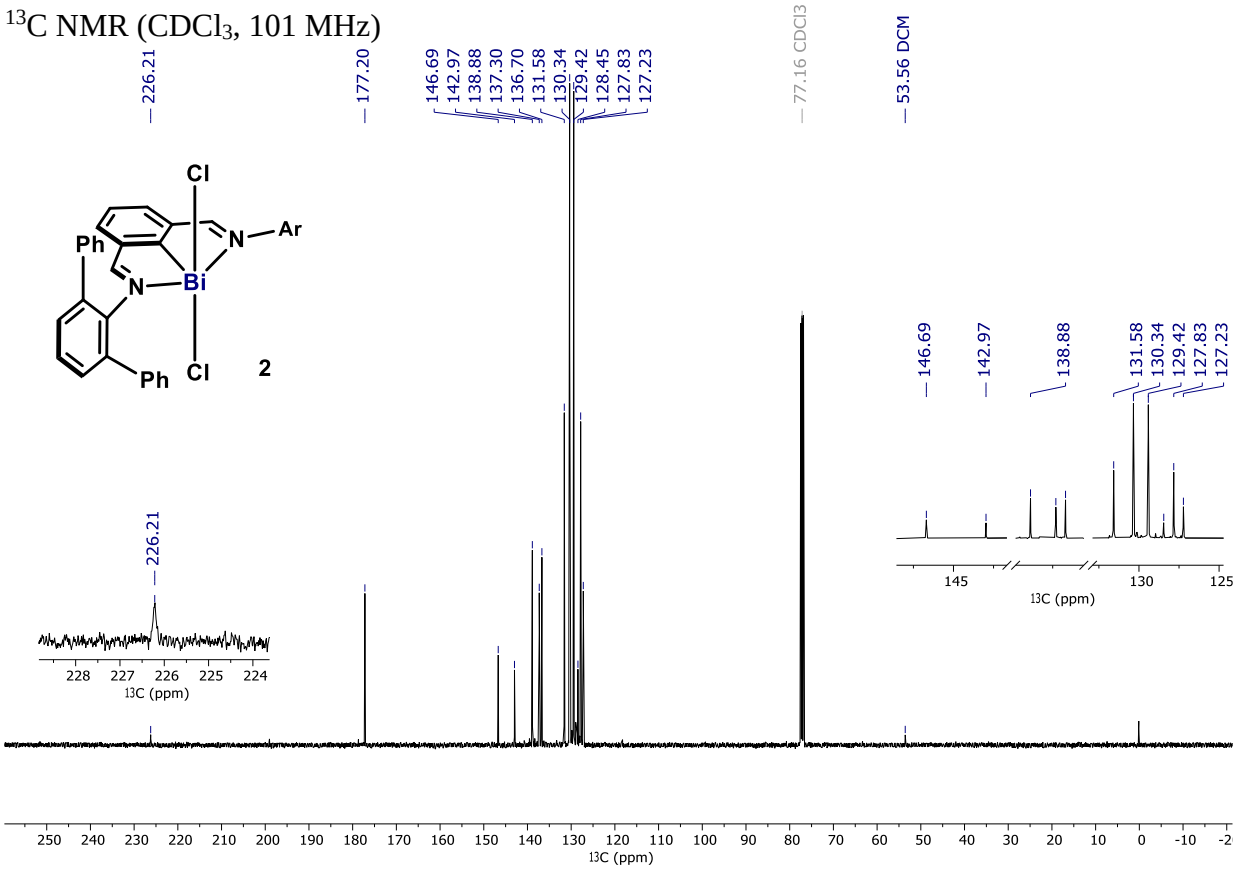

^{1}H NMR ($CDCl_3$, 400 MHz)

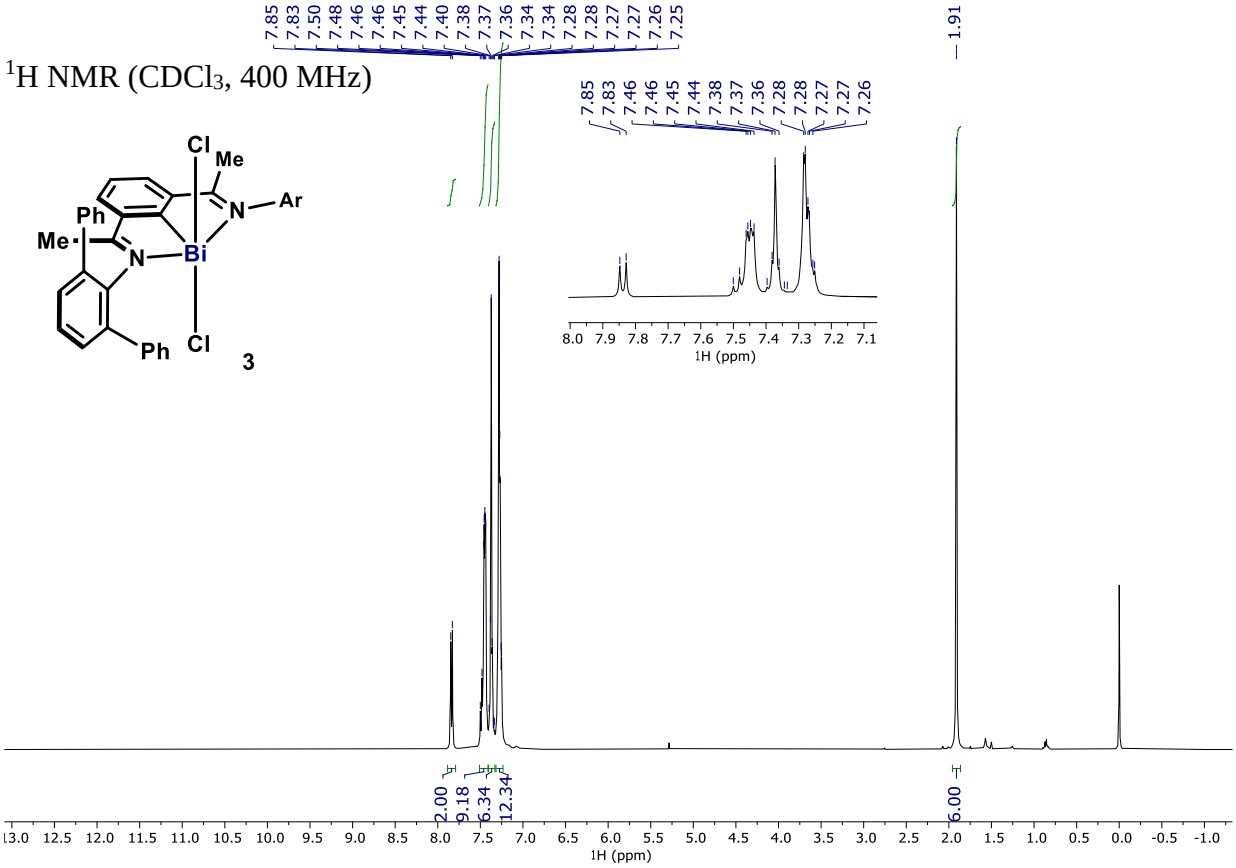

^{13}C NMR ($CDCl_3$, 101 MHz)

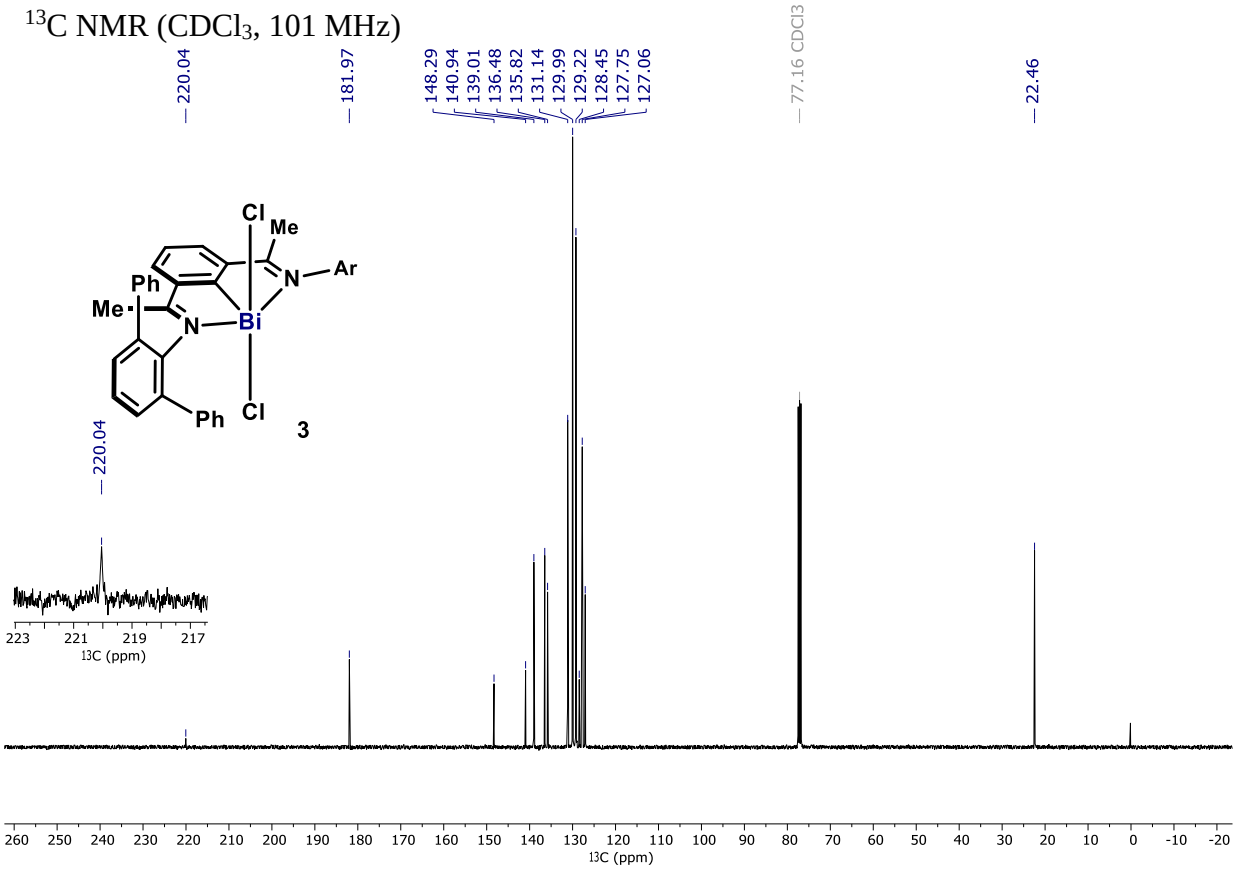

^{1}H NMR (500 MHz, THF-d_8)

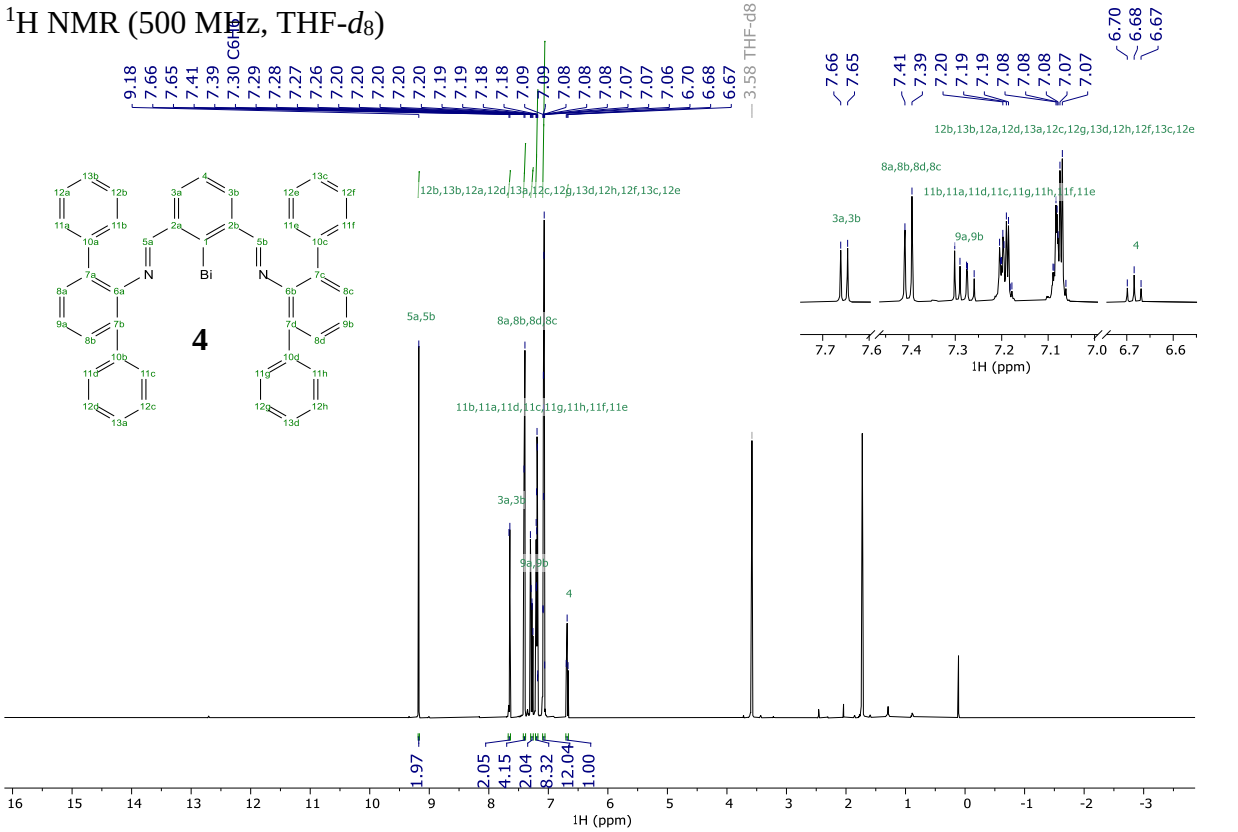

^{13}C NMR (126 MHz, THF-d_8)

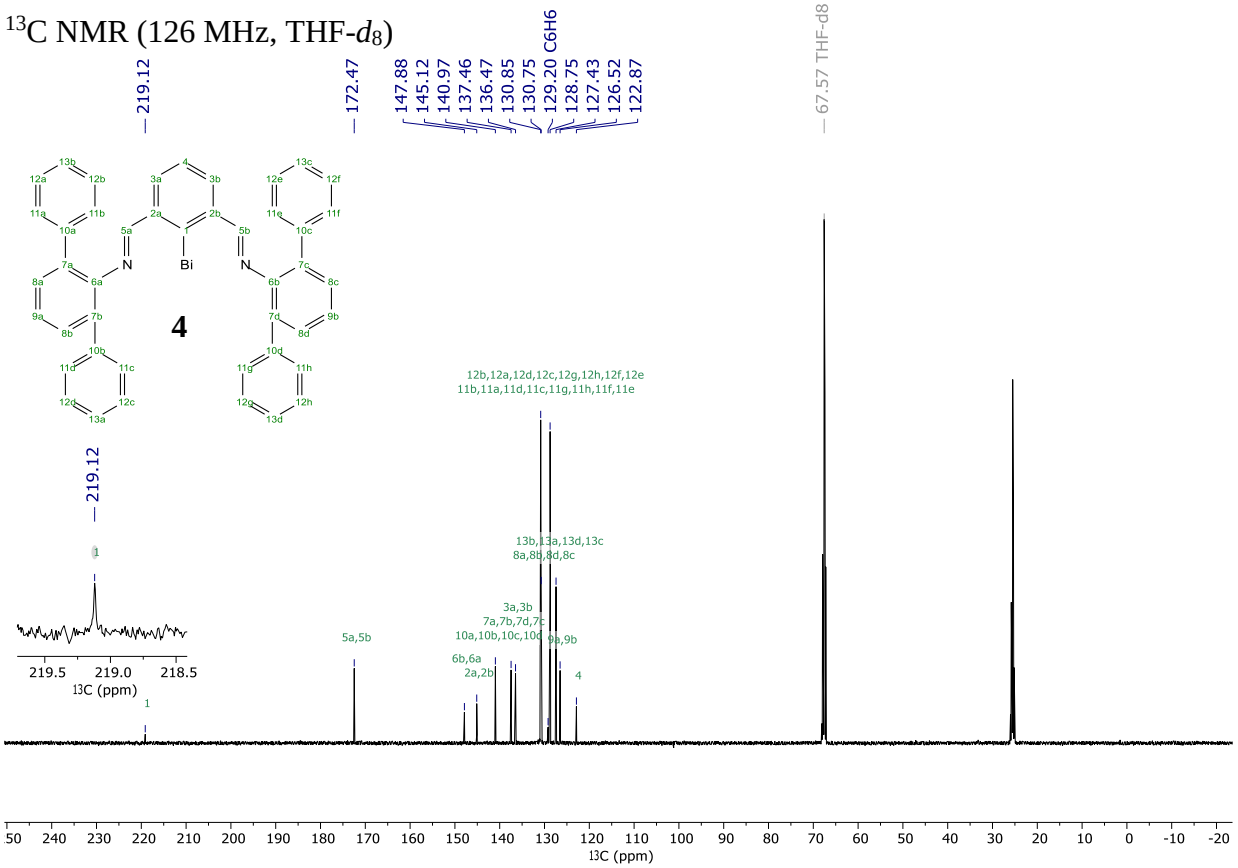

^{1}H NMR (400 MHz, THF-d_8)

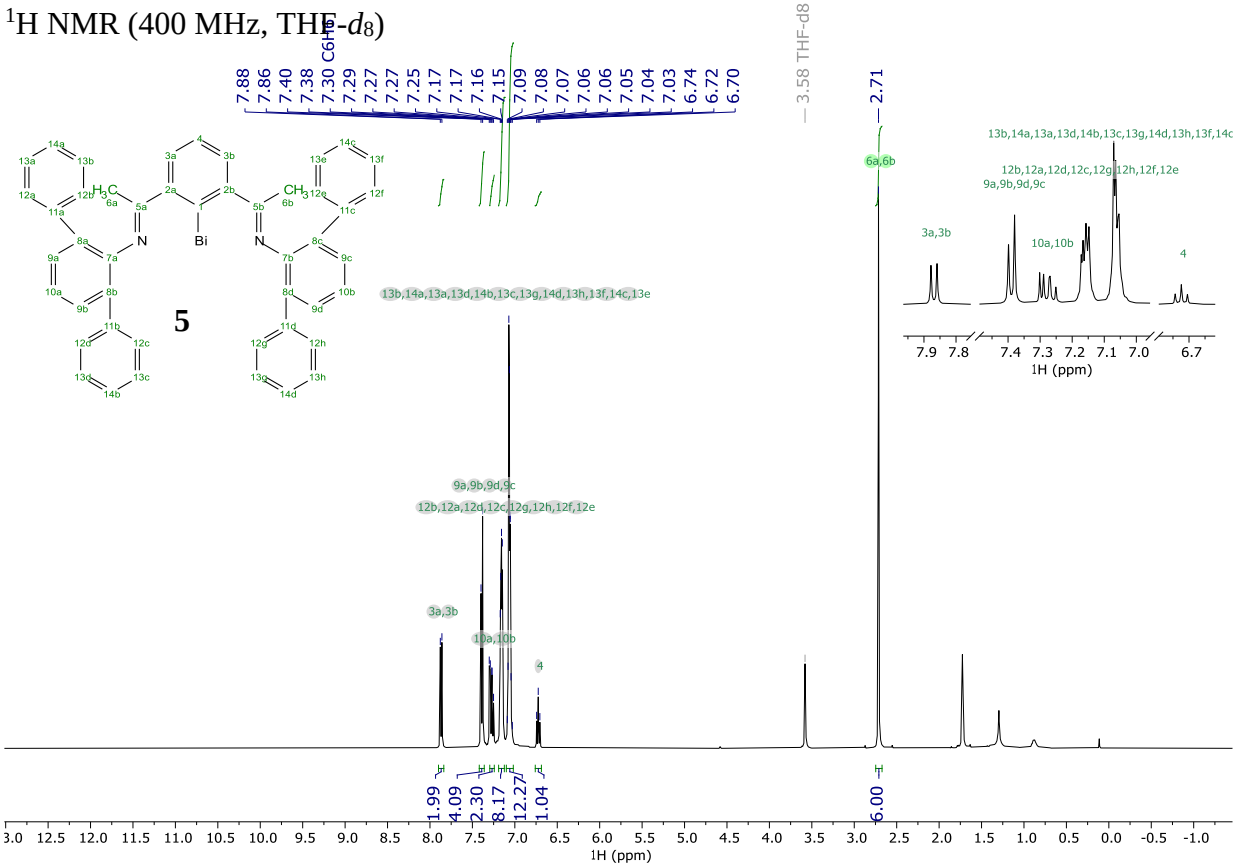

^{13}C NMR (101 MHz, THF-d_8)

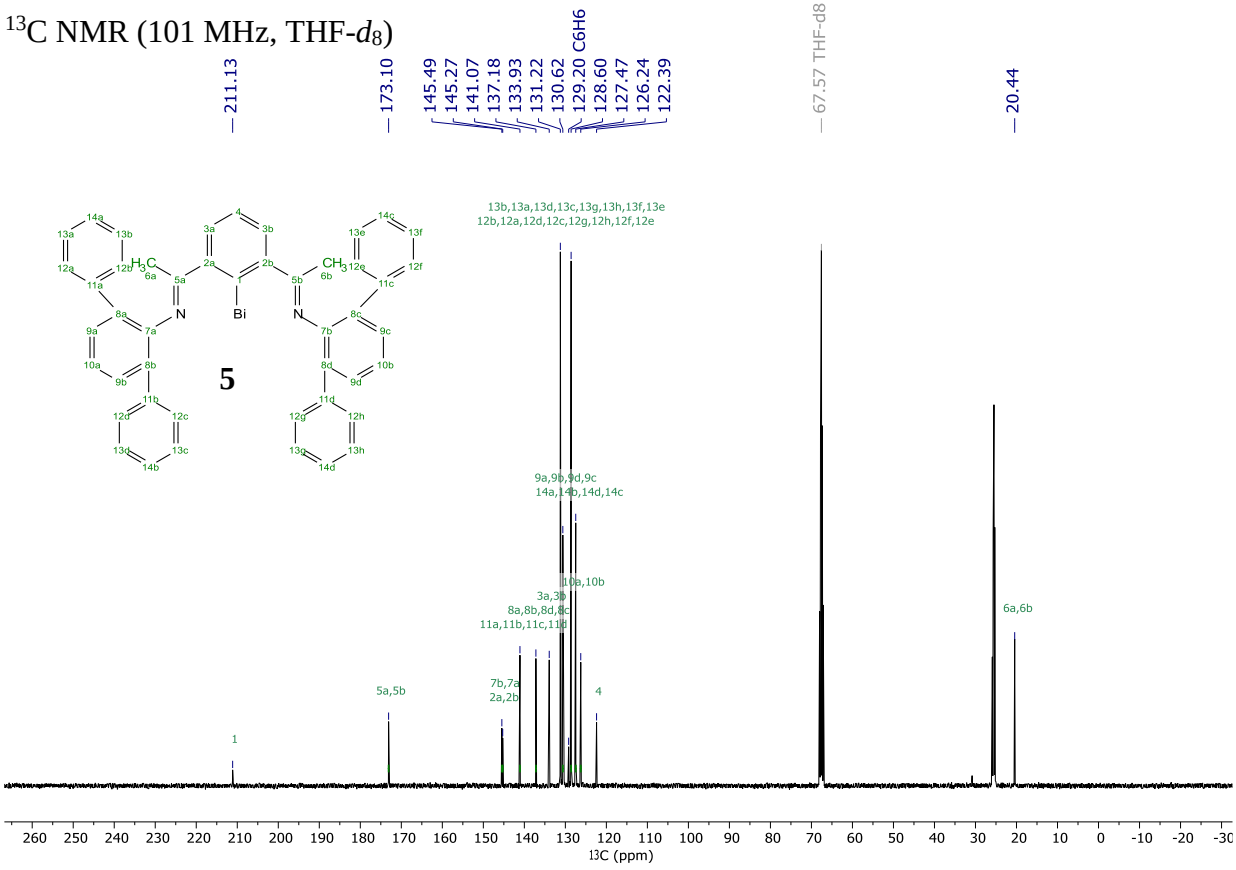

^{1}H NMR (400 MHz, THF-d_8, -50 °C)

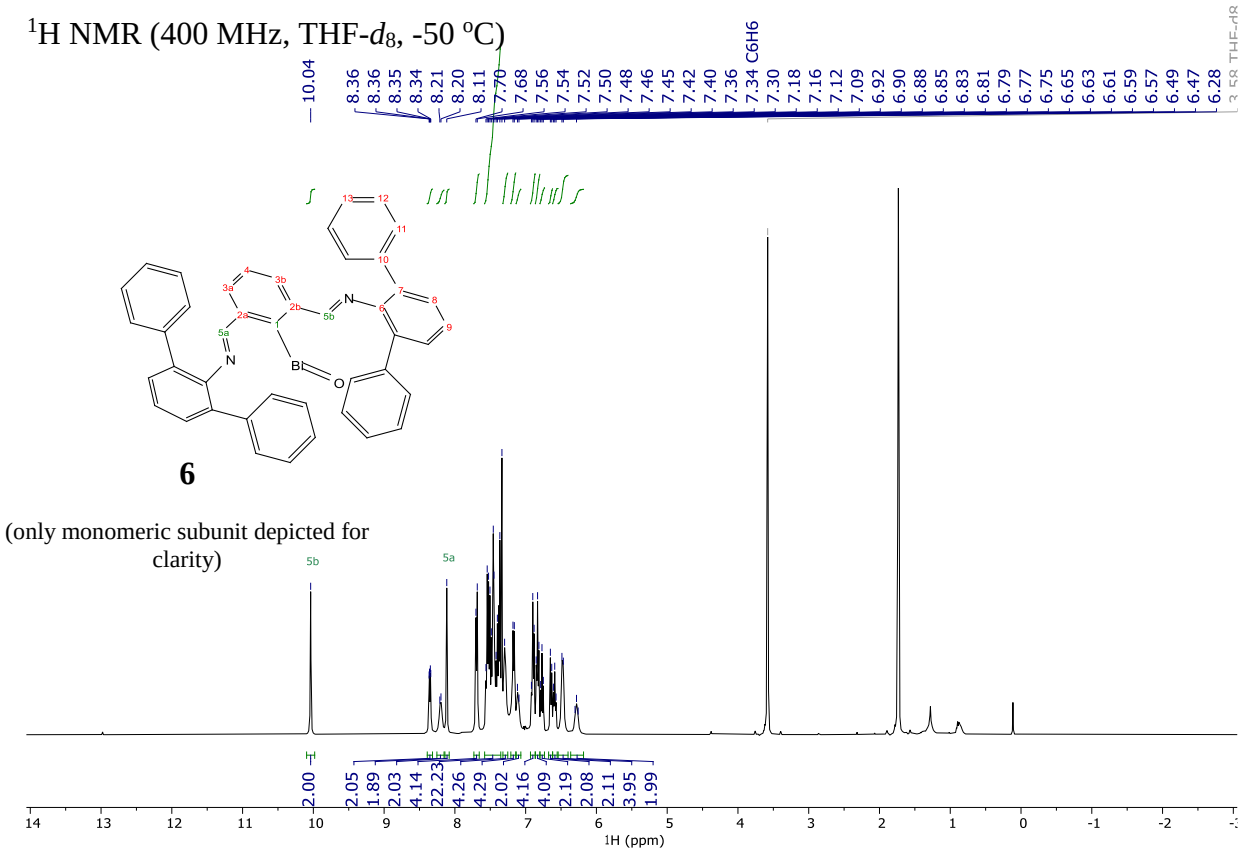

6

(only monomeric subunit depicted for clarity)

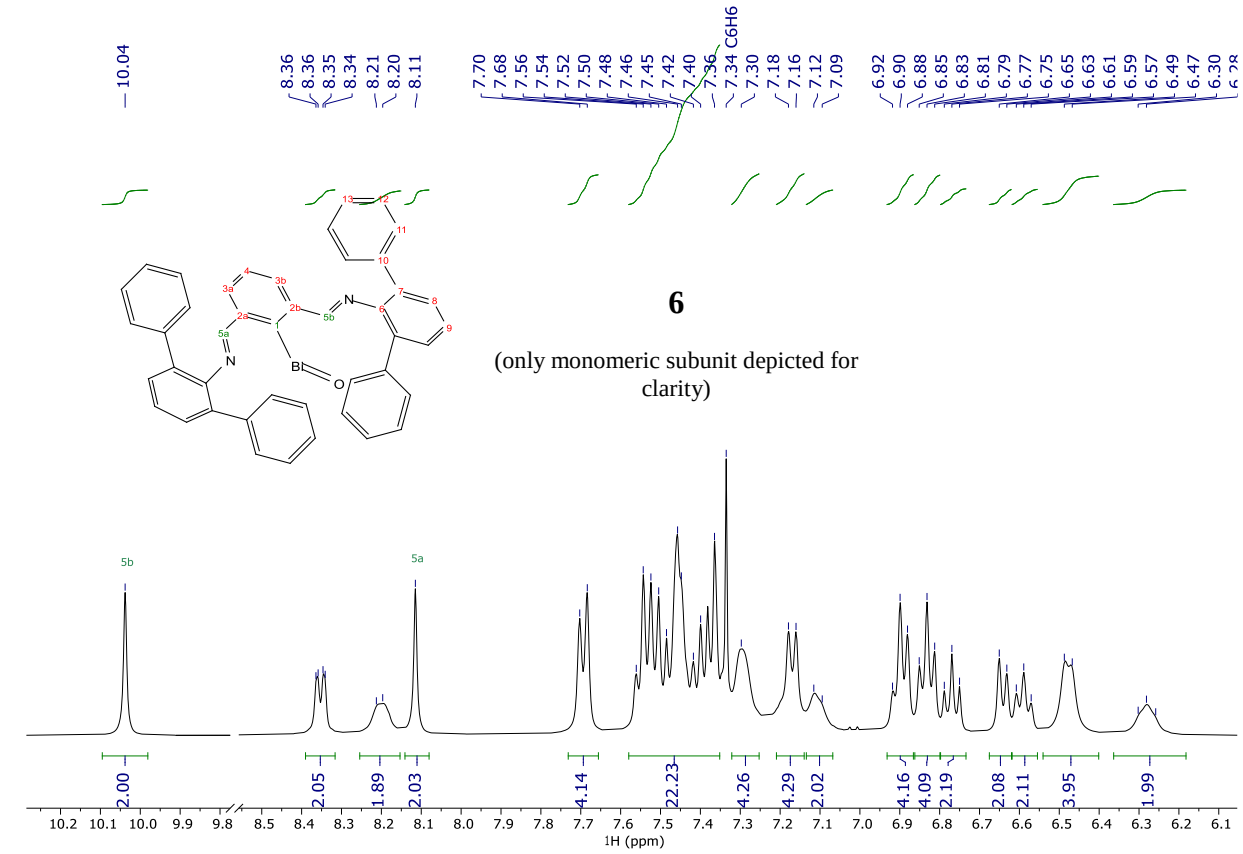

6

(only monomeric subunit depicted for clarity)

^{13}C NMR (101 MHz, THF-d_8, -50 °C)

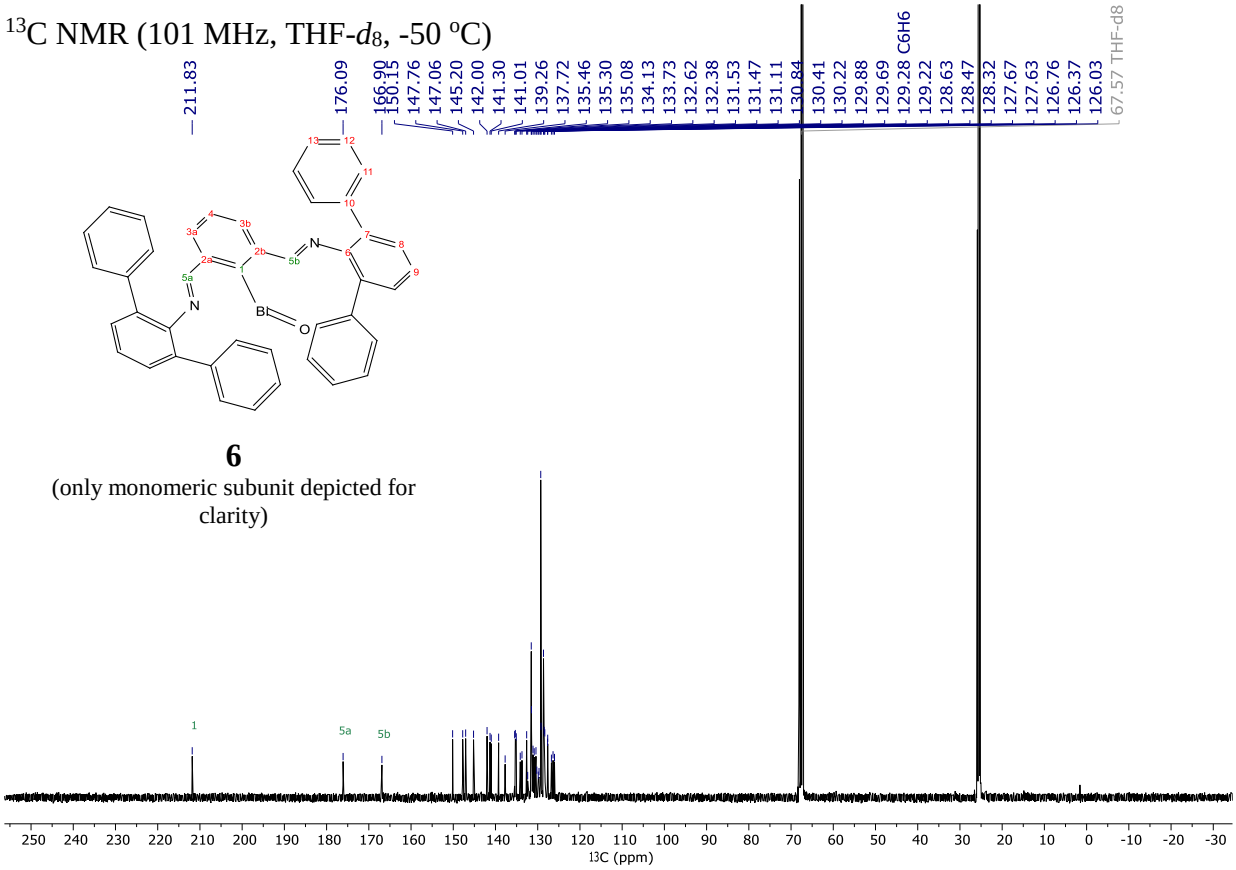

6

(only monomeric subunit depicted for clarity)

^{1}H NMR (400 MHz, THF-d_8, 60 ^{o}C)

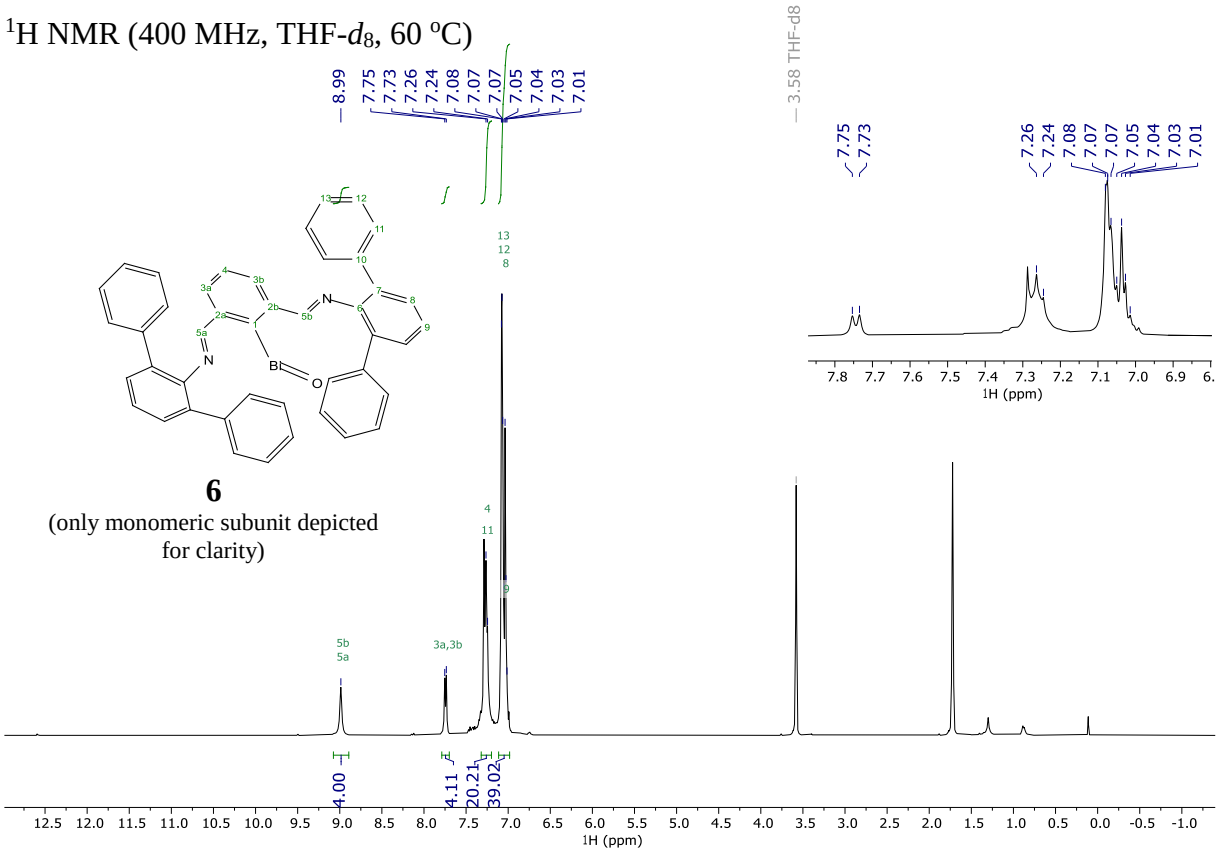

^{13}C NMR (101 MHz, THF-d_8, 60 ^{o}C)

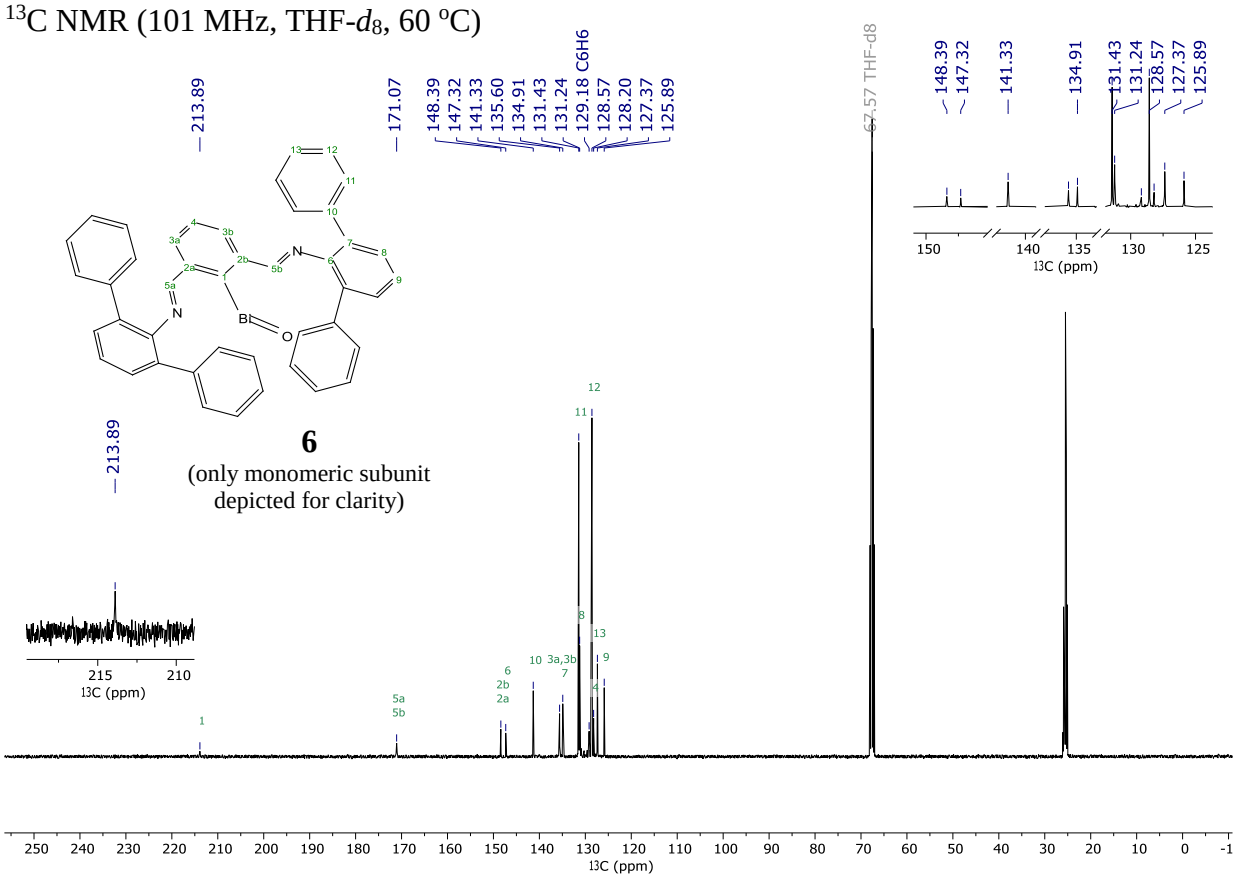

HSQC (–50 ºC)

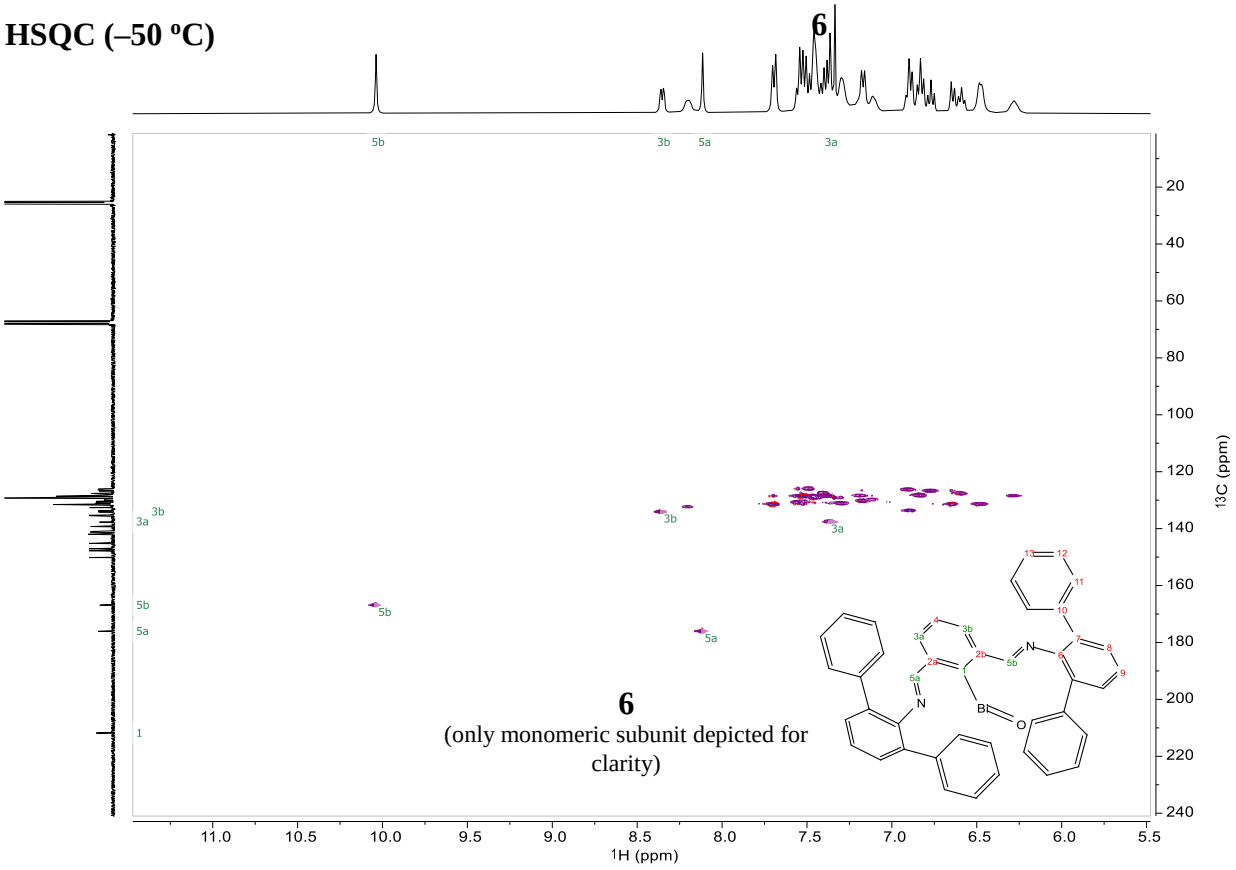

HMBC (–50 ºC)

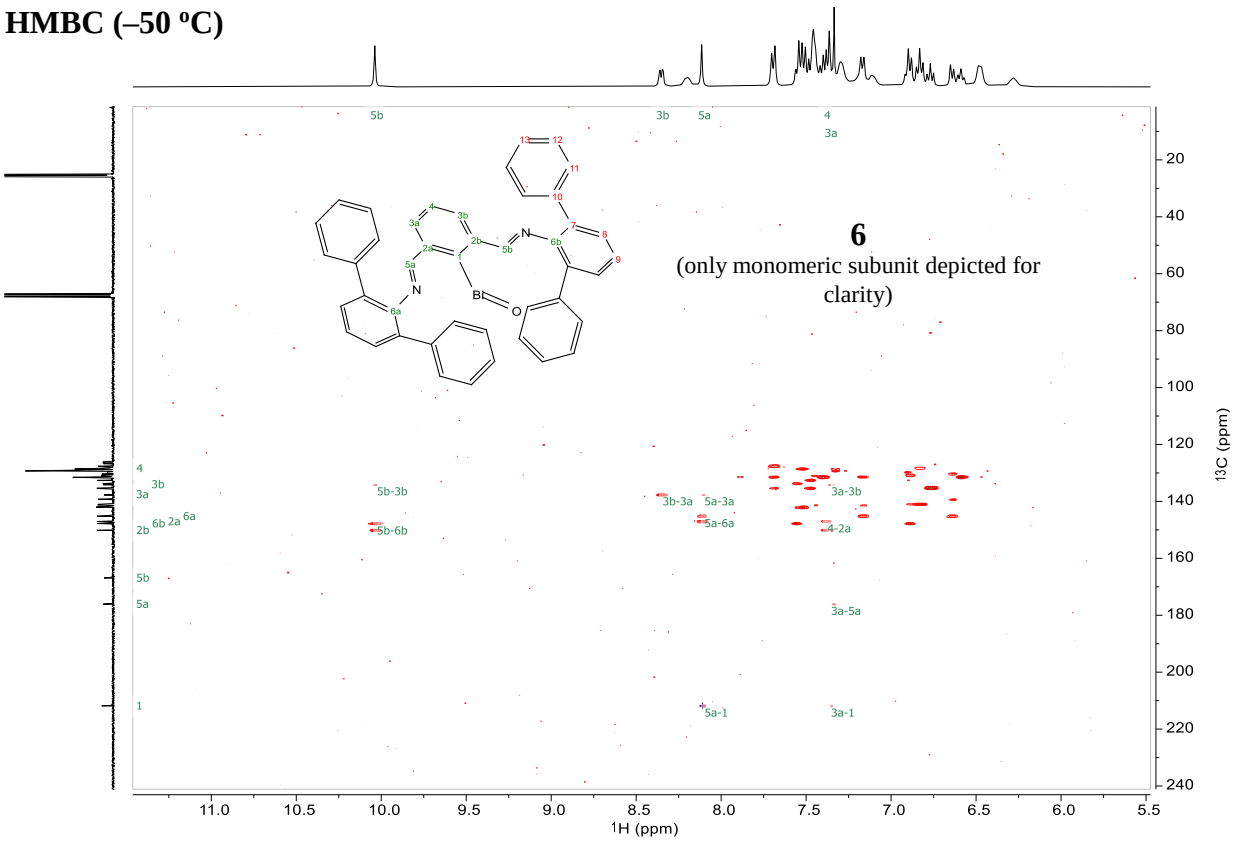

ROESY (–50 ºC)

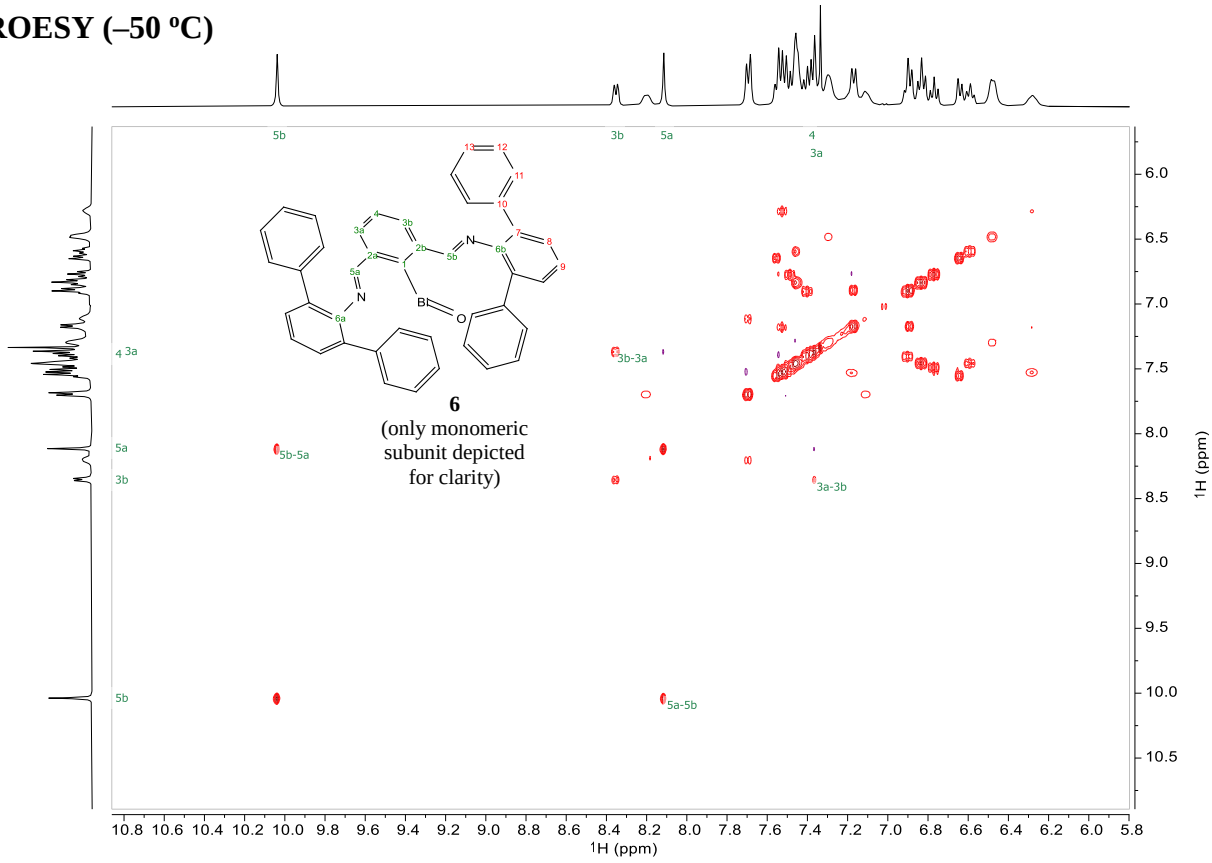

6
(only monomeric subunit depicted for clarity)

^{1}H NMR (400 MHz, THF-d_8, 25 ^{o}C)

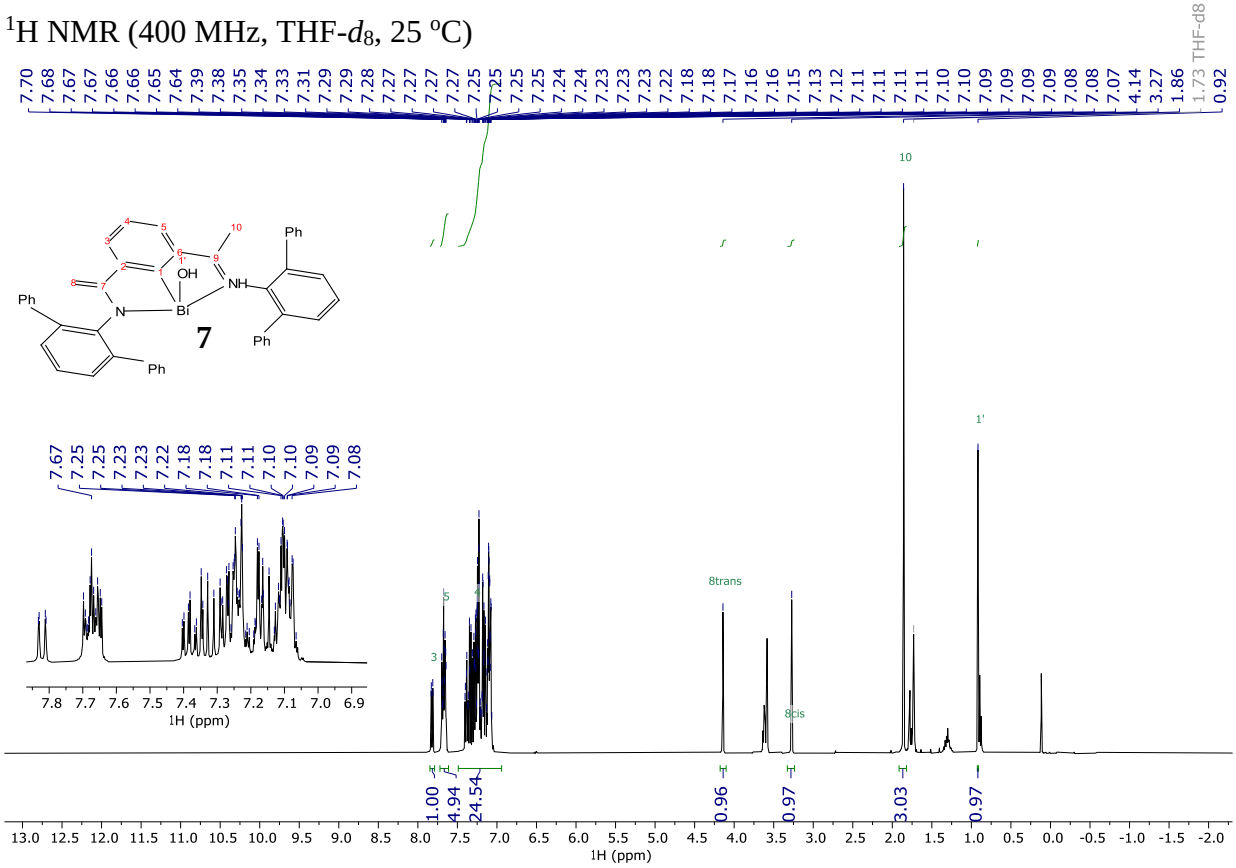

^{13}C NMR (101 MHz, THF-d_8, 25 ^{o}C)

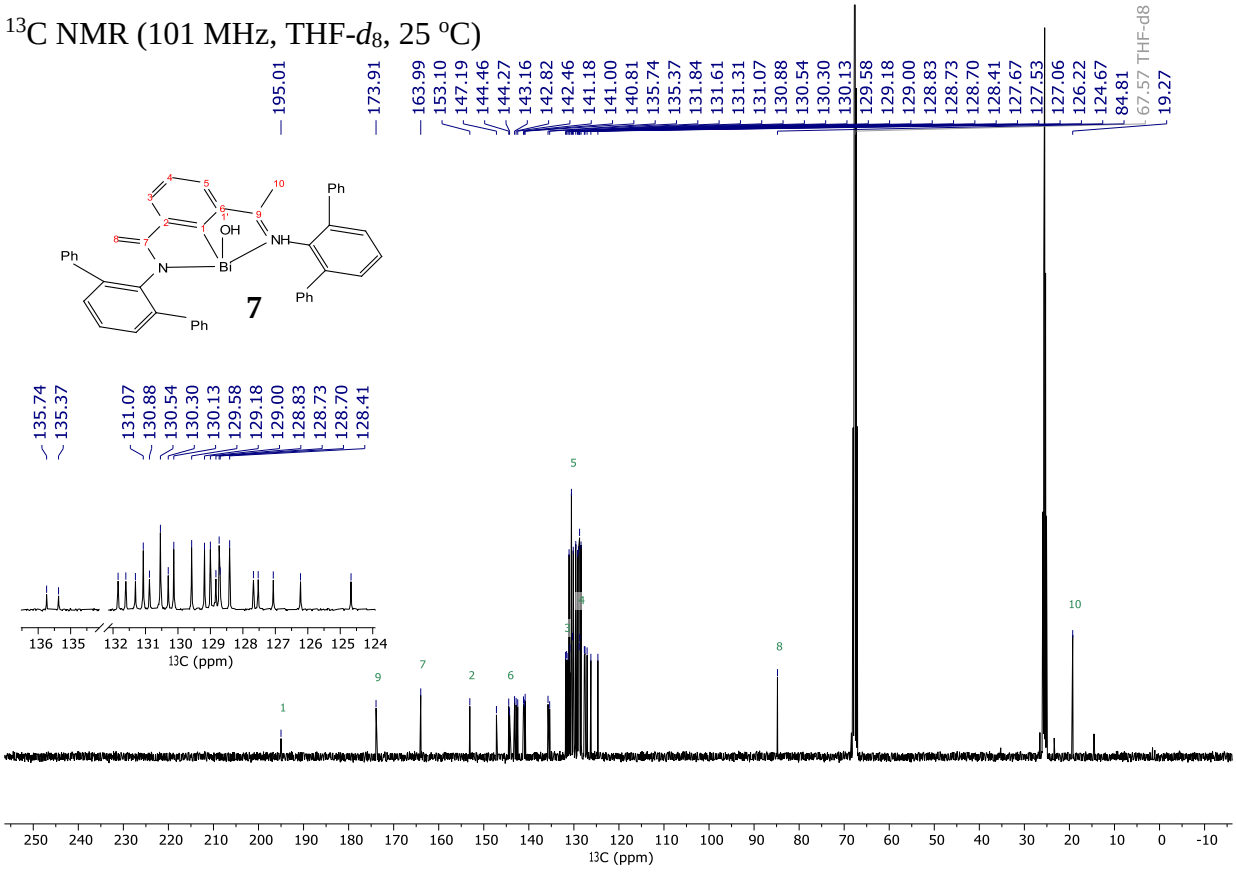

^{1}H-^{1}H COSY

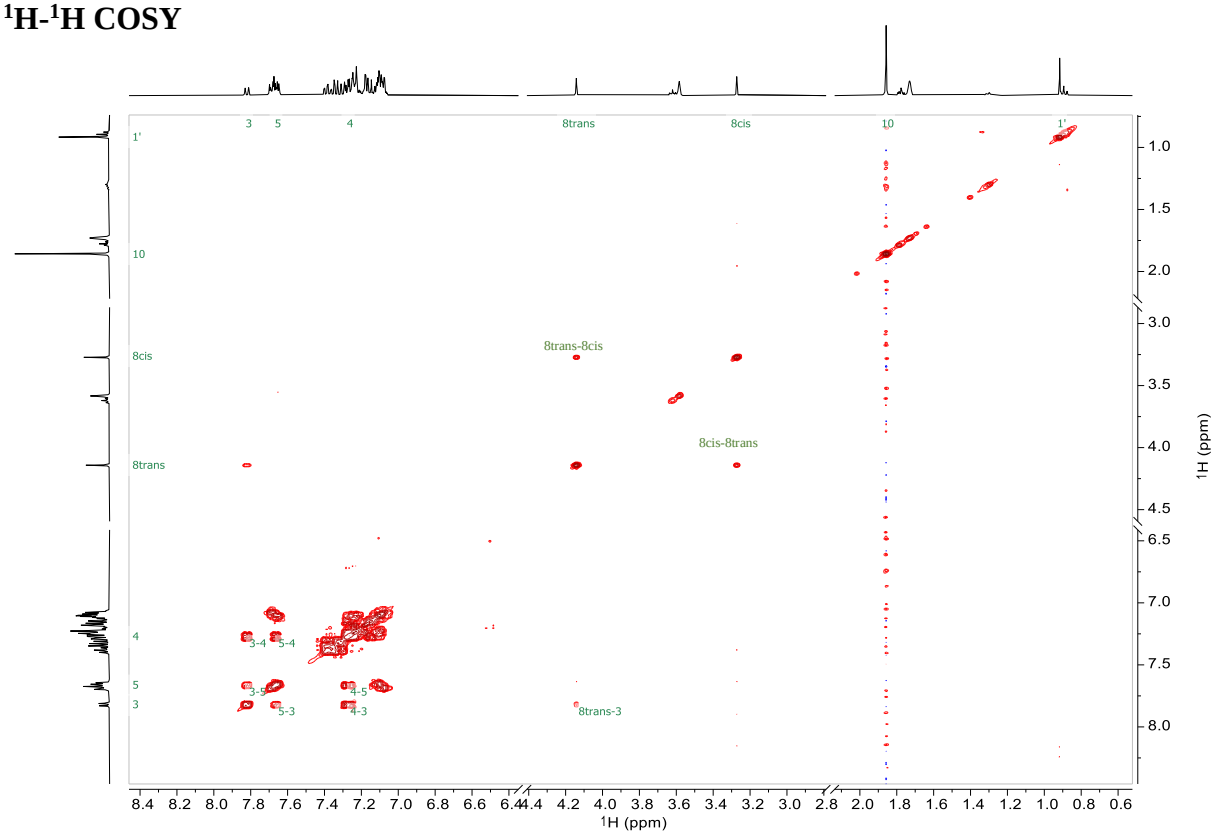

Edited-HSQC

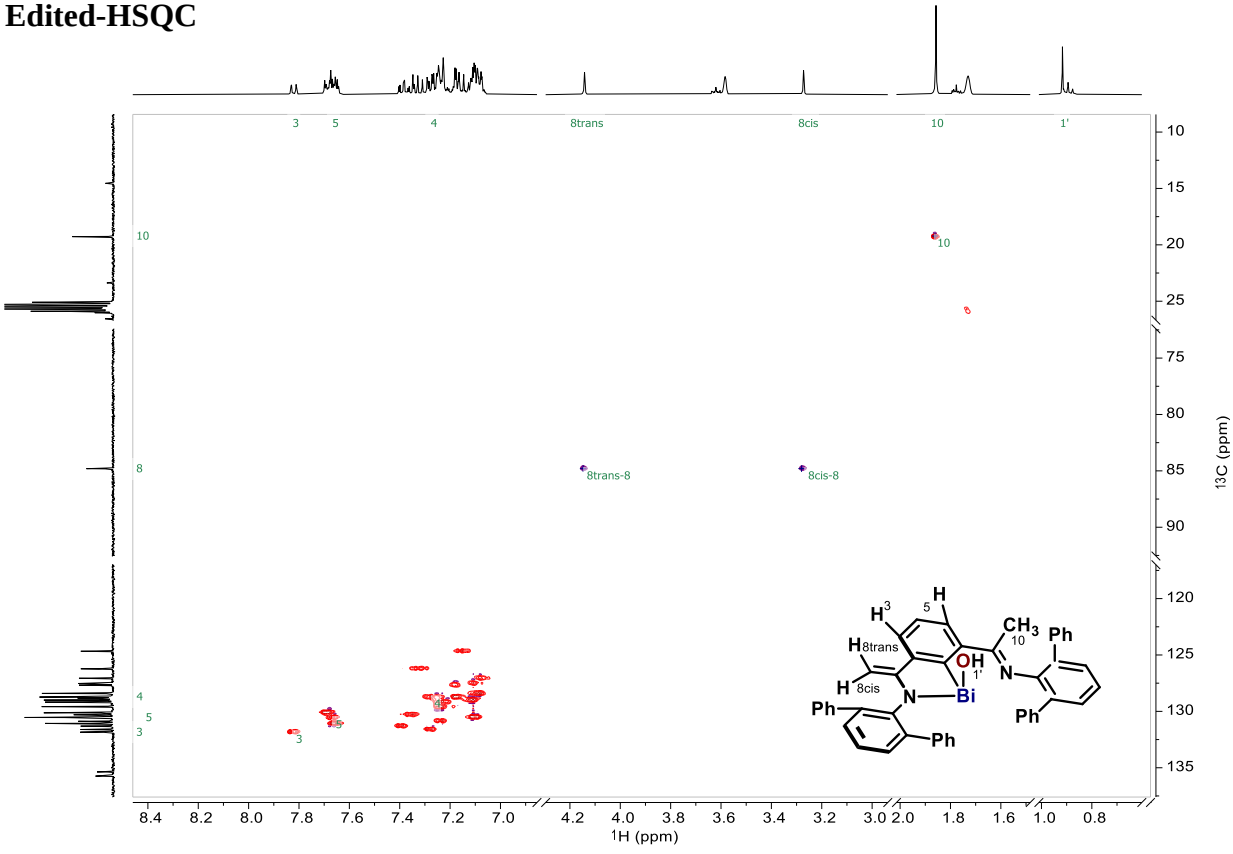

HMBC

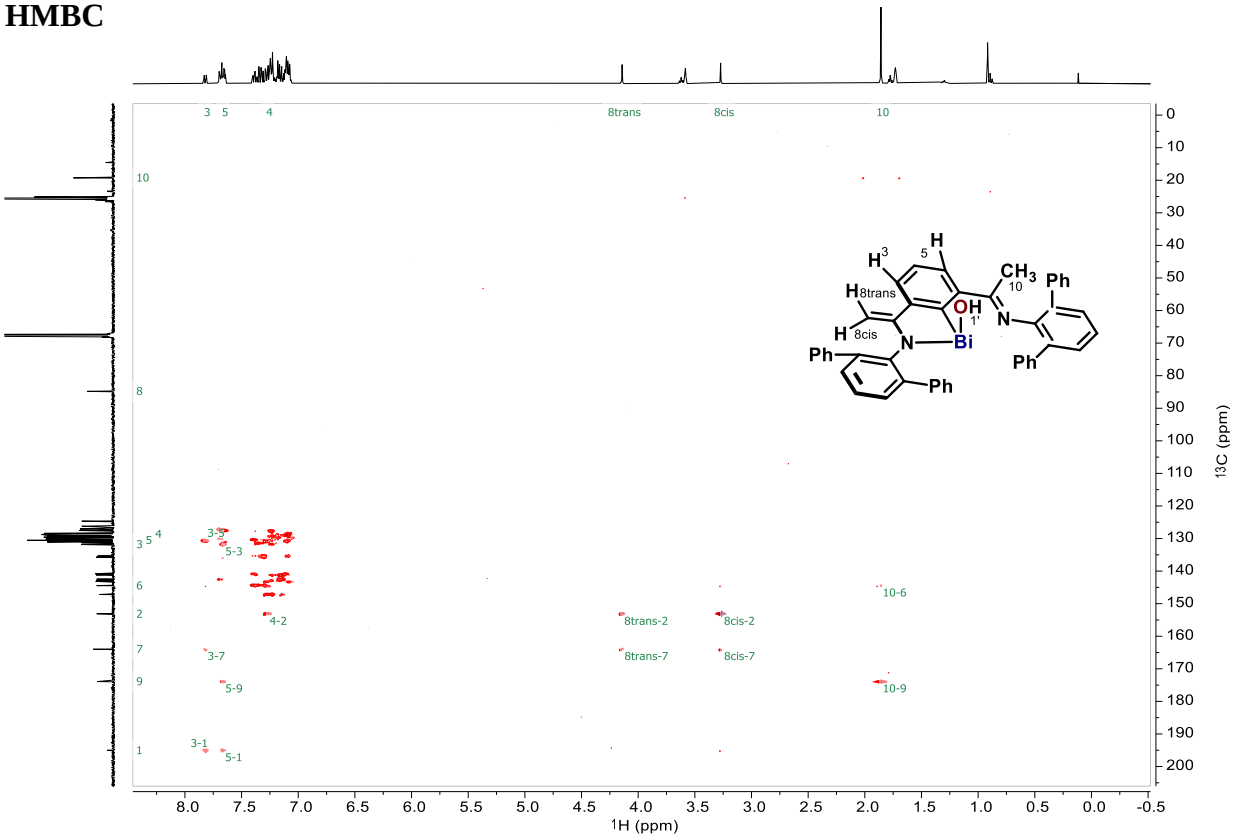
3 5 4
8trans
8cis
10
10
8
3 5 4
6
2
7
9
1
3-5
5-3
4-2
3-7
5-9
3-1
5-1
8trans-2
8cis-2
8trans-7
8cis-7
10-6
10-9
H
H3
5
CH3
10
Ph
H8trans
OH
1'
N
H 8cis
N
Bi
Ph
Ph
Ph
0
10
20
30
40
50
60
70
80
90
100
110
120
130
140
150
160
170
180
190
200
13C (ppm)
8.0
7.5
7.0
6.5
6.0
5.5
5.0
4.5
4.0
3.5
3.0
2.5
2.0
1.5
1.0
0.5
0.0
-0.5
1H (ppm)

ROESY

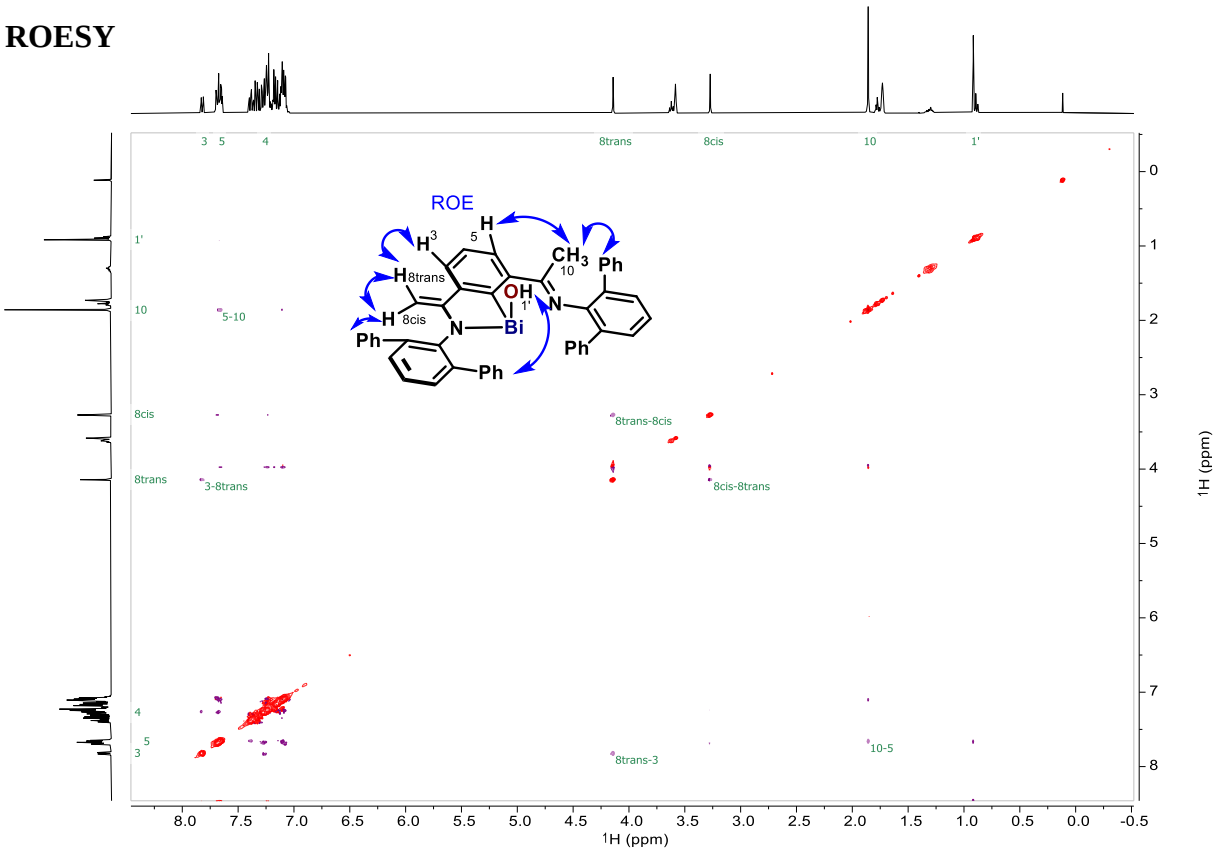
3 5 4
8trans
8cis
10
1'
1'
10
8cis
8trans
4
3 5
5-10
3-8trans
8trans-8cis
8cis-8trans
8trans-3
10-5
ROE
H
H3
5
CH3
10
Ph
H8trans
OH
1'
N
H 8cis
N
Bi
Ph
Ph
Ph
0
1
2
3
4
5
6
7
8
1H (ppm)
8.0
7.5
7.0
6.5
6.0
5.5
5.0
4.5
4.0
3.5
3.0
2.5
2.0
1.5
1.0
0.5
0.0
-0.5
1H (ppm)

^{1}H NMR (500 MHz, THF-d_8)

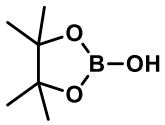

8

^{13}C NMR (126 MHz, THF-d_8)

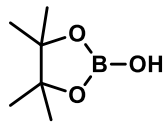

8

^{11}B NMR (160 MHz, THF-d_8)

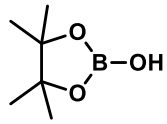

8

^{1}H NMR (500 MHz, THF-d_8)

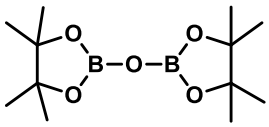

9

^{13}C NMR (126 MHz, THF-d_8)

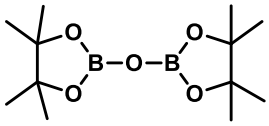

9

^{11}B NMR (160 MHz, THF-d_8)

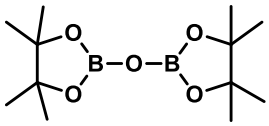

9